TECHNISCHE UNIVERSITÄT MÜNCHEN

Fakultät für Chemie

WACKER-Lehrstuhl für Makromolekulare Chemie

Copolymerization of Epoxides and CO_2: Extending the Portfolio of Aliphatic Polycarbonates

Sebastian Andreas Kernbichl

Vollständiger Abdruck der von der Fakultät für Chemie der Technischen Universität München zur Erlangung des akademischen Grades eines

Doktors der Naturwissenschaften

genehmigten Dissertation.

Vorsitzender:	apl. Prof. Dr. Wolfgang Eisenreich
Prüfer der Dissertation	1. Prof. Dr. Dr. h.c. Bernhard Rieger
	2. Prof. Dr. Klaus Köhler
	3. Prof. Dr. Gerrit Luinstra (schriftliche Beurteilung) Prof. Dr. Tom Nilges (mündliche Beurteilung)

Die Dissertation wurde am 04.03.2020 bei der Technischen Universität München eingereicht und durch die Fakultät für Chemie am 29.04.2020 angenommen.

Die vorliegende Arbeit wurde in der Zeit von Mai 2017 bis März 2020 am Wacker-Lehrstuhl für Makromolekulare Chemie, Technische Universität München, unter Betreuung von Herrn Prof. Dr. Dr. h.c. Bernhard Rieger angefertigt.

Acknowledgements

An erster Stelle bedanke ich mich bei Herrn Prof. Dr. Dr. h.c. Bernhard Rieger für die herzliche Aufnahme an seinen Lehrstuhl und die Möglichkeit, meine Doktorarbeit unter seiner Anleitung anfertigen zu dürfen. Vielen Dank für die sehr interessante Themenstellung, die gute Ausstattung des Lehrstuhls und die wertvollen Diskussionen.

Dr. Carsten Troll möchte ich für die zahlreichen Reparaturarbeiten an verschiedenen Geräten und der Unterstützung innerhalb der Industriekooperation mit Covestro danken. Weiterhin danke ich Dr. Sergei Vagin für sehr anregende, polymerchemische Diskussionen.

Bei meinen Industriepartnern von Covestro möchte ich mich für die spannenden Treffen, den Einblick in die Industrie und den durchgeführten Messungen bedanken.

Besonders danke ich meinen beiden Auszubildenden Caro Herzinger und Monika Meindl, all meinen fleißigen Studenten und dabei insbesondere meiner Masterstudentin Alina Denk für ihre Unterstützung. Daniel Bucalon gebührt Dank für synthetische Arbeit für das Tropolon-Projekt und Dr. Marina Reiter für die tolle Vorarbeit und Einarbeitung in mein Promotionsthema. Ihr habt entscheidend zum Gelingen dieser Arbeit beigetragen!

Ich werde mich immer an die sehr angenehme Arbeitsatmosphäre am Wacker-Lehrstuhl zurückerinnern. Zahlreiche Grillabende, Konferenzbesuche und Hüttenwochenenden waren ein super Ausgleich zum Laboralltag. Dabei möchte ich mich besonders bei der älteren Generation (Michl, Tom, Andi, Marc) bedanken. Aber auch die 'junge' Generation (Matthi, Chris, Alina, Kerstin, Sophia) trug zu einem sehr angenehmen Arbeitsklima im Labor, hart umkämpften Tennis-/Squashmatches und dem ein oder anderen feucht-fröhlichen Abend bei.

Abschließend möchte ich meinen Eltern für das entgegengebrachte Vertrauen in das Studium und die finanzielle Unterstützung danken. Und dir liebe Anna, vielen Dank, dass du immer an meiner Seite bist, meine Launen erträgst und wir zusammen eine gute Zeit haben!

List of Abbreviations

2VP	2-vinyl pyridine
Å	Ångström [10^{-10} m]
ATI	aminotroponiminate
BBL	*rac*-β-butyrolactone
BDI	β-diiminate
BPA-PC	bisphenol-A polycarbonate
CHO	cyclohexene oxide
CL	caprolactone
Cp	cyclopentadienyl
cPC	cyclic propylene carbonate
Đ	polydispersity
DAVP	dialkyl vinylphosphonate
DEVP	diethyl vinylphosphonate
et al.	and others (lat.: et alii)
Et	ethyl
GC-MS	gas chromatography mass spectrometry
GPC	gel permeation chromatography
GTP	group transfer polymerization
h	hour
HMBC	heteronuclear multiple bond correlation
HPPO	hydrogen peroxide to propylene oxide
HRIP	high-refractive index polymer
IPOx	2-*iso*-propenyl-2-oxazoline
^{i}Pr	isopropyl
IR	infrared
LA	*rac*-lactide
LO	limonene oxide

MA	methyl acrylate
*m*CPBA	*meta*-chloroperoxybenzoic acid
Me	methyl
MMA	methyl methacrylate
MTP	methanol-to-propylene process
NBS	*N*-bromosuccinimide
n_D	refractive index
NMR	nuclear magnetic resonance
P2VP	poly(2-vinylpyridine)
PBAT	poly(butylene adipate terephthalate)
PCHC	poly(cyclohexene carbonate)
PDEVP	poly(diethyl vinylphosphonate)
Ph	phenyl
PHB	poly(3-hyroxybutyrate)
PLA	poly(lactide)
PLC	poly(limonene carbonate)
PM	poly(*(-)*menthide)
P_m	probability of meso linkages
PO	propylene oxide
PP	poly(propylene)
PPC	poly(propylene carbonate)
ppm	part per million
PPNCl	*bis*(triphenylphosphin)iminiumchlorid
REM	rare earth metal-mediated
ROCOP	ring-opening copolymerization
ROP	ring-opening polymerization
SA	succinic acid
SKA	silyl ketene acetal

t	tons
*t*Bu	*tert*-butyl
T_g	glass transition temperature
thf	tetrahydrofuran
TMS	trimethylsilyl
TOF	turn-over frequency [h^{-1}]
TS-1	titanium-doped silicate 1
ZnGA	zinc glutarate

Publication List

- S. Kernbichl,‡ M. Reiter,‡ F. Adams, S. Vagin, B. Rieger*. CO_2-Controlled One-Pot Synthesis of AB, ABA Block, and Statistical Terpolymers from β-Butyrolactone, Epoxides, and CO_2. *J. Am. Chem. Soc.* **2017**, *139*, 6787 – 6790.
- S. Kernbichl, M. Reiter, J. Mock, B. Rieger*. Terpolymerization of β-Butyrolactone, Epoxides, and CO_2: Chemoselective CO_2-Switch and Its Impact on Kinetics and Material Properties, *Macromolecules* **2019**, *52*, 8476-848.
- A. Denk,‡ S. Kernbichl,‡ A. Schaffer, M. Kränzlein, T. Pehl and B. Rieger*. A Heteronuclear, Monomer-Selective Zn/Y Catalyst Combines Copolymerization of Epoxides and CO_2 with Group-Transfer Polymerization of Michael-type Monomers. 10.1021/acsmacrolett.9b01025
- S. Kernbichl, B. Rieger*. Aliphatic Polycarbonates Derived From Epoxides and CO_2: A Comparative Study of Poly(cyclohexene carbonate) and Poly(limonene carbonate). *Manuscript in preparation.*
- S. Kernbichl, B. Rieger*. Aliphatic Polycarbonates Derived from Epoxides and CO_2, Engineering Solutions for CO_2 Conversion; *John Wiley & Sons*, Limited, **2021**.

Publications beyond the scope of this thesis:

- S. Kernbichl, M. Reiter, D. H. Bucalon, P. J. Altmann, A. Kronast, B. Rieger*. Synthesis of Lewis Acidic, Aromatic Aminotroponiminate Zinc Complexes for the Ring-Opening Polymerization of Cyclic Esters. *Inorg. Chem.* **2018**, 57, 9931-9940.
- F. Adams, T. M. Pehl, M. Kränzlein, S. Kernbichl, J.-J Kang, C. Papadakis, B. Rieger* (Co)polymerization of (-)-Menthide and racemic β-Butyrolactone with Heteroaromatic Yttrium-bis(phenolates): Tuning Material Properties of Sustainable Polyesters. *Manuscript in preparation.*

‡These authors contributed equally; *Corresponding authors

Conference contributions:

- S. Kernbichl, M. Reiter, B. Rieger. CO_2-Controlled One-Pot Synthesis of AB, ABA Block, and Statistical Terpolymers from β-Butyrolactone, Epoxides, and CO_2, Macromolecular Colloquium **2018**, Freiburg, poster presentation.
- S. Kernbichl, B. Rieger. CO_2-Selective Terpolymerizations from β-Butyrolactone, Epoxides & CO_2 and Their Kinetic, Thermal and Mechanical Characterization, 258th American Chemical Society National Meeting & Exposition **2019**, San Diego, oral presentation.

Table of Contents

1. Introduction

With approximately 8 million tons of plastics entering the ocean each year, the necessity for efficient waste disposal as well as the development of degradable polymers becomes obvious.[1] An impressive amount of 359 million tons of plastics are produced worldwide per year. Undoubtedly, the massive variety of different types of plastics has provided the basis for today's high living standard. Plastics have both complemented and replaced conventional materials such as wood, wool, or metals. 39.9% of the worldwide plastics are used in packaging, followed by the sectors building & construction (19.8%) and automotive (9.9%) (Figure 1).[2]

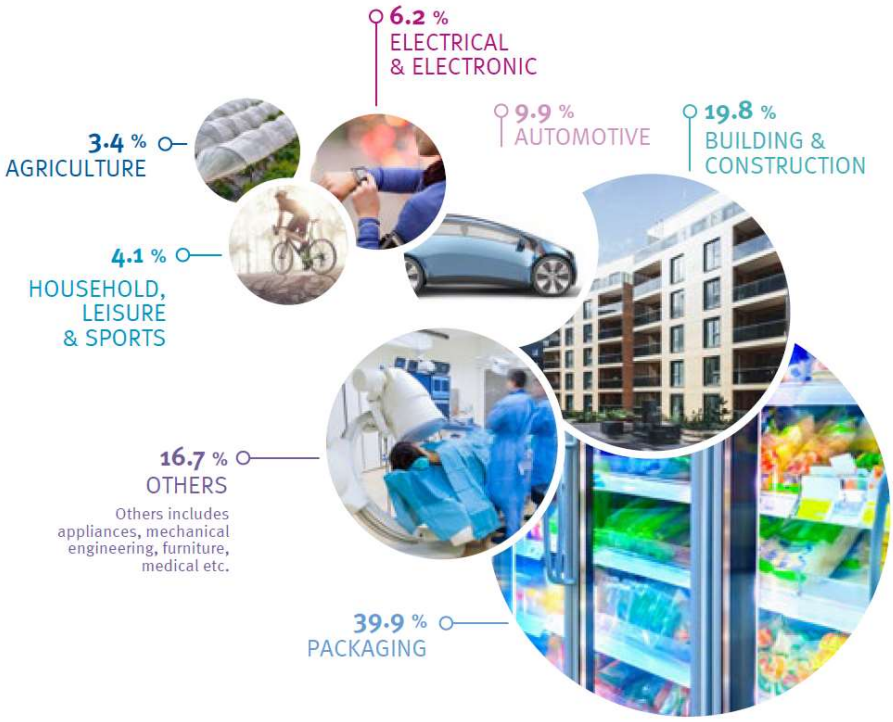

Figure 1. European plastics demand in 2018 by segments.[2]

Clearly, this amount and variety of polymers has only been enabled by the use and development of suitable catalysts. One of the most important milestones in polymerization catalysis is the initial discovery of the polymerization of ethylene with a mixture of $TiCl_4$ and $AlEt_3$ by Ziegler and Natta.[3] It represents the origin of the field of coordinative and stereoselective polymerization catalysis. Referring to coordinative polymerizations, the difference in terminology of initiator and catalyst should be addressed shortly. In general, every polymerization reaction is catalytic since certain equivalents of the monomer are built up to polymer chains by one initiating molecule. In metal-catalyzed polymerizations, the definition is broader since a metal complex can both act as an initiator of the reaction and as catalyst via (pre-)activating the monomer.[4-5] Catalysts help to minimize energy costs, facilitate the formation of the desired product and make novel types of polymers possible, anyway.

One group of polymers that increasingly gains attention are biopolymers. In the context of bioplastics, it must be differentiated between the bio-based and the biodegradable character of a material. A polymer

is considered to be biodegradable if it decomposes into water, carbon dioxide and biomass upon exposure to suitable environmental conditions. In contrast, a material can have a bio-based origin but is not necessarily biodegradable.[6] In 2019, 1% of the total plastics production is ascribed to bioplastics (bio-based and biodegradable combined). Within the class of biodegradable plastics, the most important polymers are starch blends (21%), poly(lactide) (PLA) (14%), and poly(butylene adipate terephthalate) (PBAT), commercialized under Ecoflex® (13%, Figure 2). Despite their non-biodegradable nature, the production of bio-based polymers is continuously increasing as well. Bio-based polypropylene (PP), for instance, entered the market on a commercial scale in 2019 and its production is predicted to sextuple by 2024.[7] Most of these bioplastics are designed for an application as commodity polymers, mainly packaging. Although commodity polymers are not regarded as high-performance polymers, they must meet high demands with regard to thermal and mechanical performance.

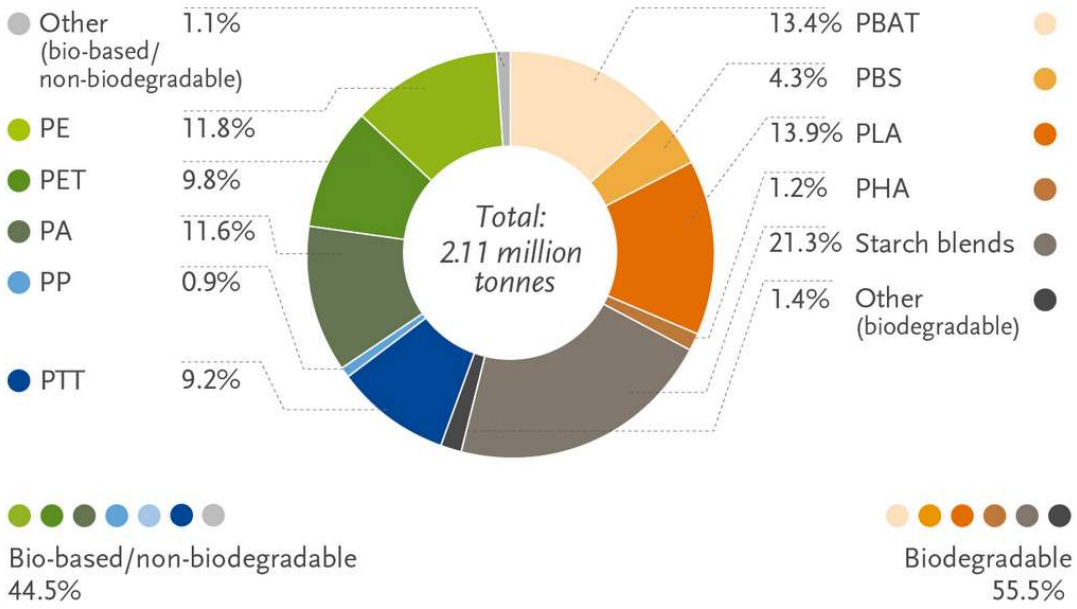

Figure 2. Global production of bioplastics in 2019 by material type.[7]

A different approach to render chemical syntheses sustainable is the utilization of carbon dioxide as a C-1 feedstock. CO_2 is a nontoxic, abundantly available and nonflammable feedstock which, on the downside, is thermodynamically stable with a Gibbs free energy $\Delta G_f = -394$ kJ/mol . To overcome this high energy barrier, highly reactive reagents for a possible coupling with CO_2 have been explored. The utilization of CO_2 is already industrially implemented in various processes such as the synthesis of urea (146 mt/a), methanol (6 mt/a), salicylic acid (60 kt/a), and cyclic carbonates (40 kt/a). Altogether, these reactions only contribute to a conversion of 1% of the total amount of anthropogenic CO_2 emission.[8-9] Another encouraging strategy to incorporate carbon dioxide is the coupling of epoxides and CO_2 to form polycarbonates (Scheme 1).

Scheme 1. Alternating ring-opening copolymerization (ROCOP) of epoxides and CO_2 to polycarbonates and the two possible byproducts, cyclic carbonate, and polyether

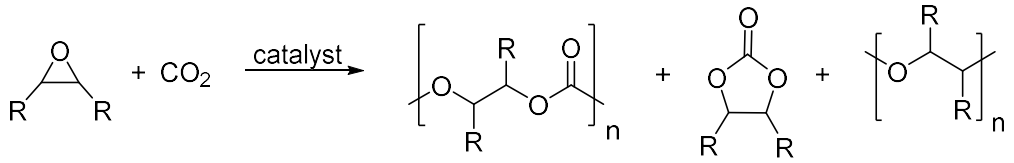

CO_2-based polycarbonates can generally serve as a valuable feedstock depending on their molecular weight. Low molecular weight (MW) polycarbonates in a polyol structure are interesting building blocks for polyurethane production whereas the high MW polycarbonates find application as rigid plastics. Like most coordinative polymerizations, also the epoxide/CO_2 copolymerization is subject to various factors and influences. The increasing viscosity of the reaction mixture during polymerization limits monomer diffusion and therefore hampers high monomer conversions. Addressing this by diluting the polymerization ensures a lowered viscosity but also lets the activities often drop due to a decreasing monomer concentration and a spatial separation of active catalyst molecules. The second concern that must be considered are side- and chain-transfer reactions (also illustrated in Scheme 1). The consecutive insertion of epoxides leads to polyether linkages while a nucleophilic backbiting reaction gives cyclic carbonates. Moreover, protic impurities affect a dissociation of the growing polymer chain and the catalytic center and produce polymers in reduced molecular weight. All these issues can be met by a judicious choice of catalyst and a wise adjustment of the reaction parameters and enable the synthesis of different CO_2-based polycarbonates, for which the three most important examples are illustrated in Figure 3.

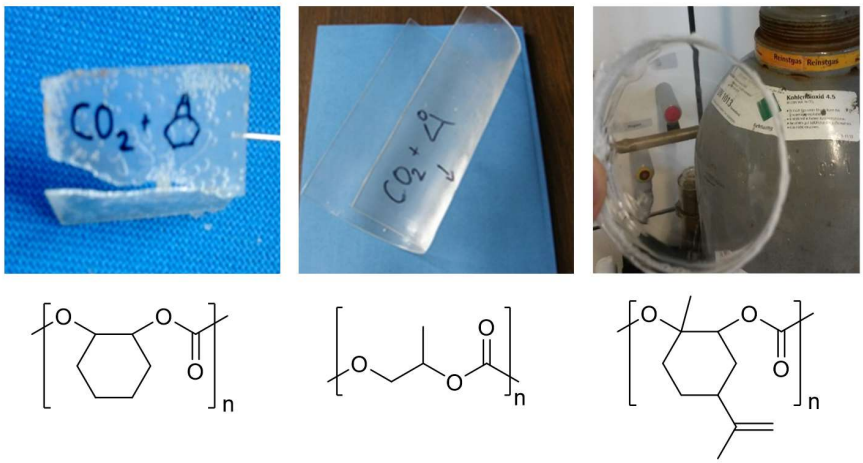

Figure 3. Chemical structure and appearance of the three most important aliphatic polycarbonates: Poly(cyclohexene carbonate) (PCHC), poly(propylene carbonate) (PPC), and poly(limonene carbonate) (PLC).

Poly(propylene carbonate) is regarded as biodegradable and is very promising for large scale productions because propylene oxide (PO) is industrially abundant, and the CO_2 content of the polymer is high (43wt%). Poly(limonene carbonate) is a bio-based material since limonene can be gained from

the peel of oranges and is polymerized upon epoxidation with CO_2. Different companies continuously work on the industrialization of processes to produce CO_2-based polymers. *Novomer*, to only name one example, established a 7 kt/a production of poly(propylene carbonate) in 2013.[10] Also, *Covestro* is running a pilot-scale production of poly(ether carbonates). The CO_2-content in the final polyol, which is used for the production of polyurethane foams, can be selectively adjusted and reduces the use of fossil fuels by 20%.[11-12]

2. Copolymerization of Epoxides and CO_2 to Aliphatic Polycarbonates

Aliphatic polycarbonates derived from epoxides and CO_2 are often considered to be a possible alternative to bisphenol-A polycarbonate (BPA-PC). Although this novel class of polymers shows very interesting properties such as biodegradability (for PPC), lightness, high transparency as well as UV resistance, their large-scale commercialization has not been realized yet. To further shine light on the reasons for its limited industrialization, a detailed discussion about the most important properties is presented (Table 1). Starting with the thermal properties, the glass transition temperatures (T_g) of the polycarbonates listed in Table 1 differ significantly. While BPA-PC shows a high T_g of around 150 °C, only the cyclic aliphatic polycarbonates PCHC and PLC display glass transitions higher than 100 °C.[13-14] PPC has a very low T_g which varies from 20 – 40 °C depending on the molecular weight and the amount of ether linkages.[15] The second key feature in terms of thermal properties is thermal degradation. It has been discussed for a long time since an overall lower decomposition has been observed compared to BPA-PC. Generally, thermal decomposition can either occur via random chain scission or via chain unzipping (a nucleophile is located at the polymer chain end and causes backbiting to cyclic carbonates). Due the very low activation energy for the cyclic carbonate in case of PPC, the thermal stability of the polymer is a big issue. Approaches to suppress backbiting mainly focus on end-capping the polymer with functional groups which are less prone to promote the cyclic propylene carbonate (cPC) formation.[16]

Table 1. Comparison of the thermal and mechanical data of BPA-PC with three aliphatic polycarbonates

polycarbonate	T_g [°C]	T_{max} [°C]	Young modulus [MPa]	tensile strength [MPa]	elongation at break [%]
BPA-PC[13,17]	149	365	2400 ± 400	47 ± 4	40 ± 35
PCHC[13,18]	115	240	3600 ± 100	43 ± 2	1.7 ± 0.6
PPC[15,19]	40	180	831 ± 23	22 ± 2	330 ± 9
PLC[14]	130	265	950	55	15

The widespread commercialization of BPA-PC is mainly based on its high impact resistance, the glass-like transparency, a good heat resistance as well as an easy processability. PCHC for example has a promising T_g of 115 °C but lacks a sufficient mechanical performance. The low elongation at break of approximately 1-2% renders this material very brittle. In contrast, the weak chain interactions of PPC cause a low T_g which makes the polymer very soft. Also, the mechanical data strongly depend on the molecular weight, the microstructure and traces of cyclic carbonate. It behaves as a rather brittle material

below 15 °C but loses strength above 40 °C, too.[20] Terpolymerization of cyclohexene oxide (CHO), PO, and CO_2 is a valuable tool to overcome these adverse properties. Lee *et al.* used a Co(III) salen complex and could tune the glass transition for the terpolymer between 52 °C and 93 °C depending on the monomer feed.[21] Although the Young modulus of the terpolymer was reduced compared to pure PCHC, the elongation at break, however, remained very low.[22] Poly(limonene carbonate) recently gained a lot of attention after its comprehensive characterization by Greiner and Rieger. A 94% transmission was found besides a T_g of 130 °C and promising mechanical data (Young modulus: 950 MPa; elongation at break: 15%).[14] The glass transition temperature of limonene oxide (LO) based copolymers was increased even further by the synthesis of poly(limonene dicarbonate) (T_g = 146 – 180 °C). This was achieved via two different routes. Kleij *et al.* has chosen the way to copolymerize LO and CO_2 first and selectively oxidize the double bond prior to the formation of the cyclic carbonate with CO_2 and *bis*(triphenylphosphin)iminiumchlorid (PPNCl) as a chloride-assisted carboxylation agent.[23] Koning and coworkers decided to start with limonene dioxide, performed the ROCOP with the help of a β-diiminate (BDI) zinc catalyst to poly(limonene-8,9-oxide carbonate) which served as an interesting platform for the synthesis of the respective dicarbonate or thiol- and dicarboxylate modified polymers.[24]

2.1 Monomer Synthesis

Among the three introduced epoxides, propylene oxide is by far the most abundant one with a production of 7.5 million t/a.[25] In the early days, PO was produced through the so called hydrochlorination route. It proceeds via the conversion of propylene to propylene chlorohydrin. The latter is then dehydro-chlorinated to get propylene oxide. For one ton PO, it requires 1.4 t tons of chlorine and 40 t wastewater are produced. Later, the styrene oxide/PO route has been established. Ethyl benzene was converted to ethylbenzene hydroperoxide which, upon oxidation of propylene, was converted to 1-phenylethanol, a useful precursor for the synthesis of styrene. But still, 2.3 t styrene as a byproduct were produced per ton PO along with 1.6 t wastewater. By far the most environmentally friendly synthesis is the hydrogen peroxide to propylene oxide (HPPO) process. A titanium-doped silicate (TS-1) serves as the active catalyst for the direct synthesis of propylene oxide from propylene with H_2O_2 and water as the only byproducts (Scheme 2a). An energy reduction by 35% compared to the other routes is one of the many reasons why it has been industrially realized so rapidly.[25-26] Cyclohexene oxide often serves as a bench-mark in ROCOP research but is industrially less relevant than PO. It can be epoxidized with peracids, e.g. peroxypropionic acid, in chloroform with a sodium acetate buffer (Scheme 2b).[27] Other approaches have been reported, such as the direct epoxidation with manganese porphyrins in the presence of molecular oxygen.[28] (*R*)-limonene is extracted from the peel of citrus fruits on a 70 kt/a scale. Most processes that directly epoxidize (*R*)-limonene yield a mixture of *cis*- and *trans*-(*R*)-limonene oxide. Due to the fact, that most homogeneous catalysts can only polymerize the *trans*-stereoisomer so far, a

stereoselective route has been established (Scheme 2c). The conversion of limonene is performed with *N*-bromosuccinimide (NBS) to the endo-cyclic bromohydrin which is readily converted to the epoxide.[14]

Scheme 2. Preparation of the epoxide, propylene oxide (a), cyclohexene oxide (b), and limonene oxide (c)

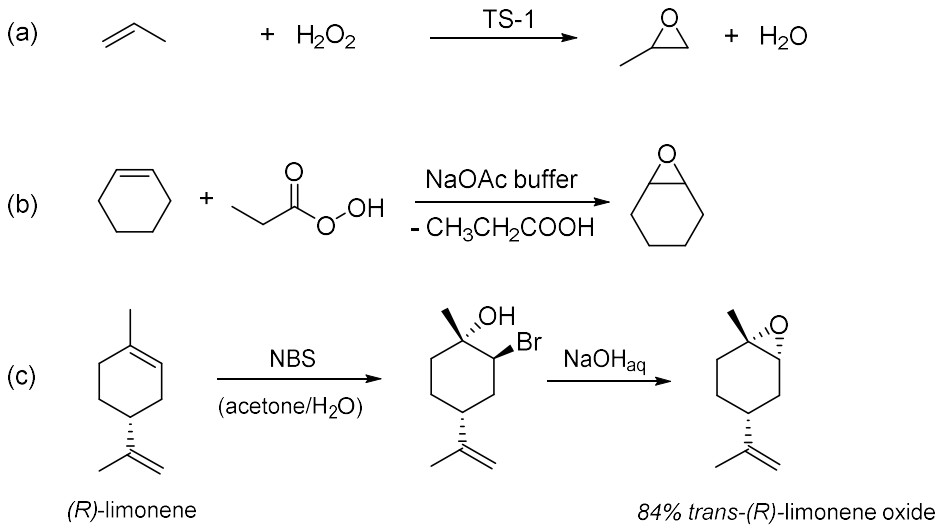

2.2 Development of Hetero- and Homogeneous Catalytic Systems

In 1969, Inoue *et al.* observed the formation of poly(propylene carbonate) by combining diethylzinc, water, propylene oxide, and CO_2.[29-30] Although very low activities were observed, different research groups picked up this idea and tried to improve the catalytic performance. The use of $Zn(OH)_2$ and various dicarboxylic acids by Soga and coworkers yielded PPC at 60 °C and 30 bar CO_2 with a TOF of 1.1 h^{-1}.[31] The cost-effective preparation of the catalyst and the fact that high molecular weight PPC could be obtained, classified this approach as an industrially relevant route towards aliphatic polycarbonates. In fact, this system is used in the industrial production of PPC since years, although the structural elucidation of the zinc glutarate (ZnGA) was incomplete for a long time. Single-crystal diffraction studies by Rieger *et al.* revealed the reason for the higher activity of ZnGA compared to its lower homologue containing succinic acid (SA).

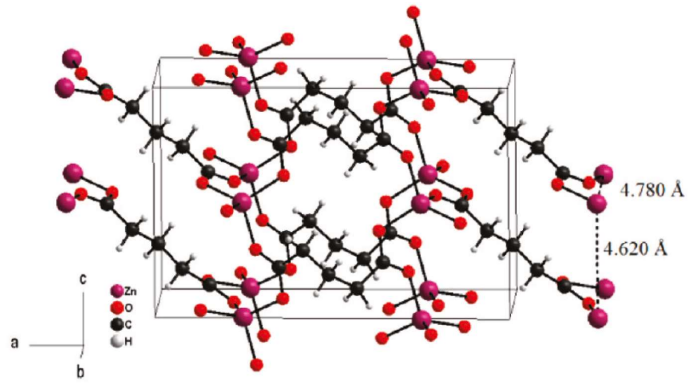

Figure 4. Solid state structure of ZnGA.[32]

Zinc-zinc surface couples (not present in ZnSA) are the prerequisite for activities in the copolymerization reaction which runs via a bimetallic mechanism. Within this study an ideal Zn-Zn distance of 4.6 – 4.8 Å was reported (Figure 4). Attempts to further increase the catalytic performance of the system (ball milling, stirring speed, etc.) did only lead to minor improvements.[32-33]

It was again Inoue *et al.* who presented the first homogeneous catalyst to the ROCOP of an epoxide and CO_2. A tetraphenylporphyrin ligand bound to an aluminum center yielded PPC in molecular weights of 3.7 – 27 kg/mol in narrow dispersities.[34] Porphyrin-based complexes have been modified regarding the metal center (Al, Cr, Co), ligand variations, and the nature of different cocatalysts (PPNCl, 4-(dimethylamino)-pyridin, Bu_4NCl) (Figure 5a).[35-36] In the 1990s, a series of zinc phenoxides with the general formula $(2,6\text{-}R_2C_6H_3O)Zn(base)_2$ was presented by Darensbourg. The effect of ligand substitution was investigated and an overall higher activity observed with decreasing substituent size.[37-38] Figure 5 gives an overview of the four most important structures in the field of epoxide/CO_2 polymerization catalysis. The different types of complexes are discussed in the following section.

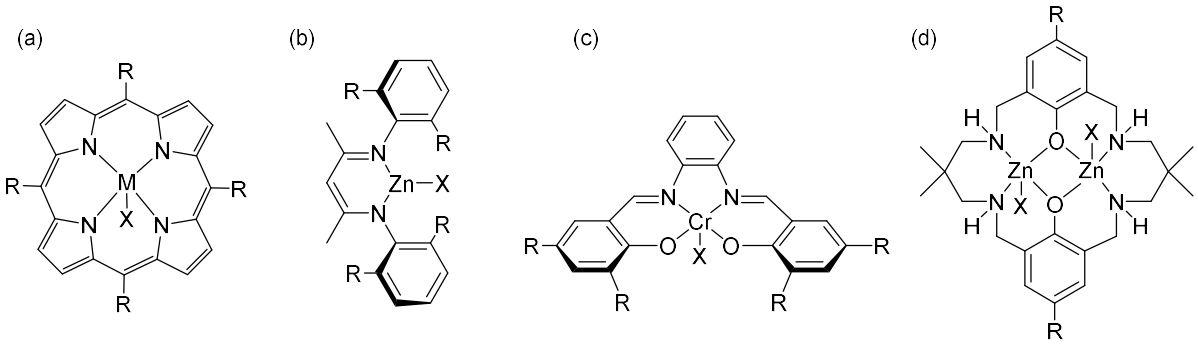

Figure 5. Most important catalyst structures in the epoxide/CO_2 copolymerization. Metal porphyrins (a), BDI zinc complexes (b), metal salen structures and a macrocyclic (c), and a Robson-type complex (d) (X = initiating group).

A breakthrough in the homogeneous catalysis of epoxides and CO_2 was achieved by the group of Coates in 1998 which introduced β-diiminate zinc complexes as active catalysts in the ROCOP (Figure 5b).[39] Due to the sterically demanding BDI ligands, *bis*-ligation is inhibited, and free coordination sites are available which are crucial for the catalytic process. In the ROCOP of CHO and CO_2, a high ratio of carbonate linkages (>95%) in high turn-over frequencies (TOF > 135 h^{-1}) was achieved. From then on, β-diiminate ligands were attached to various zinc precursors and structural modifications at the ligand structure were found to significantly influence the catalytic activity. Methyl-substituted BDI complexes are inactive in the copolymerization whereas the ethyl (Et) and isopropyl (^{i}Pr) analogs show very high activities (TOF up to 431 h^{-1}). The reason for this reactivity could be found in the monomer-dimer equilibrium. BDI complexes preferentially exist as dimers in the solid state. In solution, this equilibrium highly depends on steric and electronic factors of the ligand as well as on temperature and concentration. High activities in the ROCOP are reached with weakly linked dimers in a favorable Zn-Zn distance.

Methyl substituted BDI complex, for instance, form a strong linkage and are therefore inactive in the copolymerization. Synthetic modifications at the pentane backbone with electron-withdrawing substituents such as cyano and trifluoromethyl groups further enhanced the activity of the complexes (TOF = 917 h^{-1}).[40]

Another important class of catalysts are metal salens (Figure 5c).[41] It is the most investigated system in the copolymerization of epoxides and CO_2 with a *N*,*N*,*O*,*O*-tetradentate ligand structure. They overall suffer from lower activities in case of PO (TOF = 70 h^{-1}) compared to BDI complexes (TOF = 235 h^{-1}), but are able to introduce regioselectivity along with high polycarbonate selectivities (>99%).[42-43] On the downside, these complexes require the use of a cocatalyst and often contain chromium, a very toxic metal. Later, reports concentrated more on the use of cobalt as central metal. Moreover, binary catalysts were synthesized where a quaternary ammonium moiety is linked to the salen structure. This hinders the backbiting reaction to the cyclic propylene carbonate and enabled the highest TOF for PO/CO_2 copolymerization of 26,000 h^{-1}.[44]

The concept of flexibly linking two BDI complexes was taken up by Rieger and coworkers. They reported a flexibly tethered dinuclear zinc complex with unprecedented high activity for the ROCOP of CHO and CO_2 (Figure 6). The two zinc centers seem to have the perfect distance during the CHO/CO_2 coupling which enabled very high TOFs of 23,000 – 155,000 h^{-1} (depending in the substituents at the pentane backbone).

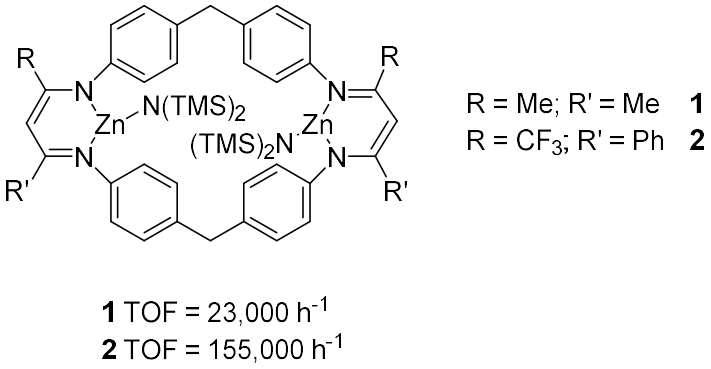

Figure 6. Structure of the flexibly bridged, dinuclear zinc complexes **1** and **2**.

Kinetic studies with mononuclear BDI complexes revealed the ring-opening of the epoxide to be the rate-determining step and therefore the epoxide has a reaction order of 1. The same kinetic investigations were performed with the dinuclear complex **1** using in situ infrared (IR) spectroscopy. At high carbon dioxide pressures (25 – 45 bar), the reaction orders are similar to those obtained for the mononuclear complex. But, interestingly, upon reducing the CO_2 pressure (5 – 25 bar) the orders with respect to CHO and CO_2 change, and CO_2 becomes rate-determining.

$$r = k\,[\mathrm{CHO}]^0[\mathrm{CO_2}]^1[\mathrm{cat}]^1 \qquad 5 - 25 \text{ bar}$$

$$r = k\,[\mathrm{CHO}]^1[\mathrm{CO_2}]^0[\mathrm{cat}]^1 \qquad 25 - 45 \text{ bar}$$

Macrocyclic ligand systems synthesized by the group of Williams used zinc and/or magnesium as central metal and bear two major advantages. On the one hand, a very low CO_2 pressure of 1 bar still ensures high polycarbonate selectivities at moderate activities (TOF for CHO/CO_2 = 20 – 620 h^{-1}).[45-46] On the other hand, the complex is highly tolerant towards protic compounds and is not decomposed rapidly like a lot of other transition metal-based complexes. Copolymerization of CHO and CO_2 can run with 10 – 30 eq. of water enabling the tailoring of low-molecular weight PCHC and the generation of polyols which can further serve as a valuable feedstock in the polyurethane production.[46] Also, these macrocyclic ligands turned out to be a valuable group of catalysts to perform terpolymerization reactions from a mixed-monomer feedstock with CHO, CO_2, and a lactone or an anhydride (see Chapter 5.2).

The very first example for the successful copolymerization of limonene oxide and CO_2 dates back to 2004. A BDI-Zn-OAc complex serves as an active initiator and is most active between 25 – 35 °C (TOF = 37 h^{-1}). Two main insights could be gathered. First, using a commercially available mixture of *cis*- and *trans*-LO resulted in the exclusive incorporation of the *trans* monomer. Secondly, at elevated temperatures (T = 50 °C) only very little conversion was observed.[47] It took 10 years until the polymerization of limonene oxide again appeared at the screen of polymer catalysis. Coates *et al.* reported the crystallization of stereocomplexed poly(limonene carbonate).[48] In the same year, the group of Kleij synthesized an amino(triphenolate) aluminum (III) complex **3** which, upon treatment with a suitable cocatalyst, showed activity in the copolymerization of LO and CO_2 (Figure 7). The activity was lower (TOF = 3 h^{-1}) compared to the BDI complex but due to the use of a cocatalyst both stereoisomers were incorporated with a preferential nucleophilic attack at the substituted position of the epoxide.[49]

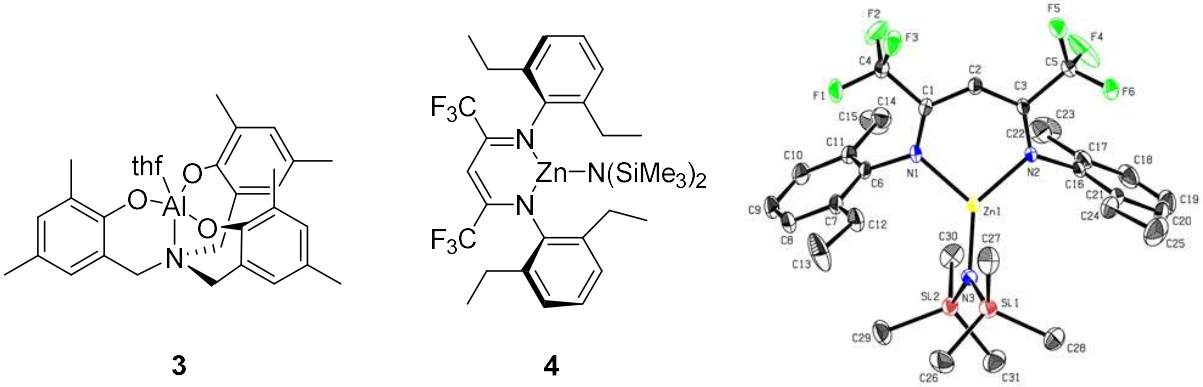

3 **4**

Figure 7. Active catalysts for the LO/CO_2 copolymerization: Amino(triphenolate) aluminum **3** and the BDI^{CF3}-Zn-N($SiMe_3$)$_2$ **4** and its ORTEP style representation with ellipsoids drawn at the 50% probability level.[50]

The introduction of two electron-withdrawing groups and the use of a *bis*(trimethylsilyl)amide initiating group rendered complex **4** the most active catalyst for LO/CO_2 copolymerization (TOF = 310 h^{-1}). Furthermore, complex **4** turned out to be active for a multitude of different epoxides such as CHO, PO, LO, octene oxide, and styrene oxide. Within the LO/CO_2 coupling, the decrease in activity for LO at

elevated temperatures could be addressed with the use of in situ infrared spectroscopy. In case of LO, the reverse reaction to the polymerization is the release of LO and CO_2 (and not the backbiting reaction to cyclic limonene carbonate). At 60 °C, a critical LO concentration is reached at which the equilibrium of the reaction shifts to the backformation of LO and CO_2. This means that the ceiling temperature of PLC is comparably lower than of other aliphatic polycarbonates and the polymerization has to be performed at temperatures not higher than 40 °C.[50]

2.3 Mechanism of the Copolymerization of Epoxides and CO_2

The copolymerization of epoxides and CO_2 is divided into three elementary steps, initiation, propagation, and termination. Termination also occurs via a chain transfer of the propagating chain through protic impurities or the addition of chain-transfer agents (CTA). Generally, the mechanism can proceed via three different pathways, with L_nM-X being the homogeneous catalyst. In the monometallic pathway, the ring-opening of the precoordinated epoxide takes place through an intramolecular attack of the nucleophile X. The second route involves an interaction between the catalyst and a cocatalyst such as tetrabutylammonium halides. Within this pathway, the cocatalyst promotes the ring-opening of the precoordinated epoxide. In the third, so called bimetallic pathway, two metal complexes intermolecularly drive the ring-opening step of the epoxide. Density functional theory calculations indicate the chain growth to occur via the attack of a metal-bound carbonate on a metal-bound epoxide.[51]

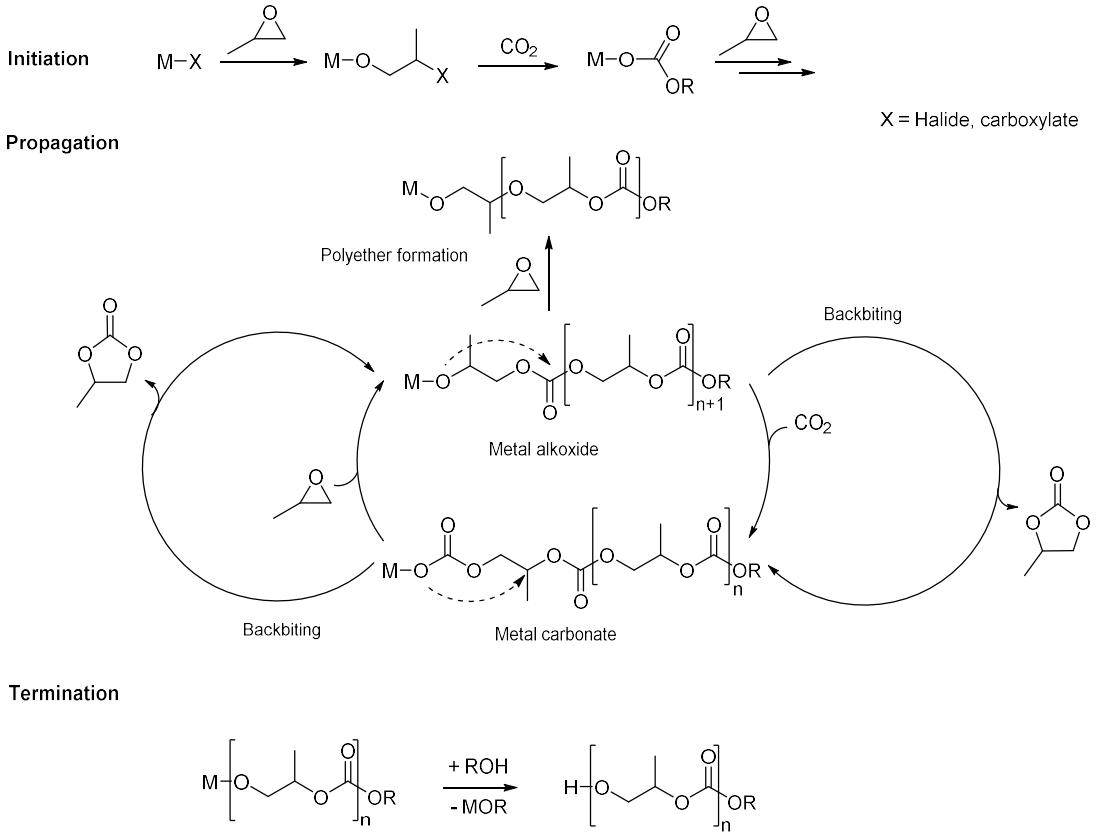

Figure 8. Mechanism of the copolymerization of epoxides and CO_2 via initiation, propagation, and termination.[52]

All three pathways in common, the coordination of the epoxide at the metal center is a crucial step. Without this pre-coordination, the initiating group X and later the growing polymer chain would not be nucleophilic enough to promote the ring-opening step. The coordination-insertion mechanism of the epoxide/CO_2 coupling is displayed in Figure 8.

The metal complex undergoes a ring-opening of the epoxide according to one of the three pathways and forms a metal-carbonate chain-end after the insertion of CO_2. The alternating insertion of an epoxide and CO_2 leads to the formation of the polycarbonate. Two possible side reactions are observed. If epoxides are inserted consecutively, polyether linkages result and if the growing carbonate chain is prone to backbiting, a cyclic carbonate byproduct is formed. The polymerization reaction is usually terminated by the addition of alcohols or water. This protonation of the growing polymer chain can either occur due to hydroxyl impurities in the reaction mixture or intentionally for the generation of low molecular weight polymers or the incorporation of a chain-transfer agent.[8]

For many metal complexes, especially zinc-based systems, the main difference in polymerizing CHO or PO with carbon dioxide, is the tendency towards the formation of cyclic carbonate. Usually, higher activities and selectivities are observed for CHO. Darensbourg reported the activation energies for both monomers in the copolymerization reaction with chromium salen complexes (Figure 9).[53] The polycarbonate PCHC is synthesized with a 20.7 kJ/mol lower activation energy than PPC. Additionally, in case of PO, the energetic difference of the polycarbonate and the cyclic carbonate accounts for only 33 kJ/mol whereas the energy difference is 86 kJ/mol for CHO. As a result, backbiting is the major challenge for propylene oxide and has to be addressed by a precise tuning of the (co)catalyst's structure and reactivity, CO_2 pressure and the temperature since high temperatures usually favor cyclic carbonate formation.

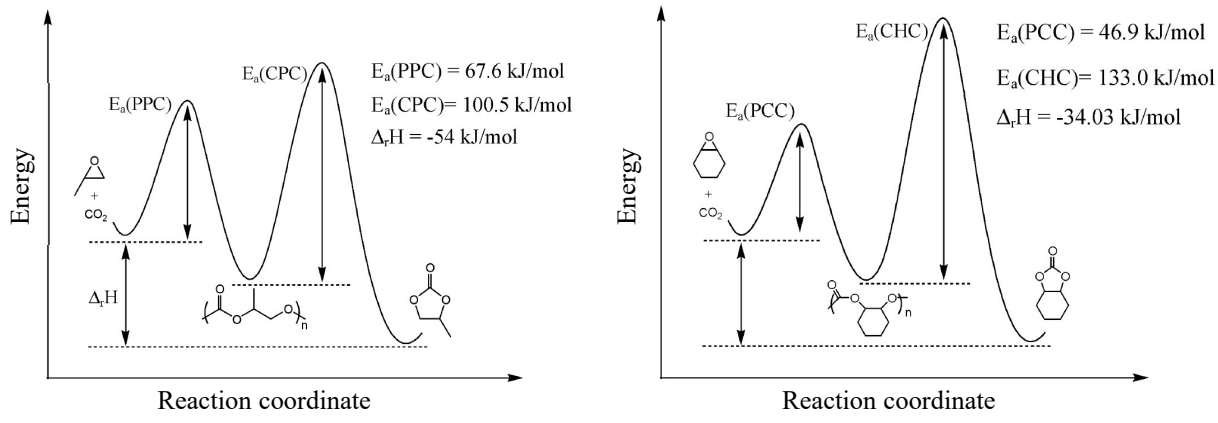

Figure 9. Reaction coordinate diagram for the coupling of PO and CO_2 (left), and the coupling of CHO and CO_2 (right).[53]

The third, very important monomer, limonene oxide, bears an additional methyl group at the epoxide moiety compared to CHO. Due to this increased steric hindrance during the copolymerization reaction, a deeper understanding of the polymerization mechanism is desirable. Two types of complexes are

known to catalyze the LO/CO_2 coupling. Amino(triphenolate) aluminum complexes **3** combined with PPNCl interestingly showed activities towards the incorporation of both stereoisomers, *cis*- and *trans*-limonene oxide. Surprisingly, the attack of the cocatalyst's chloride at the sterically hindered carbon atom of *cis*-LO in α-position is energetically favored (Figure 10). Also, for *trans* LO, the attack on the substituted position requires less energy than on the β-position. A nucleophilic attack at the α-position results in an inversion of the configuration and *trans*-PLC is obtained.

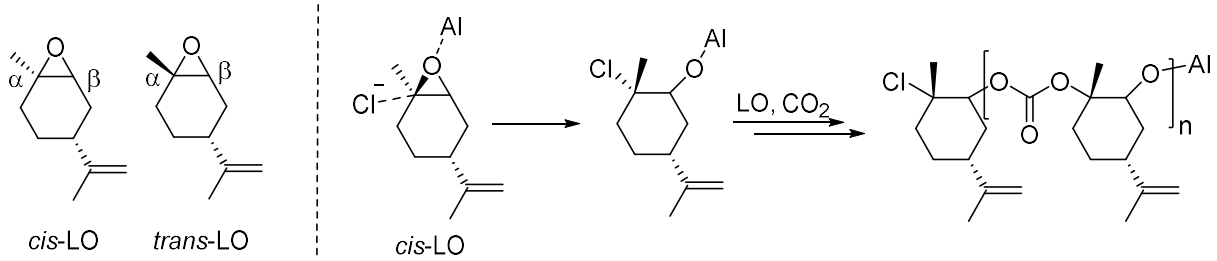

Figure 10. Possible nucleophilic attack at two different positions for *cis*-LO and *trans*-LO (left). Initiation of the polymerization with amino(triphenolate) Al complexes and PPNCl (right).

The second class of active catalysts are BDI complexes. To get further mechanistic insight, kinetic studies were performed. Thereby, the determination of the reaction orders for all reactive components, catalyst, monomer, and CO_2, delivers valuable information. Coates reported the following rate law for CHO as epoxide and 20 bar CO_2 with a BDI-Zn-OAc catalyst: $-d[CHO]/dt = k[CO_2]^0[CHO]^1[Zn]^1$.[40] The same catalyst was used in kinetic studies by Rieger and Greiner in 2016, where they observed a significant difference in the rate law for LO: $-d[LO]/dt = k[CO_2]^0[LO]^2[Zn]^1$.[14] The order with respect to the epoxide changed to the order of 2 for LO. Based on these kinetic investigations, a copolymerization mechanism for LO and CO_2 was postulated (Scheme 3).

Scheme 3. Initiation of the copolymerization of limonene oxide and CO_2 with a BDI-Zn-OAc complex[14]

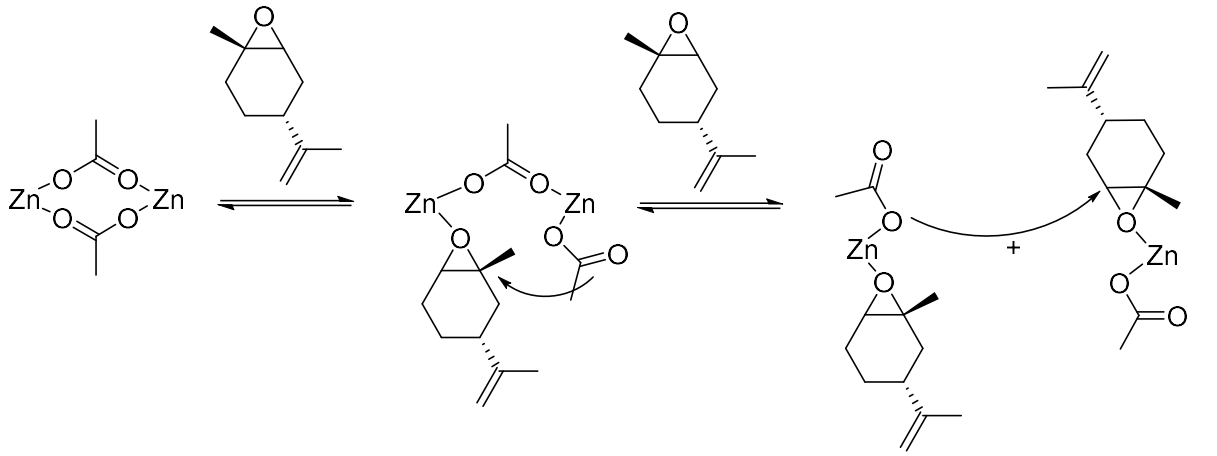

The bridged zinc catalyst coordinates one LO molecule, but due to the steric hindrance at the epoxide unit, the acetate initiating group is unable to achieve a nucleophilic attack on the epoxide. The authors rather suppose that it requires the coordination of a second LO molecule to facilitate a monometallic

arrangement which is more flexible towards the nucleophilic attack. The insertion of CO_2 regenerates the dimeric complex and a carbonate chain end is formed, which, upon coordination of a second LO, enables the alternating copolymerization.

3. Ring-Opening Polymerization of Lactones to Biodegradable Polyesters

Polyesters are globally produced on a 77 million ton scale mostly via polycondensation of a diacid and a diol.[54] Although lacking the broad range of easily accessible monomers, ring-opening polymerization (ROP) of cyclic esters evolved to a valuable method to gain access to aliphatic polyesters in high molecular weights and without the formation of small molecule byproducts. Within the class of novel polyesters, two polymers recently gained much attention, namely poly(3-hydroxybutyrate) (PHB) and poly(lactide). These two biodegradable thermoplastics can be synthesized via ring-opening of *rac*-β-butyrolactone (BBL) and *rac*-lactide (LA) with the reduction of the monomer's ring strain being the driving force of the reaction. PHB is naturally produced in its isotactic form by numerous bacteria and serves as an intercellular carbon and energy storage.[55] The fermentative synthesis gives a perfectly isotactic configuration of the chiral methyl groups, which is also the prerequisite for the desired degradation of PHB by depolymerases that selectively cleave *R*,*R*-linkages at the polymer backbone. The biotechnological production of PHB requires multiple synthesis and processing steps and thus, PHB continues to be a very expensive material.[56-58]

Comparing PHB and isotactic poly(propylene) (i-PP) in terms of mechanical properties reveals remarkable characteristics (Figure 11). A good performance regarding oxygen barrier and UV stability indicate the potential use of PHB as a packaging material. Moreover, its Young modulus, impact strength and temperature resistance seem to be comparable with other commodity polymers such as i-PP. On the downside, perfectly isotactic PHB is highly crystalline and therefore behaves as a rather brittle material with a low strain elongation. Also, the very high melting temperature of 180 °C is close to the decomposition temperature of PHB and impedes the processing via melt extrusion. As a result, the synthesis of PHB via stereoselective ring-opening polymerization of BBL is very promising to produce PHB in the desired microstructure. It is expected that isotactic-enriched PHB with a lowered crystallinity of the polymer results in a reduced melting temperature which would enable enhanced mechanical properties and a successful processing of the polymer.[15]

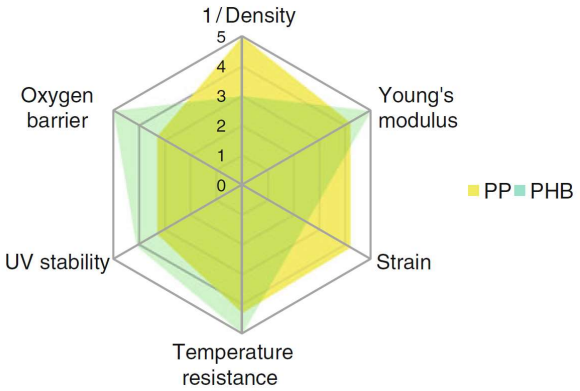

Figure 11. Qualitative comparison of the most relevant properties of naturally occurring *(R)*-PHB and i-PP.[15]

β-lactones such as BBL undergo the ring-opening step either via acyl-O cleavage or via alkyl-O cleavage leading to an alkoxy and a carboxy chain end, respectively. These two different modes are particularly important for the stereospecific polymerization of BBL since the acyl-O cleavage proceeds via retention of the methyl configuration whereas the alkyl-O cleavage involves an inversion of the stereocenter. Three different microstructures for PHB are depicted in Scheme 4. In the atactic form, the methyl groups are randomly oriented, while the orientation of the methyl groups in the isotactic (pointing in the same direction) and the syndiotactic (alternating orientation) microstructure allows enhanced polymer properties such as crystallinity along with a high melting point.

Scheme 4. Left: Ring-opening step of BBL via (a) acyl-O cleavage or (b) alkyl-O cleavage. Right: Possible microstructures of poly(3-hydroxybutyrate)[59]

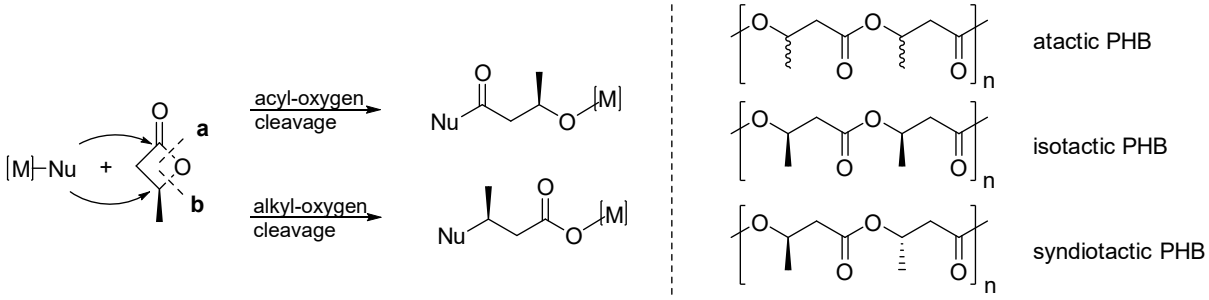

The polyesters PHB and PLA have the potential to become particularly attractive if their monomers are obtained independent from fossil fuels. Industrially relevant routes offer the possibility to produce BBL from CO_2 and render the PHB production sustainable (Scheme 5). In a first step, the catalytic hydrogenative conversion of carbon dioxide yields methanol, which, in turn, is converted to propylene via the methanol-to-propylene (MTP) process.[60-62] Then, the oxidation of propylene can be achieved with the hydrogen peroxide to propylene oxide technology with H_2O_2 serving as a clean oxidant.[63-64] In the last step, propylene oxide is successfully carbonylated to BBL by discrete complexes, e.g. [Lewis acid][$Co(CO)_4$].[15,65-66] The other lactone, lactide, was isolated for the first time, by Carl Wilhelm Scheele in 1780 from sour milk, but it took a few centuries until Pasteur identified lactic acid as a fermentation metabolite and no longer as a milk component. Nowadays, starch and corn are used as potential starting substrates to synthesize *L*-(+)-lactic acid by microbial fermentation which gives access to polylactide in a microstructure with high crystallinity and a high melting point.[67-69]

Scheme 5. Synthesis of BBL starting from CO_2 (a) and preparation of LA from corn feedstock (b)

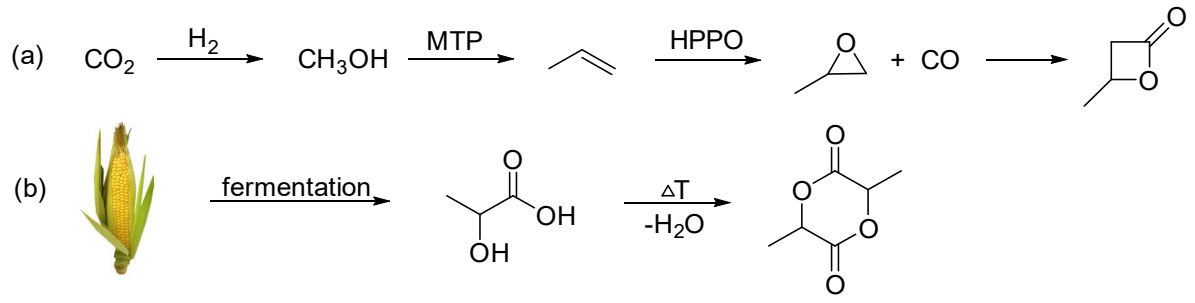

The coordinative ring-opening polymerization of lactones was first reported in the 1970s for ε-caprolactone (CL), but only a few years later, also the four-membered ring BBL was successfully polymerized with aluminum porphyrines.[70-72] Although low activities (quantitative conversion within 15 days) were observed, the living character of the polymerization was demonstrated as well as a narrow dispersity (polydispersity (*Đ)* = 1.11).[73] An important step towards a stereospecific polymerization of BBL was presented by Spassky and coworkers who used chiral initiators derived from simple metal alkyls ($ZnEt_2$, $AlEt_3$) and (*R*)-3,3-dimethylbutane-1,2-diol (Scheme 6).[74] The isotacticity is based on a kinetic resolution of the two enantiomers *(R)*-BBL and *(S)*-BBL with a ratio of 46% *ee* of the (*S*)-enantiomer at low conversions.

Scheme 6. Isospecific ROP of BBL via kinetic resolution

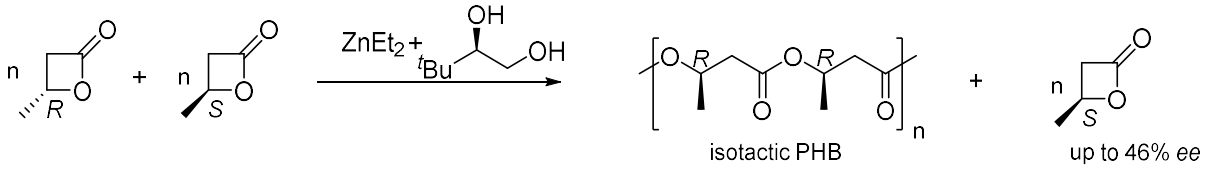

A breakthrough in the ROP of BBL was achieved by Coates *et al.* in 2002.[75] β-diiminate zinc alkoxides have previously been tested in the ROP of LA and the ROCOP of CHO and CO_2, and indeed showed also high activities for BBL. High conversions (65 – 97%) were observed for **5** within short reaction times (5 – 720 minutes) under mild conditions to polymers in adjustable molecular weights and narrow dispersities (*Đ* = 1.06 – 1.20, Figure 12). On the downside, the polymerization did not show any stereospecificity and the resulting PHB was atactic.

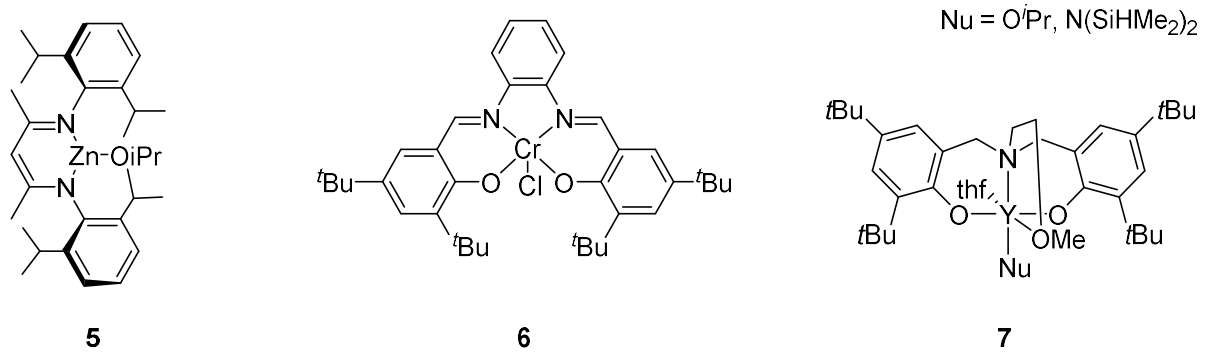

Figure 12. Selected catalysts for the ROP of BBL.

In the course of the discovery of BDI complexes, the coordination-insertion mechanism was confirmed via end-group analysis. Kinetic studies revealed a first-order dependence of both the monomer and the catalyst BDI-Zn-O^{i}Pr suggesting a monometallic active species during the polymerization. The following mechanism was postulated (Figure 13): A BBL molecule coordinates at the monometallic center. The activated monomer gets attacked by the alkoxide and undergoes an acyl-O cleavage which in turn regenerates the alkoxide chain end.[75]

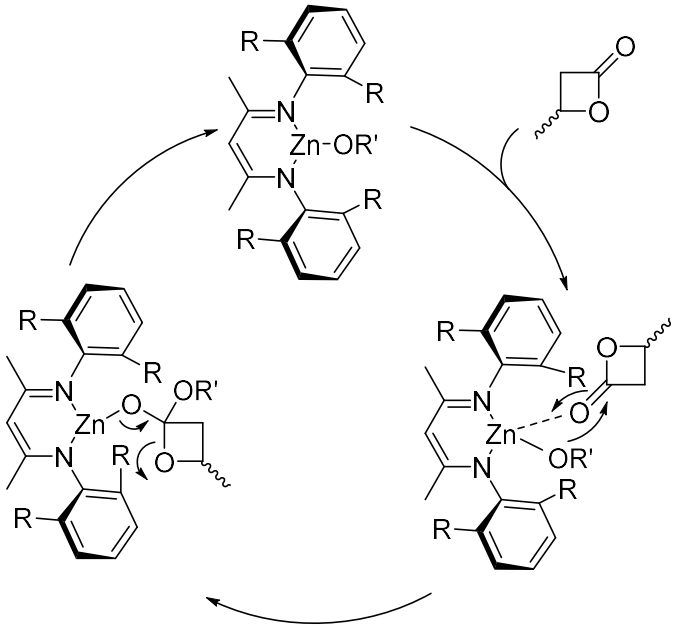

Figure 13. Proposed mechanism for the ROP of BBL with BDI-Zn-OR initiators.[75]

Focusing the original motivation of synthesizing isotactic PHB, Rieger *et al.* reported the achiral chromium salophen complex **6**.[76] Isotactic-enriched PHB ($P_m = 0.66$) was realized in high molecular weights but in relatively broad dispersities ($Đ = 5.2 – 9.6$). The degree of isotacticity seemed to be promising since perfectly isotactic PHB is very brittle and poorly processible and therefore a P_m of 0.6 – 0.8 is desired. Carpentier and coworkers tested aminoalkoxy-*bis*(phenolate) yttrium complexes **7** in the polymerization of methyl methacrylate (MMA) but found out that this ligand structure at yttrium exhibits very high activities in the ROP of BBL as well.[77] Syndiotactic PHB ($P_r = 0.81 – 0.94$) was obtained in high yields, predictable molecular weights (23 – 49 kg/mol) and narrow dispersities ($Đ = 1.03 – 1.18$).[78] The structural motif of **7** was thoroughly investigated in the following years in terms of ligand design, variation of the initiating group as well as the metal center, but no isotactic PHB could be isolated.[79-84] Nevertheless, these aminoalkoxy-*bis*(phenolate) complexes were interesting candidates for the so called immortal polymerization. In a living polymerization, protic impurities such as water or alcohols are prone to quench the propagation. In contrast, immortal polymerizations are resistant towards these impurities since the initiating group of the complex is rapidly exchanged with a chain-transfer agent, e.g. 2-propanol, whose concentration is higher than that of the catalyst molecules. Key advantage is the generation of polymers in tunable molecular weights as well as in very narrow dispersities.[58,85] Very recently, Cui *et al.* reported rare earth metal salan complexes which showed a switching tacticity in the ROP of BBL by altering the substituents at the nitrogen from aromatic to aliphatic groups (giving an isotactic and syndiotactic arrangement, respectively).[86] Another promising approach was presented by Chen and coworkers. Yttrium complexes bearing salcy ligands promote the stereoselective polymerization of a racemic mixture of the eight-membered cyclic diolide to a polymer with the same chemical structure as PHB. A tuning of the diastereomeric ratio enables a tuning ductility and toughness of the material.[87]

4. Rare Earth Metal-Mediated Group Transfer Polymerization of Nitrogen-Coordinating Monomers

In the 1980s, Webster and coworkers observed a controlled living polymerization of α,β-unsaturated esters, ketones and nitriles.[88-89] Silyl ketene acetals (SKA) thereby served as an initiator and a Lewis acid was added to activate the monomer. Initially, an associative pathway was assumed to take place, where the SKA group is transferred from the initiator to the monomer to form a new silyl group (Scheme 7). Due to this repeated conjugate addition, the term group transfer polymerization (GTP) has been established. Later studies revealed that a dissociative mechanism is present proceeding via a group transfer between the two chain ends. The ester-enolate anion thereby undergoes a poly-1,4-addition.[90-93]

Scheme 7. Associative and dissociative mechanism for the silyl ketene acetal initiators. R can be HF_2^-, F_2^{2-}, cyanide or azide[94]

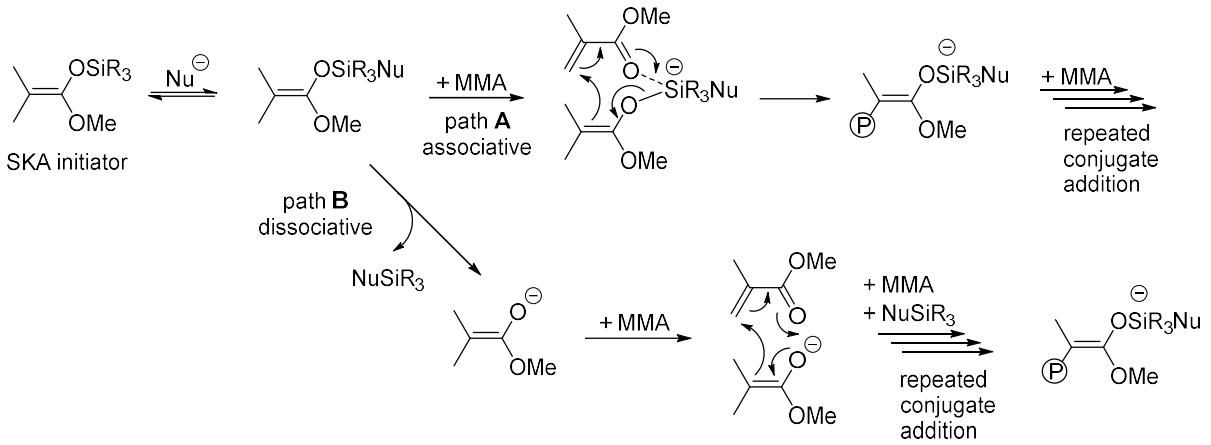

A few years later in 1992, two independent groups reported on metallocene systems catalyzing the living polymerization of acrylic monomers. Collins and Ward used neutral and cationic zirconocenes, Cp_2ZrMe_2 and $[Cp_2ZrMe(thf)][BPh_4]$, as a two-component system for the controlled polymerization of MMA.[95] Yasuda and coworkers developed a neutral samarocene $[(C_5Me_5)_2SmH]_2$ that showed high activity in the polymerization of MMA in a broad temperature range from -95 °C to 40 °C.[96] The resulting high molecular weight polymer showed a narrow dispersity ($Đ$ = 1.05) and high syndiotacticity (>95%). These observations already indicated a controlled manner of polymerization. Based on the crystal structure of a $Cp_2Sm(MMA)_2H$ adduct, a propagation via an ester enolate became evident and a monometallic anionic coordination mechanism was postulated (Scheme 8). The hydrido bridged dimer is opened after the coordination of MMA and an enolate formation takes place by a 1,4-addition of the H ligand to MMA. The second incoming MMA molecule also undergoes a 1,4-addition creating an eight-membered cyclic intermediate. Another MMA molecule cleaves off the coordinated ester group and thereby regenerates the eight-membered transition state.

Scheme 8. Polymerization of MMA via the Yasuda-type mechanism[96]

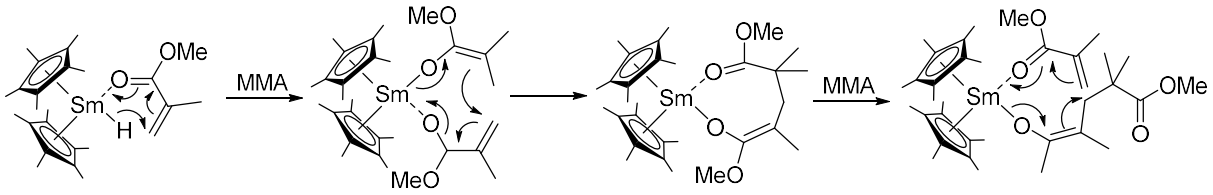

Based on this breakthrough in polymerizing acrylic monomers, rare earth metal-mediated (REM) GTP evolved into a valuable method combining both the living anionic and the coordinative polymerization. Also, the synthesis of block copolymers or the introduction of chain-end functionalities became feasible due to its living character.

In the course of the years, a wide range of possible vinylic monomers turned out to be interesting candidates for the REM-GTP (Figure 14). The nitrogen-coordinating monomers 2-vinylpyridine (2VP) and 2-isopropenyl-2-oxazoline (IPOx) form a weaker coordination to the metal center than the oxygen-coordinating monomers methyl acrylate (MA), MMA and dialkyl vinylphosphonates (DAVP). When synthesizing block copolymers, the coordination strength plays a major role: Monomers can only be polymerized in the order of increasing coordination strength.[97-98]

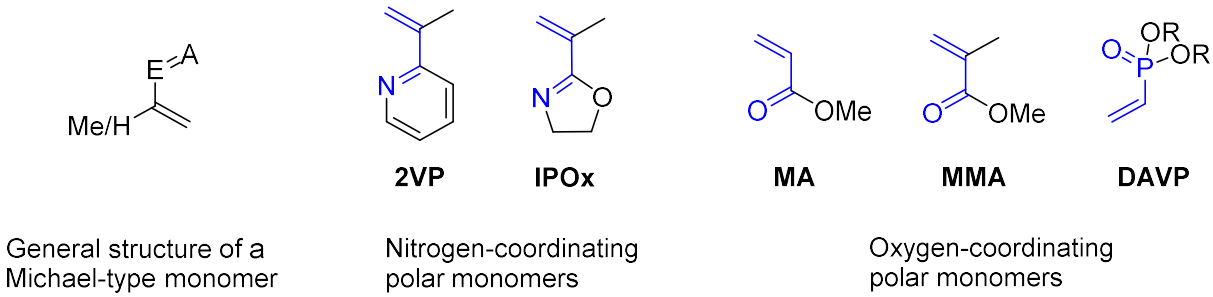

Figure 14. Scope of the most important monomers used in the REM-GTP (Michael-system highlighted).[94]

Diethyl vinylphosphonates (DEVP) belong to the group of strongly coordinating DAVPs. The polymer poly-DEVP (PDEVP) is not accessible via conventional radical or classic anionic polymerization methods. Nevertheless, its high biocompatibility combined with a decent water solubility makes it a very interesting material.[94,99] Simple metallocenes like *bis*(cyclopentadienyl)ytterbium chloride were the first catalysts for a controlled polymerization of DEVP.[100]

It was not until 2003, that Carpentier *et al.* proposed a structurally different catalyst system for REM-GTP based on a bulky amino-methoxy *bis*(phenolate) (Figure 15).[77] X-ray structures revealed an octahedral geometry of the [*ONOO*]-ligand core including the coordination of the methoxy side arm and the remaining thf molecule. The complex displayed poor activity in the polymerization of MMA, but in contrast, quantitative conversion was observed for ε-caprolactone within one minute.

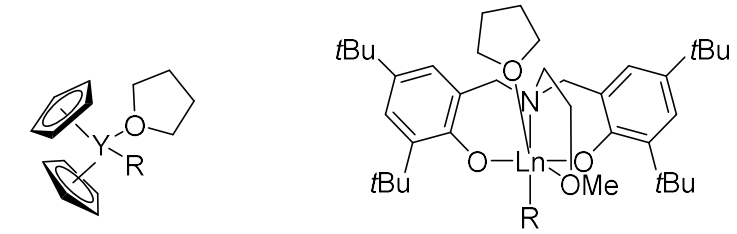

Figure 15. Illustration of the two most important catalyst structures in the REM-GTP.[101]

Generally, metallocene based catalysts have not been relevant in the stereospecific polymerization except in the case of MMA and their activities in the polymerization of 2VP and IPOx were insufficient. Hence, the structural motif of *bis*(phenolate)lanthanides became interesting and was investigated closer in the following years. Rieger *et al.* used this catalyst structure (Ln = yttrium; initiating group R = CH_2SiMe_3) and screened multiple vinylic monomers: 2VP (TOF = 1,100 h^{-1}), diethyl vinylphosphonate (480 h^{-1}), and 2-isopropenyl-2-oxazoline (1,500 h^{-1}) were polymerized in high activities to polymers in narrow dispersities ($Đ$ = 1.01 – 1.69) and molecular weights in a very controlled manner (initiator efficiency = 0.36 – 0.99). In situ attenuated total reflection IR spectroscopy revealed a living monometallic GTP according to the Yasuda-type mechanism. Attempts were undertaken to improve the stereospecificity of the polymerization of 2VP to realize highly isotactic poly-2VP (P2VP) (P_m = 0.54 – 0.97), e.g. by increasing the steric demand of one of the phenolate moieties.[102-104]

Initiator efficiency plays a crucial role in controlling the molecular weight of a catalytic living-type polymerization. The higher the initiator efficiency is, the closer the molecular weight gets to the theoretical calculated value. Yttrium complexes bearing alkyl initiators do not show satisfying initiator efficiencies for some Michael-type monomers especially in case of DEVP.[105] It was assumed that introducing a different type of initiating group would change the initiator efficiency of the yttrium metallocene. Watson *et al.* came up with the concept of CH-activation in 1983.[106] $Cp_2Ln\text{-}CH_3$ readily undergoes a [2σ-2σ]-cycloaddition with ^{13}C labeled methane to $Cp_2Ln\text{-}^{13}CH_3$. The principle of the CH-bond activation was continued by different groups and later applied in the REM-GTP. It basically offers two main advantages: First, the initiator efficiency can be improved by replacing alkyl initiators through heteroaromatic compounds such as 2,4,6-trimethylpyridine (Scheme 9). Secondly, thanks to the living-type mechanism and the fact that the initiating group represents one chain end of the polymer, introducing end-group functionality becomes accessible.[107-109]

Scheme 9. CH-bond activation of 2,4,6-trimethylpyridine with $Cp_2Y(CH_2TMS)(thf)$ and initiation of DEVP via eight-membered transition state[105,110]

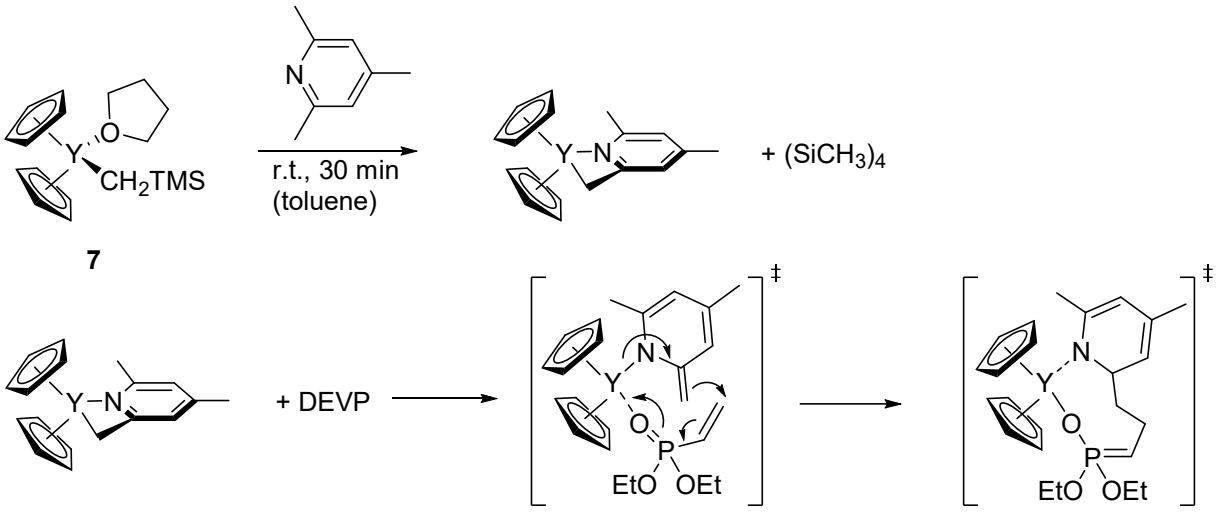

As part of the discovery of the CH-bond activation in REM-GTP, also the mechanism of the DEVP polymerization with unbridged rare earth metal metallocenes was unveiled. Generally, initiation via three different pathways is possible. It can either start via the deprotonation of the acidic α-proton through alkyl initiators, via a nucleophilic transfer of the initiating ligand to the pre-coordinated monomer or via a monomer-induced ligand-exchange reaction. Electrospray ionization mass spectrometry analysis indicated an end-group functionalization of oligomeric DEVP with (4,6-dimethylpyridin-2-yl)methyl. Combined with the dimeric crystal structure of $Cp_2Y(CH_2(C_5H_2Me_2N))$ showing a partial double bond character of the activated methyl group that enables an eight-membered transition state, the route of the nucleophilic transfer is most likely taking place.[105,110]

The other vinylic monomer 2VP was polymerized radically in the early years and atactic P2VP was obtained. In the 1960s, Natta *et al.* used magnesium, beryllium and aluminum amides and could produce isotactic P2VP.[111] But again REM-GTP turned out to be the most valuable method for synthesizing P2VP with tailored molecular weight and tacticity. Besides this, also its ability to catalyze copolymerizations with other polar vinyl monomers enabled P2VP to serve as an interesting material in different applications areas ranging from electrochemistry and medicine, especially drug delivery, but also to nano- and membrane technology.[112-115] The topic of micelles, in particular, and its extension to nanoparticles was intensively studied in the following years. Thereby, P2VP was copolymerized with different copolymer partners such as poly(ethylene oxide) or PDEVP. The latter offered the big advantage of being water-soluble and thus, the resulting P2VP-co-PDEVP polymers self-assembled to form micelles that showed pH sensitivity and a tunable lower critical solution temperature.[116-118]

5. Chemoselective Polymerizations from a Mixed-Monomer Feedstock

Synthesizing block copolymers from monomers that are not accessible via the same polymerization mechanism requires the combination of two or more distinct polymerization types. It is driven by the motivation of creating enhanced chemical complexity for special applications. Thereby, a controlled chain growth is the major prerequisite to interchange between different catalytic cycles. In literature, various types of switches are reported. An electrochemical switch was found for copper catalysts in the atom transfer radical polymerization by controlling the oxidation state. Multistep intermittent potentials switch the polymerization from a dormant to an active state.[119] The controlled radical polymerization of methyl acrylates could also be activated and deactivated via an external visible light stimulation.[120] In the ROP of lactones, interesting attempts regarding the on/off-switch of polymerizations were made, too. Group 4 metal alkoxides supported by ferrocene-based ligands could be switched between their oxidized and reduced form and thereby activated or deactivated towards the ROP of ε-CL and LA.[121] The organo-catalyzed polymerization of ε-CL and trimethylene carbonate was reversibly toggled via the absence/presence of CO_2.[122] Another approach is kinetic control based on the reactivity of the initiator towards the monomer. Coates studied the chemoselectivity of BDI complexes in the terpolymerization of epoxides, cyclic anhydrides, and CO_2. Putting all monomers together in the beginning, he observed a selective building of the polyester block before the polycarbonate was built.[123] Figure 16 gives an overview of the possible pathways based on kinetic control.

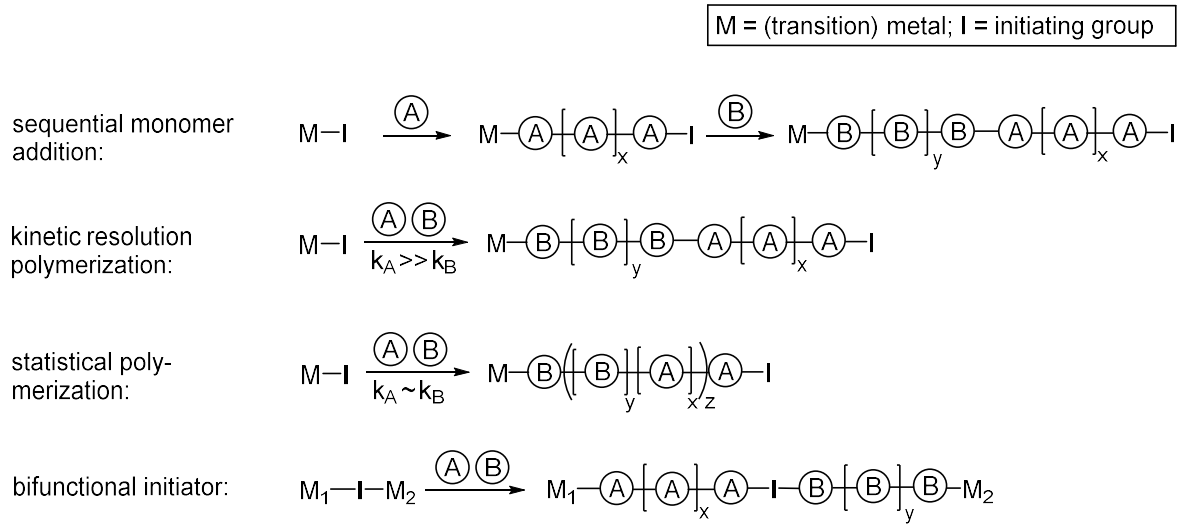

Figure 16. Illustration of the possible types of pathways for copolymerization reactions.[123]

Sequential monomer addition gives a pure diblock copolymer if the second monomer B is added after full conversion of A. One-pot polymerizations highly depend on the nature of the monomer in terms of reactivity with complex M-I. In case the rate of monomer A (k_A) is considerably higher than k_B, also diblock structures are built. The situation changes if $k_A \sim k_B$ because a statistical or gradient-like reactivity

results. To gain a different architecture control and a more diverse combination of monomers, bifunctional initiators are employed. They are able to independently incorporate monomers at each metal center and the produced blocks are interconnected via the linker I.

5.1 Terpolymerization of Two Different Epoxides and CO_2

Propylene oxide and cyclohexene oxide clearly represent the two most important epoxides used in the copolymerization of epoxides and CO_2. A multitude of metal complexes is able to catalyze the coupling of CO_2 and both epoxides individually. Since the respective copolymers display very contrary properties mainly based on their difference in the glass transition of 30 – 45 °C for PPC and 115 °C for PCHC, attempts were made to perform terpolymerizations of both epoxides and CO_2.[13,19] Zinc(II) phenoxides were one of the first complexes tested in this terpolymerization reaction. It requires a high CO_2 pressure (80 bar) and an elongated reaction time of 69 h, but remarkably, the formation of cyclic propylene carbonate is suppressed in presence of CHO (Figure 17).[124] Later, different catalysts like a salen-type cobalt(III) **9** or a chiral tetradentate Schiff-base cobalt(III) complex was employed and higher activities, tunable glass transitions and an isotactic-enriched PCHC part were observed.[21,125] Sometime later, the groups of Rieger and Kleij independently studied the terpolymerization of limonene oxide, CO_2, and either PO or CHO.[50,126] PCHC/PLC terpolymers were catalyzed by an Al(III) amino(triphenolate) combined with PPNCl as cocatalyst and the tunable amount of double bonds from PLC was used to get cross-linked polymeric networks via thiol-ene click chemistry.

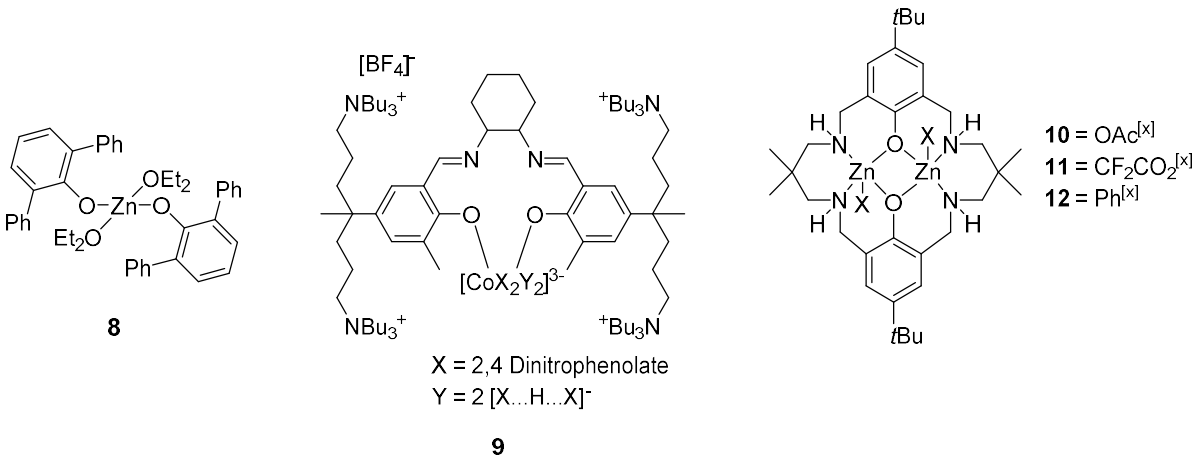

Figure 17. 8 and **9** are active initiators for the terpolymerization of CHO, PO, and CO_2. Dizinc complexes **10**-**12** can be employed in the ROCOP of epoxides and anhydrides.

5.2 Terpolymerization of Epoxides and CO_2 with Cyclic Anhydrides and Lactones

Epoxides also display an attractive feedstock for the synthesis of aliphatic polyesters by coupling them with anhydrides (Scheme 10). Commercial polyesters are usually produced via condensation polymerization. In contrast, synthesizing them via chain-growth polymerization with a suitable metal catalyst allows a tailoring of the incorporated monomers, the molecular weights as well as the resulting thermal properties.[127-129]

Scheme 10. Alternating copolymerization of epoxides and cyclic anhydrides

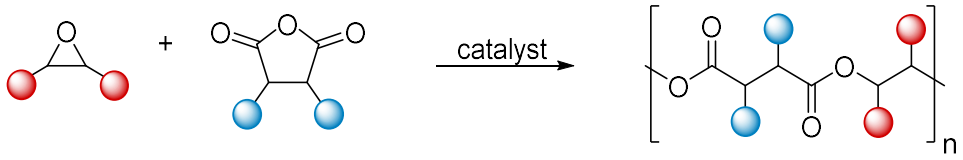

Although the ring-opening copolymerization of epoxides and CO_2 and the ring-opening polymerization of lactones bear mechanistic similarities, only a few catalysts can catalyze both polymerization types. Generally, the mechanisms can either be combined via catalysis at the same metal center or via successful chain transfer from one to another initiator. Rieger and coworkers developed a flexibly linked dimeric chromium salphen complex that was active for the ROP of BBL and the ROCOP of PO and CO_2. The dimerization of the complex results in an enhancement in activity compared to the mononuclear analogous which supports the theory of a bimetallic catalysis of the respective polymerizations in case of Cr salophen catalysts.[130] Due to the different reaction temperature that is required for the two polymerization types, a combination of both was not investigated further. Lu and Darensbourg followed the approach of a salen Co(III) catalyzed styrene oxide/CO_2 coupling to a OH-terminated polymer that served as a macroinitiator for the DBU promoted ROP of lactide.[131-132] The heterogeneous ZnGA was also found to be active in the PO/CO_2/lactone terpolymerization.[133-134] Williams *et al.* introduced a versatile group of dinuclear macrocyclic zinc complexes **10**-**12** that successfully polymerized epoxides with anhydrides and CO_2, respectively, and lactones to multiblock copolymer structures. The dizinc complex **10** was first tested towards its activity in the ROP of ε-caprolactone and the ROCOP of CHO and CO_2. **10** was only able to polymerize ε-CL in presence of CHO which inserts into the M-X bond creating an active zinc-alkoxide species.[135-136] In the following studies, this zinc-alkoxide intermediate served as an active initiator for the ROCOP of epoxides and anhydrides, the ROP of a lactone and the ROCOP of the residual epoxides with added carbon dioxide (Figure 18).[137-138] Such a polymerization pathway involves a double switch in mechanism and enabled the synthesis of polymers with tailored functionalities. The incorporation of the monomers is determined by the respective reaction rates and could only be successfully performed when adding CO_2 in the end; otherwise the ROP of ε-CL is inhibited by coordinated CO_2.

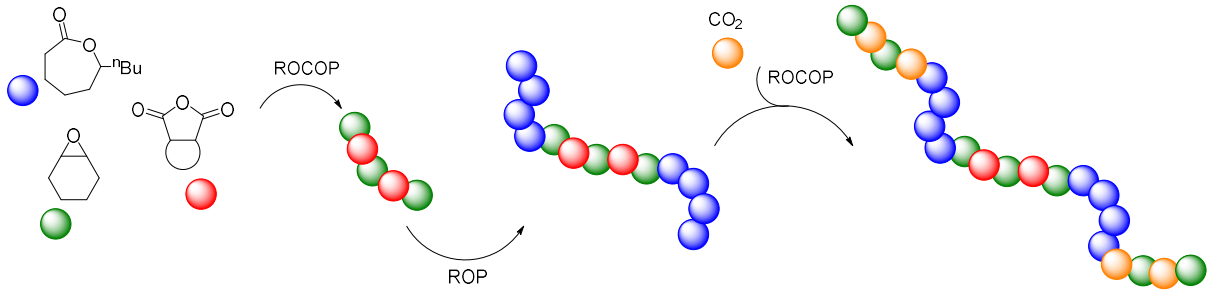

Figure 18. Combination of ring-opening copolymerization and ring-opening polymerization to pentablock copolymers.[138]

A further strategy was driven by the motivation of introducing elasticity into semiaromatic polyesters to generate thermoplastic elastomers. The three-step synthesis involved the initial ROCOP of CHO and phthalic anhydride, followed by the ROP of ε-decalactone and a subsequent diisocyanate coupling of the telechelic polymer to increase the molecular weight. The material showed high elasticity of up to 2450% in a wide temperature range (-20 – 100 °C). The elasticity was maintained over 25 cycles.[139]

5.3 Active Systems for Ring-Opening Polymerization and Group Transfer Polymerization

The combination of ring-opening polymerization and group transfer polymerization is only scarcely described in literature. Two very early examples deal with the polymerization of MMA and ε-CL or δ-valerolactone by organoaluminum catalysts[140] or organolanthanide(III) metallocenes[141-142]. The latter seemed to be more promising regarding polydispersity. The copolymerization of MMA and the lactone worked smoothly when MMA was polymerized first, and the lactone added afterwards. The very strong coordination of the lactone did not allow a subsequent incorporation of MMA. Rieger and coworkers used amino *bis*(phenolate)yttrium catalysts in the REM-GTP for a multitude of different polar vinyl monomers but, interestingly, also in the stereoselective ROP of BBL.[82] The combination of both mechanisms was investigated, but no copolymer formation could be realized. The idea was that a coordinated P2VP chain end serves as macroinitiator for the ring-opening step of the lactone. Indeed, conversion of the lactone was observed but two blocks could be easily separated via precipitation indicating no copolymer formation. A lot of follow-up reactions were performed to elucidate the reason and a deprotonation of the BBL followed by an anionic ROP or chain scission was proposed. In 2018, Wang and coworkers developed a one-step approach for CO_2-based block copolymers derived from epoxides, CO_2, and vinyl monomers.[143] Aluminum porphyrins promote the coupling of CHO or PO with CO_2 and then, a trithiocarbonate compound serves as a bifunctional chain-transfer agent which enables the reversible addition-fragmentation chain transfer polymerization of vinyl monomers such as MMA or styrene. A precise control of the molecular weight and very narrow dispersities (1.09 – 1.14) were observed for the PPC-*co*-PMMA block copolymers. Overall, this method allows the broadening of the functionality of aliphatic polycarbonates by the introduction of PMMA or polystyrene blocks. In the same year, a bifunctional catalyst has been synthesized bearing a BDI zinc unit attached to an initiating

group that is active for RAFT. ROCOP of CHO and CO_2 gives the polycarbonate with an end-group where living RAFT of styrene and *N*-isopropylacrylamide enables copolymer formation. A thermoresponsive PCHC-co-poly(*N*-isopropylacrylamide) represents a promising example for CO_2-based functional nanomaterials.[144]

6. Aim of the Thesis

Aliphatic polycarbonates are known for more than five centuries but despite numerous promising properties such as high transparency, biodegradability (PPC) and UV stability, they do not fully meet the industrial demands, yet.[145] Various kinds of attempts have been made to overcome the two major limitations; the low glass transition temperature of poly(propylene carbonate) and the high brittleness of poly(cyclohexene carbonate). Blending polycarbonates with other materials, introducing soft units via chain-transfer agents or terpolymerizing with other monomers are possible strategies to upgrade adverse properties. The first part of this work mainly concentrates on extending the portfolio of PCHC-containing polymers by combining the ROCOP mechanism with other coordinative mechanisms.

ROCOP of epoxides and CO_2 has previously been coupled with the ROCOP of anhydrides and epoxides as a well as with the ROP of lactones such as ε-CL or ε-decalactone. Chemoselective polymerizations from a mixed-monomer feedstock allowed the synthesis of defined copolymers in a block structure. Complex **4** was reported for the coupling of CHO and CO_2 in 2017 and also similar BDI complexes have previously been tested in the ROP of BBL to atactic PHB.[50,75] Based on the low glass transition temperature of atactic PHB of 5 °C and the behavior as a rather soft material, the combination with the brittle PCHC might result in a better mechanical performance. In this work, one-pot polymerizations of the three monomers with **4** are investigated (Scheme 11). It is expected that the point of CO_2 addition regulates the incorporation of the different monomer types. This chemoselective control would enable the tailoring of different architectures, particularly a block and a statistical arrangement. After studying the possible terpolymerization mechanism, the terpolymers will be investigated toward their glass transition temperatures and their mechanical behavior. Moreover, different epoxides such as cyclopentene oxide and limonene oxide will be tested.

Scheme 11. Lewis acidic complex **4** and its application in the terpolymerization of CHO, CO_2, and BBL

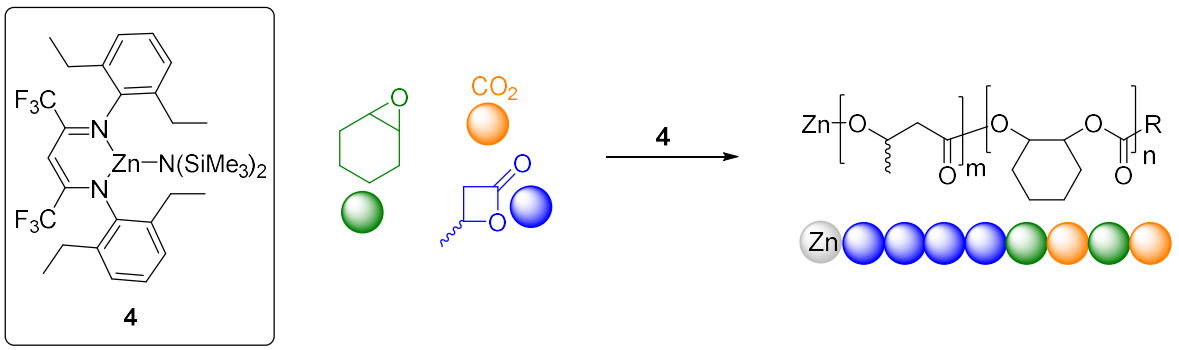

In a second approach, the combination of aliphatic polycarbonates with polar polyolefins is examined. The rare earth metal-mediated group transfer polymerization of polar vinyl monomers is a valuable method for the precise synthesis of functional materials. The polymers exhibit interesting properties such as biocompatibility and water-solubility and can show switchable properties when two different types of monomers are copolymerized. Since BDI complexes are not known to catalyze the GTP, a

bridged bifunctional catalyst is required. We aim for a complex that combines a zinc center which is active in the ROCOP of epoxides and CO_2 and an yttrium moiety that promotes the polymerization of Michael-type monomers (Scheme 12). Bridging the two centers would enable the synthesis of copolymers with the two different types of blocks connected to each other via the linking unit. This approach would result in copolymers that have not been achieved so far with unexplored properties.

Scheme 12. Combining the CHO/CO_2 coupling with the polymerization of Michael-type monomers requires the synthesis of a bifunctional catalyst

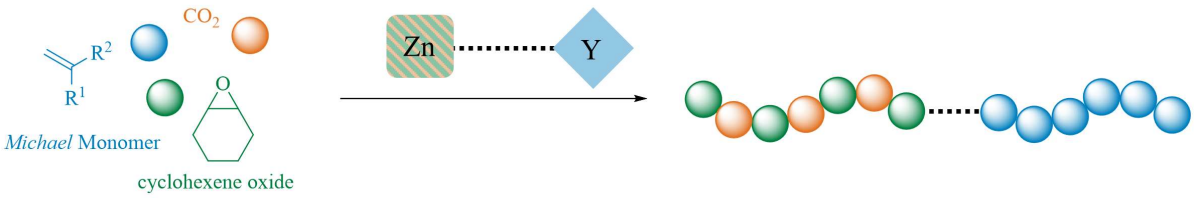

In the second part of the thesis, the established polymerizations of cyclohexene oxide with CO_2 and limonene oxide with CO_2 were put to the test regarding the upscaling of the polymerization, a thorough investigation of so far unexplored properties and the terpolymerization of the two epoxides and CO_2 was performed. The Lewis acidic zinc complex BDI^{CF3}-Zn-N(SiMe$_3$)$_2$ shows high activities in the ROCOP of various epoxides and CO_2 and is therefore best suited for the synthesis of PCHC and PLC. After a detailed screening of the reaction parameters in a 50 mL autoclave equipped with in situ IR spectroscopy to monitor the progress of the polymerization, it is planned to transfer the synthesis to a 1 L Büchi autoclave (Figure 19). It is expected to gain valuable insight into the kinetic of the reaction as well as into the purification of the resulting material. An aqueous solution of ethylenediaminetetraacetic acid is used in literature to mask the residual Zn(II) and to make the precipitation step more efficient.[14]

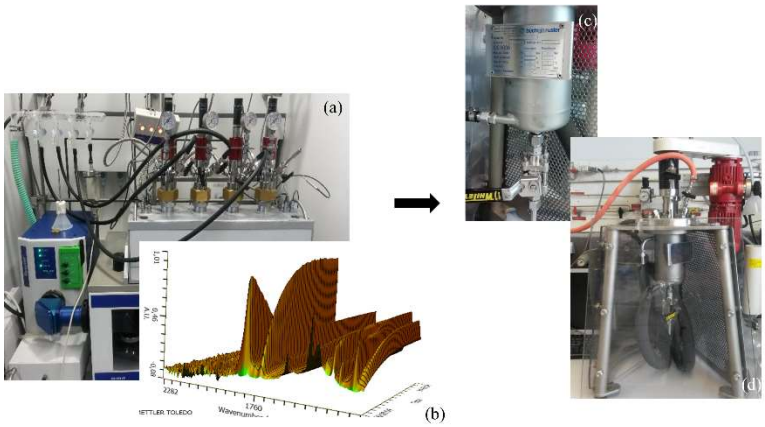

Figure 19. System for high-pressure polymerization with in situ IR monitoring in 50 mL autoclaves (a). Three-dimensional plot of wavenumber [cm^{-1}], time [min] and relative intensity [A.U.] (b). Planned upscaling of the polymerization to a 1 L Büchi reactor (c) with mechanical stirring and a heating device (d).

Data for the thermal stability of polymers is often based on thermogravimetric analysis. But with the help of this method only the converting of the polymer into volatile compounds is analyzed and no

previously occurring chain breaks get detected. Heating polymer samples to certain temperatures and analyzing them by gel-permeation chromatography would provide valuable information for designing a processing window for PCHC and PLC. Moreover, the evaluation of the mechanical properties of aliphatic polycarbonates is of special interest. After finding a suitable method for the preparation of polymer specimens, the measurement, interpretation and classification of the data is of high priority. This understanding would allow a comparison of the polymer's properties with other well-established materials such as BPA-PC and PMMA.

Scheme 13. Planned terpolymerization of CHO, LO, and CO_2

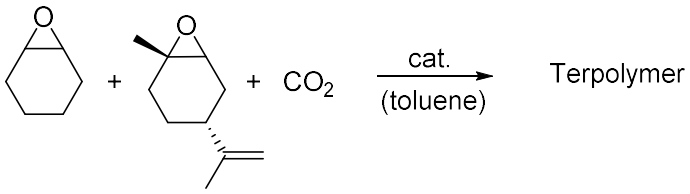

Furthermore, complex **4** is tested towards its ability to perform the terpolymerization of CHO, LO, and CO_2 for the first time (Scheme 13). Due to the very different reaction rates, it is expected that PCHC formation is predominant in the beginning of the reaction and PLC is formed after CHO is consumed. In situ IR spectroscopy and high-pressure NMR spectroscopy will provide important data on the kinetic of the terpolymerization. Besides, the combination of the two blocks might result in an enhanced performance of the material.

7. CO_2-Controlled One-Pot Synthesis of AB, ABA Block, and Statistical Terpolymers from β-Butyrolactone, Epoxides, and CO_2

Title: "CO_2-Controlled One-Pot Synthesis of AB, ABA Block, and Statistical Terpolymers from β-Butyrolactone, Epoxides, and CO_2"

Status: Communication, published online May 15, 2017

Journal: Journal of the American Chemical Society, 2017, 139, 6787-6790

Publisher: American Chemical Society

DOI: 10.1021/jacs.7b01295

Authors: Sebastian Kernbichl,[‡] Marina Reiter,[‡] Friederike Adams, Sergei Vagin, Bernhard Rieger[a]

Content

A Lewis acidic zinc complex BDI^{CF3}-Zn-$(SiMe_3)_2$ turned out to catalyze both the ring-opening polymerization of β-butyrolactone and the ring-opening copolymerization of epoxides and CO_2. Different reaction pathways were developed but all started with a one-pot situation of catalyst, epoxide, and BBL in the beginning. A high CO_2-pressure of 40 bar fully impeded the ROP of BBL and the ROCOP of CHO and CO_2 exclusively proceeded with high activity. Once the CO_2 was released, the conversion of BBL started, creating AB block copolymers. The opposite route also worked with the ROP of the lactone in the beginning and the ROCOP starting when carbon dioxide is applied (BA block). An interesting third pathway was developed once the carbon dioxide pressure was lowered to 3 bar CO_2. At this pressure, both mechanisms run with similar speed creating a statistical incorporation of the monomers. This difference in the polymer's architecture had a decisive influence on the properties of the novel poly(ester-carbonates). While the polymers in block structure showed two separated glass transitions, the ones in the statistical arrangement revealed a mixed T_g. A mechanism for this statistical terpolymerization was postulated based on polarimetry and two-dimensional NMR spectroscopy. It was shown that the ring-opening of the BBL molecule proceeds via acyl-oxygen cleavage. Additionally, HMBC-NMR indicated a coupling of the backbone proton of PCHC with the vicinal carbonyl C atom of the ester unit. Putting this together, a zinc-alkoxide intermediate either incorporates BBL or CO_2 and the zinc-carbonate can only react with a CHO molecule. The three established reaction pathways were transferred to cyclopentene oxide as epoxide demonstrating the versatility of this approach.

[‡]These authors contributed equally; [a]S. Kernbichl executed all the experiments and gave advice on the manuscript. M. Reiter had the initial idea and wrote the manuscript. F. Adams gave advice on the ring-opening polymerization of BBL. S. Vagin contributed with fruitful mechanistic discussions. All work was carried out under the supervision of B. Rieger.

JACS
JOURNAL OF THE AMERICAN CHEMICAL SOCIETY
Communication
pubs.acs.org/JACS

CO_2-Controlled One-Pot Synthesis of AB, ABA Block, and Statistical Terpolymers from β-Butyrolactone, Epoxides, and CO_2

Sebastian Kernbichl,[‡] Marina Reiter,[‡] Friederike Adams, Sergei Vagin, and Bernhard Rieger*

WACKER-Lehrstuhl für Makromolekulare Chemie, Zentralinstitut für Katalyseforschung (CRC), Technische Universität München, Lichtenbergstraße 4, 85747 Garching, Germany

Supporting Information

ABSTRACT: Terpolymerizations of (*rac*)-β-butyrolactone (BBL), cyclohexene oxide (CHO), and carbon dioxide were realized in one-pot reactions utilizing a Lewis acid BDI^{CF3}-Zn-$N(SiMe_3)_2$ (**1**) catalyst. The type of polymerization can be regulated and switched between ring-opening polymerization (ROP) of BBL and CHO/CO_2 copolymerization by the presence of CO_2 in the reaction mixture. Applying 3 bar CO_2 to the three-component system leads to similar reaction rates for copolymerization and ROP and therefore to a terpolymer with a statistical composition, whereas 40 bar CO_2 affords exclusive copolymerization of CHO/CO_2. Two-dimensional NMR spectroscopy and polarimetry provided a deeper understanding of the underlying mechanism. Furthermore, copolymerization of cyclopentene oxide (CPO) and CO_2 was performed, resulting in the highest reported TOF of 3200 h^{-1} together with 99% polycarbonate selectivity. Terpolymerizations of CPO/CO_2 and BBL were successfully conducted using the established reaction pathways.

Polycarbonates, derived from epoxides and CO_2, and poly(hydroxybutyrate) (PHB), are promising examples of thermoplastic polymers that can be synthesized independent of petroleum resources.[1] Both polymerization reactions are efficiently catalyzed by discrete, homogeneous, and metal-based complexes;[1b,2] however, there are only a few examples of catalysts that are able to perform both reactions.[2a,3] Despite the high internal strain of the four-membered butyrolactone ring, BBL seems to be a rather reluctant monomer, as it is less reactive than lactide (LA) or ε-caprolactone (ε-CL).[1b,4] Natural PHB is commonly strictly (*R*)-isotactic and is a highly crystalline thermoplastic material.[1a] Through metal-catalyzed ROP of BBL, syndiotactic, atactic, or slightly isotactic enriched PHB can be obtained, depending on the nature of the employed catalyst.[2a,b,5,6] A key challenge in polymer chemistry is the realization of polymerizations from a mixed monomer feedstock and the chemoselective control of the incorporation of the monomers to regulate the polymer structure and consequently the thermal and mechanical properties, as demonstrated by recent reports.[7] Until now, terpolymerizations of ε-CL (or lactide), CHO, and CO_2 were realized, leading to oligomers/polymers with molecular weights in the range 0.9–42 kg/mol.[7] Regarding the copolymerization of CHO and CO_2, a variety of catalysts exist,[3b,8,9] but nontoxic zinc catalysts combine high activities with high poly(cyclohexene carbonate) (PCHC) selectivity.[8c,9] Conversely, poly(cyclopentene carbonate) (PCPC) formation has been only sparsely explored and the employed complexes show TOFs between 3 and 650 h^{-1}.[10] We recently reported a Lewis acid BDI^{CF3}-Zn-$N(SiMe_3)_2$ complex (**1**), which can copolymerize various epoxides with CO_2.[9a] Herein, we investigate the activity of complex **1** toward ROP of BBL, copolymerization of cyclopentene oxide (CPO) with CO_2, and terpolymerization of CHO/CO_2/BBL or CPO/CO_2/BBL via different reaction pathways (Figure 1).

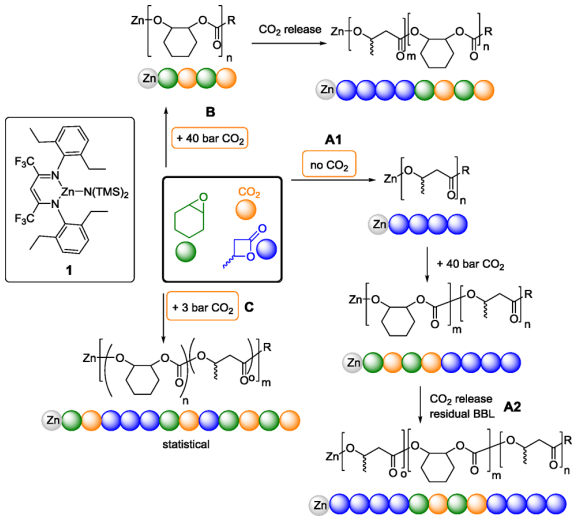

Figure 1. Copolymerization of CHO/CO_2, ROP of BBL, and chemoselective terpolymerization of CHO/BBL/CO_2 by CO_2 switching (40 vs 3 bar).

For the first time, BDI^{CF3}-Zn-$N(SiMe_3)_2$, catalyst 1, was tested with respect to its activity toward PHB formation in an autoclave with *in situ* IR monitoring (Table S1, entry S1, Figure S2). Within 4 h, 91% atactic PHB was obtained with 145 kg/mol molecular weight and a PDI of 1.6. We polymerized enantiomerically enriched *R*-BBL (ee > 95%) to determine the mechanism for this catalyst (Table S1, entry S2). Polarimetry at 365 nm of the isotactic PHB resulted in an $[\alpha]^{25}_{365}$ of +7.9° (c = 0.023 g/mL), indicating the retention of configuration

Received: February 7, 2017
Published: May 15, 2017

DOI: 10.1021/jacs.7b01295
J. Am. Chem. Soc. 2017, 139, 6787–6790

Journal of the American Chemical Society Communication

Table 1. Terpolymerization of BBL, Epoxides, and CO_2 According to Different Reaction Pathways A, B, and C (Figure 1)[a,b]

entry	[epoxide]: [BBL]: [cat]	reaction pathway[b]	CO_2 [bar]	time [h][c]	conv. BBL [%][d]	conv. epoxide [%][d]	[PC]:[PHB][e] prior to prec.	[PC]:[PHB][f] after prec.	T_g [°C][g]	M_n (PDI) [kg/mol][h]
1	500 (CHO):500:1	A1	40	1.5	66	77	54:46	56:44	2/116	76 (1.3)
2	500 (CHO):500:1	A1+A2	40	4	96	92	49:51	56:44	2/114	146 (1.2)
3	500 (CHO):500:1	B	40	2	87	90	51:49	64:36	1/118	166 (1.2)
4	500 (CHO):500:1	C	3	2	97	86	45:55[i]	47:53	36	69 (1.6)
5	650 (CHO):350:1	C	3	0.1	56	81	73:27	76:24	91	34 (1.2)
6	500 (CPO):500:1	A1	40	6	95	84	47:53	48:52	4/88	92 (1.6)
7	500 (CPO):500:1	A1 + A2	40	7	75	82	52:48[i]	61:39	5/73	143 (1.7)
8	500 (CPO):500:1	B	40	6	93	85	48:52	55:45	8/68	45 (1.8)
9	500 (CPO):500:1	C	3	2	58	47	42:58	42:58	24	68 (1.4)

[a]Reaction conditions: CHO/BBL/CO_2, 60 °C; CPO/BBL/CO_2, 50 °C; 2.0 g toluene, 40 μmol catalyst **1**. [b]According to Figure 1. [c]Complete polymerization time followed by *in situ* ATR-IR. [d]Determined by ^{1}H NMR spectroscopy of a crude polymer sample. [e]Determined by ^{1}H NMR spectroscopy of a crude polymer sample. [f]Composition of terpolymer after precipitation in MeOH (homopolymeric PHB stays in solution). [g]Determined by DSC, heating rate: 5 K/min. [h]Measured via GPC in THF. [i]Entry 4, 8%; entry 5, 4%; entry 7, 2% cyclic carbonate was formed.

(natural origin (*R*)-PHB: $[\alpha]^{25}_{365}$ of +7.4°).[2a,11,12] Therefore, acyl-oxygen cleavage is proposed, which is consistent with a coordination−insertion mechanism (Figure S4).[1b,2a,11,12b] We investigated whether CO_2 influences the polymerization of BBL. Pressurizing a mixture of BBL, toluene, and catalyst 1 with 40 bar CO_2 resulted in stagnation of the reaction after 17% PHB formation (Figure S2, Table S1, entry S3). ^{13}C NMR spectroscopy revealed that CO_2 was not incorporated into the PHB polymer structure (Figure S3) as no carbonato C atoms were detected. Therefore, the termination of the reaction could be attributed to CO_2 insertion into the Zn−O bond, leading to a carbonato chain end that is unable to ring-open another BBL (see Scheme 1). This observation is in agreement with the literature, as also ε-caprolactone cannot be ring-opened by a carbonato end group.[7a,c] A third experiment was conducted wherein the reaction mixture was pressurized with 40 bar CO_2 followed by CO_2 release after ∼3 h (Figure S2, Table S1, entry S4). As 87% PHB was obtained, the stagnation of the reaction is a reversible process. The presence of small amounts of residual CO_2 (0.8 bar CO_2 were detected after few minutes) presumably causes a lower reaction rate. Finally, CHO was added to the system (CHO:BBL = 1:1, no CO_2) to detect any side reactions with the epoxide (Table S1, entry S5). The presence of CHO afforded a higher TOF for PHB formation, perhaps owing to its suitability as a solvent, and no polyether formation was observed. Additionally, it is possible that some catalyst molecules have opened CHO, which is then also an active initiator of ROP of BBL.[1b,2a,9a] Though, in both cases the PHB chain is terminated with an alkoxy-end group coordinated to the catalyst, that enables CO_2 insertion.

Owing to the influence of CO_2 on the ROP of BBL, we conducted a terpolymerization experiment according to method A1 (Figure 1): A mixture of BBL/CHO/catalyst 1 (500:500:1) and toluene was put in an autoclave with *in situ* IR monitoring at 60 °C and no CO_2 (Figure S11a). After 66% consumption of BBL ($\nu_{(C=O,\ BBL)}$ = 1830 cm^{-1}), the reaction mixture was pressurized with 40 bar CO_2 to initiate CHO/CO_2 copolymerization (Table 1, entry 1). The resulting crude AB block terpolymer comprised 1:1/PCHC:PHB and a molecular weight of 76 kDa via GPC and two glass transition temperatures at 2 and 116 °C due to phase separation were measured. Interestingly, the amount of homopolymeric PHB increased significantly, if the reaction proceeds to full conversion for BBL and CHO (Table S5, entry S1). The major homopolymeric proportion was effected by catalyst 1 due to the longer reaction time. It promotes elimination/trans-esterification reactions at the PHB chain (SI, chapter 15), which lead to unsaturated crotonate end groups that are not able to participate in the terpolymerization anymore (Scheme S1). ABA block terpolymers could be obtained by adding CO_2 at *ca.* 50% PHB conversion. When the yield of PCHC reached 92%, CO_2 was released to activate the ROP of the residual BBL (Table 1, entry 2, Figure 2). Therefore, CO_2 acts as a reversible switching agent, as previously shown by others in related fields.[7]

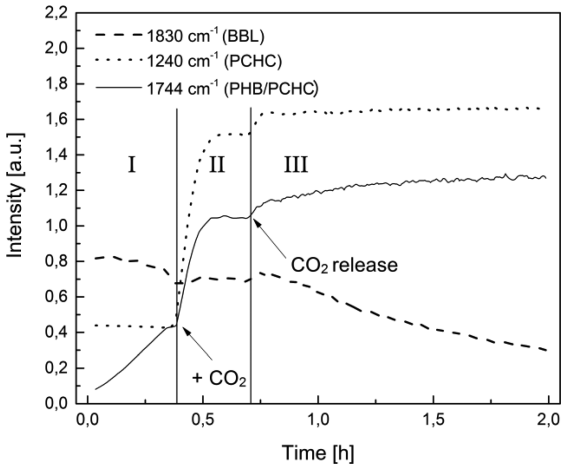

Figure 2. Formation of an ABA block terpolymer from BBL/CHO/CO_2, monitored by *in situ* IR spectroscopy. In step I, ROP of BBL occurred; afterward (step II), the system was pressurized with 40 bar CO_2 until full conversion to PCHC was achieved. Finally (step III), CO_2 was released to create the last PHB block.

A second route B was investigated to create BA block terpolymers, which was initiated by pressurizing the original mixture of BBL, CHO, catalyst 1, and toluene with 40 bar CO_2 at 60 °C (Table 1, entry 3). Owing to *in situ* IR monitoring of the carbonyl stretching bands of BBL, PHB, and PCHC, we assume that the polymerization began with the exclusive formation of PCHC and continued until all the epoxide was consumed (Figure S11b). This presumption was confirmed by an aliquot ^{1}H NMR spectrum (Figure S21a). The resulting PCHC unit has a molecular weight of 128 kDa and a bimodal mass distribution, which is often found in the literature for

DOI: 10.1021/jacs.7b01295
J. Am. Chem. Soc. 2017, 139, 6787−6790

copolymerization of CHO/CO_2 (Table S4, entry S2).[8,9] Afterward, ROP of BBL occurred (intensity of carbonyl stretching bond of BBL decreased) only upon complete CO_2 release. A polymer with a high molecular weight, narrow PDI, and two glass transition temperatures was obtained. The mass distribution of the terpolymer is again bimodal due to the first bimodal PCHC unit, so contamination of the terpolymer through PCHC copolymer is unlikely, but cannot be completely excluded.

Reducing the CO_2 pressure to 3 bar resulted in new polymerization behavior (Route C). Owing to this low pressure, the copolymerization reaction rate was much lower compared to that when 40 bar CO_2 was used and was thereby similar to the rate of the ROP of BBL. Therefore, a statistical terpolymer (Markov-distribution) was produced, which showed a mixed T_g of 36 °C (Table 1, entry 4).[13] The linkages can be assigned in the ^{1}H NMR spectrum (Figure 3), indicating that

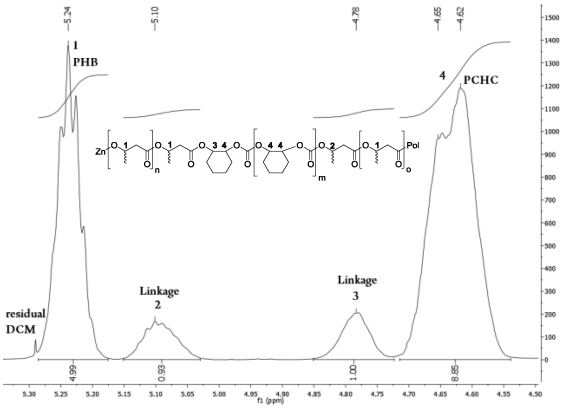

Figure 3. ^{1}H NMR (5.4–4.50 ppm) of a statistical terpolymer from BBL/CHO/CO_2 produced under 3 bar CO_2 (Table 1, entry 4).

the ring-opening of BBL under these conditions occurs again over an acyl-oxygen cleavage (Figure S4), accompanied by CO_2 insertion after a BBL unit to enable nucleophilic attack at the epoxide. The reaction pathway for ROP of BBL was confirmed by an experiment at 3 bar CO_2 with CHO and *R*-BBL (Table S2, entry S3, retention of conversion). *Via* 2D-NMR analysis (HMBC-NMR), a coupling of the H-2 atom (5.10 ppm) with the C atom of the carbonate (154 ppm) and of the ester (169 ppm) was observed (Figure S10, assignment of H atoms, Figure 3). Increasing the scan rate of HMBC to 32 scans leads to a detectable coupling signal for the H-3 atom with the vicinal

Scheme 1. Postulated Mechanism for the Terpolymerization of BBL, CHO, and 3 bar CO_2 with Catalyst 1

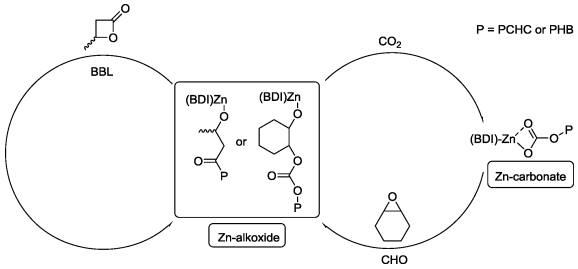

carbonyl C atom of the ester (169 ppm). Hence, we propose the following mechanism (Scheme 1): Initially, e.g., a PCHC chain grows at the zinc center and the alkoxide chain end attacks the BBL over an acyl-oxygen cleavage. Afterward, either ROP of BBL proceeds further or CO_2 is inserted into the alkoxide chain, which attacks the epoxide afterward. Then, copolymerization of CHO/CO_2 is possible or ROP of BBL occurs again. The carbonato chain end is unable to attack BBL. Terminating the experiment at 3 bar CO_2 at an earlier stage resulted in the same composition (Table S2, entry S1), indicating that the polymer is not a gradient terpolymer. Applying solely 1 bar to the one-pot mixture resulted in the preferential formation of PHB (72%) (Table S2, entry S2). Varying the CHO:BBL ratio to 650:350 at 3 bar CO_2, effected a statistical terpolymer (76:24, PCHC:PHB) with a high mixed T_g of 91 °C (Table 1, entry 5), illustrating that the T_g can be tuned by varying the ratio of BBL/CHO. We determined whether the different polymerization procedures can be transferred to other epoxides. CPO was chosen, as CHO and CPO have nearly the same ring tension and are supposed to exhibit similar reactivity. We tested catalyst 1 with respect to its activity for this copolymerization and produced poly(cyclopentene carbonate) with the highest reported TOF of 3200 h^{-1} (M_n = 122 kDa (1.3), 99% polycarbonate, Table S2, entry S7). Afterward, we performed terpolymerization experiments with BBL, CPO, and CO_2 according to reaction pathways A, B, and C (Table 1, entries 6–9). AB or ABA block terpolymers were produced with high molecular weights and two T_g values. However, pathway B (40 or 50 bar CO_2) afforded small signals for the linkages between PHB/PCPC in the ^{1}H NMR, indicating that in this case, copolymerization does not occur exclusively (Table S2, entry S8, Figure S18b). Therefore, the resulting polymer is a gradient polymer rather than a block terpolymer. Utilization of 3 bar CO_2, resulted again in the preparation of an almost statistical terpolymer with a mixed T_g of 24 °C.

In summary, we introduced BDI^{CF3}-Zn-N(SiMe$_3$)$_2$ as a versatile and capable catalyst for ROP of β-butyrolactone and copolymerization of CPO and CO_2. Three different terpolymerization procedures out of a mixed monomer feedstock comprising BBL/CHO(CPO)/CO_2 were established. There is not only a switch on/off CO_2 position possible (block polymers), but even a third option that leads to statistical terpolymers with a mixed glass transition temperature. This feature offers many opportunities in terms of polymer architecture and tuning terpolymer properties.

■ ASSOCIATED CONTENT

Supporting Information

The Supporting Information is available free of charge on the ACS Publications website at DOI: 10.1021/jacs.7b01295.

Experimental polymerization procedures, GPC, DSC, and stress–strain data, as well as NMRs of selected polymers (PDF)

■ AUTHOR INFORMATION

Corresponding Author

*rieger@tum.de

ORCID

Bernhard Rieger: 0000-0002-0023-884X

Author Contributions

‡These authors contributed equally.

DOI: 10.1021/jacs.7b01295
J. Am. Chem. Soc. 2017, 139, 6787–6790

Journal of the American Chemical Society Communication

Notes

The authors declare no competing financial interest.

■ ACKNOWLEDGMENTS

The authors thank Dr. Peter T. Altenbuchner, Martin Machat, Markus Pschenitza, and Christina Schwarzenböck for the valuable discussions. F. Adams thanks the Bavarian State Ministry of Environment and Consumer Protection for financial support within the BayBiotech research network.

■ REFERENCES

(1) (a) Rieger, B.; Künkel, A.; Coates, G. W. *Synthetic Biodegradable Polymers*; Springer, 2012. (b) Carpentier, J. F. *Macromol. Rapid Commun.* **2010**, *31*, 1696−1705.

(2) (a) Rieth, L. R.; Moore, D. R.; Lobkovsky, E. B.; Coates, G. W. *J. Am. Chem. Soc.* **2002**, *124*, 15239−15248. (b) Reichardt, R.; Vagin, S.; Reithmeier, R.; Ott, A. K.; Rieger, B. *Macromolecules* **2010**, *43*, 9311−9317. (c) Amgoune, A.; Thomas, C. M.; Ilinca, S.; Roisnel, T.; Carpentier, J. F. *Angew. Chem., Int. Ed.* **2006**, *45*, 2782−2784. (d) Darensbourg, D. J.; Wilson, S. J. *Green Chem.* **2012**, *14*, 2665−2671. (e) Romain, C.; Thevenon, A.; Saini, P. K.; Williams, C. K. *Carbon Dioxide and Organometallics*; Springer, 2016. (f) Paul, S.; Zhu, Y.; Romain, C.; Brooks, R.; Saini, P. K.; Williams, C. K. *Chem. Commun.* **2015**, *51*, 6459−6479. (g) Coates, G. W.; Moore, D. R. *Angew. Chem., Int. Ed.* **2004**, *43*, 6618−6639.

(3) (a) Vagin, S. I.; Reichardt, R.; Klaus, S.; Rieger, B. *J. Am. Chem. Soc.* **2010**, *132*, 14367−14369. (b) Moore, D. R.; Cheng, M.; Lobkovsky, E. B.; Coates, G. W. *J. Am. Chem. Soc.* **2003**, *125*, 11911−11924. (c) Zintl, M.; Molnar, F.; Urban, T.; Bernhart, V.; Preishuber-Pflügl, P.; Rieger, B. *Angew. Chem.* **2008**, *120*, 3508−3510.

(4) Dubois, P.; Coulembier, O.; Raquez, J.-M. *Handbook of Ring-Opening Polymerization*; John Wiley & Sons, 2009.

(5) Ajellal, N.; Bouyahyi, M.; Amgoune, A.; Thomas, C. M.; Bondon, A.; Pillin, I.; Grohens, Y.; Carpentier, J.-F. *Macromolecules* **2009**, *42*, 987−993.

(6) (a) Kronast, A.; Reiter, M.; Altenbuchner, P. T.; Jandl, C.; Pöthig, A.; Rieger, B. *Organometallics* **2016**, *35*, 681−685. (b) Abe, H.; Matsubara, I.; Doi, Y.; Hori, Y.; Yamaguchi, A. *Macromolecules* **1994**, *27*, 6018−6025.

(7) (a) Romain, C.; Zhu, Y.; Dingwall, P.; Paul, S.; Rzepa, H. S.; Buchard, A.; Williams, C. K. *J. Am. Chem. Soc.* **2016**, *138*, 4120−4131. (b) Paul, S.; Romain, C.; Shaw, J.; Williams, C. K. *Macromolecules* **2015**, *48*, 6047−6056. (c) Romain, C.; Williams, C. K. *Angew. Chem., Int. Ed.* **2014**, *53*, 1607−1610. (d) Kröger, M.; Folli, C.; Walter, O.; Döring, M. *Adv. Synth. Catal.* **2006**, *348*, 1908−1918. (e) Coulembier, O.; Moins, S. B.; Todd, R.; Dubois, P. *Macromolecules* **2014**, *47*, 486−491.

(8) (a) Kember, M. R.; Knight, P. D.; Reung, P. T. R.; Williams, C. K. *Angew. Chem., Int. Ed.* **2009**, *48*, 931−933. (b) Kember, M. R.; Williams, C. K. *J. Am. Chem. Soc.* **2012**, *134*, 15676−15679. (c) Cheng, M.; Moore, D. R.; Reczek, J. J.; Chamberlain, B. M.; Lobkovsky, E. B.; Coates, G. W. *J. Am. Chem. Soc.* **2001**, *123*, 8738−8749. (d) Darensbourg, D. J.; Yarbrough, J. C.; Ortiz, C.; Fang, C. C. *J. Am. Chem. Soc.* **2003**, *125*, 7586−7591.

(9) (a) Reiter, M.; Vagin, S.; Kronast, A.; Jandl, C.; Rieger, B. *Chem. Sci.* **2017**, *8*, 1876−1882. (b) Kissling, S.; Lehenmeier, M. W.; Altenbuchner, P. T.; Kronast, A.; Reiter, M.; Deglmann, P.; Seemann, U. B.; Rieger, B. *Chem. Commun.* **2015**, *51*, 4579−4582. (c) Jutz, F.; Buchard, A.; Kember, M. R.; Fredriksen, S. B.; Williams, C. K. *J. Am. Chem. Soc.* **2011**, *133*, 17395−17405.

(10) (a) Darensbourg, D. J.; Chung, W.-C.; Wilson, S. J. *ACS Catal.* **2013**, *3*, 3050−3057. (b) Liu, Y.; Ren, W.-M.; Liu, J.; Lu, X.-B. *Angew. Chem., Int. Ed.* **2013**, *52*, 11594−11598. (c) Cheng, M.; Darling, N. A.; Lobkovsky, E. B.; Coates, G. W. *Chem. Commun.* **2000**, 2007−2008. (d) Nozaki, K.; Nakano, K.; Hiyama, T. *J. Am. Chem. Soc.* **1999**, *121*, 11008−11009. (e) Liu, Y.; Ren, W.-M.; He, K.-K.; Lu, X.-B. *Nat. Commun.* **2014**, *5*, 5687.

(11) Zhang, Y.; Gross, R. A.; Lenz, R. W. *Macromolecules* **1990**, *23*, 3206−3212.

(12) (a) Alper, R.; Lundgren, D. G.; Marchessault, R. H.; Cote, W. A. *Biopolymers* **1963**, *1*, 545−556. (b) Jedliński, Z.; Kowalczuk, M.; Kurcok, P.; Adamus, G.; Matuszowicz, A.; Sikorska, W.; Gross, R. A.; Xu, J.; Lenz, R. W. *Macromolecules* **1996**, *29*, 3773−3777.

(13) Elias, H.-G. *Makromoleküle: Band 3: Industrielle Polymere und Synthesen*; John Wiley & Sons, 2009.

DOI: 10.1021/jacs.7b01295
J. Am. Chem. Soc. 2017, 139, 6787−6790

8. Terpolymerization of *β*-Butyrolactone, Epoxides, and CO_2: Chemoselective CO_2-Switch and its Impact on Kinetics and Material Properties

Title: "Terpolymerization of β-Butyrolactone, Epoxides, and CO_2: Chemoselective CO_2-Switch and its Impact on Kinetics and Material Properties"

Status: Full Paper, published online November 01, 2019

Journal: Macromolecules, 2019, 52, 8476-8483

Publisher: American Chemical Society

DOI: 10.1021/acs.macromol.9b01777

Authors: Sebastian Kernbichl, Marina Reiter, Josef Mock, Bernhard Rieger[a]

Content

In 2017, our group presented a novel approach towards the combination of two polymerization mechanisms.[146] The Lewis acidic zinc catalyst BDI^{CF3}–Zn–$N(TMS)_2$ is able to both catalyze the ring-opening polymerization of β-butyrolactone and the ring-opening copolymerization of epoxides and CO_2. The focus of this study is the synthesis of the respective terpolymers in a block and a statistical architecture by the application of a different carbon dioxide pressure (3 bar vs 40 bar). In situ IR spectroscopy provides a valuable tool for reaction order determination. Thereby, a switch in the reaction order of CO_2 was observed. At a high pressure, CO_2 is not rate-determining for the polymerization and therefore has a reaction order of zero. Lowering the pressure to 3 bar CO_2, as in the case for the statistical terpolymerization, resulted in a switch in the reaction order with respect to carbon dioxide from zero to one, indicating that CO_2 gets rate-determining at a reduced pressure. Next, thermal and mechanical properties have been investigated closer. Differential scanning calorimetry measurements revealed a tunable T_g for the statistical polymers ranging from 44 °C to 73 °C. The incorporation of the soft PHB into the brittle PCHC also resulted in a reduced Young modulus compared to pure PCHC. In case of a terpolymer in block structure exceeding 100 kg/mol, the elongation at break could be improved demonstrating the soft PHB part clearly has an impact on the brittleness of PCHC. This terpolymerization concept was successfully transferred to limonene oxide as epoxide. Again, block and statistical terpolymer were accessible and a tunable mechanical performance for PLC-PHB block copolymers achieved.

[a]S. Kernbichl had the initial idea, executed all experiments and wrote the manuscript. M. Reiter contributed with fruitful ideas. J. Mock conducted the AFM measurements and managed the processing of the respective data. All work was carried out under the supervision of B. Rieger.

Macromolecules
Article
Cite This: Macromolecules 2019, 52, 8476−8483
pubs.acs.org/Macromolecules

Terpolymerization of β-Butyrolactone, Epoxides, and CO_2: Chemoselective CO_2-Switch and Its Impact on Kinetics and Material Properties

Sebastian Kernbichl,[†] Marina Reiter,[†] Josef Mock,[‡] and Bernhard Rieger*[,†]

[†]WACKER-Chair of Macromolecular Chemistry, Catalysis Research Center, Technical University Munich, Lichtenbergstrasse 4, 85748 Garching, Germany

[‡]Chair of Nanoelectronics, Technical University Munich, Theresienstrasse 90, 80333 Munich, Germany

Supporting Information

ABSTRACT: Terpolymerization reactions with a mixed-monomer feedstock of epoxides, CO_2, and β-butyrolactone (BBL) at two different CO_2 pressures are presented. The Lewis acidic zinc complex BDI^{CF3}−Zn−$N(SiMe_3)_2$ **1** is able to catalyze both the ring-opening polymerization (ROP) of BBL and the ring-opening copolymerization of epoxides and CO_2. The carbon dioxide concentration thereby displays an attractive tool for the chemoselective tailoring of the incorporation of both monomer types to either a block or a statistical configuration. A high CO_2 pressure (40 bar) leads to a block structure, whereas 3 bar CO_2 allows the two catalytic cycles, ROP of BBL and ring-opening copolymerization of cyclohexene oxide and CO_2, to proceed with similar rates. This results in a statistical polymerization behavior. Reducing the CO_2 pressure from 40 to 3 bar involves a change in the reaction order of CO_2 from zero- to first-order dependency. The statistical polymerization pathway offers a promising route to terpolymers with one mixed-glass transition temperature that can be adjusted in a range between 5 and 115 °C. Terpolymers in block structure show two segregated glass transitions. This phase separation was also confirmed via atomic force microscopy. Referring to the mechanical behavior of the resulting terpolymers, a decrease of the Young modulus for both the block and the statistical structure compared to the very brittle poly(cyclohexene carbonate) is observed due to the incorporation of soft poly(3-hydroxybutyrate) (PHB). An enhanced elongation at break is revealed for the block structure when the molecular weights exceed 100 kg/mol. The biobased monomer limonene oxide is also successfully terpolymerized with CO_2 and BBL. Interestingly, the block structure shows a tunable stress−strain behavior depending on the amount of PHB in the terpolymer.

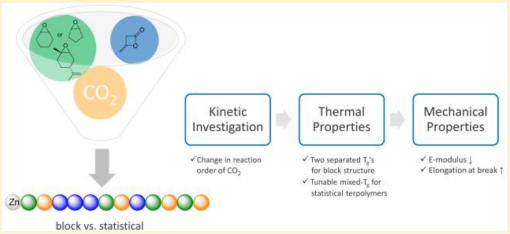

INTRODUCTION

Chemoselective polymerizations from a mixed-monomer feedstock offer the chance of synthesizing materials with tailored properties. Combining two different polymer types into one copolymer opens the option to overcome adverse properties of the respective homopolymers and create an enhanced performance of the copolymer. Block copolymers consisting of two block units linked together are best studied, but, nevertheless, the synthesis of block polymers seems to be unlimited by the choice of different monomers, block length, or degree of branching.[1] This synthetic playground was made mainly possible by the living anionic polymerization. Transferring this principle of tailoring the sequence of a polymer to the area of transition-metal-catalyzed polymerizations is ambitious. One of the general prerequisites is to have a metal complex that serves as a catalyst for two different types of monomer.

Polycarbonates derived from epoxides and CO_2 are a promising class of polymers because they display an attractive method to use carbon dioxide as a C1-feedstock; however, they suffer from poor mechanical stability.[2−11] Meanwhile, the ring-opening polymerization (ROP) of cyclic esters, e.g., β-butyrolactone (BBL), enables the synthesis of polyesters with defined tacticities and molecular weights.[12−16] Both polymer classes are industrially produced via condensation reactions but are also accessible via ring-opening of the respective monomers through a suitable catalyst.[17] The predominant class of catalysts for the copolymerization of epoxides and CO_2 and the ROP of different lactones are homogeneous complexes. Apart from β-diiminate (BDI) zinc complexes,[18] only a few complexes can catalyze both polymerization processes.[19−22] Williams introduced dinuclear zinc complexes as a versatile class of catalysts for the synthesis of polyester-carbonates.[23−26] On the one hand, these catalysts are limited to cyclohexene oxide (CHO) as epoxide and ε-caprolactone as well as lactide as cyclic ester. On the other hand, the system only allows the synthesis of block structures.

Received: August 23, 2019
Revised: October 22, 2019
Published: November 1, 2019

DOI: 10.1021/acs.macromol.9b01777
Macromolecules 2019, 52, 8476−8483

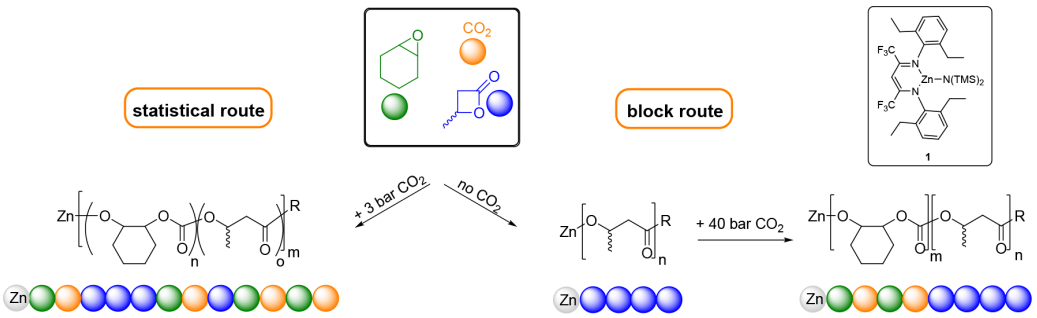

Figure 1. Illustration of the two selected polymerization routes using complex **1**. The statistical route runs at 3 bar CO_2, while the block pathway starts with the ROP of BBL and continues with the copolymerization upon addition of 40 bar CO_2.

We recently investigated the Lewis acidic BDI zinc complex **1**, focusing on the simultaneous polymerization behavior of *β*-butyrolactone and epoxides with CO_2.[27,28] Poly(cyclohexene carbonate) (PCHC) shows a glass transition at 115 °C but behaves as a very brittle material in high molecular weights.[29] In contrast, poly(3-hydroxybutyrate) (PHB) is regarded as a very soft polymer when polymerized with BDI zinc catalysts to its atactic form.[30,31] Thus far, a possible application for atactic PHB is lacking. Combining both polymers in one so-called terpolymer offers the chance to overcome adverse properties and to obtain a polymer with tunable thermal and mechanical properties. Using complex **1** in a one-pot polymerization of CHO, CO_2, and BBL, a chemoselective combination of the two catalytic cycles was observed. Applying no carbon dioxide in the beginning lets the ROP of BBL to start, followed by the epoxide/CO_2 copolymerization when the system is pressurized with 40 bar CO_2. This route gives access to defined block terpolymers with adjustable compositions and molecular weights (Figure 1). Further, when the CO_2 pressure is lowered to 3 bar, both catalytic pathways run simultaneously indicating that the two monomer types become statistically incorporated. This result opened a promising route to novel terpolymers that exhibit mixed-glass transition temperatures.

This work studied the reaction kinetics of the copolymerization reaction in detail to get a better insight into the polymerization behavior at 3 bar CO_2. In addition, the terpolymers synthesized via the two different approaches were investigated closer in terms of their thermal and mechanical behaviors to figure out if the difference in the architecture gets reflected in any change of properties. Differential scanning calorimetry (DSC) was used for glass transition and microphase separation analysis. The latter was also examined via atomic-force microscopy. Stress−strain measurements allowed the study of the mechanical behavior of the terpolymers.

RESULTS AND DISCUSSION

Kinetic Studies. The reaction orders in CO_2, CHO, and catalyst were determined for a more detailed understanding of the statistical terpolymerization process. In situ attenuated total reflection infrared (ATR-IR) spectroscopy provides a valuable tool for monitoring the reaction progress by a linear increase of the carbonyl stretching bond ($\nu_{C=O}$ = 1750 cm^{-1}). Coates and co-workers revealed the CHO ring-opening step to be rate-determining for BDI−Zn catalysts, whereas CO_2 insertion is a fast step (reaction order zero).[32] Connecting two zinc centers by a flexible BDI bridge resulted in high activities for the copolymerization reaction because it ensures the spatial proximity of two catalyst moieties.[33] A shift for carbon dioxide from zero- to first-order dependency was observed for these dinuclear complexes. The switch in the reaction order occurs at 25 bar CO_2. Carbon dioxide insertion becomes rate-limiting below this pressure, whereas the ring-opening of CHO follows a zero-order dependency. This shift can be explained by a very high copolymerization activity with these flexible tethered complexes. We were curious if a mononuclear complex like catalyst **1** also exhibits such a shift in the order of carbon dioxide. Hence, polymerizations with a varying CO_2 pressure ranging from 2 to 40 bar CO_2 were conducted. The initial slopes were plotted in a double logarithmic plot against CO_2 pressure (Figure 2). A shift of the rate-determining step became clearly visible between 5 and 10 bar CO_2.

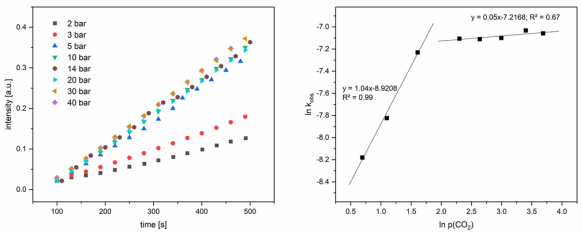

Figure 2. Determination of the order with respect to carbon dioxide pressure: plot of the intensity of the carbonyl stretching bond of the polycarbonate ($\nu_{C=O}$ = 1750 cm^{-1}) versus time dependent on the carbon dioxide pressure (2.0−40 bar) (left); double logarithmic plotting of the initial rate against CO_2 pressure (right).

Subsequently, the orders with respect to cyclohexene oxide and the catalyst were determined at two different CO_2 pressures (i.e., 3 and 30 bar (Figure 3). In contrast to the previously mentioned dinuclear zinc catalysts where CHO become zero-order dependent at low carbon dioxide concentrations, the order with respect to CHO did not change for catalyst **1**. The order in catalyst was also unaffected by the CO_2 pressure. Hence, catalyst **1** showed a rate-determining behavior of all three components at a pressure of 3 bar CO_2.

Terpolymerization of CHO/CPO, CO_2, and BBL. Terpolymers were synthesized via two different pathways. Block structure was realized via ROP of BBL, followed by the addition of 40 bar CO_2 and the consequent starting of copolymerization building the polycarbonate block (cf. Figure 1). The second pathway is called the statistical route. Accordingly, a reduced pressure of 3 bar CO_2 enabled

DOI: 10.1021/acs.macromol.9b01777
Macromolecules 2019, 52, 8476−8483

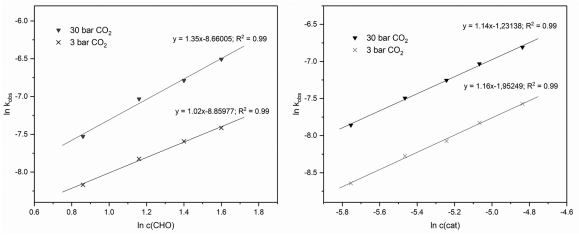

Figure 3. Reaction order in cyclohexene oxide (left) and catalyst concentration (right): plotting the initial slope against the concentration in a double logarithmic scale.

simultaneously proceeding catalytic cycles for both the ROP and the copolymerization of epoxides and CO_2.

Table 1 lists the results of the performed co- and terpolymerization experiments. The copolymerization of CHO and CO_2 (Table 1, entry 1) proceeded to high conversions within 0.2 h. PCHC showed a glass transition temperature of 116 °C and a molecular weight of 149 kg/mol ($Đ$ = 1.47). Terpolymerizations in a 50:50 ratio of CHO and BBL were successfully conducted via both the block and the statistical pathway to molecular weights in two different ranges (Table 1, entries 2−5). The synthesized block terpolymers always showed two segregated glass transitions indicating a phase-separated behavior. The statistical route enabled the synthesis of terpolymers with one single mix-T_g. Since ROP of BBL and copolymerization of epoxides and CO_2 run at similar rates at 3 bar CO_2, the initial ratio of BBL and epoxide was reflected in the composition of the terpolymer. This composition again defined the glass transition temperature and can, therefore, be purposely adjusted. Terpolymers to high contents of soft PHB were prepared (Table 1, entries 6 and 7) to check if terpolymers with a high elongation at break were also accessible.

A mixed-T_g can be obtained because of the statistical polymerization behavior at a CO_2 pressure of 3 bar. An atactic PHB homopolymer exhibits a glass transition temperature of 5 °C,[27] whereas the pure copolymer PCHC ranged at 115 °C. Depending on the composition of the terpolymer, this mixed-T_g can be tuned, and the desired temperature can be reached on purpose. It is also shown that the composition does not significantly change during the polymerization progress, meaning, e.g., a 50:50 ratio in a 500:500:1 = [CHO]:[BBL]:[cat] reaction can be observed independently of the conversion (for further compositions, see Table S4). Figure 4 shows a

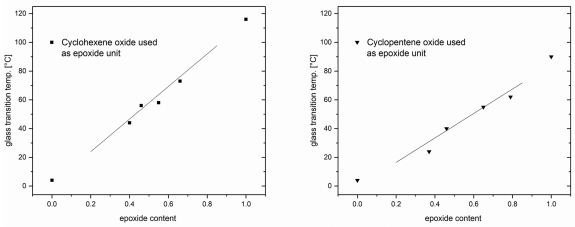

Figure 4. Dependency of the glass transition temperature (°C) from the polycarbonate content (%) in the respective terpolymer. A content of 0% corresponds to a PHB homopolymer whereas 100% represents the copolymer PCHC (left) and poly(cyclopentene carbonate) (PCPC) (right), respectively. See Table S4 for detailed polymerization conditions.

linear increase of the glass transition temperature with increasing polycarbonate content, which clearly demonstrates that the statistical terpolymerization route gives access to a group of polyester-carbonates with tunable T_g's. As early as 1956, T. G. Fox established the correlation of a copolymer's glass transition temperature and their respective mass fraction, later known as the Fox equation.[34] Taking the statistical terpolymer in Table 1, entry 3, as an example, the calculated mixed-T_g is 0.45 × 116 °C + 0.55 × 2 °C = 53 °C. Compared to the measured T_g of 57 °C, the calculated value fits well. For the statistical terpolymer in higher molecular weight (Table 1, entry 5), the calculated T_g deviates by 10 °C from the measured one.

Cyclopentene oxide (CPO) was also successfully coupled with CO_2 using complex **1** to poly(cyclopentene carbonate) in a molecular weight of 202 kg/mol ($Đ$ = 1.37) (Table 1, entry 8). The polymer showed a glass transition at 91 °C. The lowered T_g compared to PCHC is caused by the less rigid five-ringed polymer backbone. Block and statistical terpolymers were synthesized in two molecular weight regimes (Table 1,

Table 1. Co- and Terpolymerization of Epxides, CO_2, and BBL in Different Reaction Pathways[a]

entry	[epoxide]:[BBL]:[cat]	pathway[b]	time (h)[c]	conv. epoxide[d] (%)	conv. BBL[d] (%)	[PC]:[PHB][e]	T_g (°C)[f]	M_n($Đ$) (kg/mol)[g]
1	1000 (CHO):0:1	–	0.2	91	–	100:0	117	149 (1.47)
2	500 (CHO):500:1	block	1.2	77	66	55:45	2/116	76 (1.33)
3	500 (CHO):500:1	stat.	0.2	62	71	45:55	57	64 (1.20)
4	1000 (CHO):1000:1	block	1.2	84	67	60:40	3/124	115 (1.30)
5	1000 (CHO):1000:1	stat.	0.6	63	56	55:45	58	111 (1.28)
6	150 (CHO):850:1	block	4	68	59	22:78	5	73 (1.55)
7	250 (CHO):750:1	stat.	0.8	66	73	25:75	7	63 (1.90)
8	1000 (CPO):0:1	–	1	64	–	100:0	91	202 (1.37)
9	500 (CPO):500:1	block	4	85	93	55:45	8/68	45 (1.81)
10	500 (CPO):500:1	stat.	2	47	54	63:37	55	53 (1.59)
11	1000 (CPO):1000:1	block	3.2	53	58	54:46	3/88	158 (1.35)
12	1000 (CPO):1000:1	stat.	2	57	67	46:54	40	203 (1.57)

[a]Reaction conditions: CHO/BBL/CO_2, 60 °C, CPO/BBL/CO_2, 50 °C, 2.0 g of toluene. [b]Pathway according to Figure 1. [c]Polymerization time followed by in situ IR spectroscopy. [d]Conversion determined via ^{1}H NMR of a crude polymer sample. In cases of low conversions, the reaction was quenched at an early stage to check whether the two catalytic cycles run at similar rates or not. [e]According to ^{1}H NMR spectrum of the precipitated polymer. [f]Determined via DSC at a heating rate of 5 K/min. [g]Determined via GPC in THF relative to polystyrene.

DOI: 10.1021/acs.macromol.9b01777
Macromolecules 2019, 52, 8476−8483

entries 9–12) showing either two separated T_g's or one tunable mixed-T_g (see Figure 4, right).

DSC measurements indicate a phase-separated behavior for the terpolymers in block structure whereas for the statistical polymers a mixed-T_g was observed. We were curious if such a phase separation can be observed via atomic force microscopy. Dip coating of a dilute chloroform solution of the polymer onto a polished silicon wafer and consequent drying at 60 °C for 3 h revealed major differences in the surface character. Figure 5 shows the AFM topographic images of the terpolymers in a block structure (left, Table 1, entry 4) and the statistical configuration (right, Table 1, entry 5). The dark regions were caused by solvent evaporation and therefore a tapping onto the Si-wafer without any polymeric surface. In case of the block structure, the height difference of the surface was more pronounced where the statistical polymer showed a rather smooth surface. We suppose that the bright spots in Figure 5a correspond to the PCHC blocks. The respective height profile also indicated the change in surface height at the location of the white spots. Their average size of about 50 nm matches with the calculated PCHC block length (block polymer in Table 1, entry 4) of 50–100 nm depending on the coiling behavior. Performing AFM in tapping mode also allows the recording of the phase shift signal. The respective phase images are presented in Figure 5b and d.[35−38] In case of the block structure, the isolated PCHC blocks get visible again. For the polymer in the statistical structure, the phase shift of the area around the holes and at the small, homogeneously distributed spots is more pronounced than expected (Figure 5d). Generally, the phase shift always depends on both the effective Young modulus and the tip–sample contact area; for soft materials the latter has a higher influence on the phase shift.[39] In case of the statistical terpolymer, the higher Young modulus might be a reason why the phase shift became relatively more intense. The regions around the holes show a very high phase shift. This is most likely caused by the phase shift of the tip reaching the Si-wafer and not by a change of the polymeric surface. Taking this into account when comparing the two phase images, the one for the statistical terpolymer may show higher phase shifts at some spots, but in combination with the topographic images, the phase separation is much less existent. Nevertheless, we cannot exclude that the spots with a relatively higher phase shift are little isolated PCHC parts originating from the statistical terpolymer where an unusual high number of PCHC repeating units is present. Bearing in mind that AFM scans only represent a small section of the polymeric surface, it is concluded that phase separation in case of the block structure became clearly visible.

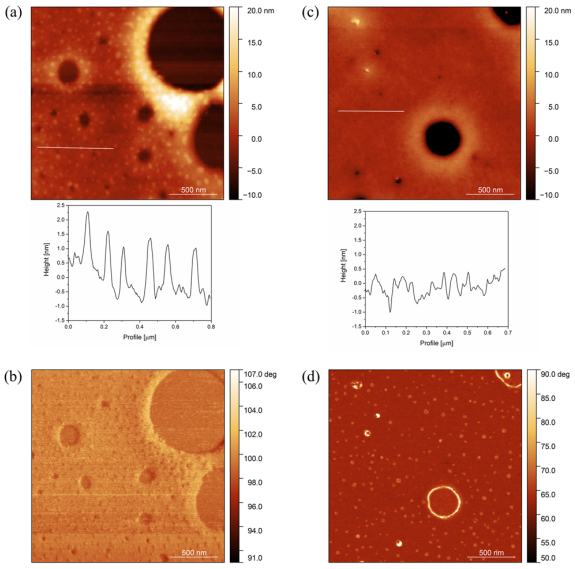

Figure 5. AFM images of two terpolymers in a different architecture. (a) AFM topographic image of a polymer in a block structure (Table 1, entry 4) with phase image (b) and (c) AFM topographic image of the polymer in a statistical configuration (Table 1, entry 5) with phase image (d).

Mechanical Properties. Considering our initial motivation of combining a hard and a soft segment together in one terpolymer, the polymers were hot-pressed to dog-bone-shaped specimens and investigated with a stress–strain machine. A thickness of 0.5 ± 0.1 mm was set for all test specimens. Poly(cyclohexene carbonate) is regarded as a very brittle polycarbonate in the literature.[29] This has been confirmed for PCHC with a molecular weight of 149 kg/mol which showed a Young modulus of 2500 MPa and an elongation at break of 1% (Table 2, entry 1). The overall aim was to reduce the brittleness of PCHC by the introduction of soft PHB units. Terpolymers with a 50:50 PCHC/PHB composition of both block and statistical structure were tested (Table 2, entries 2 and 3). Both polymers were considered to be "low MW" in this context with a MW lower than 100 kg/mol relative to polystyrene. Interestingly, Young moduli decreased to 1200–1350 MPa, but the elongation at break remained low at about 1–2%. No difference was observed between the block and the statistical structure. The decrease of

Table 2. Mechanical Properties of Different CHO Containing Co- and Terpolymers Measured with Dog-Bone-Shaped Specimens Obtained via Hot Pressing[a]

entry	structure	[PCHC]: [PHB]	M_n($Đ$) (kg/mol)	Young modulus (MPa)	tensile strength (MPa)	elongation at break (%)
1	–	100:0	149 (1.47)	2500 (±100)	43 (±5)	1 (±0.3)
2	block, low MW	55:45	76 (1.34)	1200 (±50)	17 (±3)	1.3 (±0.3)
3	stat., low MW	45:55	64 (1.20)	1350 (±60)	18 (±3)	1.8 (±0.2)
4	block, high MW	60:40	115 (1.29)	1170 (±50)	26 (±3)	5 (±0.2)
5	stat., high MW	55:45	111 (1.28)	1600 (±100)	23 (±2)	1.5 (±0.3)
6	block, high PHB	22:78	73 (1.53)	261 (±30)	5 (±0.6)	225 (±40)
7	stat., high PHB	25:75	101 (1.37)	150 (±20)	5 (±0.5)	350 (±50)

[a]The Young modulus of all polymers is determined at the initial region of the linear stress–strain. Dog-bone-shaped specimens have a thickness of 0.5 ± 0.1 mm and are tested with a strain rate of 5 mm/min.

DOI: 10.1021/acs.macromol.9b01777
Macromolecules 2019, 52, 8476–8483

Table 3. Co- and Terpolymerization of LO, CO_2, and BBL in Different Reaction Pathways[a]

entry	[*trans*-LO]: [BBL]:[cat]	pathway	time (h)[b]	conv. *trans*-LO[c](%)	conv. BBL[c] (%)	[PLC]:[PHB][d]	T_g (°C)[e]	M_n($Đ$) (kg/mol)[f]
1	200:0:1	–	7	62	–	100:0	126	80 (1.42)
2	350:0:1	–	8	69	-	100:0	131	244 (1.24)
3	250:250:1	block, B	10	6	7	48:52	n.d.	n.d.
4	250:250:1	block, A	6	63	74	46:54	2/126	90 (1.30)
5	375:125:1	block, A	8	74	78	79:21	1/129	149 (1.23)
6	250:250:1	stat.	22	22	26	55:45	53	9 (1.39)
7	400:400:1	block, A	16	65	66	58:42	3/131	211 (1.37)
8	600:200:1	block, A	16	66	60	75:25	1/133	233 (1.34)

[a]Reaction conditions for the different pathways, see the Supporting Information. [b]Complete polymerization time followed by in situ ATR-IR. [c]Determined by ^{1}H NMR spectroscopy of a crude polymer sample. [d]According to ^{1}H NMR spectrum of the precipitated polymer. [e]Determined by DSC at a heating rate of 5 K/min. [f]Measured via GPC in $CHCl_3$ relative to polystyrene standards.

the Young moduli clearly indicates an impact of the PHB, but nevertheless the poor elongation at break is still dominated by the brittle PCHC part. Doubling the MW of the terpolymers ("high" MW) revealed an attractive difference between the two structures (Table 2, entries 4 and 5). While the block terpolymer exhibited a lower Young modulus (1170 vs 1600 MPa) than the statistical terpolymer, the elongation at break was remarkably higher (5% vs 1.5%). This finding clearly demonstrates the impact of the polymers' architecture on the mechanical behavior on the one hand and represents an explicit improvement of the brittleness of PCHC on the other hand. In the case of the block structure, a coiling of the two different segments is assumed to be possible more easily, enabling this enhanced elongation at break.

In the case of increasing the PHB content to 75%, a drastic decrease of the Young modulus was observed accompanied by an elongation at break of more than 200% for both architectures. This behavior can solely be explained by a predominant influence of the soft poly(3-hydroxybutyrate) block and gives access to a useful application of atactic PHB.

Co- and terpolymers bearing poly(cyclopentene carbonate) moieties were also investigated as regards their mechanical performance (Table S6). PCPC itself behaved like a very rigid plastic but showed a slightly increased elongation at break compared to PCHC because of the lower T_g of 91 vs 115 °C. All the conclusions drawn from the results of Table 2 were confirmed by the PCPC-containing terpolymers. The incorporation of PHB lowered Young moduli, but it took high MW and the block structure to end up with enhanced properties.

Terpolymerization of LO, CO_2, and BBL. Limonene oxide displays a promising biobased alternative to the established epoxide monomers, especially cyclohexene oxide and propylene oxide. The respective polymer poly(limonene carbonate) (PLC) shows a high glass transition temperature of 130 °C; therefore, it is also represents an interesting candidate for the terpolymerization with β-butyrolactone.[40] First, copolymerization reactions with limonene oxide and CO_2 were conducted to obtain PLC in different molecular weights (Table 3, entries 1 and 2). BDI complexes are known to only incorporate *trans*-limonene oxide; hence, conversions were indicated based on *trans*-LO.[28,41] Tunable molecular weights could be obtained in a range suitable for the application as rigid plastics depending on the catalyst-to-monomer ratio. The established reaction pathways for the terpolymerization of epoxides, CO_2, and BBL were transferred to limonene oxide. Applying 40 bar CO_2 in the beginning of the reaction successfully started the coupling of LO and CO_2 (Table 3, entry 3, called pathway B). A complete release of CO_2 was required for the PHB block formation. Figure 6 illustrates the in situ IR monitoring of the polymerization reaction. The

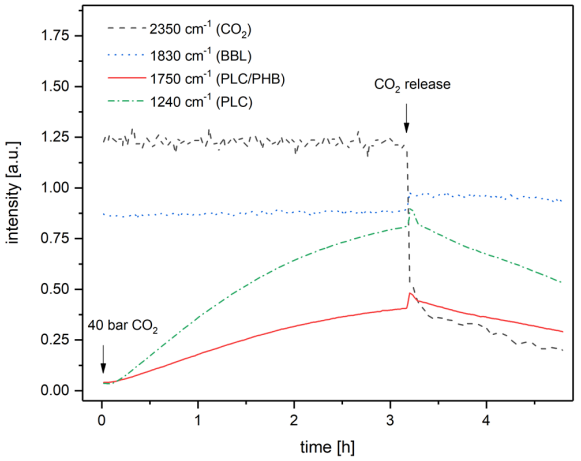

Figure 6. Monitoring of the terpolymerization of LO, CO_2, and BBL via in situ IR spectroscopy. 40 bar CO_2 was applied in the beginning and released after 3.25 h. A decrease of the carbonyl stretching bond at 1750 cm^{-1} indicates the depolymerization of PLC.

intensity of the carbonyl stretching bond of PLC increased in the presence of carbon dioxide. When CO_2 was released after 3.25 h, the start of the BBL ring-opening polymerization was expected, observable with a further increase of the intensity of $\nu_{C=O}$ = 1750 cm^{-1}. Surprisingly, a depolymerization of PLC occurred instead of the initiation of the ROP. Our group recently investigated the ceiling temperature of PLC and observed depolymerization at 60 °C at elevated conversions.[28] A release of carbon dioxide like that in pathway B strongly favors depolymerization. The reaction ran for an additional 6 h and led to a total conversion of LO of 6% and BBL of 7%. Switching to pathway A means starting with the ROP and enabling copolymerization by the addition of CO_2 after almost full conversion of BBL. Terpolymerizations were successfully performed to adjustable compositions (Table 3, entries 4 and 5) bearing two glass transition temperatures due to phase separation. Selective block formation was verified via aliquot GPC analysis (Table S5, entry S1, Figure S5).

Attempts were made to realize a statistical incorporation of both monomer types (Table 3, entry 6), despite the relatively low ceiling temperature of PLC. An optimum CO_2 pressure of 9 bar was applied, where copolymerization and ROP exhibited

DOI: 10.1021/acs.macromol.9b01777
Macromolecules 2019, 52, 8476−8483

Table 4. Mechanical Properties of Different Limonene Oxide Containing Co- and Terpolymers Measured with Dog-Bone-Shaped Specimens Obtained via Solvent Casting[a]

entry	structure	[PLC]: [PHB]	M_n($Đ$) (kg/mol)	Young modulus (MPa)	tensile strength (MPa)	elongation at break (%)
1	low MW	100:0	80 (1.42)	2250 ± 200	58 ± 3	6 ± 1
2	block, low MW	46:54	90 (1.30)	1800 ± 100	44 ± 1	4 ± 1
3	high MW	100:0	244 (1.24)	2350 ± 100	52 ± 2	3.5 ± 0.5
4	block, high MW	46:54	211 (1.37)	1450 ± 100	38 ± 2	18 ± 9
5	block, high MW	79:21	233 (1.34)	1800 ± 200	45 ± 3	13 ± 4

[a]The Young modulus of all polymers is determined at the initial region of the linear stress−strain regime. Dog-bone-shaped specimens have a thickness of 0.25 ± 0.05 mm and are tested with a strain rate of 5 mm/min.

the same reaction rates. As expected, conversions were low because of the possible depolymerization of PLC at low LO/CO_2 concentrations and a lower activity of the ROP of BBL at 40 °C compared to 60 °C. Even an extended reaction time of 22 h only led to conversions of 22% and 26%, respectively. Additionally, two terpolymers in block structure (Table 3, entries 7 and 8) were synthesized in different compositions to high molecular weight polymers for mechanical testing.

Mechanical Properties. PLC displayed a very attractive property regarding processability because polymer films could be readily obtained via solvent casting from a polymeric solution in dichloromethane. The solvent became fully evaporated without creating any surface irregularities like bubbles. This marks a very interesting difference from the terpolymers derived from cyclohexene oxide because they could hardly be used for solvent casting. The aim was to produce dog-bone-shaped specimens for further testing in a stress−strain machine. A thickness of 250 ± 50 μm was set for all polymer specimens. First, PLC in different molecular weights (80 and 244 kg/mol) was tested. Independent of the molecular weight, high Young moduli (2250 and 2350 MPa) and a similar elongation at break of 6% and 4% were obtained.

Testing the terpolymer in block structure (Table 4, entry 2) revealed a softer behavior based on the reduced Young modulus but did not show an enhanced elongation at break. Indeed, the latter could be improved when molecular weights were increased (Table 4, entries 4 and 5). The elongation at break could be successfully tuned from 13 ± 4% to 18 ± 9% simply via a higher PHB content (Figure 7). This finding again emphasizes the necessity of high molecular weights and a block structure to realize enhanced material properties via terpolymerization.

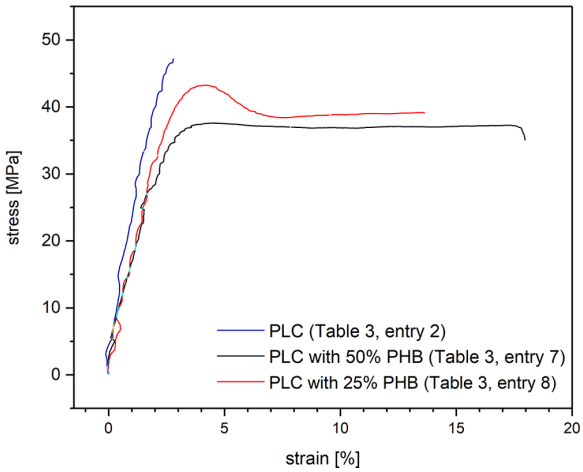

Figure 7. Stress−strain curves of poly(limonene carbonate) specimens with a varying poly(3-hydroxybutyrate) content in the terpolymer.

CONCLUSION

The terpolymerization behavior of a Lewis acidic BDI zinc complex **1** with a mixed-monomer feedstock of epoxide, CO_2, and BBL was reported herein. Two different polymerization pathways were used to selectively realize polyester-carbonates in both a block and a statistical configuration. The block structure was realized by ring-opening polymerization of BBL in the beginning, followed by the addition of 40 bar CO_2 and the start of the epoxide/CO_2 copolymerization. Lowering the carbon dioxide pressure to 3 bar allowed the two catalytic cycles to run at similar rates, thereby enabling a statistical incorporation of both monomer types. A kinetic study of the pressure-dependent copolymerization of CHO and CO_2 revealed a change in the reaction order with respect to carbon dioxide from zero- to first-order dependency. The switch in the reaction order occurred at a pressure of 5 bar CO_2. Apart from CHO, cyclopentene oxide and limonene oxide were used as epoxides in the terpolymerization to both the block and the statistical structure. The terpolymers were tested in terms of their thermal and mechanical behaviors using DSC and stress−strain analysis. The polymers in block structure showed two glass transitions (i.e., 5 and 115 °C) because of the phase separation, whereas only one mixed-T_g was observed for the statistical architecture. AFM images show severe differences in the height profile between the two structures. The terpolymer in block structure reveals a rougher surface with phase-separated PCHC spots. In the case of the epoxides CHO or CPO, statistical terpolymers were obtained in different compositions disclosing a tunable glass transition temperature. The mechanical analysis revealed an overall lower Young modulus for the terpolymers compared to PCHC because of the incorporation of soft PHB. To realize an enhanced elongation at break, high molecular weights (>100 kg/mol) and a block structure were required. The two polymerization pathways were transferred to the biobased monomer LO. PLC−PHB block polymers were then synthesized to high molecular weights and showed a tunable elongation at break depending on the amount of PHB incorporation. Overall, this terpolymerization behavior opens the possibility of modifying CO_2-based polycarbonates specifically depending on the area of application. Statistical terpolymers are T_g-tunable whereas the block structure shows enhanced mechanical properties.

EXPERIMENTAL SECTION

General. All reactions containing air- and/or moisture-sensitive compounds were performed under dry argon atmosphere using standard Schlenk or glovebox techniques. All chemicals were

DOI: 10.1021/acs.macromol.9b01777
Macromolecules 2019, 52, 8476−8483

purchased from Aldrich or TCI. Monomers were dried over calcium hydride or sodium hydride and distilled prior to polymerization. Limonene oxide used in this work contained 54% *trans*-LO and 46% *cis*-LO. CO_2 was purchased from Westfalen (purity 4.6). Dry toluene was purified with an MBraun MB-SPS-800 solvent purification system.

NMR (^{1}H and ^{13}C) measurements were recorded on a Bruker AVIII500 Cryo and an AVHD500 spectrometer. Chemical shifts δ were reported in ppm relative to tetramethylsilane and calibrated to the residual ^{1}H or ^{13}C signal of the deuterated solvent. Deuterated solvents were obtained from Aldrich and dried over a 3 Å molecular sieve.

In situ IR measurements were performed under argon atmosphere using an ATR IR MettlerToledo system. Kinetic investigations were all performed in the same reactor under identical conditions. GPC was performed on a Varian PL-GPC 50 using THF (HPLC grade) with 0.22 g L^{-1} 2.6 di-*tert*-butyl-4-methylphenol and a flow rate of 1 mL/min at 40 °C. Poly(limonene carbonate)-containing polymers were measured at a Varian PL-GPC 50 using chloroform (HPLC grade) with a flow rate of 1 mL/min at 25 °C. Polystyrene standards were used for calibration.

DSC was conducted on a DSC Q2000 instrument. First 3−6 mg of the polymer was filled into a DSC aluminum pan and heated from −30 to 170 °C at a rate of 5 K/min. The reported values were determined with TA Universal Analysis from the second heating cycle.

Stress−strain measurements were performed on a ZwickRoell machine with a strain rate of 5 mm/min and analyzed with testXpert II software. First, the polymer was grinded and dried in vacuo to constant weight. The solvent-free polymer was checked via ^{1}H NMR. Specimens (dog-bone-shaped, 50 mm long, 4 mm wide (smallest point)) were produced by pressing the polymeric powder at a certain temperature (usually 30 °C above the T_g) at 50−100 bar for 3 h. A thickness of 0.5 ± 0.1 mm was set. The specimens were checked with regard to a homogeneous surface. At least three specimens were tested for all the different polymers investigated in this work. All poly(limonene carbonate)-containing co- and terpolymers were solvent-cast from a polymeric solution in dichloromethane. The solvent was then slowly evaporated overnight, and the film was dried to constant weight at 80 °C for 1 h. The thickness of the film was 0.25 ± 0.05 mm. The dog-bone-shaped specimens were obtained through a polymer film stamping. AFM measurements were obtained with an Asylum Research AFM MFP-3D from Oxford instruments in the tapping mode and analyzed with Gwyddion software.

Synthesis. Both the ligand and the catalyst were synthesized according to the literature procedures.[28,42]

Polymerization. All polymerizations were performed with in situ monitoring using a React-IR Mettler-Toledo system. The 50 mL steel autoclaves were equipped with a diamond window, a heating device, and mechanic stirring. The autoclaves were heated to 130 °C under vacuum overnight prior to polymerization at the desired temperature. All chemicals were weighed in the glovebox, stored in syringes, and rapidly transported to the reactor. The reaction was terminated by adding dichloromethane and a drop of methanol and transferred to a flask. The consequent removal of the solvent under a reduced pressure allowed the determination of yield and selectivity via NMR/weight of the polymer. The dissolved polymer (dichloromethane) was precipitated in methanol and dried to constant weight. See the Supporting Information for the detailed polymerization procedures.

■ ASSOCIATED CONTENT

Supporting Information

The Supporting Information is available free of charge on the ACS Publications website at DOI: 10.1021/acs.macromol.9b01777.

Experimental polymerization procedures, GPC, DSC, and stress−strain data (PDF)

■ AUTHOR INFORMATION

Corresponding Author

*E-mail: rieger@tum.de. Tel.: +49-89-289-13570. Fax: +49-89-289-13562.

ORCID

Bernhard Rieger: 0000-0002-0023-884X

Author Contributions

The manuscript was written through contributions of all authors. All authors have given approval to the final version of the manuscript.

Notes

The authors declare no competing financial interest.

■ ACKNOWLEDGMENTS

We are grateful to the Covestro AG for financial support. M.R. substantially contributed to this work during her time as a co-worker of the Wacker-Chair of Macromolecular Chemistry. J. M. performed the AFM measurements and thanks the DFG and the NSERC for financial support of the Alberta/(Technische Universität München Graduate School for Functional Hybrid Materials ATUMS (IRTG2022, NSERC CREATE). The authors thank Sergei Vagin and Andreas Schaffer for valuable discussions and proofreading the manuscript.

■ REFERENCES

(1) Bates, F. S.; Hillmyer, M. A.; Lodge, T. P.; Bates, C. M.; Delaney, K. T.; Fredrickson, G. H. Multiblock Polymers: Panacea or Pandora's Box? *Science* **2012**, *336*, 434−440.

(2) Coates, G. W.; Moore, D. R. Discrete Metal-Based Catalysts for the Copolymerization of CO2 and Epoxides: Discovery, Reactivity, Optimization, and Mechanism. *Angew. Chem., Int. Ed.* **2004**, *43*, 6618−6639.

(3) Darensbourg, D. J. Making Plastics from Carbon Dioxide: ; Salen Metal Complexes as Catalysts for the Production of Polycarbonates from Epoxides and CO2. *Chem. Rev.* **2007**, *107*, 2388−2410.

(4) Klaus, S.; Lehenmeier, M. W.; Anderson, C. E.; Rieger, B. Recent advances in CO2/epoxide copolymerization—New strategies and cooperative mechanisms. *Coord. Chem. Rev.* **2011**, *255*, 1460−1479.

(5) Rieger, B.; Künkel, A.; Coates, G. W. *Synthetic Biodegradable Polymers*; Springer: Berlin/Heidelberg, Germany, 2012.

(6) Kember, M. R.; Buchard, A.; Williams, C. K. Catalysts for CO2/epoxide copolymerisation. *Chem. Commun.* **2011**, *47*, 141−163.

(7) Kissling, S.; Altenbuchner, P. T.; Niemi, T.; Repo, T.; Rieger, B. *Zinc Catalysis*; Wiley-VCH Verlag: Weinheim, Germany, 2015.

(8) Romain, C.; Thevenon, A.; Saini, P. K.; Williams, C. K. *Carbon Dioxide and Organometallics*; Springer: Cambridge, U.K., 2016.

(9) Kozak, C. M.; Ambrose, K.; Anderson, T. S. Copolymerization of carbon dioxide and epoxides by metal coordination complexes. *Coord. Chem. Rev.* **2018**, *376*, 565−587.

(10) Wang, Y.; Darensbourg, D. J. Carbon dioxide-based functional polycarbonates: Metal catalyzed copolymerization of CO2 and epoxides. *Coord. Chem. Rev.* **2018**, *372*, 85−100.

(11) Kim, J. G.; Cowman, C. D.; LaPointe, A. M.; Wiesner, U.; Coates, G. W. Tailored Living Block Copolymerization: Multiblock Poly(cyclohexene carbonate)s with Sequence Control. *Macromolecules* **2011**, *44*, 1110−1113.

(12) Rieth, L. R.; Moore, D. R.; Lobkovsky, E. B.; Coates, G. W. Single-Site β-Diiminate Zinc Catalysts for the Ring-Opening Polymerization of β-Butyrolactone and β-Valerolactone to Poly(3-hydroxyalkanoates). *J. Am. Chem. Soc.* **2002**, *124*, 15239−15248.

(13) Thomas, C. M. Stereocontrolled ring-opening polymerization of cyclic esters: synthesis of new polyester microstructures. *Chem. Soc. Rev.* **2010**, *39*, 165−173.

(14) Carpentier, J.-F. Rare-Earth Complexes Supported by Tripodal Tetradentate Bis(phenolate) Ligands: A Privileged Class of Catalysts for Ring-Opening Polymerization of Cyclic Esters. *Organometallics* **2015**, *34*, 4175−4189.
(15) Carpentier, J.-F. Discrete Metal Catalysts for Stereoselective Ring-Opening Polymerization of Chiral Racemic β-Lactones. *Macromol. Rapid Commun.* **2010**, *31*, 1696−1705.
(16) Schneiderman, D. K.; Hill, E. M.; Martello, M. T.; Hillmyer, M. A. Poly(lactide)-block-poly(ε-caprolactone-co-ε-decalactone)-block-poly(lactide) copolymer elastomers. *Polym. Chem.* **2015**, *6*, 3641−3651.
(17) Paul, S.; Zhu, Y.; Romain, C.; Brooks, R.; Saini, P. K.; Williams, C. K. Ring-opening copolymerization (ROCOP): synthesis and properties of polyesters and polycarbonates. *Chem. Commun.* **2015**, *51*, 6459−6479.
(18) Cheng, M.; Lobkovsky, E. B.; Coates, G. W. Catalytic Reactions Involving C1 Feedstocks: ; New High-Activity Zn(II)-Based Catalysts for the Alternating Copolymerization of Carbon Dioxide and Epoxides. *J. Am. Chem. Soc.* **1998**, *120*, 11018−11019.
(19) Wu, G.-P.; Darensbourg, D. J.; Lu, X.-B. Tandem Metal-Coordination Copolymerization and Organocatalytic Ring-Opening Polymerization via Water To Synthesize Diblock Copolymers of Styrene Oxide/CO2 and Lactide. *J. Am. Chem. Soc.* **2012**, *134*, 17739−17745.
(20) Darensbourg, D. J.; Wu, G.-P. A One-Pot Synthesis of a Triblock Copolymer from Propylene Oxide/Carbon Dioxide and Lactide: Intermediacy of Polyol Initiators. *Angew. Chem., Int. Ed.* **2013**, *52*, 10602−10606.
(21) Duan, Z.; Wang, X.; Gao, Q.; Zhang, L.; Liu, B.; Kim, I. Highly active bifunctional cobalt-salen complexes for the synthesis of poly(ester-block-carbonate) copolymer via terpolymerization of carbon dioxide, propylene oxide, and norbornene anhydride isomer: Roles of anhydride conformation consideration. *J. Polym. Sci., Part A: Polym. Chem.* **2014**, *52*, 789−795.
(22) Vagin, S. I.; Reichardt, R.; Klaus, S.; Rieger, B. Conformationally Flexible Dimeric Salphen Complexes for Bifunctional Catalysis. *J. Am. Chem. Soc.* **2010**, *132*, 14367−14369.
(23) Romain, C.; Williams, C. K. Chemoselective Polymerization Control: From Mixed-Monomer Feedstock to Copolymers. *Angew. Chem., Int. Ed.* **2014**, *53*, 1607−1610.
(24) Romain, C.; Zhu, Y.; Dingwall, P.; Paul, S.; Rzepa, H. S.; Buchard, A.; Williams, C. K. Chemoselective Polymerizations from Mixtures of Epoxide, Lactone, Anhydride, and Carbon Dioxide. *J. Am. Chem. Soc.* **2016**, *138*, 4120−4131.
(25) Chen, T. T. D.; Zhu, Y.; Williams, C. K. Pentablock Copolymer from Tetracomponent Monomer Mixture Using a Switchable Dizinc Catalyst. *Macromolecules* **2018**, *51*, 5346−5351.
(26) Zhu, Y.; Radlauer, M. R.; Schneiderman, D. K.; Shaffer, M. S. P.; Hillmyer, M. A.; Williams, C. K. Multiblock Polyesters Demonstrating High Elasticity and Shape Memory Effects. *Macromolecules* **2018**, *51*, 2466−2475.
(27) Kernbichl, S.; Reiter, M.; Adams, F.; Vagin, S.; Rieger, B. CO_2-Controlled One-Pot Synthesis of AB, ABA Block, and Statistical Terpolymers from β-Butyrolactone, Epoxides, and CO_2. *J. Am. Chem. Soc.* **2017**, *139*, 6787−6790.
(28) Reiter, M.; Vagin, S.; Kronast, A.; Jandl, C.; Rieger, B. A Lewis acid [small beta]-diiminato-zinc-complex as all-rounder for co- and terpolymerisation of various epoxides with carbon dioxide. *Chem. Sci.* **2017**, *8*, 1876−1882.
(29) Koning, C.; Wildeson, J.; Parton, R.; Plum, B.; Steeman, P.; Darensbourg, D. J. Synthesis and physical characterization of poly(cyclohexane carbonate), synthesized from CO2 and cyclohexene oxide. *Polymer* **2001**, *42*, 3995−4004.
(30) Adamus, G.; Sikorska, W.; Janeczek, H.; Kwiecień, M.; Sobota, M.; Kowalczuk, M. Novel block copolymers of atactic PHB with natural PHA for cardiovascular engineering: Synthesis and characterization. *Eur. Polym. J.* **2012**, *48*, 621−631.
(31) Aluthge, D. C.; Xu, C.; Othman, N.; Noroozi, N.; Hatzikiriakos, S. G.; Mehrkhodavandi, P. PLA−PHB−PLA Triblock Copolymers: Synthesis by Sequential Addition and Investigation of Mechanical and Rheological Properties. *Macromolecules* **2013**, *46*, 3965−3974.
(32) Moore, D. R.; Cheng, M.; Lobkovsky, E. B.; Coates, G. W. Mechanism of the Alternating Copolymerization of Epoxides and CO2 Using β-Diiminate Zinc Catalysts: ; Evidence for a Bimetallic Epoxide Enchainment. *J. Am. Chem. Soc.* **2003**, *125*, 11911−11924.
(33) Lehenmeier, M. W.; Kissling, S.; Altenbuchner, P. T.; Bruckmeier, C.; Deglmann, P.; Brym, A.-K.; Rieger, B. Flexibly Tethered Dinuclear Zinc Complexes: A Solution to the Entropy Problem in CO_2/Epoxide Copolymerization Catalysis? *Angew. Chem., Int. Ed.* **2013**, *52*, 9821−9826.
(34) Fox, T. G. Influence of Diluent and of Copolymer Composition on the Glass Temperature of a Poly-mer System. *Bull. Am. Phys. Soc.* **1956**, *1*, 123.
(35) Leclère, P.; Lazzaroni, R.; Brédas, J. L.; Yu, J. M.; Dubois, P.; Jérôme, R. Microdomain Morphology Analysis of Block Copolymers by Atomic Force Microscopy with Phase Detection Imaging. *Langmuir* **1996**, *12*, 4317.
(36) Kim, S. H.; Misner, M. J.; Xu, T.; Kimura, M.; Russell, T. P. Highly Oriented and Ordered Arrays from Block Copolymers via Solvent Evaporation. *Adv. Mater.* **2004**, *16*, 226−231.
(37) Albert, J. N. L.; Epps, T. H. Self-assembly of block copolymer thin films. *Mater. Today* **2010**, *13*, 24−33.
(38) Zhang, Q.; Tsui, O. K. C.; Du, B.; Zhang, F.; Tang, T.; He, T. Observation of Inverted Phases in Poly(styrene-b-butadiene-b-styrene) Triblock Copolymer by Solvent-Induced Order-Disorder Phase Transition. *Macromolecules* **2000**, *33*, 9561−9567.
(39) Bar, G.; Thomann, Y.; Brandsch, R.; Cantow, H. J.; Whangbo, M. H. Factors Affecting the Height and Phase Images in Tapping Mode Atomic Force Microscopy. Study of Phase-Separated Polymer Blends of Poly(ethene-co-styrene) and Poly(2,6-dimethyl-1,4-phenylene oxide). *Langmuir* **1997**, *13*, 3807−3812.
(40) Hauenstein, O.; Reiter, M.; Agarwal, S.; Rieger, B.; Greiner, A. Bio-based polycarbonate from limonene oxide and CO2 with high molecular weight, excellent thermal resistance, hardness and transparency. *Green Chem.* **2016**, *18*, 760−770.
(41) Byrne, C. M.; Allen, S. D.; Lobkovsky, E. B.; Coates, G. W. Alternating Copolymerization of Limonene Oxide and Carbon Dioxide. *J. Am. Chem. Soc.* **2004**, *126*, 11404−11405.
(42) Kronast, A.; Reiter, M.; Altenbuchner, P. T.; Jandl, C.; Pöthig, A.; Rieger, B. Electron-Deficient β-Diiminato-Zinc-Ethyl Complexes: Synthesis, Structure, and Reactivity in Ring-Opening Polymerization of Lactones. *Organometallics* **2016**, *35*, 681−685.

DOI: 10.1021/acs.macromol.9b01777
Macromolecules 2019, 52, 8476−8483

9. A Heteronuclear, Monomer-Selective Zn/Y Catalyst Combines Copolymerization of Epoxides and CO_2 with Group Transfer Polymerization of Michael-type Monomers

Title: "A Heteronuclear, Monomer-Selective Zn/Y Catalyst Combines Copolymerization of Epoxides and CO_2 with Group Transfer Polymerization of Michael-type Monomers"

Status: Communication, accepted February 19, 2020

Journal: ACS Macro Letters

Publisher: American Chemical Society

DOI: 10.1021/acsmacrolett.9b01025

Authors: Alina Denk,[‡] Sebastian Kernbichl,[‡] Andreas Schaffer, Moritz Kränzlein, Thomas Pehl, Bernhard Rieger[a]

Content

Extending the portfolio of CO_2-based polycarbonates can be achieved via the introduction of a different type of monomer which brings along interesting properties. The group transfer polymerization of Michael-type monomers yields polar polyolefins which stand out with water-solubility and a pH- and temperature-dependent solubility behavior for its copolymers. Since BDI complexes are known to not catalyze the GTP of monomers such as 2-vinylpyridine, a heterobifunctional complex has been designed. Its zinc unit promotes the ROCOP of CHO and CO_2 while the yttrium moiety, introduced via CH-bond activation, runs the GTP. End-group analysis by matrix-assisted laser desorption/ionization time-of-flight mass spectrometry of the CHO/CO_2 coupling product and the P2VP, obtained from the homopolymerization of 2VP, confirmed the successful transfer of the catalyst's linking unit onto the polymers. Terpolymerizations were performed with CHO, CO_2, and 2-vinylpyridine and IPOx, respectively. NMR studies revealed a decomposition of the catalyst upon treatment with CO_2. Therefore, the GTP was always performed in the beginning prior to the addition of CHO and CO_2. Copolymer formation was examined using aliquot gel permeation chromatography (GPC) analysis and solubility behavior tests which clearly show the presence of a terpolymer structure. Overall, a new class of polymers becomes accessible with promising properties which will be closer investigated in future studies.

[‡]These authors contributed equally; [a]A. Denk executed all the experiments and gave advice on the manuscript. S. Kernbichl had the initial idea and wrote the manuscript. A. Schaffer, M. Kränzlein and T. Pehl contributed within valuable ideas and discussions. All work was carried out under the supervision of B. Rieger.

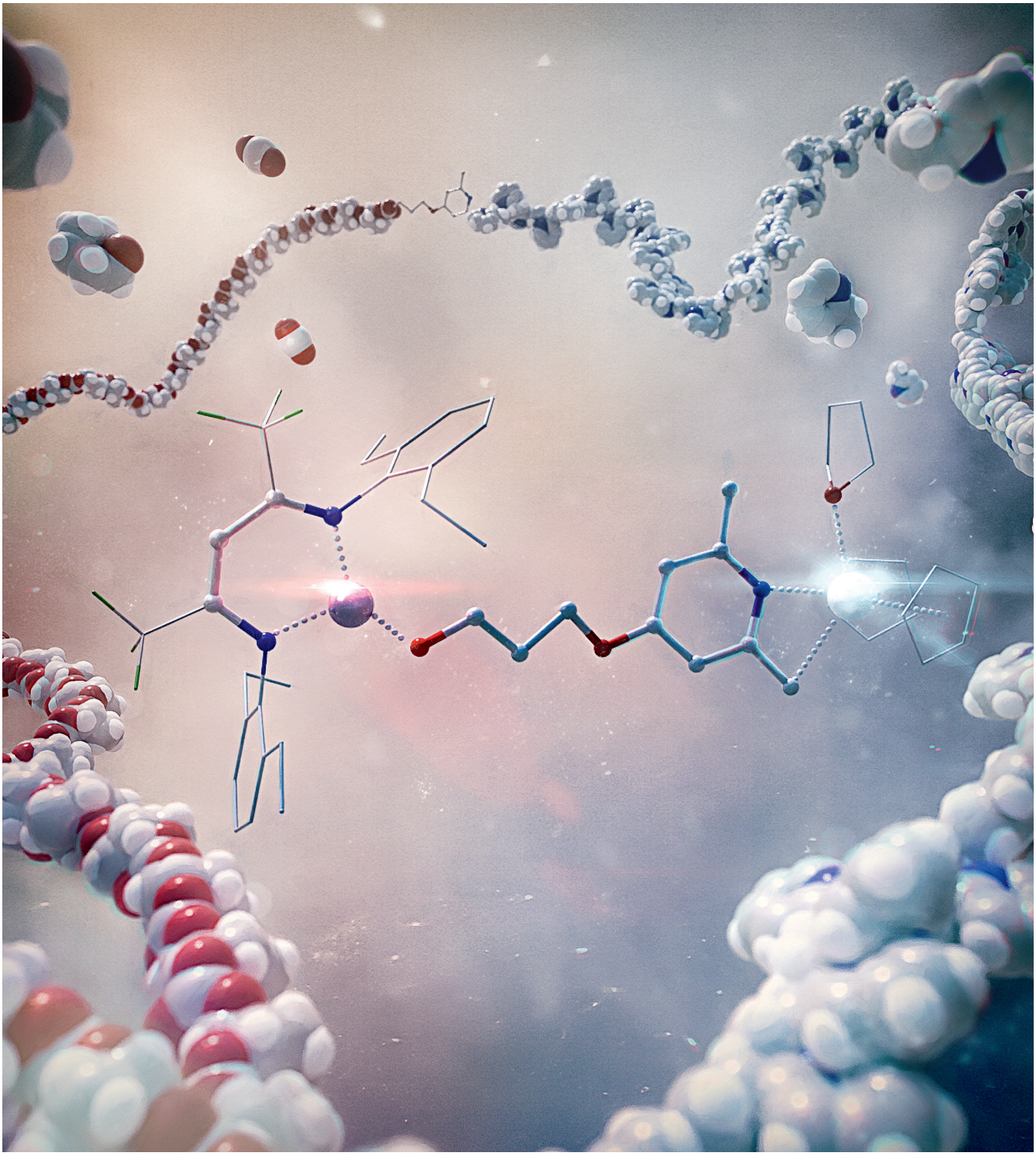

Cover art designed and created by Dr. Johannes Richers

ACS Macro Letters

pubs.acs.org/macroletters Letter

Heteronuclear, Monomer-Selective Zn/Y Catalyst Combines Copolymerization of Epoxides and CO_2 with Group-Transfer Polymerization of Michael-Type Monomers

Alina Denk,[†] Sebastian Kernbichl,[†] Andreas Schaffer, Moritz Kränzlein, Thomas Pehl, and Bernhard Rieger*

Cite This: https://dx.doi.org/10.1021/acsmacrolett.9b01025 Read Online

ACCESS | Metrics & More | Article Recommendations | Supporting Information

ABSTRACT: Terpolymerizations of cyclohexene oxide (CHO), CO_2, and the Michael-type monomer 2-vinylpyridine (2VP) are presented. The combination of two distinct polymerization mechanisms was enabled by the synthesis of a heterobifunctional complex (**3**). Its β-diiminate zinc moiety allows the ring-opening copolymerization of CHO and CO_2, whereas the yttrium metallocene catalyzed the rare earth metal-mediated group-transfer polymerization of the polar vinyl monomer. Both units were connected via the CH-bond activation of a pyridyl-alkoxide linker. Matrix-assisted laser desorption/ionization time-of-flight mass spectrometry (MALDI-TOF-MS) revealed the successful transfer of the linker to the end-group of the respective homopolymers poly(cyclohexene carbonate) (PCHC) and poly(2VP) (P2VP) being the prerequisite for copolymer formation. Aliquot gel-permeation chromatography (GPC) analysis and solubility behavior tests confirmed the P2VP-*block*(*b*)-PCHC terpolymer formation via two pathways, a sequential and a one-pot procedure. Furthermore, the versatility of the method was demonstrated by introducing 2-isopropenyl-2-oxazoline (IPOx) as the second Michael-type monomer that yielded the terpolymer poly(IPOx)-*b*-PCHC.

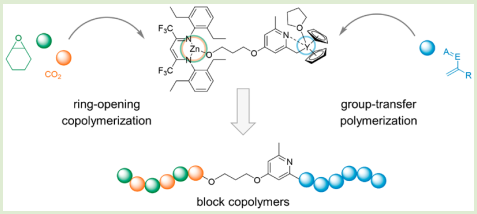

Although the ring-opening copolymerization (ROCOP) of epoxides and CO_2 was first reported 50 years ago, it remains a field of intense research.[1] The resulting aliphatic polycarbonates display attractive properties, such as biodegradability and high transparency, but the industrial demands in terms of thermal and mechanical performance have not been met yet.[2−4] The utilization of discrete, homogeneous transition metal catalysts allowed the precise synthesis of CO_2-based polymers in high activities and selectivities.[5−8] In order to improve the functionality of epoxide/CO_2-based aliphatic polycarbonates, block copolymers have been widely exploited in the last years. First, they were coupled with anhydrides to afford a novel class of polyesters.[9,10] Later, different lactones were incorporated as an additional block sequence by combining the ring-opening polymerization of lactones and the ROCOP of epoxides and CO_2.[11−20] Only a few catalysts were able to catalyze both reactions simultaneously, mainly β-diiminate zinc and dizinc phenoxide systems. Recently, our group reported the Lewis acidic BDI-Zn-N$(SiMe_3)_2$ complex **1**, which catalyzed the ROP of β-butyrolactone and the ROCOP of cyclohexene oxide and CO_2 to terpolymers in a block and statistical configuration, depending on the applied CO_2 pressure.[21]

The current study aimed to investigate the potential combination of aliphatic polycarbonates with polar polyolefins, derived from the polymerization of Michael-type monomers. The group-transfer polymerization (GTP) was initially observed by Webster et al. in 1983, where organosilicon compounds served as the initiators for the methyl methacrylate (MMA) polymerization.[22] Since then, GTP of polar monomers evolved to a valuable tool for the precise synthesis of tailor-made functional materials.[23,24] Rare-earth metal (REM) mediated GTP thereby plays an important role since high activities and the living character of the polymerization allow the synthesis of high-performance (co)polymers using monomers that range from diethyl vinylphosphonate to MMA and 2-vinylpyridine (2VP).[25−30] Currently, few studies have reported the generation of block copolymers consisting of polar polyolefins, such as PMMA and a polyester block from the ROP of a lactone.[31−34] The groups of Wang and Wu reported catalytic systems where the metal center catalyzes ROCOP of an epoxide and CO_2, and through the introduction of a second functional group, the reversible addition−fragmentation chain transfer polymerization of vinyl monomers was enabled.[35,36] Also, a Co(III) salen complex was presented that can be switched from radical polymerization to ROCOP by applying O_2 as an external stimulus.[37] But, none of these approaches combined GTP and ROCOP. Since BDI

Received: December 30, 2019
Accepted: February 19, 2020

https://dx.doi.org/10.1021/acsmacrolett.9b01025
ACS Macro Lett. XXXX, XXX, XXX−XXX

complexes are not known to catalyze the GTP of polar vinyl monomers, a heterobifunctional catalyst is required which connects two catalytically active moieties. Thereby, the zinc center would enable the coupling of the epoxide with CO_2, while the yttrium metallocene unit would precisely control the REM-GTP (Figure 1).

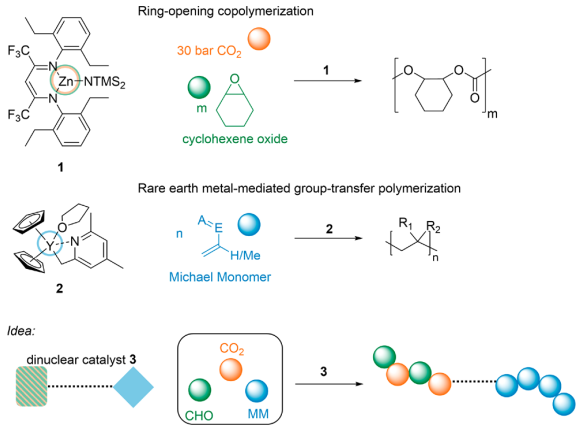

Figure 1. Top: ROCOP of CHO and CO_2 with the Lewis acidic zinc catalyst **1** to PCHC. Middle: REM-GTP of Michael-type monomers (MM) with the yttrium metallocene complex **2**. Bottom: Structure of a heteronuclear complex **3**, bearing both an yttrium and a zinc center displays the concept for the terpolymerization reaction.

Herein, we report the synthesis of a novel bifunctional catalyst **3** via the CH-bond activation of a BDI-Zn-O-pyridyl and $Cp_2Y(CH_2TMS)(thf)$. The successful end-group functionalization of the respective homopolymers, PCHC, P2VP, and PIPOx, was confirmed via MALDI-TOF MS. Catalyst **3** displayed high activity and chemoselectivity toward the ROCOP of CHO and CO_2 and the REM-GTP of 2VP and IPOx to give block copolymers using a sequential and a one-pot procedure. The resulting terpolymers were analyzed via GPC, solubility behavior, and differential scanning calorimetry (DSC).

The introduction of a suitable linking moiety was required in order to combine two different, catalytically active centers. As displayed in Scheme 1, the $-N(TMS)_2$ initiating group of **1** was successfully replaced by a pyridyl alcohol, yielding **3′**, which in turn underwent a σ-bond metathesis between one adjacent methyl group and $Cp_2Y(CH_2TMS)(thf)$ and afforded the dinuclear complex **3**. The CH-activation was monitored via ^1H NMR spectroscopy and was completed after stirring for 4 h at rt (Figure S5).

Scheme 1. Replacement of the Initiating Group of 1, Followed by the CH-Bond Activation of 3′ with $Cp_2Y(CH_2TMS)(thf)$, Yielding the Bifunctional Complex 3

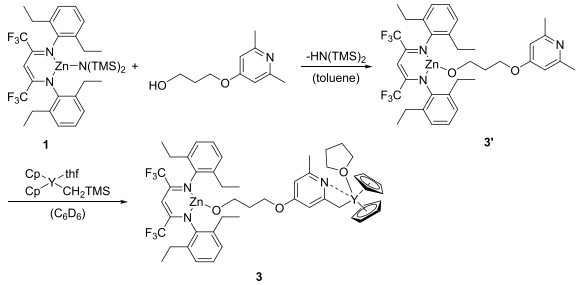

The homopolymerization of the Michael-type monomer 2VP with complex **3** was performed to check the effect of the two transition metal centers on the activity of the complex in the GTP which solely proceeded at the yttrium center (Figure S7). P2VP was produced and the subsequent MALDI-MS end-group analysis of the oligomerization experiment revealed that the pyridyl moiety was linked to the polymer (Figure S8). Due to the high structural flexibility of the linking unit in **3**, the isolation of crystals for single-crystal X-ray diffraction failed. Although BDI complexes, bearing zinc alkoxide initiators, are known to catalyze the coupling of CHO and CO_2, complex **3** was tested in the copolymerization of CHO and CO_2 (Table 1, entry 1).[5] In situ attenuated total reflection infrared spectroscopy of the polymerization at 30 bar CO_2 disclosed a reaction time of 10 h (Figure S9). Compared with the already reported complex **1**, the bifunctional complex **3** was less active for the coupling of CHO and CO_2, but full conversion could still be achieved (yttrium metallocene **2** did not show conversion for the CHO/CO_2 coupling, Figure S6).[7] This prolonged reaction time could not be explained in detail, but a steric shielding of the zinc center and a competing coordination of CO_2 at the yttrium center was assumed. Electrospray ionization mass spectrometry (ESI-MS) and MALDI-MS measurements confirmed the presence of the pyridyl initiator as the polymer end-group, which was essential for the successful linking of the two planned polymer blocks (Figures S10 and S11).

Complex **3** was first tested in the sequential route with the ROCOP of CHO and CO_2 in the beginning, yielding PCHC in >99% conversion (Table 1, entry 2). Surprisingly, no P2VP formation could be observed upon adding 100 equiv of 2VP. The reason could be addressed via ^1H NMR spectroscopy by applying solely CO_2 on **3** (Figure S12). Carbon dioxide affected the dissociation of the coordinated thf molecule as well as the η^5-coordination of the Cp ligands. Moreover, the signal of the CH_2 group resulting from the CH-activation disappears, implying that the yttrium moiety was no longer bound to the pyridyl linker. GPC analysis of the PCHC block revealed a monomodal distribution, although bimodality for PCHC is well-known in literature and can be caused by catalytic traces of water that act as a chain-transfer agent.[38−41] Considering that such a chain-transfer may generate homopolymeric byproducts, the polymerizations with catalyst **3** were performed under inert conditions and freshly distilled monomers are used to prevent this side reaction. The second possibility for a sequential route starts with the homopolymerization of 2VP prior to the addition of CHO and CO_2. Indeed, conversion both to P2VP and PCHC could be observed (Table 1, entry 3). Scheme 2 presents the possible reaction pathways for the sequential route and a one-pot procedure.

In order to confirm that both polymer blocks were connected to each other and no homopolymeric byproducts were formed, an aliquot was taken before the epoxide was added. The absolute molecular weight for the P2VP block was determined by GPC analysis in DMF. A good agreement between the experimentally determined and theoretically expected M_n values indicates a high initiator efficiency of 70%. GPC analysis of the P2VP aliquot and the final terpolymer revealed a shift of the GPC traces to lower retention times (Figure 2).

https://dx.doi.org/10.1021/acsmacrolett.9b01025
ACS Macro Lett. XXXX, XXX, XXX−XXX

ACS Macro Letters pubs.acs.org/macroletters Letter

Table 1. Terpolymerization of CHO and CO_2 with 2VP and IPOx, Respectively, Using the Bifunctional Catalyst 3

entry	feed[a]	reaction pathway[b]	conv. A[c] [%]	M_n (A)[d] (Đ)[e] [kg/mol]	I[f]	conv. B[c] [%]	M_n (A-b-BC)[g] (Đ) [kg/mol]	[A]:[BC][h]
1[i]	CHO_{100}					98	28.2 (1.32)	0:100
2	$2VP_{100}$:CHO_{100}	sequential	0			>99	17.5 (1.20)[j]	0:100
3	$2VP_{100}$:CHO_{100}	sequential	58	8.7 (1.16)	0.70	97	20.0 (1.25)	34:66
4	$2VP_{100}$:CHO_{200}	sequential	57	7.0 (1.33)	0.86	93	37.2 (1.37)	18:82
5	$2VP_{100}$:CHO_{100}	one pot	30	4.7[k] (1.13)	0.68	93	17.0 (1.30)	23:77
6	$IPOx_{100}$:CHO_{100}	sequential	82	14.9[k] (1.41)	0.61	99	23.0 (1.37)	50:50
7	$IPOx_{100}$:CHO_{100}	one pot	77	9.7[k] (1.56)	0.88	97	17.7 (1.40)	41:59

[a]Monomer feed of the respective monomers, [3] = 8.39 μmol in 1.2 mL toluene. [b]Reaction pathway according to Scheme 2. [c]Conversion determined via ^{1}H NMR spectroscopy. [d]Absolute molecular weight of block *A* (P2VP) determined via triple detection GPC analysis in DMF as eluent at 30 °C (d*n*/d*c* = 0.149 mL/g). [e]Polydispersity calculated from $M_{w,GPC}/M_{n,GPC}$ determined via GPC in DMF. [f]Initiator efficiency $I = M_{n,\,theo}/M_n(A)$, $M_{n,\,theo}$ = eq (2VP/IPOx) × M_n (2VP/IPOx) × conversion. [g]Molecular weight of the final terpolymer determined via GPC analysis in DMF as eluent at 30 °C relative to PMMA standards. [h]Composition of the terpolymer after precipitation in pentane determined via ^{1}H NMR spectroscopy. [i]Polymerization performed in an autoclave with in situ IR monitoring. [j]Only PCHC was produced. [k]Absolute molecular weight of block *A* determined via ^{1}H NMR spectroscopy.

Scheme 2. Overview of the Two Possible Polymerization Pathways

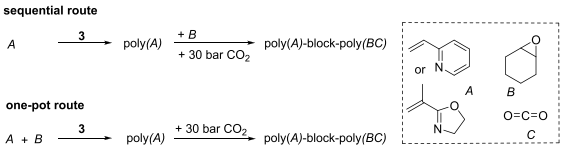

Solubility experiments were also performed. PCHC has no solubility in methanol, but the terpolymer consisting of 34% P2VP and 66% PCHC was soluble in methanol, as confirmed by ^{1}H NMR spectroscopy (Figure 2). It was also observed that the composition slightly changed to P2VP:PCHC = 41:59, owing to traces of homopolymeric PCHC. The same solubility test was conducted for an artificial polymer blend, where no PCHC was found in the methanol phase (Figure S13). Next, 200 equiv of CHO were added to the reaction mixture after successful 2VP polymerization, and again, a terpolymer was formed (Table 1, entry 4). GPC analysis confirmed the successful block formation (Figure 2). Due to the very high PCHC content, the terpolymer was not soluble in methanol any longer. The insoluble part was characterized via ^{1}H NMR, and the same P2VP:PCHC composition was found, indicating that the P2VP block was connected to the PCHC unit (homopolymeric P2VP is soluble in methanol; Figure S31). Also, for this polymerization, a slight shouldering of the GPC trace is observed that is most likely caused by homopolymeric PCHC. We were curious if the one-pot pathway also yields P2VP/PCHC terpolymers. Since CO_2 led to the decomposition of the yttrium unit, both monomers, 2VP and CHO, were mixed with **3** in the autoclave, and after stirring for 4 h, 30 bar CO_2 was applied. The conversion of 2VP decreased, probably due to the competing coordination of CHO at the yttrium moiety. Nevertheless, a terpolymer with a monomodal distribution and a dispersity of 1.30 was obtained (Table 1, entry 5). This finding demonstrates that the one-pot procedure allows the switch from the REM-GTP to the ROCOP by the addition of carbon dioxide. DSC measurements of a P2VP-*b*-PCHC terpolymer revealed a mixed glass transition temperature (T_g) of 110 °C ($T_{g,PCHC}$ = 117 °C, $T_{g,P2VP}$ = 97 °C), while thermogravimetric analysis indicated a decomposition temperature of T_{max} = 280 °C (Figures S33 and S34). In addition, IPOx as a second Michael-type monomer was selected to test the versatility of the system. ESI-MS end-group analysis of the oligomerization experiments showed the successful transfer of the pyridyl-initiating group to the PIPOx polymer (Figure S35). Terpolymerization attempts were conducted in both pathways (Table 1, entries 6 and 7), and high IPOx conversions (>77%) in high initiator efficiencies (*I* > 61%) resulted in PIPOx/PCHC terpolymers of equimolar composition. Two glass transitions were observed at 125 and 185 °C ($T_{g,PCHC}$ = 117 °C, $T_{g,PIPOx}$ = 174 °C; Figure S36).

In conclusion, we introduced a bifunctional complex bearing a Lewis acidic zinc moiety and an yttrium metallocene unit, linked via a pyridyl-alkoxide linker. Terpolymerizations were achieved by connecting the ROCOP of epoxides and CO_2 at the zinc center and the REM-GTP of Michael-type monomers

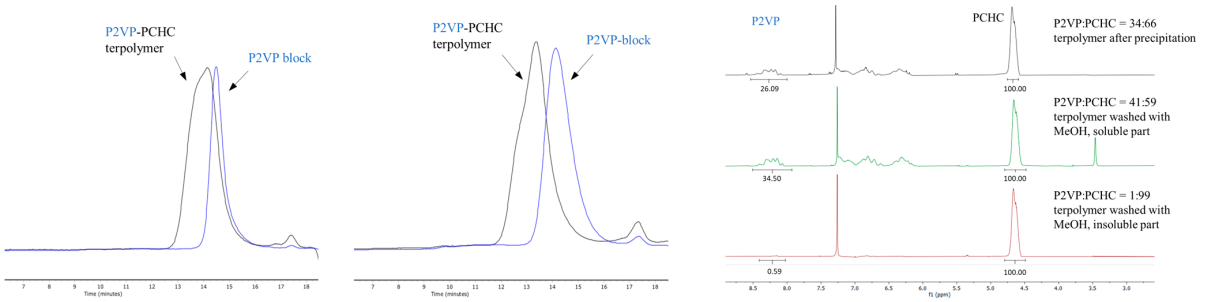

Figure 2. GPC traces. Left and middle: shift of signal from P2VP block (blue) to P2VP-PCHC terpolymer (black) for Table 1, entries 3 and 4, respectively. Right: ^{1}H NMR spectra (right) of a P2VP-PCHC terpolymer (Table 1, entry 3) prior to (black) and after (green) washing with methanol compared with the spectrum of the insoluble part (red).

https://dx.doi.org/10.1021/acsmacrolett.9b01025
ACS Macro Lett. XXXX, XXX, XXX−XXX

at the yttrium side. The resulting two-block terpolymers could be obtained both via a sequential and a one-pot procedure and consist of P2VP-*b*-PCHC and PIPOx-*b*-PCHC. This combination of aliphatic polycarbonates and polar polyolefins, therefore, offers many possibilities in terms of synthetic variations and terpolymer properties that are not accessible with the respective homopolymers.

■ ASSOCIATED CONTENT

Supporting Information

The Supporting Information is available free of charge at https://pubs.acs.org/doi/10.1021/acsmacrolett.9b01025.

Detailed experimental procedures for catalyst synthesis and polymerizations, ESI-MS and MALDI-MS end-group analysis, NMRs of selected polymers, GPC, DSC, and TGA data (PDF)

■ AUTHOR INFORMATION

Corresponding Author

Bernhard Rieger − *WACKER-Chair of Macromolecular Chemistry, Catalysis Research Center, Technical University Munich 85748 Garching, Germany;* orcid.org/0000-0002-0023-884X; Phone: +49-89-289-13570; Email: rieger@tum.de; Fax: +49-89-289-13562

Authors

Alina Denk − *WACKER-Chair of Macromolecular Chemistry, Catalysis Research Center, Technical University Munich 85748 Garching, Germany*

Sebastian Kernbichl − *WACKER-Chair of Macromolecular Chemistry, Catalysis Research Center, Technical University Munich 85748 Garching, Germany*

Andreas Schaffer − *WACKER-Chair of Macromolecular Chemistry, Catalysis Research Center, Technical University Munich 85748 Garching, Germany*

Moritz Kränzlein − *WACKER-Chair of Macromolecular Chemistry, Catalysis Research Center, Technical University Munich 85748 Garching, Germany*

Thomas Pehl − *WACKER-Chair of Macromolecular Chemistry, Catalysis Research Center, Technical University Munich 85748 Garching, Germany*

Complete contact information is available at: https://pubs.acs.org/10.1021/acsmacrolett.9b01025

Author Contributions

†These authors contributed equally to this work.

Notes

The authors declare no competing financial interest.

■ REFERENCES

(1) Inoue, S.; Koinuma, H.; Tsuruta, T. Copolymerization of carbon dioxide and epoxide. *J. Polym. Sci., Part B: Polym. Lett.* **1969**, *7*, 287−292.

(2) Rieger, B.; Künkel, A.; Coates, G. W. *Synthetic Biodegradable Polymers Springer*; Berlin/Heidelberg: Germany, 2012.

(3) Lu, X. B. *Carbon Dioxide and Organometallics*; Springer International Publishing, 2015.

(4) Kozak, C. M.; Ambrose, K.; Anderson, T. S. Copolymerization of carbon dioxide and epoxides by metal coordination complexes. *Coord. Chem. Rev.* **2018**, *376*, 565−587.

(5) Cheng, M.; Lobkovsky, E. B.; Coates, G. W. Catalytic Reactions Involving C1 Feedstocks: New High-Activity Zn(II)-Based Catalysts for the Alternating Copolymerization of Carbon Dioxide and Epoxides. *J. Am. Chem. Soc.* **1998**, *120*, 11018−11019.

(6) Coates, G. W.; Moore, D. R. Discrete Metal-Based Catalysts for the Copolymerization of CO2 and Epoxides: Discovery, Reactivity, Optimization, and Mechanism. *Angew. Chem., Int. Ed.* **2004**, *43*, 6618−6639.

(7) Reiter, M.; Vagin, S.; Kronast, A.; Jandl, C.; Rieger, B. A Lewis acid [small beta]-diiminato-zinc-complex as all-rounder for co- and terpolymerisation of various epoxides with carbon dioxide. *Chem. Sci.* **2017**, *8*, 1876−1882.

(8) Kissling, S.; Lehenmeier, M. W.; Altenbuchner, P. T.; Kronast, A.; Reiter, M.; Deglmann, P.; Seemann, U. B.; Rieger, B. Dinuclear zinc catalysts with unprecedented activities for the copolymerization of cyclohexene oxide and CO_2. *Chem. Commun.* **2015**, *51*, 4579−4582.

(9) Jeske, R. C.; DiCiccio, A. M.; Coates, G. W. Alternating Copolymerization of Epoxides and Cyclic Anhydrides: An Improved Route to Aliphatic Polyesters. *J. Am. Chem. Soc.* **2007**, *129*, 11330−11331.

(10) Jeske, R. C.; Rowley, J. M.; Coates, G. W. Pre-Rate-Determining Selectivity in the Terpolymerization of Epoxides, Cyclic Anhydrides, and CO2: A One-Step Route to Diblock Copolymers. *Angew. Chem., Int. Ed.* **2008**, *47*, 6041−6044.

(11) Romain, C.; Zhu, Y.; Dingwall, P.; Paul, S.; Rzepa, H. S.; Buchard, A.; Williams, C. K. Chemoselective Polymerizations from Mixtures of Epoxide, Lactone, Anhydride, and Carbon Dioxide. *J. Am. Chem. Soc.* **2016**, *138*, 4120−4131.

(12) Wu, G.-P.; Darensbourg, D. J.; Lu, X.-B. Tandem Metal-Coordination Copolymerization and Organocatalytic Ring-Opening Polymerization via Water To Synthesize Diblock Copolymers of Styrene Oxide/CO2 and Lactide. *J. Am. Chem. Soc.* **2012**, *134*, 17739−17745.

(13) Darensbourg, D. J.; Wu, G.-P. A One-Pot Synthesis of a Triblock Copolymer from Propylene Oxide/Carbon Dioxide and Lactide: Intermediacy of Polyol Initiators. *Angew. Chem., Int. Ed.* **2013**, *52*, 10602−10606.

(14) Zhu, Y.; Romain, C.; Williams, C. K. Selective Polymerization Catalysis: Controlling the Metal Chain End Group to Prepare Block Copolyesters. *J. Am. Chem. Soc.* **2015**, *137*, 12179−12182.

(15) Hwang, Y.; Jung, J.; Ree, M.; Kim, H. Terpolymerization of CO2 with Propylene Oxide and ε-Caprolactone Using Zinc Glutarate Catalyst. *Macromolecules* **2003**, *36*, 8210−8212.

(16) Hwang, Y.; Kim, H.; Ree, M. Zinc Glutarate Catalyzed Synthesis and Biodegradability of Poly(carbonate-co-ester)s from CO_2, Propylene Oxide, and ε-Caprolactone. *Macromol. Symp.* **2005**, *224*, 227−238.

(17) Kernbichl, S.; Reiter, M.; Mock, J.; Rieger, B. Terpolymerization of β-Butyrolactone, Epoxides, and CO_2: Chemoselective CO_2-Switch and Its Impact on Kinetics and Material Properties. *Macromolecules* **2019**, *52*, 8476.

(18) Kröger, M.; Folli, C.; Walter, O.; Döring, M. Alternating Copolymerization of Carbon Dioxide and Cyclohexene Oxide and Their Terpolymerization with Lactide Catalyzed by Zinc Complexes of N. *Adv. Synth. Catal.* **2006**, *348*, 1908−1918.

(19) Romain, C.; Williams, C. K. Chemoselective Polymerization Control: From Mixed-Monomer Feedstock to Copolymers. *Angew. Chem., Int. Ed.* **2014**, *53*, 1607−1610.

(20) Paul, S.; Romain, C.; Shaw, J.; Williams, C. K. Sequence Selective Polymerization Catalysis: A New Route to ABA Block Copoly(ester-b-carbonate-b-ester). *Macromolecules* **2015**, *48*, 6047−6056.

(21) Kernbichl, S.; Reiter, M.; Adams, F.; Vagin, S.; Rieger, B. CO_2-Controlled One-Pot Synthesis of AB, ABA Block, and Statistical Terpolymers from β-Butyrolactone, Epoxides, and CO_2. *J. Am. Chem. Soc.* **2017**, *139*, 6787−6790.

(22) Webster, O. W.; Hertler, W. R.; Sogah, D. Y.; Farnham, W. B.; RajanBabu, T. V.; et al. *J. Am. Chem. Soc.* **1983**, *105*, 5706−5708.

https://dx.doi.org/10.1021/acsmacrolett.9b01025
ACS Macro Lett. XXXX, XXX, XXX−XXX

(23) Chen, E. Y. X. Coordination Polymerization of Polar Vinyl Monomers by Single-Site Metal Catalysts. *Chem. Rev.* **2009**, *109*, 5157−5214.
(24) Soller, B. S.; Salzinger, S.; Rieger, B. Rare Earth Metal-Mediated Precision Polymerization of Vinylphosphonates and Conjugated Nitrogen-Containing Vinyl Monomers. *Chem. Rev.* **2016**, *116*, 1993−2022.
(25) Yasuda, H.; Ihara, E. Rare earth metal initiated polymerizations of polar and nonpolar monomers to give high molecular weight polymers with extremely narrow molecular weight distribution. *Macromol. Chem. Phys.* **1995**, *196*, 2417−2441.
(26) Soller, B. S.; Salzinger, S.; Jandl, C.; Pöthig, A.; Rieger, B. C−H Bond Activation by σ-Bond Metathesis as a Versatile Route toward Highly Efficient Initiators for the Catalytic Precision Polymerization of Polar Monomers. *Organometallics* **2015**, *34*, 2703−2706.
(27) Altenbuchner, P. T.; Soller, B. S.; Kissling, S.; Bachmann, T.; Kronast, A.; Vagin, S. I.; Rieger, B. Versatile 2-Methoxyethylaminobis-(phenolate)yttrium Catalysts: Catalytic Precision Polymerization of Polar Monomers via Rare Earth Metal-Mediated Group Transfer Polymerization. *Macromolecules* **2014**, *47*, 7742−7749.
(28) Adams, F.; Pahl, P.; Rieger, B. Metal-Catalyzed Group-Transfer Polymerization: A Versatile Tool for Tailor-Made Functional (Co)Polymers. *Chem. - Eur. J.* **2018**, *24*, 509−518.
(29) Kaneko, H.; Nagae, H.; Tsurugi, H.; Mashima, K. End-Functionalized Polymerization of 2-Vinylpyridine through Initial C−H Bond Activation of N-Heteroaromatics and Internal Alkynes by Yttrium Ene−Diamido Complexes. *J. Am. Chem. Soc.* **2011**, *133*, 19626−19629.
(30) Wang, Q.; Chen, S.; Liang, Y.; Dong, D.; Zhang, N. Bottle-Brush Brushes: Surface-Initiated Rare Earth Metal Mediated Group Transfer Polymerization from a Poly(3-((2,6-dimethylpyridin-4-yl)-oxy)propyl methacrylate) Backbone. *Macromolecules* **2017**, *50*, 8456−8463.
(31) Kostakis, K.; Mourmouris, S.; Karanikolopoulos, G.; Pitsikalis, M.; Hadjichristidis, N. Ring-opening polymerization of lactones using zirconocene catalytic systems: Block copolymerization with methyl methacrylate. *J. Polym. Sci., Part A: Polym. Chem.* **2007**, *45*, 3524−3537.
(32) Solaro, R.; Cantoni, G.; Chiellini, E. Polymerisability of different lactones and methyl methacrylate in the presence of various organoaluminium catalysts. *Eur. Polym. J.* **1997**, *33*, 205−211.
(33) Dove, A. P.; Gibson, V. C.; Marshall, E. L.; White, A. J. P.; Williams, D. J. A well-defined magnesium enolate initiator for the living and highly syndioselective polymerisation of methylmethacrylate. *Chem. Commun.* **2002**, 1208−1209.
(34) Kajiwara, A.; Matyjaszewski, K. Formation of Block Copolymers by Transformation of Cationic Ring-Opening Polymerization to Atom Transfer Radical Polymerization (ATRP). *Macromolecules* **1998**, *31*, 3489−3493.
(35) Wang, Y.; Zhao, Y.; Ye, Y.; Peng, H.; Zhou, X.; Xie, X.; Wang, X.; Wang, F. A One-Step Route to CO2-Based Block Copolymers by Simultaneous ROCOP of CO2/Epoxides and RAFT Polymerization of Vinyl Monomers. *Angew. Chem., Int. Ed.* **2018**, *57*, 3593−3597.
(36) Zhang, Y.-Y.; Yang, G.-W.; Wu, G.-P. A Bifunctional β-Diiminate Zinc Catalyst with CO2/Epoxides Copolymerization and RAFT Polymerization Capacities for Versatile Block Copolymers Construction. *Macromolecules* **2018**, *51*, 3640−3646.
(37) Zhao, Y.; Wang, Y.; Zhou, X.; Xue, Z.; Wang, X.; Xie, X.; Poli, R. Oxygen-Triggered Switchable Polymerization for the One-Pot Synthesis of CO2-Based Block Copolymers from Monomer Mixtures. *Angew. Chem.* **2019**, *131*, 14449−14456.
(38) Nakano, K.; Kamada, T.; Nozaki, K. Selective Formation of Polycarbonate over Cyclic Carbonate: Copolymerization of Epoxides with Carbon Dioxide Catalyzed by a Cobalt(III) Complex with a Piperidinium End-Capping Arm. *Angew. Chem., Int. Ed.* **2006**, *45*, 7274−7277.
(39) Moore, D. R.; Cheng, M.; Lobkovsky, E. B.; Coates, G. W. Mechanism of the Alternating Copolymerization of Epoxides and CO2 Using β-Diiminate Zinc Catalysts: Evidence for a Bimetallic Epoxide Enchainment. *J. Am. Chem. Soc.* **2003**, *125*, 11911−11924.
(40) Kember, M. R.; Williams, C. K. Efficient Magnesium Catalysts for the Copolymerization of Epoxides and CO2; Using Water to Synthesize Polycarbonate Polyols. *J. Am. Chem. Soc.* **2012**, *134*, 15676−15679.
(41) Na, S. J.; Sujith, S.; Cyriac, A.; Kim, B. E.; Yoo, J.; Kang, Y. K.; Han, S. J.; Lee, C.; Lee, B. Y. Elucidation of the Structure of a Highly Active Catalytic System for CO2/Epoxide Copolymerization: A salen-Cobaltate Complex of an Unusual Binding Mode. *Inorg. Chem.* **2009**, *48*, 10455−10465.

https://dx.doi.org/10.1021/acsmacrolett.9b01025
ACS Macro Lett. XXXX, XXX, XXX−XXX

10. Aliphatic Polycarbonates Derived From Epoxides and CO_2: A Comparative Study of Poly(cyclohexene carbonate) and Poly(limonene carbonate)

Title: "Aliphatic Polycarbonates Derived From Epoxides and CO_2: A Comparative Study of Poly(cyclohexene carbonate) and Poly(limonene carbonate)"

Status: Full Paper, manuscript in preparation

Journal: Polymer

Publisher: Elsevier

Authors: Sebastian Kernbichl, Bernhard Rieger[a]

Content

Poly(cyclohexene carbonate) is considered as the benchmark system in the context of ROCOP of epoxides and CO_2 catalyzed by various complexes. In contrast, the novel poly(limonene carbonate) is only accessible by two different catalysts. In this study, a BDI^{CF3}-Zn-$N(SiMe_3)_2$ serves as an active initiator for both CHO and LO with CO_2. The synthesis of the two copolymers was studied with in situ IR spectroscopy to gain valuable information for the upscaling process which was performed in a 1 L reactor to yield 125 g PCHC and 45 g PLC. After removal of the catalyst, the polymers were characterized regarding thermal stability in a muffle oven and consequent GPC analysis to detect chain breaks. Also, the grinded polymer was used for the preparation of round-shaped specimens. Multiaxial pressure tests and DMA analysis reveal major differences compared to the commercial polymers Makrolon®, Durabio®, and PMMA. The aliphatic polycarbonates turned out to be less brittle than PMMA but also less impact resistant than Makrolon® and Durabio®. Additionally, terpolymerization reactions with CHO, LO, and CO_2 were performed. Polymerization with in situ NMR spectroscopy indicate the exclusive polymerization of CHO/CO_2 in the beginning and full CHO conversion is reached prior to LO/CO_2 polymerization. Diffusion-ordered NMR spectroscopy confirmed the presence of a terpolymer with one diffusion coefficient.

[a]S. Kernbichl had the initial idea, performed all experiments and wrote the manuscript. All work was carried out under the supervision of B. Rieger

Manuscript draft

Aliphatic Polycarbonates Derived From Epoxides and CO_2: A Comparative Study of Poly(cyclohexene carbonate) and Poly(limonene carbonate)

Sebastian Kernbichl, and Bernhard Rieger*

WACKER-Chair of Macromolecular Chemistry, Catalysis Research Center, Technical University Munich, Lichtenbergstr. 4, 85748 Garching, Germany

Keywords: copolymerization, epoxide, carbon dioxide, limonene oxide, zinc catalysis

Abstract

The ring-opening copolymerization (ROCOP) of epoxides and CO_2 provides an alternative approach towards polycarbonates and due to their aliphatic nature represents an interesting alternative to bisphenol-A based polycarbonates. A Lewis acidic BDI^{CF3}-Zn-$Si(Me_3)_2$ complex **1** is used in the ROCOP of CO_2 with cyclohexene oxide (CHO) and limonene oxide (LO), respectively. The knowledge gained from polymerizations monitored via in situ IR spectroscopy was used to upscale the reaction to a 1 L reactor. The two products poly(cyclohexene carbonate) (PCHC) and poly(limonene carbonate) (PLC) were then characterized via thermal analysis, a multiaxial pressure test, and dynamic mechanical analysis and compared with commercial polymers. While PCHC and PLC were both thermally stable at 150 °C for 20 minutes and only minor decomposition occurred at 180 °C, PLC is prone to cross-linking at elevated temperatures. This could be prevented by hydrogenation of the double bond or by the addition of an antioxidant. In the mechanical performance, the aliphatic polymers ranged between the highly impact resistant Durabio® and the brittle PMMA but broke without a splintering of the material. Overall, this study enabled a classification of CO_2-based polycarbonates, especially of the novel PLC. Additionally, complex **1** was active in the terpolymerization of CHO, LO, and CO_2. The formation of an actual terpolymer was confirmed via aliquot gel-permeation chromatography and diffusion-ordered NMR spectroscopy. High-pressure NMR techniques reveal an interesting kinetic feature. CHO gets copolymerized with CO_2 exclusively, and LO incorporation only starts when CHO is fully consumed.

1. Introduction

When Inoue and coworkers applied carbon dioxide to a mixture of diethylzinc, water and propylene oxide in 1969, they produced the aliphatic poly(propylene carbonate) (PPC) for the first time.[1-2] Although the heterogeneous zinc glutarate enabled a small scale industrialization of PPC, research focused more on homogeneous systems in the last centuries since they exhibit the highest activities and selectivities for the ring-opening copolymerization of epoxides and CO_2.[3-4] The most important ligand structures have turned out to be porphyrines,[5] salens,[6-7] phenoxides,[8-9] or β-diiminates (BDI)[10-12]. The copolymerization of cyclohexene oxide (CHO) and CO_2 usually serves as a benchmark in catalysis research regarding polymerization activity.[13-17] Propylene oxide (PO) and the bio-based epoxide

limonene oxide (LO) are also studied intensively but overall lower activities are observed. Especially in case of limonene oxide, only two catalytic systems are known to promote the coupling with CO_2. In 2004, Coates *et al.* tested a BDI-Zn-OAc complex for the copolymerization of limonene oxide and CO_2 and observed a TOF of 37 h^{-1}.[18] Interestingly, only the *trans*-isomer was consumed during the polymerization. It was not until 2015 that Kleij and coworkers synthesized an amino(triphenolate) aluminum complex showing a moderate activity of 3 h^{-1} but the incorporation of both stereoisomers.[19] In 2017, our group reported a BDI zinc complex bearing two electron-withdrawing groups and an -$N(SiMe_3)_2$ initiating group.[20] This BDI^{CF3}-Zn-$N(SiMe_3)_2$ **1** showed a TOF of 310 h^{-1} for the copolymerization of LO and CO_2 but also a very high activity for other epoxides such as CHO, PO or the rather exotic octene oxide and styrene oxide.

Scheme 1. Complex 1 in the copolymerization of CHO and CO_2 to poly(cyclohexene carbonate) and limonene oxide and CO_2 to poly(limonene carbonate).

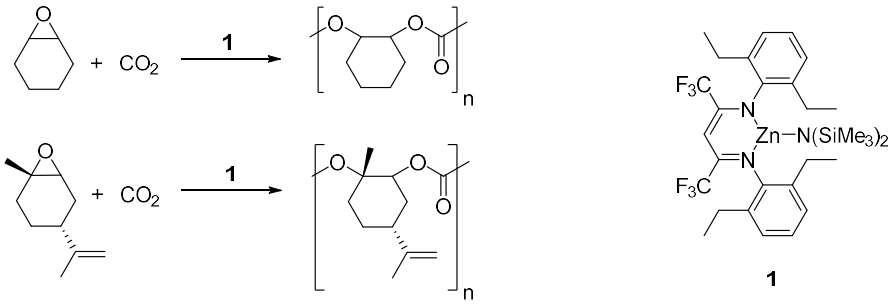

In case of poly(cyclohexene carbonate) (PCHC), the material properties including most of the thermal and mechanical characterizations have well been reported.[21-25] On the contrary, poly(limonene carbonate) (PLC) is rather sparsely described in literature and aside from that, not directly compared to PCHC.[26-29] Thanks to the high activity of complex **1** in the copolymerization of both CHO and LO with CO_2, we herein report on the in situ IR monitoring and the scale-up of both copolymerization reactions. Based on this, a detailed thermal analysis of the two resulting polymers PCHC and PLC has been conducted. Extrusion attempts in a micro-scale twin screw extruder, a multiaxial pressure test and a dynamic mechanical analysis were performed. Furthermore, one-pot terpolymerizations with CHO, LO, and CO_2 were realized and investigated regarding the kinetics of the two different epoxides.

2. Experimental Section

2.1 Materials

All reactions containing air- and/or moisture sensitive compounds were performed under argon conditions using standard Schlenk techniques. All chemicals were purchased from Aldrich or TCI. Monomers were dried over calcium hydride or sodium hydride and distilled prior to polymerization. CO_2 was purchased from Westfalen (purity 4.6). Dry toluene was purified with an MBraun MB-SPS-800 solvent purification system.

2.2 Synthesis

Limonene oxide used in this work consisted of 85% *trans*-LO and 15% *cis*-LO and was prepared according to literature procedures.[26] BDI-Zn-$NTMS_2$ complex **1** was prepared according to a literature procedure and purified via recrystallization.[20,30]

2.3 Characterization Techniques

NMR (^1H and ^{13}C) measurements were recorded on a Bruker AVIII500 Cryo and an AV300 spectrometer. Chemical shifts δ were reported in ppm relative to tetramethylsilane and calibrated to the residual ^1H or ^{13}C signal of the deuterated solvent. Deuterated solvents were obtained from Aldrich and dried over a 3 Å molecular sieve. In situ IR measurements were performed under argon atmosphere using an ATR IR MettlerToledo system. Kinetic investigations were all performed in the same reactor under identical conditions. GPC was performed on a Varian PL-GPC 50 using THF (HPLC grade) with 0.22 g L-1 2.6 di-tert-butyl-4-methylphenol and a flow rate of 1 mL/min at 40 °C. Poly(limonene carbonate) was measured at a Varian PL-GPC 50 using chloroform (HPLC grade) with a flow rate of 1 mL/min at 25 °C. Polystyrene standards were used for calibration. DSC was conducted on a DSC Q2000 instrument. 3-6 mg of the polymer was filled into a DSC aluminum pan and heated from -30 °C to 170 °C at a rate of 5 K/min. The reported values were determined with TA Universal Analysis from the second heating cycle. DMA measurements were performed with rectangular specimens (10x1x50 mm) on an Anton Parr machine MCR502. A frequency of 1 Hz and a shear deformation of 0.2% in a temperature range from -150 to 180 °C were applied. The multiaxial pressure test was conducted with round-shaped specimens with a diameter of 25 mm and a thickness of 1.0 mm on an Instron machine 5566. A speed of 1 mm/min was applied. Transmission measurements were carried out at a Cary 50 UV-vis spectrophotometer (Varian) in a range from 300–800 nm. Extrusion attempts were performed at a DACA Instruments microcompounder. For the thermal stability tests, the polymer samples were tempered in a Nabertherm muffle oven at the indicated temperature. The polymers were put into the oven and heated to the desired temperature within exact five minutes. Upon reaching the temperature, the polymers were heated for 20 minutes, immediately removed from the oven and cooled down to room temperature in air. Consequently, GPC measurements were performed to check whether the polymer chain is degraded or not.

3. Results and Discussion

Upscaling. Only a few reports deal with the question how the homogeneously catalyzed lab-scale copolymerization of an epoxide and CO_2 can be upscaled.[21,31] Most importantly, this upscaling should be performed under economical aspects especially the amount and the synthesis costs of a suitable catalyst and the yield of the polymerization. Greiner and co-workers showed one example of the copolymerization of limonene oxide and CO_2 using a BDI-Zn-OAc catalyst yielding >1 kg PLC.[26] The authors give only little information on the polymerization parameters like amount of employed catalyst

and solvent and on the molecular weight and dispersity of the resulting polymer. In this work, a stepwise upscaling was performed for both CHO and LO. Initial polymerization attempts were always performed in a 50 mL autoclave with in situ IR monitoring to get further insight into the reaction kinetics (Figure 1). Major differences between the two monomers arise from the reaction time and the catalyst-to-monomer ratio. Whereas CHO can be coupled with CO_2 by **1** in high turn-over frequencies (time <1 h) and high catalyst-to-monomer ratios (1:2000), LO behaves as a rather reluctant monomer (time >6 h) (Table 1, entries 1 and 2).

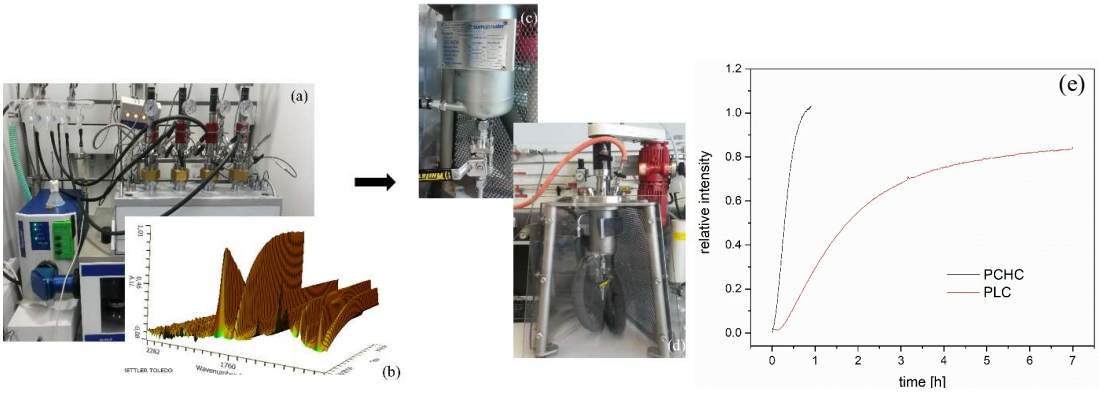

Figure 1. In situ IR monitored copolymerization of CHO/LO with CO_2 utilizing **1** under the conditions used in the upscaling polymerizations (a) and (b). 1 L Buchi reactor (c) equipped with a heating, a stirring and a pressurization device. (e) Plot of the change of $\nu_{C=O}$ = 1740 cm^{-1} vs time.

As a next step, a 1 L Buchi reactor was equipped with a mechanical stirring, a heating device and a volumetric dosing unit for carbon dioxide pressure. Kinetic investigations of BDI zinc complexes in the copolymerization reactions of CHO and CO_2 revealed that at a pressure of 10 bar CO_2, the reaction order of carbon dioxide is still zero, meaning that the rate-determining step is solely the ring-opening of the epoxide.[26,32] 50 g of the epoxide were employed for the first upscaling step; twenty times the amount that is usually polymerized in the in situ autoclave (Table 1, entries 3-5). In case of CHO, again almost quantitative conversion was reached within 2 h to poly(cyclohexene carbonate) with a molecular weight of 115 kg/mol ($Đ$ = 1.49). An interesting polymerization prerequisite was revealed for limonene oxide. Applying the same amount of toluene as solvent for the LO polymerization as in the case of CHO results very low yields (Table 1, entry 4). The reason can again be attributed to the required catalyst concentration in the reaction solution. Mechanistic studies from Rieger *et al.* revealed a reaction order of 2 for the monomer limonene oxide.[26] This study clearly indicates the reason behind the dilution findings reported in Table 1, entry 4. It requires a high concentration of active catalytic centers and monomer molecules to enable to ring-opening of the sterically hindered epoxy group at the limonene oxide.

Table 1. Copolymerization of CHO/LO and CO_2 in the 50 mL in situ IR autoclave or 1 L Buchi reactor[a]

entry	[epoxide]:[cat]	epoxide (g)	toluene (g)	time (h)	conv. epoxide (%)[b]	M_n ($Đ$) (kg/mol)[c]
1[d]	2000(CHO):1	2.5	2.5	0.7	>99	219 (1.23)
2[d]	350(LO):1	2.5	2.5	7	68	142 (1.41)
3[e]	2000(CHO):1	50	150	2	>99	176 (1.51)
4[e]	350(LO):1	50	150	15	10	21 (1.39)
5[e]	350(LO):1	50	70	15	71	117 (1.31)
6[e]	2500(CHO):1	90	250	2	97	275 (1.42)

[a]Polymerizations of CHO with CO_2 were conducted at 60 °C, whereas LO copolymerization were performed at 40 °C. 40 bar CO_2 were applied in a continuous mode. [b]Conversion determined via ^{1}H NMR spectroscopy. [c]Determined via GPC analysis in THF (in case of PCHC) and $CHCl_3$ (in case of PLC) relative to polystyrene. [d]Polymerization conducted in 50 mL in situ IR autoclave. [e]Polymerization conducted in 1 L Buchi reactor.

Lowering the dilution (Table 1, entry 5) enables successful copolymerization of limonene oxide and CO_2 of 71% conversion within 15 h to PLC with a MW of 117 kg/mol (1.31). A narrow dispersity was still guaranteed despite the upscaled polymerization and the prolonged reaction time. Also, molecular weights of >50 kg/mol are achieved which are needed to ensure a sufficient mechanical performance. PLC of lower MW (Table 1, entry 4, 21 kg/mol) is a very brittle material. Even solvent casting, usually an outstanding property of PLC, failed when low-MW polymer was used. In case of cyclohexene oxide, a further upscaling step was applied with 90 g CHO yielding 125 g PCHC after precipitation in methanol (Table 1, entry 6).

Catalyst Removal. Residues of zinc catalysts are known to accelerate thermal degradation of the polymer at elevated temperatures.[3,24,33] Figure 2 shows the transmission of a polymeric solution of the respective aliphatic polycarbonate in chloroform. The β-diiminate ligand shows a strong absorption at 300-400 nm. The more intense this band, the higher the amount of catalytic residues. Aqueous EDTA was used as chelating agent to fully remove zinc residues from the polymeric solution. Since a lower catalyst concentration was employed for the polymerization of CHO compared to LO, it only takes one extraction step with aqueous EDTA whereas for PLC a second extraction step was required. Once the polymer was dried to constant weight in vacuo, it was grinded and used as such for all following thermal and mechanical characterization methods.

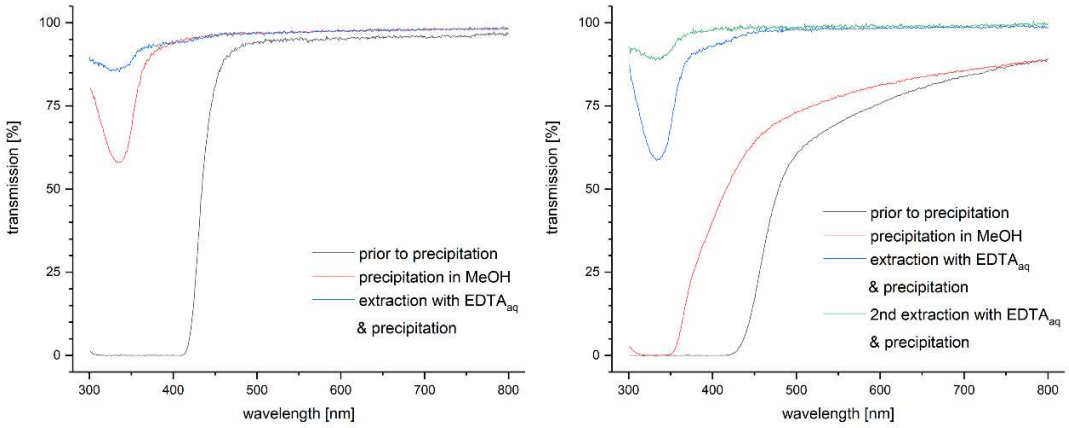

Figure 2. Transmission of a polymeric solution of PCHC (left) and PLC (right) in chloroform in the range of 300-800 nm.

Thermal analysis. Thermogravimetric analysis is a powerful method to study the decomposition of polymers. On the downside, only the conversion into volatile compounds can be detected and chain breaks to oligomeric decomposition products stay unidentified. Therefore, a different analysis method was developed. First, the polymer samples were tempered in a muffle oven at a certain temperature for 20 minutes. Next, the sample was dissolved for GPC analysis and a possible change in molecular weight and polydispersity examined. Although, TGA measurements indicate a $T_{5\%}$ of 278 °C (PCHC) and 217 °C (PLC), it was assumed that the first decomposition processes take place at much lower temperatures (Figure SX). The PCHC polymer samples were tempered under air and under argon atmosphere in a temperature range from 120 °C to 200 °C and subsequently analyzed via GPC (Figure 3). PCHC experiences no degradation at the polymer chain until 150 °C and only a slight decrease of the MW accompanied by a little increase of the polydispersity at 180 °C. Increasing the temperature further results in a more significant drop of the MW and a substantial broadening of the dispersity. Degradation is reduced in case the thermal tempering is performed under argon atmosphere. With the T_g of 116 °C in mind, a processing window of at least 40 °C creates a valuable prerequisite for the extrusion experiments.

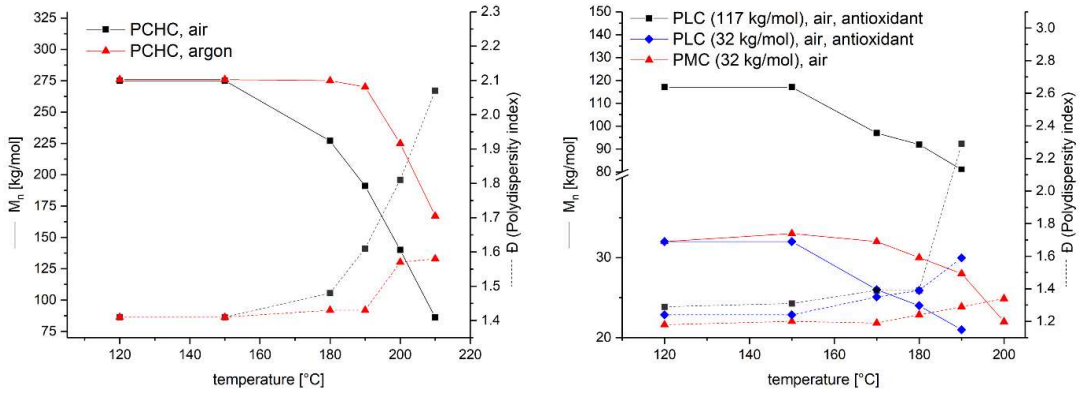

Figure 3. GPC analysis of tempered polymer samples (PCHC left; PLC, right). Plot of molecular weight M_n (kg/mol) and polydispersity *Đ* against the temperature at which the sample has been tempered in the muffle oven.

The same thermal treatment was applied for PLC and interesting differences were unveiled. Poly(limonene carbonate) did not show complete solubility in chloroform (which was necessary for GPC analysis) once the sample was heated above 160 °C. A partial cross-linking at the double bond was assumed to take place, but could not be verified via NMR (no solubility in any solvent even at high temperatures) nor via IR (concentration of cross-linked parts presumably too low). Irganox® was added to check whether this cross-linking can be prevented or not. Indeed, all tempered PLC samples could be dissolved completely in chloroform and analyzed via GPC. PLC shows the very first decomposition processes taking place at 170 °C. The comparably low ceiling temperature of poly(limonene carbonate) is assumed to be the major reason for this slightly lower thermal stability.[20] Overall, these thermal investigations demonstrate a possible processability of both polymers since a processing window spanning at least for 35 °C (for PLC) to 40 °C (for PCHC) from the T_g to the very first decomposition is guaranteed. To examine the role of the double bond in more detail, limonene oxide was hydrated with H_2 and catalytic amounts of PtO_2 to the so-called menthene oxide. This novel epoxide was readily copolymerized with CO_2 to a MW of 37 kg/mol (*Đ* = 1.16). The product poly(menthene carbonate) was also tested towards its thermal stability but besides the fact that no solubility problems and hence no crosslinking problems occurred, the decomposition of the aliphatic polycarbonate is neither hampered nor accelerated compared to PLC.

Extrusion. A further step towards the processability of a polymer is to test its behavior and stability in an extruder. The apparatus used in this work is a small, twin-screw microscale batch mixer suitable for investigating various processing parameters. A mixing volume of 4.5 mL allows the testing of a low amount of substance (Figure 4a). The grinded polymers were rapidly introduced into the extruder, stirred to ensure a homogeneous heating and released through a 1 mm wide nozzle.

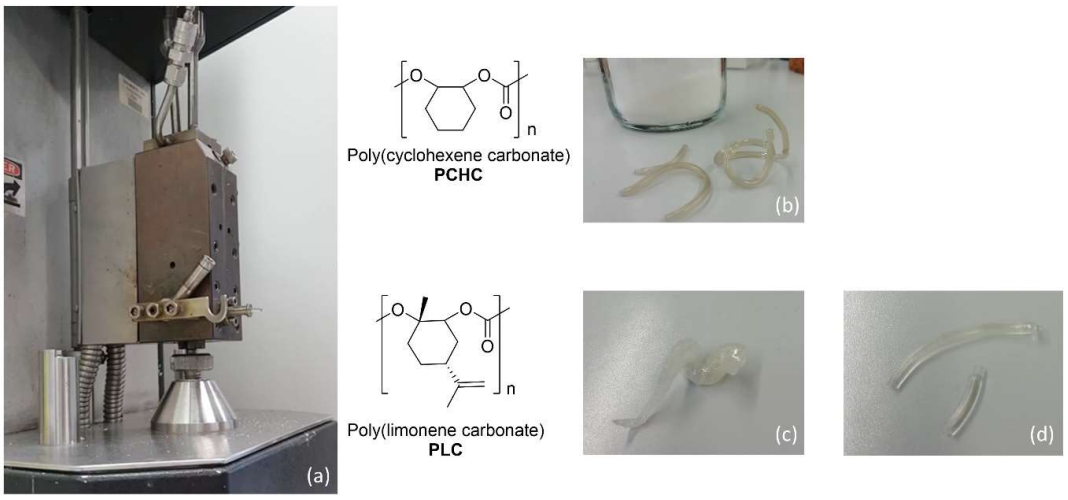

Figure 4. Twin-screw extruder (a); extruded PCHC at 180 °C (b) and PLC at 175 °C (c) and 165 °C (d).

First, PCHC was introduced into the mixer at 180 °C and a homogeneous polymer strand with a light greyish color was obtained. We performed GPC analysis to check whether the molecular weight of the polymer stayed intact, or unwanted decomposition processes took place. Table 2 gives an overview of the temperatures screened ranging from 165 to 200 °C and the results of the GPC measurements for the molecular weight analysis and the width of the polydispersity.

Table 2. Conditions and results of the extrusion experiments of PCHC and PLC[a]

entry	polymer	extrusion temp. (°C)	Irganox®[b]	M_n (kg/mol) ($Đ$)[c] original polymer	M_n (kg/mol) ($Đ$)[c] extruded polymer
1	PCHC	180	no	275 (1.42)	239 (1.44)
2	PCHC	200	no	275 (1.42)	110 (1.95)
3	PCHC	180	yes	275 (1.42)	270 (1.42)
4	PLC	165	no	117 (1.30)	48 (1.95)
5	PLC	175	no	117 (1.30)	23 (1.96)
6	PLC	165	yes	117 (1.30)	41 (1.65)

[a]Extrusion attempts conducted in a 4.5 mL twin-crew, microscale batch mixer at 80 rpm. [b]Irganox® used as antioxidant in a concentration of 500 ppm. [c]Determined via GPC analysis in THF (in case of PCHC) and $CHCl_3$ (in case of PLC) relative to polystyrene.

Due to the high molecular weight of PCHC, it requires 180 °C for a thorough mixing inside the extruder and a constant release of the polymer via the nozzle. GPC measurements indicate a slight degradation

of PCHC since the molecular weight decreases from 275 kg/mol to 239 kg/mol (Table 2, entry 1). Increasing the temperature to 200 °C, results in a severer decomposition (Table 2, entry 2). Using the antioxidant Irganox® at a concentration of 500 ppm, helps the polymer PCHC to remain transparent and to fully prevent degradation (Table 2, entry 3). In case of PLC, the temperature was lowered and PLC was extruded successfully at 165 °C to slight greyish, but fully homogeneous polymer strands, which showed a degradation from 117 kg/mol (1.30) to 48 kg/mol (1.95) (Table 2, entry 4). Increasing the processing temperature changed the extruded polymer drastically since severe degradation lead to a release of volatile compounds which caused an intense bubbling of the polymer (Table 2, entry 5). Again, the use of Irganox® helped the PLC to give a fully transparent extrudate but did not fully prevent degradation processes (Table 2, entry 6).

Mechanical Characterization. Commonly, the mechanical analysis of polymers is performed at a stress-strain machine with dog-bone shaped specimens. The preparation of such is prone to create surface irregularities and possible cracks on the edges of the specimen. Therefore, a different characterization method was chosen where round-shaped samples were tested in a multiaxial pressure test. A pin with a diameter of 0.7 mm approached the surface of the polymer and pushed with a rate of 1 mm/min for 300 s. Both the plot of the force against time (Figure 5a) and the fracture patterns (Figure 5b) provided important insight into the mechanical behavior of aliphatic polycarbonates in comparison with industrially applied aliphatic polymers, in this instance PMMA and Durabio®.

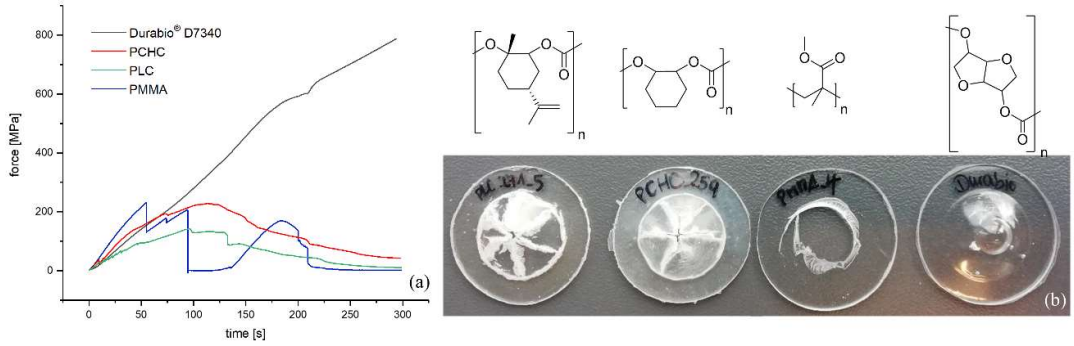

Figure 5. Multiaxial pressure test on round-shaped specimens with a pin of 7.0 mm diameter and a rate of 1 mm/min. (a) Plot of the force (MPa) versus time (s) and (b) fracture pattern of the tested polymers.

Durabio® displayed a high-impact resistance behavior whereas PMMA severely splintered in three stages releasing all the polymeric material with about the size of the pin. The two aliphatic polycarbonates showed a performance in between the mentioned benchmarks. They both were not able to fully absorb the energy but did also not splinter and show a rather homogeneous uptake of the exposed force. The green curve in Figure 5 represents PLC and shows a lower force with which the polymer tries to resist the approaching pin compared to PCHC. This clearly indicates a lower modulus of PLC.

Mechanical spectroscopy experiments like the dynamic mechanical analysis (DMA) helped to find an explanation for the high ductility of the bisphenol-A based polycarbonate Makrolon®. First, DMA is the most sensitive technique for the determination of the glass transition temperature. A large drop in the storage modulus combined with a clear peak in the loss modulus indicates the transition from the glassy to a rubbery state at 155 °C (Figure 6).

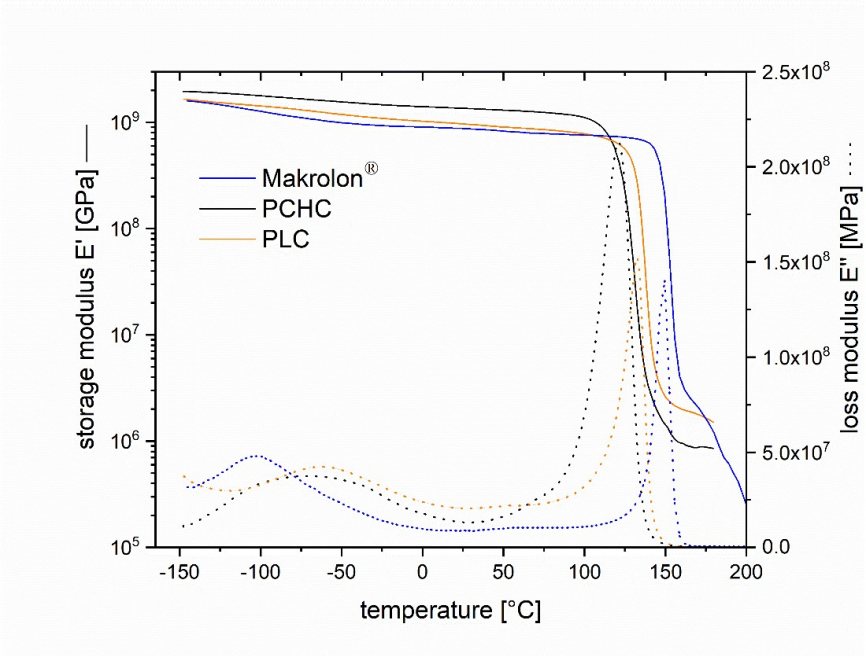

Figure 6. Dynamic mechanical analysis of Makrolon®, PCHC, and PLC in the range of -150 °C to 180 °C.

Besides the glass transition, sub-T_g relaxations, often called β- and γ-transitions, are crucial for the toughness of a material. Generally, these transitions result from the onset of the motion of side chains.[34] In early studies, the relaxations at low temperatures were assigned to the rotation of the phenylene rings and the carbonate group of BPA-PC.[35-36] They allow the material to absorb energy below the T_g. Looking at the storage and loss modulus of PCHC and PLC, a similar curve but with some important differences can be observed. The aliphatic polycarbonates, PCHC and PLC, both show a lowered T_g of 120 °C and 132 °C, respectively, which are in good agreement with the values measured via DSC (Figure SX). Besides, they also exhibit a low temperature transition which is shifted towards higher temperatures compared to the one of BPA-PC. Also, the magnitude is lower than for the classical polycarbonate. Based on this, it is assumed that the main chain of PCHC and PLC is less flexible than the one of BPA-PC. In 2001, Koning *et al.* investigated the role of the cyclohexyl rings and the entanglement density on the stiffness of the polymer.[21] They postulated that the sub-T_g relaxation corresponds to chair-chair transitions of the cyclohexyl rings. However, these cyclohexyl rings are regarded as side groups and can therefore not contribute to the toughness of the material. Comparing the loss modulus of PCHC

and PLC reveals that the amplitude for PLC is slightly enhanced indicating a higher flexibility of the polymer chain.

Terpolymerization of CHO, LO, and CO_2.

Since BDI^{CF3}-Zn-$NTMS_2$ **1** is able to catalyze the copolymerization of both CHO and LO with CO_2 to aliphatic polycarbonates, we were curious if **1** can serve as an active initiator for the terpolymerization of CHO, LO and CO_2. A one-pot attempt gave a polymer consisting of 66:34 PCHC:PLC (Table 3, entry 1). A second polymerization experiment revealed an interesting kinetic property regarding the polymerization rate of the respective epoxides (Table 3, entry 2). Running the reaction for 1 h, lead to the exclusive coupling of the CHO molecule with CO_2. No conversion of LO was observed within one hour. This observation rose the question if it requires full CHO conversion before limonene oxide gets consumed.

Table 3. Terpolymerization of CHO, LO, and CO_2 with complex **1**

entry	(CHO):(*trans*-LO) :(cat)	time (h)	conv. CHO (%)[b]	conv. LO (%)[b]	(PCHC):(PLC)[c]	M_n ($Đ$) (kg/mol)[d]
1	300:200:1	15	>99	60	66:34	316 (1.48)
2	250:250:1	1	36	0	100:0	38 (1.32)
3	150:350:1	15	>99	70	40:60	300 (1.40)

[a]Terpolymerizations of CHO, LO, and CO_2 were conducted at 40 °C in a 50 mL in situ IR autoclave. 40 bar CO_2 were applied in a continuous mode. [b]Conversion determined via ^{1}H NMR spectroscopy. [d]Determined via GPC analysis in $CHCl_3$ relative to polystyrene.

High-pressure NMR tubes allowed a detailed monitoring of the reaction progress (Figure 7). Generally, due to the lack of stirring and a reduced carbon dioxide pressure of 9 bar, a higher catalyst loading was employed and the reaction time is prolonged. Indeed, quantitative conversion of CHO is taking place prior to the start of the copolymerization of limonene oxide and CO_2. After 7 h reaction time, CHO is fully consumed, and the ring-opening of limonene oxide starts. LO is sterically more hindered than CHO by the additional methyl group, and thus the ring-opening step on the epoxy group is hampered. Hence, this terpolymerization reaction can be considered as an in situ-controlled block copolymerization driven by the reaction kinetics of the respective monomers.

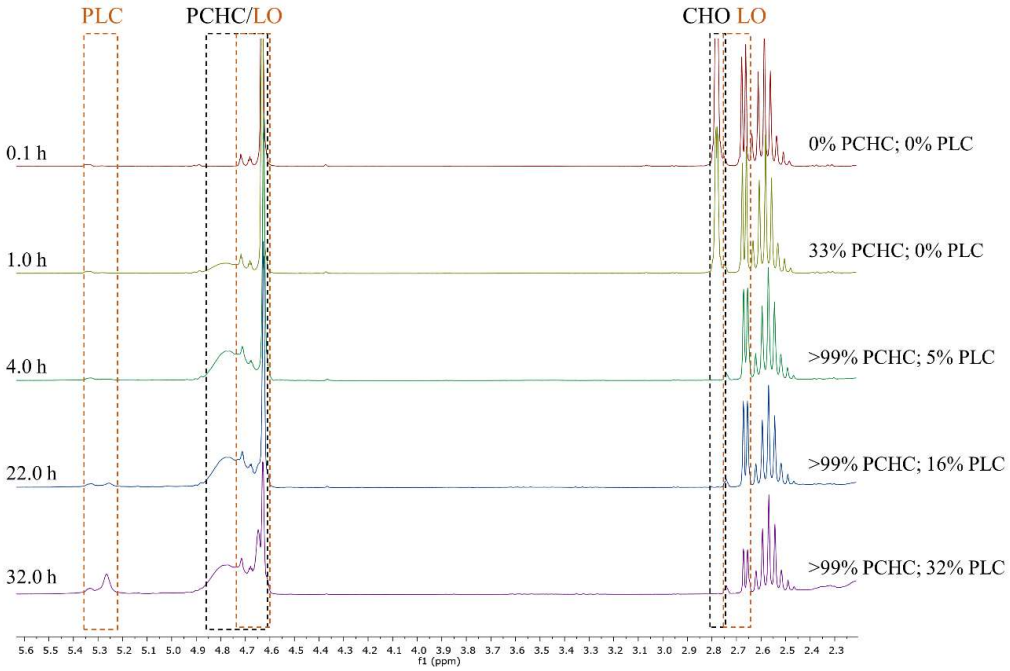

Figure 7. NMR spectra of the terpolymerization of CHO, LO, and CO_2 performed in a high-pressure NMR tube at the respective reaction time.

With the kinetic insight in hand, it remained to be proven if both types of polymer are chemically linked with each other and an actual terpolymer was produced. GPC traces of PCHC regularly show a bimodality due to the in situ formed cyclohexene diol acting as a chain-transfer agent. Hence, a bimodal distribution by itself does not indicate the presence of individual polymers as a blend. Aliquot GPC analysis and DOSY NMR experiments were performed to confirm the terpolymer's architecture. After 40 min reaction time, CO_2 was released from the reactor, an aliquot was taken, and the system was repressurized with 30 bar CO_2. Comparison of the aliquot's GPC trace with the one of the final polymer revealed a shift in molecular weight from 86 kg/mol to 127 kg/mol (Figure SX).

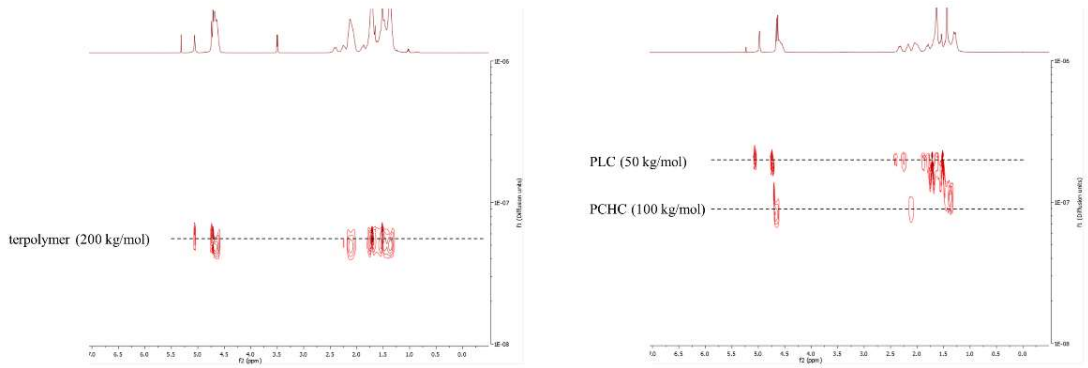

Figure 8. DOSY NMR spectrum of the PCHC-PLC terpolymer (Table 3, entry 1) (left) and DOSY NMR spectrum of an artificial blend of PCHC and PLC.

DOSY NMR spectroscopy of the final terpolymer showed that all the signals have the same diffusion coefficient. An artificial blend consisting of two copolymers of comparable molecular weights exhibits the presence of two separated species owing to two different diffusion coefficients.

4. Conclusion

The use of a BDI^{CF3}-Zn-$N(SiMe_3)_2$ catalyst allowed the ring-opening copolymerization of CO_2 with CHO and LO, respectively. An upscaling of the reaction in a 1 L reactor provided access to the polymers poly(cyclohexene carbonate) and poly(limonene carbonate), which were used for further characterizations. Thermal analysis indicated only minor decomposition upon tempering the polymers to 180 °C for 20 minutes. Multiaxial pressure tests and dynamic mechanical analysis enabled a comparison of the two CO_2-based polycarbonates with commercial plastics in terms of mechanical performance. Also, terpolymerizations of CHO, LO, and CO_2 were successful. High-pressure NMR spectroscopy revealed the exclusive incorporation of CHO in the beginning of the one-pot polymerization, and LO is only incorporated when CHO is fully consumed. In total, this study provides important data regarding upscaling and the thermal and mechanical performance of PLC. Moreover, the PCHC/PLC terpolymers represent a promising approach to combine the properties of the respective copolymers.

Acknowledgments

The authors thank Alina Denk for proof-reading the manuscript.

Appendix A: Supplementary data.

References

(1) Inoue, S.; Koinuma, H.; Tsuruta, T. Copolymerization of carbon dioxide and epoxide with organometallic compounds. *Die Makromolekulare Chemie* **1969**, *130*, 210-220.

(2) Inoue, S.; Koinuma, H.; Tsuruta, T. Copolymerization of carbon dioxide and epoxide. *J. Polym. Sci.* **1969**, *7*, 287-292.

(3) Luinstra, G. A. Poly(Propylene Carbonate), Old Copolymers of Propylene Oxide and Carbon Dioxide with New Interests: Catalysis and Material Properties. *Poly. Rev.* **2008**, *48*, 192-219.

(4) Langanke, J.; Wolf, A.; Hofmann, J.; Böhm, K.; Subhani, M. A.; Müller, T. E.; Leitner, W.; Gürtler, C. Carbon dioxide (CO2) as sustainable feedstock for polyurethane production. *Green Chem.* **2014**, *16*, 1865-1870.

(5) Takeda, N.; Inoue, S. Polymerization of 1,2-epoxypropane and copolymerization with carbon dioxide catalyzed by metalloporphyrins. *Die Makromolekulare Chemie* **1978**, *179*, 1377-1381.

(6) Qin, Z.; Thomas, C. M.; Lee, S.; Coates, G. W. Cobalt-Based Complexes for the Copolymerization of Propylene Oxide and CO2: Active and Selective Catalysts for Polycarbonate Synthesis. *Angew. Chem. Int. Ed.* **2003**, *42*, 5484-5487.

(7) Jacobson, N. E.; Tokunaga, M.; Larrow, J. F. 2000, PCT Int. Appl. WO 00/09463.

(8) Kember, M. R.; Knight, P. D.; Reung, P. T. R.; Williams, C. K. Highly Active Dizinc Catalyst for the Copolymerization of Carbon Dioxide and Cyclohexene Oxide at One Atmosphere Pressure. *Angew. Chem. Int. Ed.* **2009**, *48*, 931-933.

(9) Darensbourg, D. J.; Holtcamp, M. W. Catalytic Activity of Zinc(II) Phenoxides Which Possess Readily Accessible Coordination Sites. Copolymerization and Terpolymerization of Epoxides and Carbon Dioxide. *Macromolecules* **1995**, *28*, 7577-7579.

(10) Cheng, M.; Lobkovsky, E. B.; Coates, G. W. Catalytic Reactions Involving C1 Feedstocks: New High-Activity Zn(II)-Based Catalysts for the Alternating Copolymerization of Carbon Dioxide and Epoxides. *J. Am. Chem. Soc.* **1998**, *120*, 11018-11019.

(11) Coates, G. W.; Moore, D. R. Discrete Metal-Based Catalysts for the Copolymerization of CO2 and Epoxides: Discovery, Reactivity, Optimization, and Mechanism. *Angew. Chem. Int. Ed.* **2004**, *43*, 6618-6639.

(12) Kissling, S.; Lehenmeier, M. W.; Altenbuchner, P. T.; Kronast, A.; Reiter, M.; Deglmann, P.; Seemann, U. B.; Rieger, B. Dinuclear zinc catalysts with unprecedented activities for the copolymerization of cyclohexene oxide and CO_2. *Chem. Comm.* **2015**, *51*, 4579-4582.

(13) Kozak, C. M.; Ambrose, K.; Anderson, T. S. Copolymerization of carbon dioxide and epoxides by metal coordination complexes. *Coord. Chem. Rev.* **2018**, *376*, 565-587.

(14) Klaus, S.; Lehenmeier, M. W.; Anderson, C. E.; Rieger, B. Recent advances in CO2/epoxide copolymerization—New strategies and cooperative mechanisms. *Coord. Chem. Rev.* **2011**, *255*, 1460-1479.

(15) Kissling, S.; Altenbuchner, P. T.; Niemi, T.; Repo, T.; Rieger, B. *Zinc Catalysis*; Wiley-VCH Verlag, 2015.

(16) Darensbourg, D. J.; Holtcamp, M. W. Catalysts for the reactions of epoxides and carbon dioxide. *Coord. Chem. Rev.* **1996**, *153*, 155-174.

(17) Wang, Y.; Darensbourg, D. J. Carbon dioxide-based functional polycarbonates: Metal catalyzed copolymerization of CO2 and epoxides. *Coord. Chem. Rev.* **2018**, *372*, 85-100.

(18) Byrne, C. M.; Allen, S. D.; Lobkovsky, E. B.; Coates, G. W. Alternating Copolymerization of Limonene Oxide and Carbon Dioxide. *J. Am. Chem. Soc.* **2004**, *126*, 11404-11405.

(19) Peña Carrodeguas, L.; González-Fabra, J.; Castro-Gómez, F.; Bo, C.; Kleij, A. W. AlIII-Catalysed Formation of Poly(limonene)carbonate: DFT Analysis of the Origin of Stereoregularity. *Chem. Eur. J.* **2015**, *21*, 6115-6122.

(20) Reiter, M.; Vagin, S.; Kronast, A.; Jandl, C.; Rieger, B. A Lewis acid [small beta]-diiminato-zinc-complex as all-rounder for co- and terpolymerisation of various epoxides with carbon dioxide. *Chem. Sci.* **2017**, *8*, 1876-1882.

(21) Koning, C.; Wildeson, J.; Parton, R.; Plum, B.; Steeman, P.; Darensbourg, D. J. Synthesis and physical characterization of poly(cyclohexane carbonate), synthesized from CO2 and cyclohexene oxide. *Polymer* **2001**, *42*, 3995-4004.

(22) Darensbourg, D. J.; Yarbrough, J. C.; Ortiz, C.; Fang, C. C. Comparative Kinetic Studies of the Copolymerization of Cyclohexene Oxide and Propylene Oxide with Carbon Dioxide in the Presence of Chromium Salen Derivatives. In Situ FTIR Measurements of Copolymer vs Cyclic Carbonate Production. *J. Am. Chem. Soc.* **2003**, *125*, 7586-7591.

(23) Thorat, S. D.; Phillips, P. J.; Semenov, V.; Gakh, A. Physical properties of aliphatic polycarbonates made from CO2 and epoxides. *J. Appl. Polym. Sci.* **2003**, *89*, 1163-1176.

(24) Li, G.; Qin, Y.; Wang, X.; Zhao, X.; Wang, F. Study on the influence of metal residue on thermal degradation of poly(cyclohexene carbonate). *Journal of Polymer Research* **2011**, *18*, 1177-1183.

(25) Cohen, C. T.; Thomas, C. M.; Peretti, K. L.; Lobkovsky, E. B.; Coates, G. W. Copolymerization of cyclohexene oxide and carbon dioxide using (salen)Co(iii) complexes: synthesis and characterization of syndiotactic poly(cyclohexene carbonate). *Dalton Trans.* **2006**, 237-249.

(26) Hauenstein, O.; Reiter, M.; Agarwal, S.; Rieger, B.; Greiner, A. Bio-based polycarbonate from limonene oxide and CO2 with high molecular weight, excellent thermal resistance, hardness and transparency. *Green Chem.* **2016**, *18*, 760-770.

(27) Hauenstein, O.; Agarwal, S.; Greiner, A. Bio-based polycarbonate as synthetic toolbox. *Nat. Comm.* **2016**, *7*, 11862.

(28) Zhang, D.; del Rio-Chanona, E. A.; Wagner, J. L.; Shah, N. Life cycle assessments of bio-based sustainable polylimonene carbonate production processes. *Sus. Prod. Cons.* **2018**, *14*, 152-160.

(29) Li, C.; Sablong, R. J.; Koning, C. E. Synthesis and characterization of fully-biobased α,ω-dihydroxyl poly(limonene carbonate)s and their initial evaluation in coating applications. *Eur. Polym. J.* **2015**, *67*, 449-458.

(30) Kronast, A.; Reiter, M.; Altenbuchner, P. T.; Jandl, C.; Pöthig, A.; Rieger, B. Electron-Deficient β-Diiminato-Zinc-Ethyl Complexes: Synthesis, Structure, and Reactivity in Ring-Opening Polymerization of Lactones. *Organometallics* **2016**, *35*, 681-685.

(31) Quadrelli, E. A.; Centi, G.; Duplan, J.-L.; Perathoner, S. Carbon Dioxide Recycling: Emerging Large-Scale Technologies with Industrial Potential. *ChemSusChem* **2011**, *4*, 1194-1215.

(32) Kernbichl, S.; Reiter, M.; Mock, J.; Rieger, B. Terpolymerization of β-Butyrolactone, Epoxides, and CO2: Chemoselective CO2-Switch and Its Impact on Kinetics and Material Properties. *Macromolecules* **2019**.

(33) Rieger, B.; Künkel, A.; Coates, G. W. *Synthetic Biodegradable Polymers* Springer, Berlin/Heidelberg, Germany, 2012.

(34) Nelson, A. M.; Long, T. E. A perspective on emerging polymer technologies for bisphenol-A replacement. *Polym. Int.* **2012**, *61*, 1485-1491.

(35) Yee, A. F.; Smith, S. A. Molecular structure effects on the dynamic mechanical spectra of polycarbonates. *Macromolecules* **1981**, *14*, 54-64.

(36) Locati, G.; Tobolsky, A. V. Studies of the toughness of polycarbonate of bisphenol a in light of its secondary transition. *Advances in Molecular Relaxation Processes* **1970**, *1*, 375-408.

11. Aliphatic Polycarbonates Derived from Epoxides and CO_2

Title: **"**Aliphatic Polycarbonates Derived from Epoxides and CO_2"

Status: Review article, submitted online September 09, 2019

Publisher *John Wiley & Sons*

ISBN 3527346392

Authors: Sebastian Kernbichl, Bernhard Rieger[a]

Content

Aliphatic polycarbonates have been known for more than 50 years but remain highly interesting in a variety of research areas. While poly(propylene carbonate), derived from propylene oxide and CO_2, has already found its industrial application in small scale processes, poly(cyclohexene carbonate) continues to serve as an academic benchmark for catalysis research. Although heterogeneous systems dominate the industrial PO/CO_2 copolymerization, with homogeneous catalysts dramatic improvements become possible in the last decade. β-diiminate zinc systems seem to be the most active catalysts for the copolymerization of cyclohexene oxide and CO_2. Besides BDI complexes, macrocyclic diphenolate systems allow the coupling of CO_2 and epoxides as well as the incorporation of another type of monomer like cyclic esters or anhydrides. These one-pot terpolymerizations can be nicely controlled via the carbon dioxide pressure. The combination of various polymerization cycles by a single catalyst represents an interesting tool for chemoselectively building up block copolymers with different features. BDI complexes also enable the coupling of the bio-based epoxide limonene oxide and CO_2 to the very promising material poly(limonene carbonate). Intense research in recent years has revealed possible areas of application for PLC: In addition to the use as a non-isocyanate building block in polyurethane production or in coating applications, the detailed determination of its thermal, optical and mechanical properties has made it a potential rigid plastic alternative to bisphenol-A polycarbonate. However, turnover numbers still need to be increased for limonene oxide, and it will be very interesting to see whether this limitation can be solved in the near future in order to make an industrial process possible.

[a]S. Kernbichl wrote the manuscript. All work was carried out under the supervision of B. Rieger.

Chapter X

Aliphatic Polycarbonates Derived from Epoxides and CO_2

Sebastian Kernbichl, and Bernhard Rieger

Contents

S. Kernbichl, and B. Rieger
WACKER-Chair of Macromolecular Chemistry, Technical University Munich, Lichtenbergstr. 4, 85747 Garching
email. rieger@tum.de

Abbreviations

BDI	β-diiminate
BPA-PC	Bisphenol-A polycarbonate
CCU	Carbon capture and utilization
CHO	Cyclohexene oxide
Đ	Polydispersity index
DFT	Density functional theory
DMAP	4-(Dimethylamino)pyridine
HPPO	Hydrogen peroxide to propylene oxide
LO	Limonene oxide
MW	Molecular weight
NBS	N-bromosuccinimide
PCHC	Poly(cyclohexene carbonate)
PLC	Poly(limonene carbonate)
PO	Propylene oxide
PPC	Poly(propylene carbonate)
PPNCl	Bis(triphenylphosphine)iminium chloride
TMS	Trimethylsilyl
TOF	Turn-over frequency
TPP	Tetraphenylporphyrine
ZnGA	Zinc glutarate
ZnSA	Zinc succinate

1. Introduction

In light of its increasing concentration in the atmosphere and its industrial emergence, carbon dioxide is clearly a topic of intense research. Carbon dioxide capture and utilization (CCU) deals with the aim of using industrially produced CO_2 as a C1-feedstock for high-quality chemical products. Since carbon dioxide is chemically rather inert, high energy barriers must be overcome.[1] The coupling of CO_2 with an epoxide offers the possibility of using carbon dioxide for the preparation of cyclic carbonates or polycarbonates. Cyclic carbonates are applied as electrolytes in lithium ion batteries or as high boiling aprotic polar solvents.[2-3] Depending on their molecular weight (MW) and their kind of end-groups, polycarbonates are used in the polyurethane production (low MW, hydroxyl terminated) or in the fabrication of rigid plastics

(high MW) as a possible alternative to bisphenol-A polycarbonate (BPA-PC).[4] Polycarbonates derived from epoxides and CO_2 offer promising properties such as high transparency, UV stability and high Young's moduli.[5] The coupling of propylene oxide (PO) and CO_2 offers the most promising polymer poly(propylene carbonate) (PPC) since PO is industrially available in large quantities and a higher CO_2 content is generated compared to other aliphatic polycarbonates (Figure 1a). The widespread commercialization of PPC although was hindered due to the low glass transition temperature of 30 - 40 °C. Polyurethane foams from Bayer based on poly(ether carbonates) made of PO and CO_2 proof the potential use of carbon dioxide in large scale polymerizations.[6] The industrial feasibility of such processes always depends on the activity of the employed catalyst. Since the initial discovery in 1969 of diethylzinc and water serving as a heterogeneous catalyst in the synthesis of PPC, much research has been made on the question of how the activity of the catalysts can be improved.[7] Efforts mainly concentrate on homogeneous systems and often initially use cyclohexene oxide (CHO) as it can be copolymerized more easily due to its ring-strain to poly(cyclohexene carbonate) (PCHC) (Figure 1b). Poly(limonene carbonate) (PLC) was reported for the first time in 2004, but gained attention only very recently (Figure 1c).[8] The bio-based origin of limonene oxide (LO) and the polymers' very promising properties expand the class of the well-known aliphatic polycarbonates PPC and PCHC. This review gives an overview of the catalytic copolymerization of various epoxides and CO_2 and focuses on the latest findings especially in the field of poly(limonene carbonate).

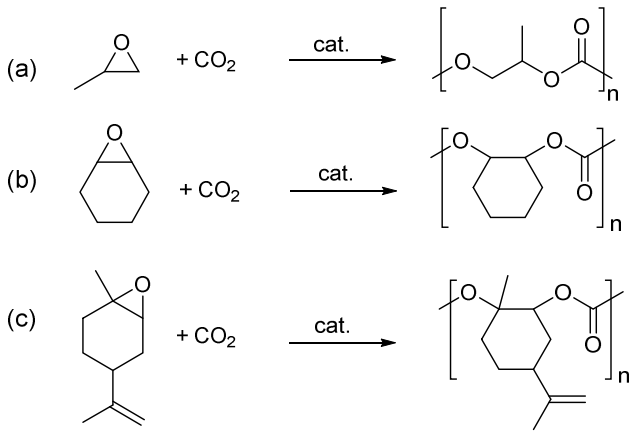

Figure 1. Alternating copolymerization of CO_2 with (a) propylene oxide, (b) cyclohexene oxide, and (c) limonene oxide.

2. Aliphatic polycarbonates

2.1 Synthesis of the monomers

During recent decades, several processes for the production of propylene oxide have been established, starting with the hydrochlorination route in 1930.[9] Due to the high costs of the starting materials and arising by-products, the preparation has been improved several times. The hydrogen peroxide to propylene oxide (HPPO) process works with the aid of a titanium-doped silicalite catalyst and produces water as the only by-product.[10] 7.5 mio. t/a PO were produced this way in 2015.[11]

Despite the industrial abundance of propylene oxide, cyclohexene oxide is often used in an initial attempt at testing a catalyst. Due to the ring strain of the cyclohexane ring, this epoxide can be ring-opened more easily after coordination to a suitable catalyst. Cyclohexene oxide itself is usually prepared through epoxidation with peracids or even catalytically with manganese porphyrins and oxygen.[12-13]

Carbon dioxide used in the copolymerization process in academic research is usually taken from gas bottles in high purity. Williams and coworkers reported in 2015 whether CO_2 from a nearby power station can be copolymerized with epoxides using established catalysts.[14] Three homogeneous dinuclear Zn/Mg systems showed a high tolerance towards gaseous impurities. Polyols from CHO and CO_2 were obtained in a controlled manner, demonstrating the possibility to apply industrially emitted carbon dioxide without further purification.

The third type of epoxide discussed in this chapter is limonene oxide. It is obtained via the epoxidation of limonene. One enantiomer, (*R)*-limonene, can be found in orange peels and gets extracted at a volume of 70 kt/a.[15] Categorized as a cyclic monoterpene, limonene bears one chiral C-atom and two unsaturated carbon bonds prone to chemical modification. This renewable non-food resource represents a promising class of feedstock because the 1,2 epoxidation products displays an auspicious candidate for the copolymerization with CO_2.[16] In addition, it shows strong resemblance to the well-studied epoxide cyclohexene oxide. The topic of sustainable epoxide/CO_2 copolymerization was summarized by Darensbourg *et al.* in 2017.[17] Limonene oxide is commercially available in a 46:54 cis:trans mixture usually obtained via acid-catalyzed oxidation of *(R)*-limonene (Figure 2a).[18] Due to the fact that the most active catalysts almost exclusively polymerize the trans diastereomer, a route towards a higher trans-content was established in 2016 by first treating limonene with N-bromosuccinimide (NBS) to enable the more selective ring closure in the second step (Figure 2b).[16]

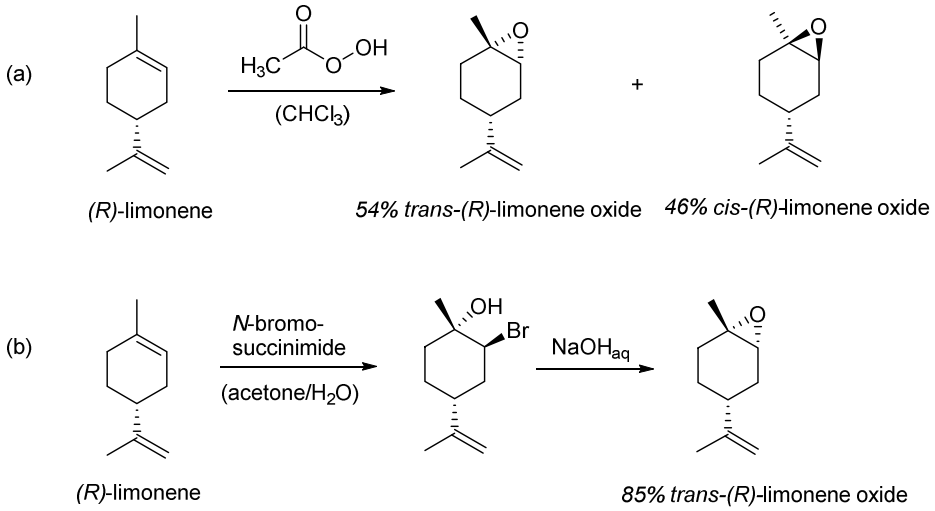

Figure 2. Oxidation of *(R)*-limonene via two different routes to different *trans-(R)*-limonene oxide contents.[16, 18]

2.2 Mechanistic aspects of the copolymerization of epoxides and CO_2

The process of the CO_2/epoxide copolymerization can be divided into three catalytic steps, namely initiation, propagation, and termination (Scheme 1). During initiation, either carbon dioxide or the epoxide inserts into the M-X bond, creating a metal-carboxylate or a metal-alkoxide species. The nature of the catalyst decides which of the two monomers is more likely to be inserted in the first step. The alternating incorporation of CO_2 and epoxide marks the period of propagation, in which the metal alkoxide and the metal carbonate are interconverted. There are two important side reactions during propagation that occur to a varying extent, which depends on the type of epoxide and the catalyst as well as the general polymerization conditions like reaction temperature or CO_2 pressure. The consecutive insertion of two (or more) epoxide molecules results in the formation of polyether units. In contrast to that, the so-called backbiting reaction to a 5-membered carbonate ring is the thermodynamically favored product. It is the predominant side reaction for the copolymerization of propylene oxide and CO_2.

For most catalysts, the copolymerization reaction can be described as an immortal reaction. On the one hand, this allows the synthesis of polymers in well-defined molecular weights since an inverse relationship exists between the catalyst concentration and the resulting molecular weight. On the other hand, this living character also enables the formation of block copolymers by the addition of a second type of epoxide. The polymerizations are usually terminated by the addition of a protic compound like methanol. The underlying mechanism is a chain-transfer reaction between the polymeric chain end and the proton. This chain-transfer can also occur

during the polymerization if any protic impurities like water are present in the reaction mixture. This automatically leads to polymers of lower molecular weight. In case of cyclohexene oxide chain-transfer also explains the often observed bimodal molecular weight distribution due to the in situ formed cyclohexanediol that again acts as a chain-transfer agent.

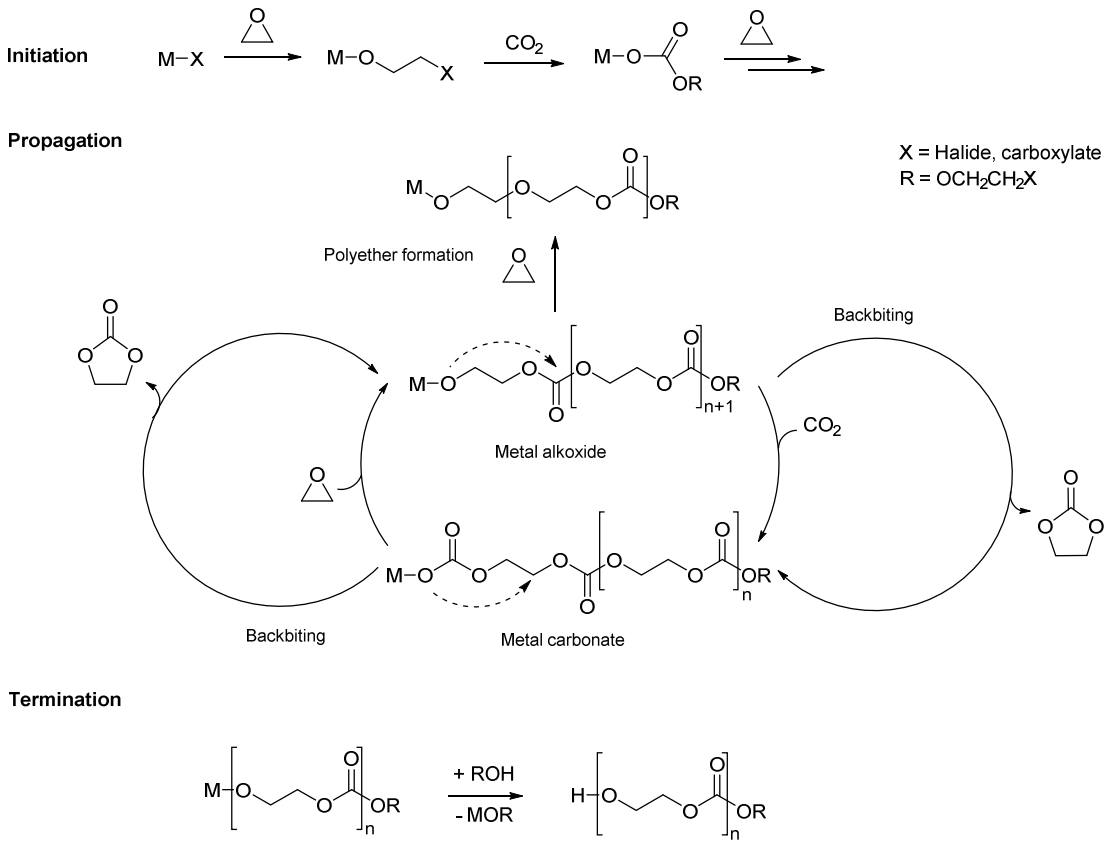

Scheme 1. Copolymerization of CO_2 and epoxides in three elementary steps. Initiation, propagation, and termination.

Applying the same reaction conditions for the two epoxide types, CHO and PO, in the copolymerization with CO_2 results in a major difference regarding reactivity and selectivity. The reason was investigated more closely by the group of Darensbourg in 2003 using a chromium salen catalyst.[19] Activation energies were determined by *in situ* IR kinetic measurements showing that, for both monomers, the respective cyclic product requires a higher activation energy than the polycarbonate (Figure 3). However, the decisive difference is the smaller energy gap between the two products in the case of PO (33 kJ/mol), explaining the lower selectivity for polycarbonate formation at elevated temperatures.

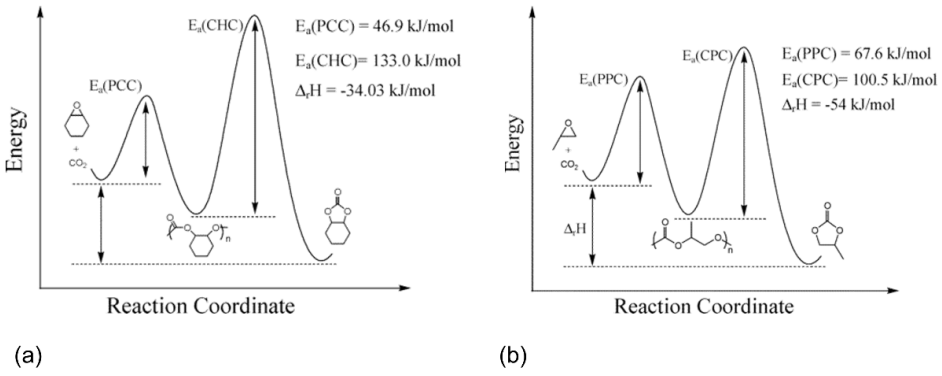

Figure 3. Reaction coordinate diagram for the coupling of (a) CHO and (b) PO with CO_2 using a chromium salen catalyst. Reproduced with permission from [19], Copyright © 2003 American Chemical Society.

2.3 Thermal stability and possible degradation pathways

Processability of polymers is always strongly linked to the question of thermal stability. A multitude of works is dealing with the thermal degradation of aliphatic polycarbonates, especially poly(propylene carbonate).[20-25] Two main decomposition pathways have been observed thereby. On the one hand, the intramolecular backbiting reaction to cyclic carbonates is facilitated by OH-end groups (Scheme 2a). These hydroxy end groups are usually obtained if the catalytic copolymerization is terminated by the addition of acidified methanol. On the other hand, chain unzipping occurs if a nucleophile is located at a polymer chain end (Scheme 2b). Catalyst residues accelerate the backbiting reaction severely in the temperature range of 150-180 °C.[26] At higher temperatures (~200 °C) random chain scission has been mostly observed leading to the splitting of a polymer chain with the release of CO_2.

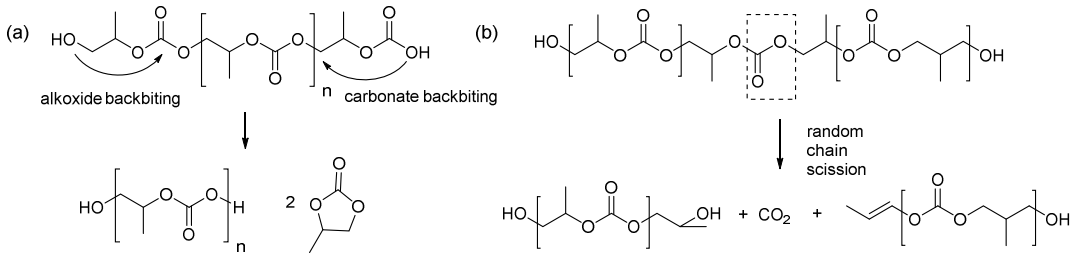

Scheme 2. Degradation mechanism for PPC: chain scission (a) and backbiting (b).[24]

Decomposition temperatures reported in the literature are difficult to compare due to varying conditions, the type of analysis, and the kind of polymer. Most publications indicate 180 °C as the upper processability limit for PPC. Different attempts have been made to further increase

the thermal stability of aliphatic polycarbonates. The backbiting reaction can be prevented to some extent via an endcapping of the polymer chain ends.[24] Anhydrides seem to be the most promising candidates along with acetates and chlorophosphates as they are less reactive than the hydroxy functionality.

Thermogravimetric analysis of poly(limonene carbonate) revealed a $T_{5\%}$ of 225 °C, meaning that, at 225 °C, 5% of the sample was converted to volatile compounds.[16] Endcapping with maleic anhydride further increased the decomposition temperature to a $T_{5\%}$ of 240 °C. GC-MS measurement of a hydroxy-terminated PLC sample heated to 230 °C for 20 minutes did not show any cyclic limonene carbonate, exhibiting instead a variety of different decomposition products including limonene oxide.[16] This circumstance was transferred to the base-initiated depolymerization of PLC by Koning *et al*.[27] A similar base-assisted depolymerization was previously observed for poly(cyclopentene carbonate) yielding both the epoxide and the cyclic carbonate.[28] In the case of PLC, the strong organic base triazabicyclodec-5-ene leads to the deprotonation of the hydroxyl polymer chain end enabling fast backbiting to limonene oxide and CO_2 at 110 °C. The controlled depolymerization of aliphatic polycarbonates represents an interesting approach in terms of recyclability and sustainability.

2.4 Mechanical properties

Figure 4 illustrates the three copolymers derived from CO_2 and the respective epoxide. The main advantages and disadvantages are clearly visible: While PCHC struggles with brittleness and PPC exhibits a soft, deformable property, PLC is best suited for solvent casting along with a high transmission of the polymer film.

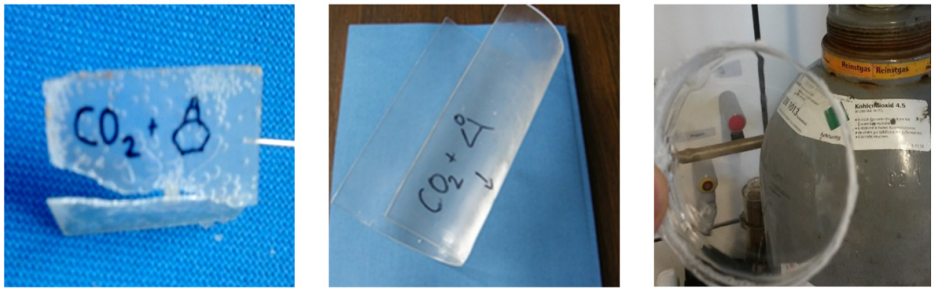

(a) (b) (c)

Figure 4. Poly(cyclohexene carbonate) (a), poly(propylene carbonate) (b), and poly(limonene carbonate) (c).

Similar to the determination of the thermal stability of aliphatic polycarbonates, mechanical properties cannot be easily compared since they are strongly dependent on the respective microstructure, the molecular weight, and cyclic carbonate impurities. In the case of poly(propylene carbonate) the glass transition temperature is highly dependent on the molecular weight of the polymer and ranges between 30 - 40 °C. PPC with a T_g of 30 °C exhibits Young's moduli of 200 – 1000 MPa, whereas the polymer with a higher T_g shows an increased stiffness of 700 – 1400 MPa.[5, 26, 29] Aliphatic polycarbonates are often compared with the aromatic bisphenol-A based polycarbonate. Apart from a Young's modulus of 2400±400 MPa, the aromatic polymer shows an elongation at break of 40±35%, opening up a multitude of different areas of application. PCHC is a much stiffer material than PPC and resembles BPA-PC in some aspects. The main disadvantage of PCHC thus far arises from its brittleness reflected in a Young's modulus of 3600±100 MPa and an elongation at break of 1.7±0.6%.[30]

Efforts to overcome the main problems in terms of material properties for both PPC and PCHC were made by using a second type of epoxide in the polymerization. The so-called terpolymerization enables the synthesis of polymers in an adjustable composition and hence in a tunable glass transition temperature.[31] Terpolymerization of CHO, PO, and CO_2 was thought to improve the brittleness of PCHC, but it only resulted in a reduced E-modulus (2100 MPa) with an otherwise unchanged elongation at break.[32] Other epoxides like hexene oxide or styrene oxide were also successfully polymerized with the established monomers PO and CHO.[33-34]

The mechanical behavior of poly(limonene carbonate) was tested for the first time in 2016.[16] Hot-pressed polymer specimen could be produced at a thickness of 300 µm and tested using a stress-strain machine. A Young's modulus of 950 MPa, a tensile strength of 55 MPa, and an elongation at break of 15% were obtained. These promising properties indicate that PLC is a possible alternative to BPA-PC.

3. Catalyst systems for the CO_2/epoxide copolymerization

Like for other classes of polymerization, early catalytic attempts started with heterogeneous systems. Although the number and the kind of active sites is difficult to determine for such systems, they have already been industrially applied for centuries in PPC production.[26, 35-36] In contrast, homogeneous catalysts are the subject of intense research due to their solubility, tunability, and the possibility of determining the underlying mechanism in situ. The viscosity of the polymerization solution plays an important role regarding polymer processability and activity. A low amount of solvent enables high activity but reduces diffusion of the monomer, whereas

an increased dilution lowers the activity, to some extent due to spatially separated metal centers, but allows higher yields and improved processability.[37]

3.1 Heterogeneous catalysts

The development of catalysts that are active in the copolymerization of epoxides and CO_2 has been excellently reviewed by a number of groups.[37-47] Following a brief historical overview of the most important milestones in the catalysis of copolymerization, the focus of this chapter will be on the possibility for the terpolymerization of epoxides with other types of monomers. In addition, the coupling of limonene oxide and CO_2 giving the fully bio-based polymer poly(limonene carbonate) will be discussed in detail. The copolymerization of carbon dioxide and epoxides was observed for the very first time when Inoue *et al.* mixed diethylzinc and water with propylene oxide and CO_2 in 1969.[7, 48]. Despite the low activity of 0.12 h^{-1} as well as low molecular weights, this finding marks the beginning of an intensively studied research field. Soga *et al.* changed to a system of $Zn(OH)_2$ and various dicarboxylic acids and in this way created the first well-defined heterogeneous catalyst.[49] Glutaric acid turned out to be the most active partner to $Zn(OH)_2$, enabling an activity of 1.1 h^{-1}. The easy preparation along with the nontoxicity of zinc made this system industrially relevant for the preparation of poly(propylene carbonate). Nevertheless, the reaction mechanism remained unknown for a long time. Single-crystal X-ray spectroscopy revealed a tetrahedral coordination of four carboxylic groups around the zinc center, which prevents monomer diffusion, thus limiting the catalyst's activity.[50] Attempts to increase the ZnGA (zinc glutarate) surface area by ball milling, modification of the stirring procedure, or the use of additives such as SiO_2 did not lead to significantly higher activity.[51-53]

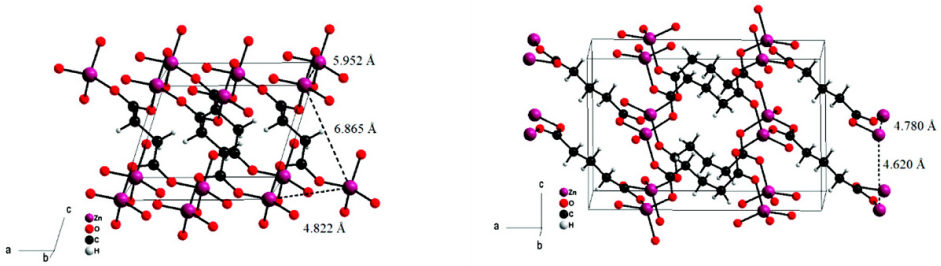

Figure 5. Representation of part of the repeating unit in two different zinc carboxylates: (a) zinc succinate and (b) zinc glutarate. Reproduced with permission from [51], Copyright © 2011 American Chemical Society.

In 2011, Rieger and coworkers demonstrated the importance of the Zn-Zn distance by varying the chain length of the carboxylic acid ranging from succinic acid (C_4) to pimelic acid (C_7).[51] Interestingly, zinc succinate (ZnSA) indeed showed nearly no activity in the copolymerization of PO and CO_2, whereas ZnGA, zinc adipate, and zinc pimelate exhibited similar activity. The reason could be addressed by measuring the solid-state structures, indicating a Zn-Zn distance only for the latter three systems of 4.6-4.8 Å, whereas ZnSA did not show such a defined spatial proximity (Figure 5). This principle of two interacting zinc centers was later transferred to the development of homogeneous catalysts.

3.2 Overview of the homogeneous catalytic systems

Although heterogeneous catalysts display numerous advantages, including sufficient activities in the copolymerization, defining the active sites in these systems is challenging. As a result, improvements to the catalyst's structure as well as the study of reaction kinetics are difficult to address. Regarding polymer chemistry, the variety of active sites also causes broad polydispersity indices (*Đ*) with severe effects on thermal and mechanical properties. In 1978, Inoue *et al.* was again first in developing an aluminum tetraphenylporphyrin (TPP) complex (**1a**, M = Al, X = OMe).[54-56] By using $EtPh_3PBr$ as a cocatalyst, the complex successfully catalyzed the CHO/CO_2 and PO/CO_2 polymerization. Figure 6 illustrates the four main complex structures used in the copolymerization of CO_2 and epoxides.

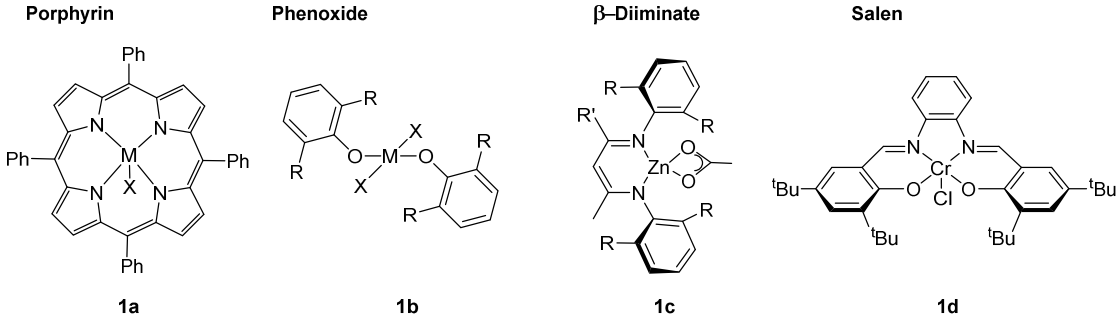

Figure 6. Types of homogeneous catalysts active in the copolymerization of CO_2 and epoxides.[4]

When Kruper and Dellar used chromium as the central metal for porphyrin based complexes in combination with the cocatalysts 4-(dimethylamino)pyridine (DMAP) and bis(triphenylphosphine)iminium chloride (PPNCl), they observed mostly cyclic carbonate formation both for cyclohexene oxide and propylene oxide.[57] In contrast, switching to cobalt (**1a**, M = Co, X = halide) led to a decrease in activity due to the reduced Lewis acidity of the metal, but it yielded high polycarbonate selectivities, especially for PO/CO_2 (99% polycarbonate,

turn-over frequency (TOF) = 188 h^{-1}).[58] Various porphyrin-based catalysts were synthesized and tested in the copolymerization of propylene oxide and CO_2.[59-66]

The first aryl-oxide zinc complex paved the way for a novel class of catalysts, namely the phenoxide system (**1b**) bearing the advantage of being soluble, and as a result more easily characterized and improved.[67] Their activity in the copolymerization reaction is mainly dependent on the aryl ligand framework and the base ligand at the metal center.[68] Substituents in ortho position were screened systematically, which show the trend of increased activity along with decreasing substituent size and increasing electronegativity (F>Cl>Br, X = thf).[69] Apart from one of the first successful terpolymerizations from CHO, PO and CO_2, this class of catalysts also indicated that epoxide activation is more decisive for high activities than the carbon dioxide insertion step.[30, 34, 70]

A breakthrough in the copolymerization of epoxides and CO_2 was achieved by Coates in 1998 with the complexation of a β-diiminate (BDI) ligand to zinc (**1c**).[71] A variety of modifications were performed at the pentane backbone as well as at the aniline moieties and the nucleophilic initiating group.[39, 72-75] Having a closer look at the reaction kinetics again a bimetallic mechanism was observed with a reaction order of $[Zn]_{tot}$ = 1.73.[76] The complexes are usually in a monomer-dimer equilibrium and form these dimeric species via a bridging of the initiating group. Scheme 3 shows the ring-opening step of CHO in a bimetallic transition state and the consecutive insertion of CO_2 into the metal alkoxide bond.

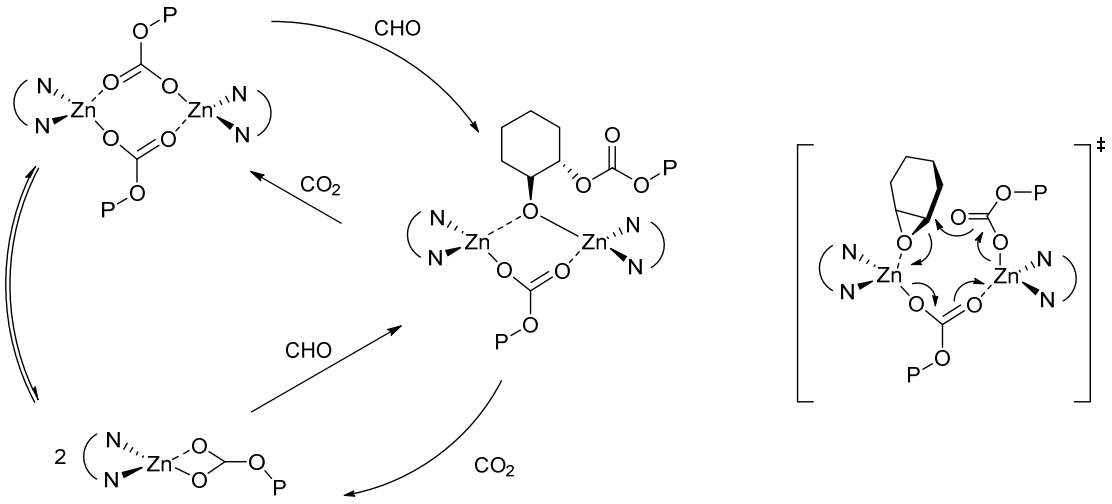

Scheme 3. Proposed copolymerization mechanism for BDI-Zn catalysts (left) and transition state of the epoxide ring-opening step (right).[39, 76]

The synthetic realization of a flexibly tethered bimetallic catalyst was done by Rieger and coworkers (Figure 7). In the copolymerization of CHO with CO_2, the bimetallic catalyst showed a TOF of 23,000 h^{-1} at 100 °C and 30 bar.[77] Further increasing the Lewis acidity at the zinc center by introducing CF_3-groups at the pentane backbone even increased the activity to the highest reported TOF for CHO with 155,000 h^{-1}.[77] The two zinc centers seem to have the perfect distance for enabling a rapid CHO coordination and ring-opening. The reaction orders have been determined for catalyst **2a** and a switch in der rate-determining step observed.[78] At CO_2 pressures below 25 bar, the insertion of CO_2 becomes rate-limiting whereas the insertion of CHO is no longer bearing the reaction order of 1, but shows zero-order dependency.

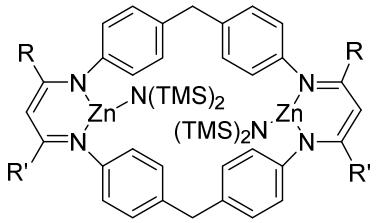

R = Me; R' = Me **2a**
R = CF_3; R' = Ph **2b**

2a TOF = 23,000 h^{-1}
2b TOF = 155,000 h^{-1}

Figure 7. Flexibly tethered bimetallic zinc complex.[77]

Applying catalyst **2a** in the copolymerization of propylene oxide and CO_2 resulted in very low activities and selectivities towards polycarbonate formation.[79-80] Density functional theory (DFT) calculations indicate a thermodynamically stable six-membered transition state consisting of an alkoxide-terminated chain end, the catalyst, and a carbonate moiety with 104.8 kJ/mol to be overcome in the case of propylene oxide as epoxide. The incorporation of a carbon dioxide molecule in the polymerization of CHO as epoxide is less hindered explaining this discrepancy in the activity for both epoxides. A great deal of efforts was put into the modification of dimeric complexes, but no major improvements were achieved for propylene oxide. Returning to the mononuclear structure and introducing two electron withdrawing CF_3-groups at the pentane backbone revealed an 'all-rounder' for the copolymerization of various epoxides and CO_2 (Figure 8).[81] In the case of CHO high turn-over frequencies (TOF = 5520 h^{-1}) were again observed. In addition, however, challenging epoxides like PO (TOF = 53 h^{-1}), styrene oxide (TOF = 26 h^{-1}), or the less explored limonene oxide (TOF = 310 h^{-1}) were copolymerized to high molecular weights (M_n = 21.0-134 kg/mol) in a controlled manner ($Đ$ = 1.2-1.8). A more detailed overview of the copolymerization of limonene oxide with CO_2 is presented in Chapter 3.4.

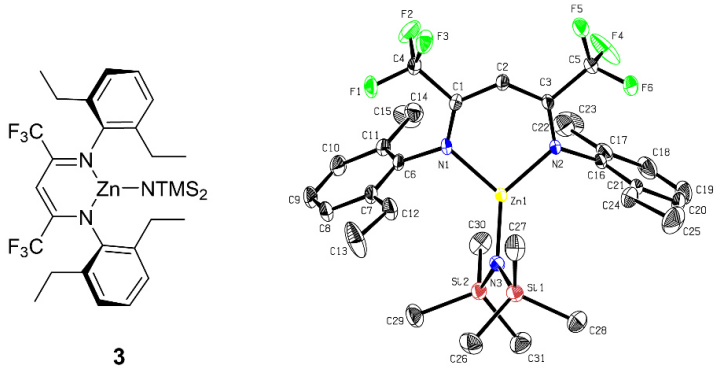

Figure 8. Structure of the β-diiminato-zinc-$NTMS_2$ complex **3** and its ORTEP style representation with ellipsoids drawn at the 50% probability level. Reproduced with permission from [81], Copyright © 2017 Royal Society of Chemistry.

The most intensively studied system for the copolymerization of epoxides and CO_2 is the metal salen system (**1d**). It has been excellently reviewed by a number of groups and will only be discussed briefly within this chapter.[41-42, 82] Although suffering from overall lower activities than BDI complexes, salen ligands coordinated to a suitable transition metal (Cr, Co, etc.) allow high polymer selectivity under mild conditions and the introduction of regioselectivity. The first cobalt salen complex was published by Coates *et al.* in 2003.[83] For the coupling of PO and CO_2 high polymer selectivities (>99%) for polymerization temperatures between 15 - 40 °C and molecular weights of up to 21.7 kg/mol were achieved. The N,N,O,O-tetradentate ligand structure has been optimized but, also the cocatalyst plays an important role. The axial X group at the metal center should be an electrophile of poor leaving ability (e.g. 2,4-dinitrophenoxy or halide), whereas bulky nucleophiles with low coordination ability are good candidates for a cocatalyst (e.g. Bu_4NCl, PPNCl). Head-to-tail connectivities of >95% were able to be realized.[84] Based on these results, the salen systems have been improved in terms of activity, stereo- and regioselectivity.[85-88]

A series of bimetallic complexes supported by a macrocyclic ligand system based on diphenolates were prepared by Williams *et al.* (Figure 9).[89] The complexes were active in the copolymerization of CHO and CO_2 even at very low pressures (p_{CO2} = 1 bar) with the polycarbonate selectivity remaining high. The introduction of defined equivalents of H_2O acting as chain-transfer agents allowed the synthesis of polyols in controlled molecular weights. These polyols represent an interesting group of candidates for the production of polyurethanes.[90] Synthetic modifications both at the metal center and at the nucleophilic leaving group led to improvements in terms of activity and selectivity.[91-94]

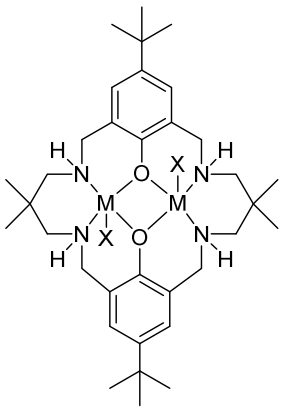

4

4a M = Zn, X = OAc
4b M = Mg, X = OAc
4c M = Mg, X = Br
4d M = Zn, X = CF_3CO_2
4e M = Zn, X = Ph

Figure 9. Macrocyclic diphenolate complexes with Zn or Mg as central metal.[90-91, 95-96]

3.3 Terpolymerization pathways

The class of macrocyclic diphenolate complexes was also able to catalyze the ring-opening polymerization of other types of monomers such as lactones and anhydrides in combination with epoxides. In a first example, terpolymers from CHO, CO_2 and ε-caprolactone were synthesized to ABA block copolymers consisting of polyester and polycarbonate units. The catalyst exclusively initiated the copolymerization of CHO and CO_2, followed by the ring-opening polymerization of ε-CL only after releasing CO_2 completely from the reaction atmosphere.[95] In this case, CHO served as an situ formed alkoxide initiator enabling ring-opening step of the lactone. The monomer scope was even extended to anhydrides, allowing the chemoselective synthesis of copolyesters and copolyester-carbonates.[97] Using mixtures of three different monomers limits the synthesis of polymers to ABA block copolymers.[98] Pentablocks were realized by activating a similar dizinc catalyst with cyclohexanediol.[96] The diol enables the in situ formation of two alkoxide initiators, allowing the combination of three different catalytic cycles in a one-pot polymerization of four different types of monomer, namely phthalic anhydride, ε-decalactone, CHO, and CO_2. Another approach for the combination of different catalytic cycles was presented by Wang *et al.* in 2018.[99] The terpolymerization of CO_2, epoxides and vinyl monomers by a porphyrin aluminum complex is presented. The advantage of this catalyst is its compatibility with the reversible addition-fragmentation chain-transfer (RAFT) polymerization, which enables the synthesis of PPC-b-PMMA copolymers to M_n = 11.9-21.6 kg/mol in narrow dispersities (1.09-1.14). The switch in the catalytic cycle was realized by a bifunctional chain-transfer agent. A different approach was done by our group in order to realize both consecutively and simultaneously proceeding catalytic cycles.[100] BDI-Zn-$NTMS_2$

complex **3** shows high activity for both the ring-opening polymerization of β-butyrolactone and the copolymerization of CO_2 and epoxides.[81, 101] CO_2 controlled AB and BA block copolymers were able to be prepared in one-pot polymerizations. Specifically, the polymerization procedure starting with the copolymerization of CO_2 and CHO ran in a highly selective manner since no incorporation of BBL was observed at that stage, and the ROP of BBL did not start until the excess of the carbon dioxide pressure was released. By lowering the CO_2 pressure to 3 bar, similar reaction rates for the two types of polymerization led to a statistical composition of the terpolymers. Molecular weights between 34 kg/mol and 166 kg/mol were obtained. Interestingly, the block copolymers exhibit two glass transition temperatures ($T_{g,\,PHB}$ ~ 2 °C, $T_{g,\,PCHC}$ ~ 115 °C) due to phase separation, whereas the mix-T_g of the statistical terpolymer ranges between 36-91 °C. Mechanistic insights could be gained using in situ IR spectroscopy, 2D NMR spectroscopy and polarimetry, thus suggesting two zinc-alkoxide intermediates that can coordinate either BBL or CO_2 (Figure 10). Following carbon dioxide insertion the respective zinc-carbonate facilitates the ring-opening of CHO.

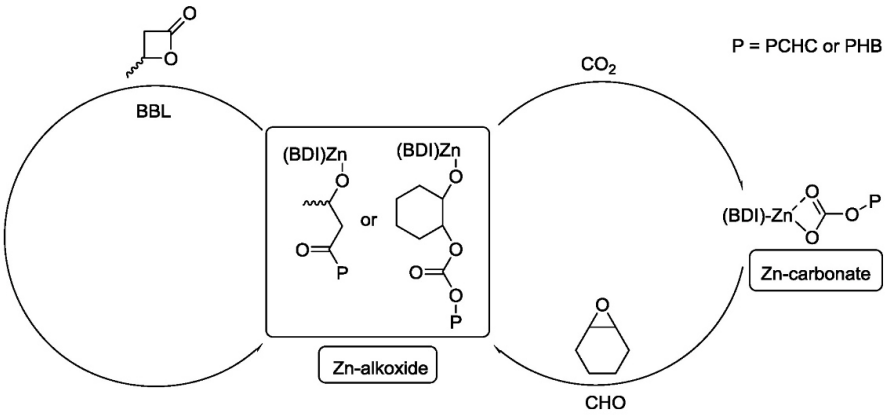

Figure 10. Postulated mechanism for the terpolymerization reaction of BBL, CHO and CO_2 under 3 bar CO_2 pressure with catalyst **3**. Reproduced with permission from [100], Copyright © 2018 American Chemical Society.

3.4 Limonene oxide: Recent advances in catalysis and mechanism elucidation

The bio-based limonene oxide was successfully copolymerized with CO_2 by Coates *et al.* in 2004 using the Lewis acidic zinc catalyst **5** (Figure 11).[8] This catalyst bears one electron-withdrawing CF_3-group in the pentane backbone and an acetate moiety serving as a nucleophilic initiating group. A maximum TOF of 37 h^{-1} was achieved at a reaction temperature of 25 °C. Surprisingly, the activity decreased drastically for temperatures above 35 °C. The reason for this was later

explained by a relatively low ceiling temperature of PLC in the presence of a catalyst.[81] The second interesting observation was the exclusive incorporation of the trans-limonene oxide into the polymer even though the initial monomer consisted of a 46:54 cis:trans mixture. This fact renders the synthesis of PLC with BDI-Zn catalysts economically unfriendly. One approach was achieved by the group of Kleij with the introduction of an amino-triphenolate aluminum complex **6** with PPNCl as cocatalyst.[102] Based on DFT calculations, it was shown that a precoordinated LO is prone to a nucleophilic attack by the chloride of PPNCl. This ring-opening step of the epoxide can occur on both positions of the oxirane ring. Surprisingly, the attack on the α-C-atom (position of methyl-group) requires the lowest energy but overall, both diastereomers are incorporated into the polymer. In the same year, Coates changed the nucleophilic initiating group of system **5** from acetate to a trimethylsilylamide group.[103] The crystal structure of a 1:1 mixture of amorphous poly(R-limonene carbonate) and poly(S-limonene carbonate) indicate a semi-crystalline nature of the packed polymer chains.[104]

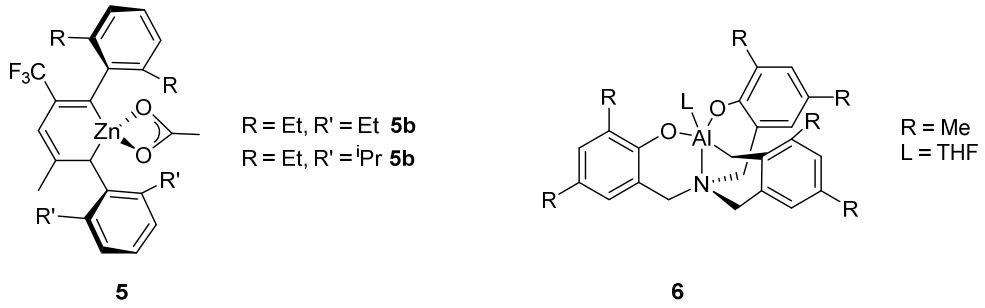

5 **6**

Figure 11. Active initiators for the copolymerization of CO_2 and limonene oxide: BDI-Zn-OAc **5** and the amino-triphenolate aluminum complex **6**.[8, 102]

A second approach was demonstrated by Greiner and Rieger:[16] The stereoselective epoxidation route from *(+)*-limonene with *N*-bromosuccinimide enables the synthesis of 90% trans-limonene oxide allowing the use of BDI-Zn catalysts in a more economic way. In addition, higher molecular weights (> 100 kDa) were achieved, and the most important thermal, optical and mechanical properties were determined. A glass transition temperature of 130 °C along with a transmission of a polymer film of 97% and a Young's modulus of 0.95 GPa with an elongation at break of 15% demonstrate the high potential of PLC for use as a rigid plastic alternative. Within this work, the reaction orders were determined for the polymerization with a BDI-Zn-OAc catalyst, and a possible mechanism could be postulated. In the case of CHO as an epoxide the overall rate equation is $-d[CHO]/dt = k \cdot [CO_2]^0 \cdot [CHO]^1 \cdot [Zn]^1$ for the same catalyst.[76] This demonstrates that the coordination of CHO is the rate-determining step, whereas the incorporation of CO_2 is very fast. The decisive difference in the rate law for limonene oxide was observed for the order with respect to limonene oxide: $-d[LO]/dt = k \cdot [CO_2]^0 \cdot [LO]^2 \cdot [Zn]^1$. Due to

the higher steric demand of the limonene oxide molecule, it is assumed that a nucleophilic attack of the acetate group is not possible within the first step (Figure 12). It rather requires the coordination of a second LO molecule to spatially separate the two zinc centers. After a rearrangement, the initiating group can finally successfully ring-open the epoxide, and the alternating addition of carbon dioxide and limonene oxide can take place.

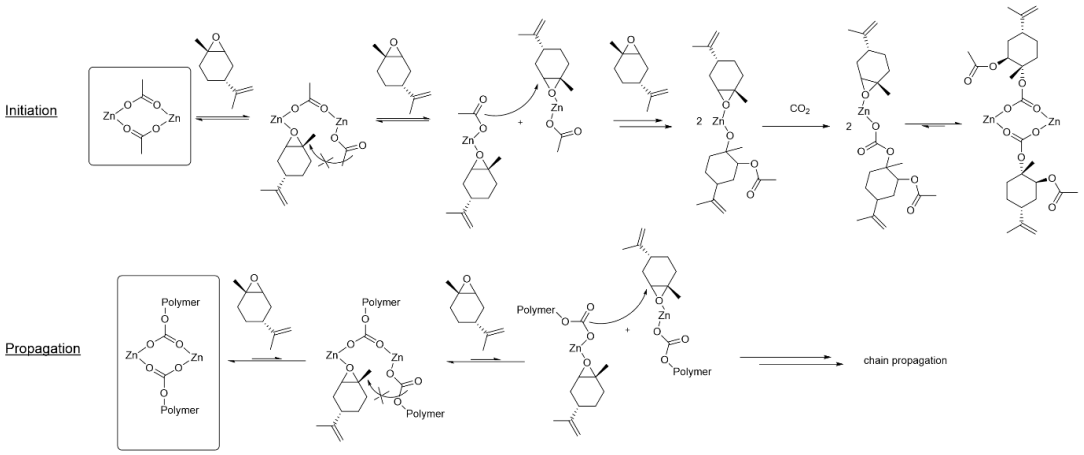

Figure 12. Postulated mechanism for the copolymerization of limonene oxide and CO_2 with BDI-Zn-OAc. Reproduced with permission from [16], Copyright © 2016 Royal Society of Chemistry.

Modifying the BDI structure by the introduction two electron withdrawing groups and an $NTMS_2$-initiating group led to the highest activity in the copolymerization of LO and CO_2 at a TOF of 310 h^{-1}.[81] In this work, the reason for low conversions at elevated temperatures was addressed in more detail. As previously observed by Coates, the polymerization to PLC hardly reaches high conversions and actually results in lower yields when polymerized at 60 °C instead of at 40 °C. It was assumed that either cis-LO that stays in the reaction mixture and is not polymerized or the double bond of LO might act as catalyst poison preventing the polymerization from proceeding to high conversion. Both using 99% trans-LO and fully hydrated LO, also called menthene oxide, indeed showed the same polymerization behavior and no increase in yield at 60 °C. Using *in situ* IR spectroscopy, a deeper insight into polymerization activity at certain temperatures could be gained indicating a relatively low ceiling temperature at 60 °C for LO concentrations of 3.5 mol/L.[81] Until now, a multitude of different synthetic modifications were performed and possible applications investigated.[27, 105-110] Kleij *et al.* developed a stepwise approach to poly(limonene dicarbonate) via PLC followed by the epoxidation of the isopropenyl group that again can be transformed into the respective carbonate with the help of CO_2 and PPNCl.[111] Glass transition temperatures of up to 180 °C were obtained for molar masses of 15 kg/mol ($Đ$ = 1.31). The group of Koning also investigated the synthesis and use of

poly(limonene-8,9-oxide carbonate).[112] They obtained this aliphatic epoxy polycarbonate through the alternating copolymerization of limonene dioxide and CO_2 with a BDI-Zn-$NTMS_2$ catalyst. The epoxy group opens a magnitude of possibilities for post-modification: Thiols, carboxylic acids or CO_2 again afford functional polymers for different areas of application like epoxy resins or non-isocyanate polyurethanes.

4. Conclusion

Aliphatic polycarbonates have been known for more than 50 years but remain highly interesting in a variety of research areas. While poly(propylene carbonate), derived from propylene oxide and CO_2, has already found its industrial application in small scale processes, poly(cyclohexene carbonate) continues to serve as an academic bench mark for catalysis research. Although heterogeneous systems dominate the industrial PO/CO_2 copolymerization, with homogeneous catalysts dramatic improvements become possible in the last decade. β-diiminate zinc systems seem to be the most active catalysts for the copolymerization of cyclohexene oxide and CO_2. Besides BDI complexes, macrocyclic diphenolate systems allow the coupling of CO_2 and epoxides as well as the incorporation of another type of monomer like cyclic esters or anhydrides. These one-pot terpolymerizations can be nicely controlled via the carbon dioxide pressure. The combination of various polymerization cycles by a single catalyst represents an interesting tool for chemoselectively building up block copolymers with different features. BDI complexes also enable the coupling of the bio-based epoxide limonene oxide and CO_2 to the very promising material poly(limonene carbonate). Intense research in recent years has revealed possible areas of application for PLC: In addition to the use as a non-isocyanate building block in polyurethane production or in coating applications, the detailed determination of its thermal, optical and mechanical properties has made it a potential rigid plastic alternative to bisphenol-A polycarbonate. However, turnover numbers still need to be increased for limonene oxide, and it will be very interesting to see whether this limitation can be solved in the near future in order to make an industrial process possible.

5. References

[1] B. M. Bhanage, M. Arai, *Transformation and Utilization of Carbon Dioxide*, Springer, Berlin/Heidelberg, Germany, **2014**.
[2] T. Sakakura, K. Kohno, *Chem. Comm.* **2009**, 1312-1330.
[3] H. Büttner, L. Longwitz, J. Steinbauer, C. Wulf, T. Werner, *Top. Curr. Chem.* **2017**, *375*, 50.
[4] X. B. Lu, *Carbon Dioxide and Organometallics*, Springer International Publishing, **2015**.
[5] G. A. Luinstra, *Poly. Rev.* **2008**, *48*, 192-219.
[6] J. Langanke, A. Wolf, J. Hofmann, K. Böhm, M. A. Subhani, T. E. Müller, W. Leitner, C. Gürtler, *Green Chem.* **2014**, *16*, 1865-1870.
[7] S. Inoue, H. Koinuma, T. Tsuruta, *Die Makromolekulare Chemie* **1969**, *130*, 210-220.

[8] C. M. Byrne, S. D. Allen, E. B. Lobkovsky, G. W. Coates, *J. Am. Chem. Soc.* **2004**, *126*, 11404-11405.

[9] H. Baer, M. Bergamo, A. Forlin, L. H. Pottenger, J. Lindner, in *Ullmann's Encyclopedia of Industrial Chemistry*, **2012**.

[10] B. Yilmaz, U. Müller, *Top. Catal.* **2009**, *52*, 888-895.

[11] A. Kreimeyer, P. Eckes, C. Fischer, H. Lauke, P. Schuhmacher, *Angew. Chem. Int. Ed.* **2015**, *54*, 3178-3195.

[12] X.-T. Zhou, H.-B. Ji, J.-C. Xu, L.-X. Pei, L.-F. Wang, X.-D. Yao, *Tetrahedron Lett.* **2007**, *48*, 2691-2695.

[13] R. J. Gall, F. P. Greenspan, Google Patents US2745848 A, **1956**.

[14] A. M. Chapman, C. Keyworth, M. R. Kember, A. J. J. Lennox, C. K. Williams, *ACS Catal.* **2015**, *5*, 1581-1588.

[15] R. Ciriminna, M. Lomeli-Rodriguez, P. Demma Carà, J. A. Lopez-Sanchez, M. Pagliaro, *Chem. Comm.* **2014**, *50*, 15288-15296.

[16] O. Hauenstein, M. Reiter, S. Agarwal, B. Rieger, A. Greiner, *Green Chem.* **2016**, *18*, 760-770.

[17] S. J. Poland, D. J. Darensbourg, *Green Chem.* **2017**, *19*, 4990-5011.

[18] F. P. Greenspan, S. M. Linder, Google Patents US3014929 A, **1961**.

[19] D. J. Darensbourg, J. C. Yarbrough, C. Ortiz, C. C. Fang, *J. Am. Chem. Soc.* **2003**, *125*, 7586-7591.

[20] M. H. Chisholm, D. Navarro-Llobet, Z. Zhou, *Macromolecules* **2002**, *35*, 6494-6504.

[21] B. Liu, X. Zhao, X. Wang, F. Wang, *J. Appl. Polym. Sci.* **2003**, *90*, 947-953.

[22] J. K. Varghese, S. J. Na, J. H. Park, D. Woo, I. Yang, B. Y. Lee, *Polym. Degrad. Stab.* **2010**, *95*, 1039-1044.

[23] S. Lin, W. Yu, X. Wang, C. Zhou, *Ind. Eng. Chem. Res.* **2014**, *53*, 18411-18419.

[24] O. Phillips, J. M. Schwartz, P. A. Kohl, *Polym. Degrad. Stab.* **2016**, *125*, 129-139.

[25] D. J. Darensbourg, *Polym. Degrad. Stab.* **2018**, *149*, 45-51.

[26] B. Rieger, A. Künkel, G. W. Coates, *Synthetic Biodegradable Polymers*, Springer, Berlin/Heidelberg, Germany, **2012**.

[27] C. Li, R. J. Sablong, R. A. T. M. van Benthem, C. E. Koning, *ACS Macro Lett* **2017**, *6*, 684-688.

[28] D. J. Darensbourg, S.-H. Wei, A. D. Yeung, W. C. Ellis, *Macromolecules* **2013**, *46*, 5850-5855.

[29] Y. Qin, X. Wang, *Biotechnol. J.* **2010**, *5*, 1164-1180.

[30] C. Koning, J. Wildeson, R. Parton, B. Plum, P. Steeman, D. J. Darensbourg, *Polymer* **2001**, *42*, 3995-4004.

[31] J. E. Seong, S. J. Na, A. Cyriac, B.-W. Kim, B. Y. Lee, *Macromolecules* **2010**, *43*, 903-908.

[32] S. D. Thorat, P. J. Phillips, V. Semenov, A. Gakh, *J. Appl. Polym. Sci.* **2003**, *89*, 1163-1176.

[33] L. Shi, X.-B. Lu, R. Zhang, X.-J. Peng, C.-Q. Zhang, J.-F. Li, X.-M. Peng, *Macromolecules* **2006**, *39*, 5679-5685.

[34] D. J. Darensbourg, M. W. Holtcamp, *Macromolecules* **1995**, *28*, 7577-7579.

[35] Y. Demirel, *J. Chem. Eng. Process Technol.* **2015**, *6*, 236.

[36] X. L. Wang, F. G. Du, J. Jiao, Y. Z. Meng, R. K. Y. Li, *J. Biomed. Mater. Res. B* **2007**, *83B*, 373-379.

[37] S. Klaus, M. W. Lehenmeier, C. E. Anderson, B. Rieger, *Coord. Chem. Rev.* **2011**, *255*, 1460-1479.

[38] D. J. Darensbourg, M. W. Holtcamp, *Coord. Chem. Rev.* **1996**, *153*, 155-174.

[39] G. W. Coates, D. R. Moore, *Angew. Chem. Int. Ed.* **2004**, *43*, 6618-6639.

[40] H. Sugimoto, S. Inoue, *J. Polym. Sci. Pol. Chem.* **2004**, *42*, 5561-5573.

[41] D. J. Darensbourg, R. M. Mackiewicz, A. L. Phelps, D. R. Billodeaux, *Acc. Chem. Res.* **2004**, *37*, 836-844.

[42] D. J. Darensbourg, *Chem. Rev.* **2007**, *107*, 2388-2410.

[43] M. R. Kember, A. Buchard, C. K. Williams, *Chem. Comm.* **2011**, *47*, 141-163.

[44] D. J. Darensbourg, S. J. Wilson, *Green Chem.* **2012**, *14*, 2665-2671.

[45] M. I. Childers, J. M. Longo, N. J. Van Zee, A. M. LaPointe, G. W. Coates, *Chem. Rev.* **2014**, *114*, 8129-8152.

[46] Y. Wang, D. J. Darensbourg, *Coord. Chem. Rev.* **2018**, *372*, 85-100.

[47] C. M. Kozak, K. Ambrose, T. S. Anderson, *Coord. Chem. Rev.* **2018**, *376*, 565-587.
[48] S. Inoue, H. Koinuma, T. Tsuruta, *J. Polym. Sci.* **1969**, *7*, 287-292.
[49] K. Soga, E. Imai, I. Hattori, *Polym. J.* **1981**, *13*, 407-410.
[50] M. Ree, Y. Hwang, J.-S. Kim, H. Kim, G. Kim, H. Kim, *Catal. Today* **2006**, *115*, 134-145.
[51] S. Klaus, M. W. Lehenmeier, E. Herdtweck, P. Deglmann, A. K. Ott, B. Rieger, *J. Am. Chem. Soc.* **2011**, *133*, 13151-13161.
[52] Y. Z. Meng, L. C. Du, S. C. Tiong, Q. Zhu, A. S. Hay, *J. Polym. Sci. Pol. Chem.* **2002**, *40*, 3579-3591.
[53] L. J. Gao, M. Xiao, S. J. Wang, F. G. Du, Y. Z. Meng, *J. Appl. Polym. Sci.* **2007**, *104*, 15-20.
[54] N. Takeda, S. Inoue, *Die Makromolekulare Chemie* **1978**, *179*, 1377-1381.
[55] T. Aida, S. Inoue, *J. Am. Chem. Soc.* **1985**, *107*, 1358-1364.
[56] F. Kojima, T. Aida, S. Inoue, *J. Am. Chem. Soc.* **1986**, *108*, 391-395.
[57] W. J. Kruper, D. D. Dellar, *J. Org. Chem.* **1995**, *60*, 725-727.
[58] Y. Qin, X. Wang, S. Zhang, X. Zhao, F. Wang, *J. Polym. Sci. Pol. Chem.* **2008**, *46*, 5959-5967.
[59] M. H. Chisholm, Z. Zhou, *J. Am. Chem. Soc.* **2004**, *126*, 11030-11039.
[60] P. Chen, M. H. Chisholm, J. C. Gallucci, X. Zhang, Z. Zhou, *Inorg. Chem.* **2005**, *44*, 2588-2595.
[61] C. E. Anderson, S. I. Vagin, W. Xia, H. Jin, B. Rieger, *Macromolecules* **2012**, *45*, 6840-6849.
[62] C. Chatterjee, M. H. Chisholm, *Inorg. Chem.* **2012**, *51*, 12041-12052.
[63] C. E. Anderson, S. I. Vagin, M. Hammann, L. Zimmermann, B. Rieger, *ChemCatChem* **2013**, *5*, 3269-3280.
[64] W. Xia, S. I. Vagin, B. Rieger, *Chem. Eur. J.* **2014**, *20*, 15499-15504.
[65] X. Sheng, Y. Wang, Y. Qin, X. Wang, F. Wang, *RSC Adv.* **2014**, *4*, 54043-54050.
[66] W. Wu, X. Sheng, Y. Qin, L. Qiao, Y. Miao, X. Wang, F. Wang, *J. Polym. Sci. Pol. Chem.* **2014**, *52*, 2346-2355.
[67] R. L. Geerts, J. C. Huffman, K. G. Caulton, *Inorg. Chem.* **1986**, *25*, 1803-1805.
[68] D. J. Darensbourg, S. A. Niezgoda, J. D. Draper, J. H. Reibenspies, *J. Am. Chem. Soc.* **1998**, *120*, 4690-4698.
[69] D. J. Darensbourg, J. R. Wildeson, J. C. Yarbrough, J. H. Reibenspies, *J. Am. Chem. Soc.* **2000**, *122*, 12487-12496.
[70] D. J. Darensbourg, M. W. Holtcamp, G. E. Struck, M. S. Zimmer, S. A. Niezgoda, P. Rainey, J. B. Robertson, J. D. Draper, J. H. Reibenspies, *J. Am. Chem. Soc.* **1999**, *121*, 107-116.
[71] M. Cheng, E. B. Lobkovsky, G. W. Coates, *J. Am. Chem. Soc.* **1998**, *120*, 11018-11019.
[72] M. Cheng, D. R. Moore, J. J. Reczek, B. M. Chamberlain, E. B. Lobkovsky, G. W. Coates, *J. Am. Chem. Soc.* **2001**, *123*, 8738-8749.
[73] D. R. Moore, M. Cheng, E. B. Lobkovsky, G. W. Coates, *Angew. Chem. Int. Ed.* **2002**, *41*, 2599-2602.
[74] L. Bourget-Merle, M. F. Lappert, J. R. Severn, *Chem. Rev.* **2002**, *102*, 3031-3066.
[75] M. Cheng, N. A. Darling, E. B. Lobkovsky, G. W. Coates, *Chem. Comm.* **2000**, 2007-2008.
[76] D. R. Moore, M. Cheng, E. B. Lobkovsky, G. W. Coates, *J. Am. Chem. Soc.* **2003**, *125*, 11911-11924.
[77] S. Kissling, M. W. Lehenmeier, P. T. Altenbuchner, A. Kronast, M. Reiter, P. Deglmann, U. B. Seemann, B. Rieger, *Chem. Comm.* **2015**, *51*, 4579-4582.
[78] M. W. Lehenmeier, S. Kissling, P. T. Altenbuchner, C. Bruckmeier, P. Deglmann, A.-K. Brym, B. Rieger, *Angew. Chem. Int. Ed.* **2013**, *52*, 9821-9826.
[79] S. Kissling, P. T. Altenbuchner, M. W. Lehenmeier, E. Herdtweck, P. Deglmann, U. B. Seemann, B. Rieger, *Chem. Eur. J.* **2015**, *21*, 8148-8157.
[80] S. D. Allen, D. R. Moore, E. B. Lobkovsky, G. W. Coates, *J. Am. Chem. Soc.* **2002**, *124*, 14284-14285.
[81] M. Reiter, S. Vagin, A. Kronast, C. Jandl, B. Rieger, *Chem. Sci.* **2017**, *8*, 1876-1882.
[82] X.-B. Lu, D. J. Darensbourg, *Chem. Soc. Rev.* **2012**, *41*, 1462-1484.
[83] Z. Qin, C. M. Thomas, S. Lee, G. W. Coates, *Angew. Chem. Int. Ed.* **2003**, *42*, 5484-5487.
[84] X.-B. Lu, L. Shi, Y.-M. Wang, R. Zhang, Y.-J. Zhang, X.-J. Peng, Z.-C. Zhang, B. Li, *J. Am. Chem. Soc.* **2006**, *128*, 1664-1674.

[85] D. J. Darensbourg, J. C. Yarbrough, *J. Am. Chem. Soc.* **2002**, *124*, 6335-6342.
[86] C. T. Cohen, T. Chu, G. W. Coates, *J. Am. Chem. Soc.* **2005**, *127*, 10869-10878.
[87] X.-B. Lu, Y. Wang, *Angew. Chem. Int. Ed.* **2004**, *43*, 3574-3577.
[88] R. L. Paddock, S. T. Nguyen, *Macromolecules* **2005**, *38*, 6251-6253.
[89] A. Buchard, M. R. Kember, K. G. Sandeman, C. K. Williams, *Chem. Comm.* **2011**, *47*, 212-214.
[90] M. R. Kember, C. K. Williams, *J. Am. Chem. Soc.* **2012**, *134*, 15676-15679.
[91] M. R. Kember, P. D. Knight, P. T. R. Reung, C. K. Williams, *Angew. Chem. Int. Ed.* **2009**, *48*, 931-933.
[92] M. R. Kember, A. J. P. White, C. K. Williams, *Macromolecules* **2010**, *43*, 2291-2298.
[93] A. Buchard, F. Jutz, M. R. Kember, A. J. P. White, H. S. Rzepa, C. K. Williams, *Macromolecules* **2012**, *45*, 6781-6795.
[94] F. Jutz, A. Buchard, M. R. Kember, S. B. Fredriksen, C. K. Williams, *J. Am. Chem. Soc.* **2011**, *133*, 17395-17405.
[95] S. Paul, C. Romain, J. Shaw, C. K. Williams, *Macromolecules* **2015**, *48*, 6047-6056.
[96] T. T. D. Chen, Y. Zhu, C. K. Williams, *Macromolecules* **2018**, *51*, 5346-5351.
[97] C. Romain, Y. Zhu, P. Dingwall, S. Paul, H. S. Rzepa, A. Buchard, C. K. Williams, *J. Am. Chem. Soc.* **2016**, *138*, 4120-4131.
[98] T. Stößer, C. K. Williams, *Angew. Chem. Int. Ed.* **2018**, *57*, 6337-6341.
[99] Y. Wang, Y. Zhao, Y. Ye, H. Peng, X. Zhou, X. Xie, X. Wang, F. Wang, *Angew. Chem. Int. Ed.* **2018**, *57*, 3593-3597.
[100] S. Kernbichl, M. Reiter, F. Adams, S. Vagin, B. Rieger, *J. Am. Chem. Soc.* **2017**, *139*, 6787-6790.
[101] A. Kronast, M. Reiter, P. T. Altenbuchner, C. Jandl, A. Pöthig, B. Rieger, *Organometallics* **2016**, *35*, 681-685.
[102] L. Peña Carrodeguas, J. González-Fabra, F. Castro-Gómez, C. Bo, A. W. Kleij, *Chem. Eur. J.* **2015**, *21*, 6115-6122.
[103] F. Auriemma, C. De Rosa, M. R. Di Caprio, R. Di Girolamo, W. C. Ellis, G. W. Coates, *Angew. Chem. Int. Ed.* **2015**, *54*, 1215-1218.
[104] F. Auriemma, C. De Rosa, M. R. Di Caprio, R. Di Girolamo, G. W. Coates, *Macromolecules* **2015**, *48*, 2534-2550.
[105] O. Hauenstein, S. Agarwal, A. Greiner, *Nat. Comm.* **2016**, *7*, 11862.
[106] C. Li, R. J. Sablong, C. E. Koning, *Eur. Polym. J.* **2015**, *67*, 449-458.
[107] C. Li, M. Johansson, R. J. Sablong, C. E. Koning, *Eur. Polym. J.* **2017**, *96*, 337-349.
[108] T. Stößer, C. Li, J. Unruangsri, P. K. Saini, R. J. Sablong, M. A. R. Meier, C. K. Williams, C. Koning, *Polymer Chem.* **2017**, *8*, 6099-6105.
[109] O. Hauenstein, M. M. Rahman, M. Elsayed, R. Krause-Rehberg, S. Agarwal, V. Abetz, A. Greiner, *Adv. Mater. Technol.* **2017**, *2*, 1700026.
[110] F. Parrino, A. Fidalgo, L. Palmisano, L. M. Ilharco, M. Pagliaro, R. Ciriminna, *ACS Omega* **2018**, *3*, 4884-4890.
[111] N. Kindermann, À. Cristòfol, A. W. Kleij, *ACS Catal.* **2017**, *7*, 3860-3863.
[112] C. Li, R. J. Sablong, C. E. Koning, *Angew. Chem.* **2016**, *128*, 11744-11748.

12. Excursus: Synthesis of Novel Epoxy Monomers and Their Copolymerization with CO_2

12.1 Monomers for the Synthesis of High Refractive Index Polymers (HRIP)

In the past few centuries, optical devices such as eye glasses, sensors and display devices have experienced a tremendous change. For quite a long time, all eyeglass lenses were made of glass. Within the discovery and development of synthetic plastics, glass lenses were more and more replaced. PMMA was one of the first polymers used to produce eyeglasses followed by poly(allyldiglycol carbonate) and Makrolon® (Figure 20). Synthetic HRIP bear some outstanding advantages. Injection molding allows the mass production of the polymers at low costs to materials which withstand high mechanical stress. Due to the lowered density compared to glass, the material has a reduced weight. Most importantly, the refractive index (n_D) of synthetic polymers can be tuned via the introduction of suitable side groups or heavy metal elements. The remaining challenges for HRIPs in high-performance applications are a high chemical resistance, a good thermal stability as well as an improved scratch resistance.[147-148]

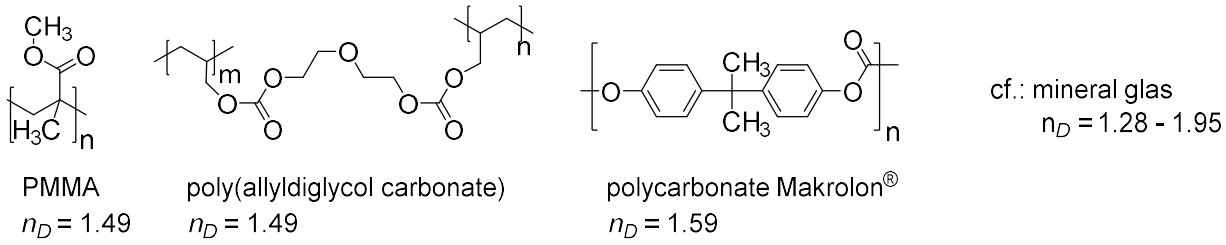

Figure 20. Development of commercial high-refractive index polymers.[148]

The patent of the synthesis of polythiourethanes by *Mitsui Chemical Inc.* in 1987 fueled the discussion about introducing heteroatoms into the polymeric network to generate HRIPs.[149] The use of sulfur containing polymers was not only restricted to polyurethanes but also polycarbonates have been closely investigated. (Salen)CrCl complexes display high activities in the copolymerization of episulfide and CS_2 and in the coupling of CHO and CS_2 to polythiocarbonates.[150-152] In this respect, the introduction of silicon was considered to be a valuable alternative approach to the generation of HRIPs.

Scheme 14. Epoxidation of vinyltrimethylsilane and its coupling with CO_2

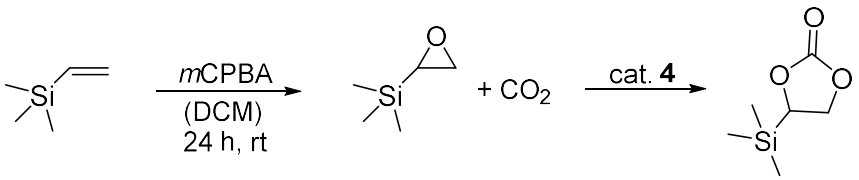

The structural motif of poly(propylene carbonate) was chosen and a silicon moiety was planned to be attached instead of the methyl group (Scheme 14). Epoxidation of vinyltrimethylsilane with *meta*-

chloroperbenzoic acid (*m*CPBA) yielded trimethylsilyloxirane which, upon treatment with CO_2 and complex **4**, did not yield the desired polycarbonate structure but the cyclic carbonate instead.

12.2 Terpene-Based Epoxides

The synthesis of sustainable polymers can be generally classified into two approaches, namely a polymer approach (natural polymers are used) and a monomer approach, where natural monomers are polymerized. Within the latter group, hydrocarbon-rich biomass as for instance terpenes represent an interesting renewable feedstock. α- and β-pinenes are the most abundant natural terpenes and can be obtained from non-edible parts of plants. The very high steric hindrance of α-pinene makes its polymerization very difficult (Figure 21). In contrast, polymers derived from β-pinene are a lot more accessible via cationic or radical polymerization methods and aliphatic cycloolefins can be obtained.[153] Another bicyclic monoterpene is 3-carene. Its chemical structure bears similarities to the well-known limonene with a dimethylcyclopropyl ring instead of the isopropenyl group.

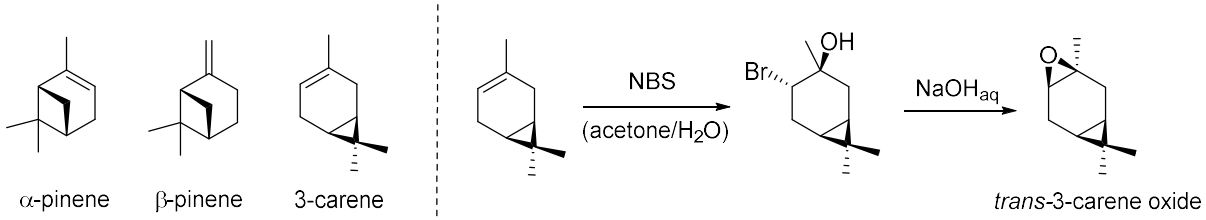

Figure 21. Terpenes as a possible feedstock for epoxidation (left). *trans*-selective epoxidation of 3-carene (right).

Since BDI complexes are known to only incorporate the *trans* monomer in the copolymerization of limonene oxide and CO_2, also for 3-carene the *trans*-selective epoxidation route was chosen. The 2-step reaction yielded 3-carene oxide in 100% *trans*-selectivity. After drying over NaH, the freshly distilled monomer was added to complex **4** and pressurized with CO_2. No conversion to the polycarbonate nor to the cyclic by-product could be observed in the ^{1}H NMR spectrum.

13. Summary

The ring-opening copolymerization of epoxides and CO_2 is a valuable method for the synthesis of aliphatic polycarbonates (Scheme 15). Carbon dioxide is used as a non-toxic, abundant C1-feedstock to produce polycarbonates independent of fossil fuels. In this work, a Lewis acidic zinc complex was used as a catalyst for the polymerization of carbon dioxide with cyclohexene oxide and limonene oxide, respectively.

Scheme 15. Ring-opening copolymerization of epoxides and CO_2 with the Lewis acidic zinc complex **4**.

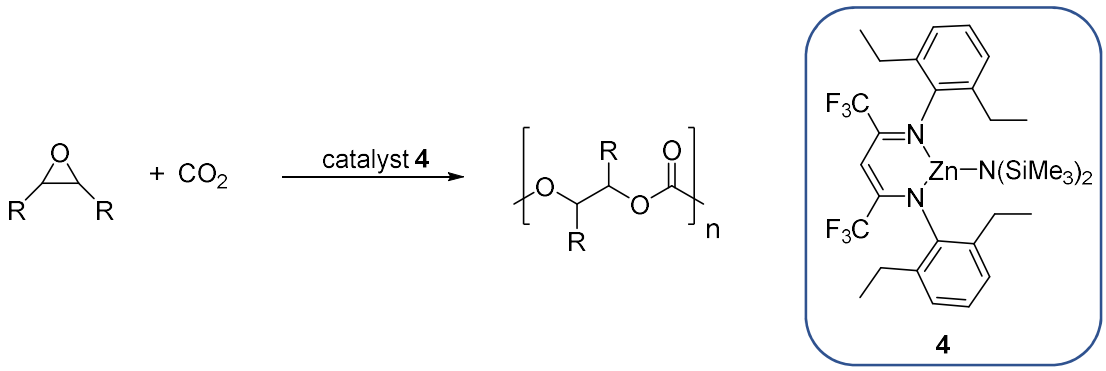

In the first part of the thesis, two approaches for the combination of the ring-opening copolymerization of epoxides and CO_2 with other mechanisms were investigated. This allowed for the introduction of an additional type of monomer into the polymer structure. The so-called terpolymerization is expected to serve as a promising method for the synthesis of polymers with an enhanced portfolio of properties. The first approach was based on the catalytic activity of the BDI^{CF3}-Zn-$N(SiMe_3)_2$ **4** for ROCOP of CHO and CO_2 but also for the ROP of lactones such as β-butyrolactone. One-pot polymerizations consisting of CHO, BBL, CO_2, and catalyst were studied towards block formation and the influence of CO_2 on the incorporation of the respective monomers. In total, three pathways were established (Figure 22). Adding no CO_2 in the beginning resulted in polyester formation with consequent polycarbonate polymerization upon CO_2 addition (AB block, route A). When 40 bar CO_2 are added at the start, exclusive polycarbonate formation was observed, and the polyester block was only formed by the time carbon dioxide was completely released from the autoclave (route B). An interesting third route has been developed by lowering the pressure to 3 bar CO_2 (route C). Due to similar reaction rates of **4** for ROCOP and ROP, both monomer types (CHO/CO_2 and BBL) were polymerized to a statistical polymer. A possible mechanism for this statistical polymerization was postulated based on polarimetry measurements of PHB and two-dimensional NMR spectroscopy. Taking a closer look at the reaction orders of the ROCOP by varying the carbon dioxide pressure revealed an interesting shift. While CO_2 is not rate-limiting (reaction order zero) in the CHO/CO_2 copolymerization at a pressure of 40 bar, the reaction order changed to a first-order dependency at lower CO_2 concentrations. The change in polymer architecture (block vs statistical) also severely influenced thermal and mechanical characteristics. PHB/PCHC terpolymers in block structure showed two separated glass transition temperatures due to phase

separation (PHB block ~5 °C; PCHC block ~115 °C) whereas those in statistical structure exhibited a mixed T_g which was tunable depending on the polymer composition.

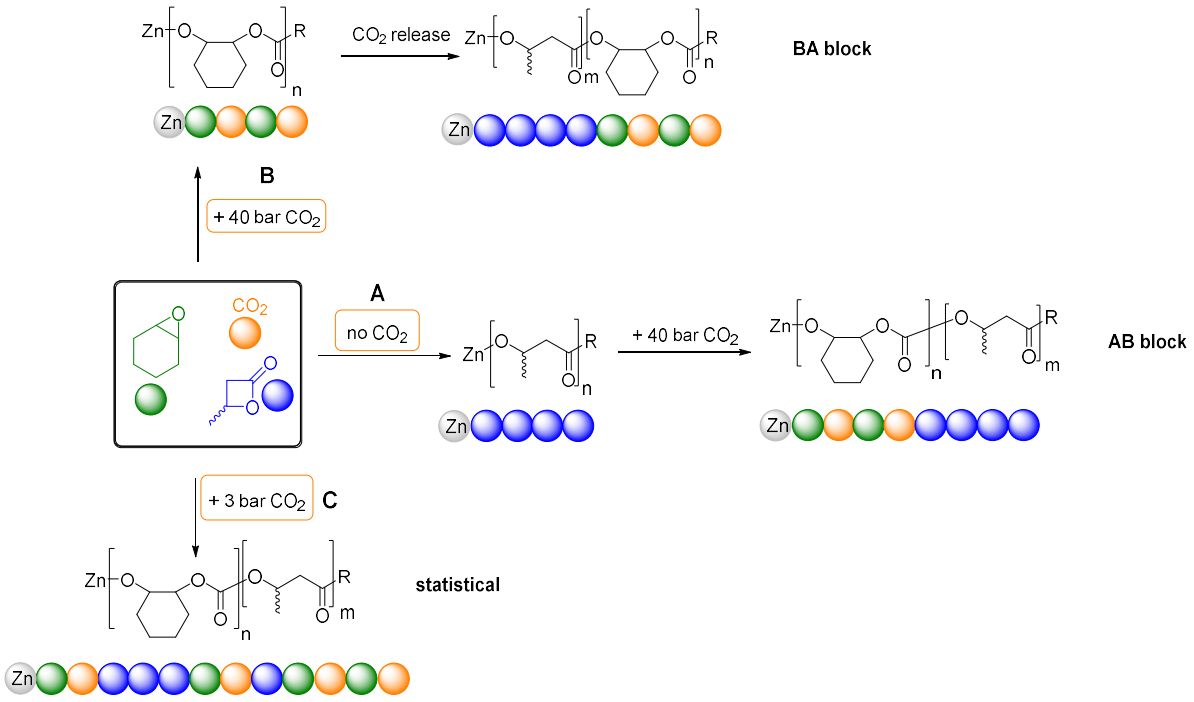

Figure 22. Illustration of the three possible polymerization pathways.

Additionally, the terpolymers were characterized towards their mechanical performance through hot-pressing into dog-bone shaped specimens and their stress-strain analysis. The overall goal was to overcome the brittleness of PCHC (Young modulus: 3600 MPa, elongation at break: 1.7%[13]) by the introduction of soft PHB blocks. Terpolymers in statistical structure showed reduced Young moduli but a similar elongation at break. Switching to PCHC/PHB polymers in high molecular weight ($M_{n,\,rel.}$>100 kg/mol) revealed an improved performance of the material (1170 MPa, 5.0%) compared to pure PCHC. Subsequently, the established reaction pathways were tested towards different types of epoxides, namely cyclopentene oxide (CPO) and limonene oxide. In case of CPO, a very similar reactivity behavior was observed, and all three polymerization routes yielded the desired terpolymers. Pure poly(cyclopentene oxide) showed a reduced T_g of 91 °C compared to PCHC due to the change in the ring size of the epoxide. The resulting terpolymers again revealed a phase separated behavior in case of the block structure and a tunable T_g when polymerized at 3 bar CO_2. An interesting reactivity change was disclosed when using limonene oxide. Applying CO_2 in the beginning of the polymerization successfully led to the formation of PLC, but upon releasing carbon dioxide to enable the polyester formation, the depolymerization of PLC started. The BDI zinc catalyzed copolymerization of LO and CO_2 was studied in detail in 2017.[50] Thereby, the depolymerization of the polycarbonate was found to become predominant at elevated temperatures at moderate to high conversions. Now, also the carbon dioxide pressure was found to be crucial for the polymerization-depolymerization equilibrium. As a result of this depolymerization, the second route starting with the polyester formation followed by the

poly(limonene carbonate) formation was chosen and yielded the PHB/PLC terpolymer in a block structure (route A). The latter showed very promising mechanical data. Adjusting the PHB/PLC composition gave materials with a varying elongation at break. Pure PLC with a Young modulus of 2350 MPa usually got destroyed at an elongation at break of 4 – 6 %. Incorporating soft PHB in a ratio of 20% and 50% let the Young modulus drop to 1800 MPa and 1450 MPa and the specimens endured 13% and 18% elongation, respectively.

In the second approach of combining different mechanisms, the aim was to couple the ring-opening copolymerization of epoxides and CO_2 with the rare earth metal-mediated group transfer polymerization. Since the BDI zinc complex **4** did not show any activity for the polymerization of Michael-type monomers such as 2-vinylpyridine and 2-*iso*-propenyl-2-oxazoline, a different concept has been established. Instead of performing the polymerization at one metal center, two metal centers are planned to be linked via a flexible linking unit (Figure 23). The initiating group of the established BDI complex was exchanged with a pyridyl alcoholate. The latter was then used to couple it with an yttrium metallocene via CH-bond activation. This heteronuclear complex **14** was tested towards the terpolymerization of CHO, CO_2, and 2VP. Previous MALDI-TOF-MS measurements confirmed the linking unit attached to the respective homopolymer PCHC and P2VP being the premise for a successful connection of the two different polymer blocks.

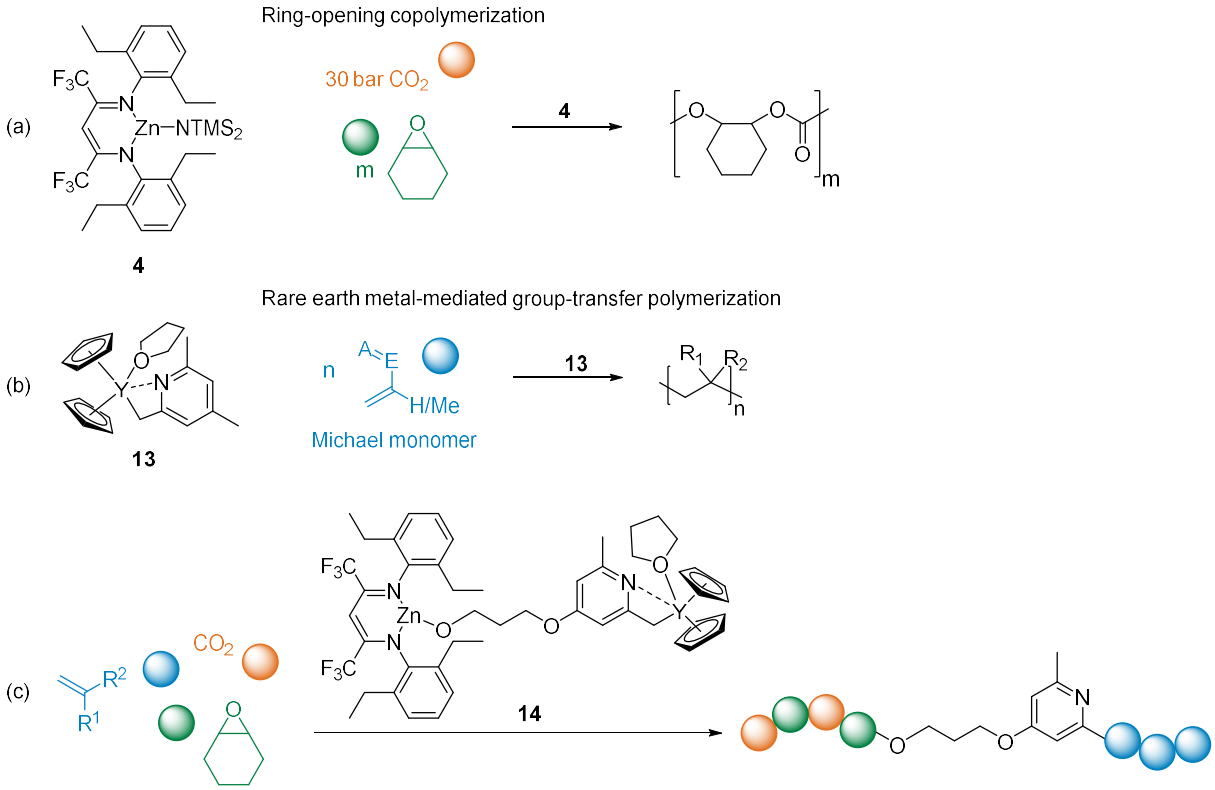

Figure 23. Ring-opening copolymerization of epoxide and CO_2 (a), rate earth metal-mediated group transfer polymerization of vinyl monomers (b), and the idea of linking two metal centers to create a heterobifunctional catalyst for the terpolymerization of epoxides, CO_2, and vinyl monomers (c).

Mixing complex **14** with CHO and CO_2, yielded PCHC but upon addition of 2VP, no P2VP was observed. The reason for this behavior could be addressed with NMR spectroscopy by applying CO_2 on complex **14**. The yttrium moiety lost its functionality because carbon dioxide afforded a dissociation of the coordinated thf molecule along with a change at the CH_2-Y bond, indicating that the pyridyl was no longer bound to yttrium. The second pathway started with the REM-GTP of 2VP and the addition of CHO and CO_2 after four hours. Indeed, conversion to P2VP and PCHC could be observed. To proof a successful block formation, aliquot GPC analysis and solubility behavior tests were conducted. A shift in the retention time of the P2VP/PCHC terpolymer relative to the P2VP aliquot was revealed. Also, solubility of a terpolymer consisting of 34% P2VP and 66% PCHC in methanol confirmed a linking of the two blocks because pure PCHC is insoluble in methanol. Additionally, one-pot polymerizations were accessible when 2VP and CHO were mixed with the catalyst in the beginning and carbon dioxide was applied at a certain 2VP conversion. The versatility of the method could be demonstrated by successfully introducing IPOx as a second type of Michael type monomer. Overall, this approach gives access to a group of terpolymers that could not be synthesized before. In future studies, properties such as thermal and mechanical performance should be investigated in more detail. Moreover, P2VP copolymers are often used in creating temperature and pH dependent micelles, but no polycarbonate units have been tested so far.

In the second part of the thesis, a thorough investigation of the two polymers, poly(cyclohexene carbonate) and poly(limonene carbonate) was performed. In situ IR spectroscopy provided a valuable method to optimize polymerization parameters and to gain insight into the kinetics of the reactions (Figure 24).

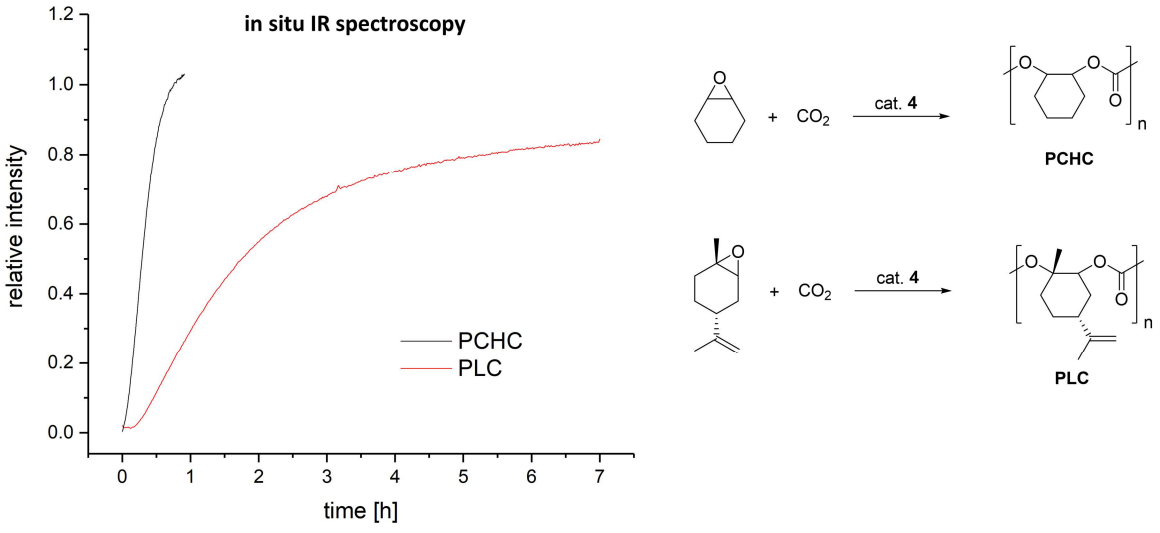

Figure 24. Monitoring of the ROCOP of carbon dioxide with CHO and LO, respectively ($\nu_{C=O}$ = 1745 cm^{-1}).

Two important parameters regarding the polymerization of LO have been revealed. A previous study already reported a reaction order with respect to limonene oxide of two (in contrast to one in case of CHO).[14] That implies, that it requires a certain concentration of active catalytic centers and monomer

molecules to enable the coordination-insertion mechanism to proceed. First, the catalyst-to-monomer ratio could not be increased higher than 1:500 while CHO was polymerized in 1:2500. Therefore, a significant amount of catalyst is needed for upscaling reactions in case of limonene oxide. Secondly, the amount of solvent could also not be increased arbitrarily because this also lowers the concentration of active centers. Usually, polymerizations were conducted in a 50 mL autoclave. Upscaling the reaction in a 1 L Buchi reactor was successful and gave access to an amount of polymer that was later used in characterizing the polymer. The thermal stability of the two polymers was tested by tempering them at certain temperatures for 20 minutes and consequently analyzing them via GPC analysis. Both PCHC and PLC were stable at 150 °C and only little degradation was observed at 180 °C. Thermally induced cross-linking of poly(limonene carbonate) occurred at elevated temperatures but could be prevented by adding 500 ppm Irganox®. Multiaxial pressure tests revealed mechanical performance which ranges between the two used commercialized polymers PMMA and Durabio®. PCHC and PLC are rather brittle materials but did not show a splintering of the material. Dynamic mechanical analysis allowed the determination of the glass transition temperatures and the examination of low-T_g transitions. Since catalyst **4** shows polymerization activity for both CHO and LO, terpolymerizations of CHO, LO, and CO_2 were performed. A successful formation of a terpolymer was confirmed via aliquot GPC analysis and DOSY NMR spectroscopy. An interesting kinetic feature was revealed using pressure NMR techniques, too. CHO is incorporated in the beginning and it takes full CHO conversion before LO polymerization starts. All in all, these comprehensive characterizations allow a better understanding of the novel CO_2-based polymers and facilitate a comparison with commercialized plastics.

14. Zusammenfassung

Die Copolymerisation von Epoxiden und CO_2 ist eine wertvolle Methode zur Herstellung von aliphatischen Polycarbonaten (Scheme 16). Kohlenstoffdioxid dient als ungiftiger, großtechnisch verfügbarer C1-Rohstoff, um Polycarbonate unabhängig von fossilen Energieträgern herzustellen. In dieser Arbeit diente ein Lewis azider Zinkkomplex als Katalysator für die Polymerisation von CO_2 mit Cyclohexenoxid bzw. Limonenoxid.

Scheme 16. Copolymerisation von Epoxiden und CO_2 mit dem Lewis aziden Zinkkomplex **4**.

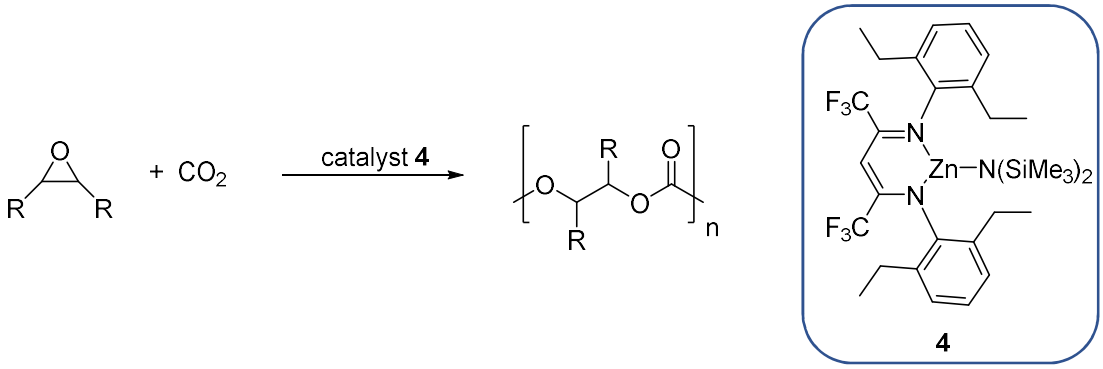

Im ersten Teil der Arbeit wurden zwei Methoden der Kombination der Copolymerisation von Epoxiden und CO_2 mit anderen Mechanismen getestet. Eine solche Kombination würde das Einführen einer zusätzlichen Art von Monomer in die Polymerstruktur erlauben. Es wird erwartet, dass diese sogenannte Terpolymerisation eine vielversprechende Methode zur Herstellung von Polymeren mit einem verbessertem Eigenschaftsportfolio darstellt. Der erste Ansatz basiert auf der katalytischen Aktivität von BDI^{CF3}-Zn-$N(SiMe_3)_2$ **4** für die Copolymerisation von CHO und CO_2 und der Ringöffnungspolymerisation von Lactonen, wie beispielsweise β-Butyrolacton. Eintopf-Polymerisationen bestehend aus CHO, BBL, CO_2 und Katalysator **4** wurden hinsichtlich der Blockbildung und des Einflusses von CO_2 auf den Einbau der jeweiligen Monomere untersucht. Insgesamt wurden drei verschiedene Reaktionsrouten etabliert (Figure 25). Wird zu Beginn der Reaktion kein CO_2 angelegt, so kam es zur Bildung des Polyesterblocks. Auch der Polycarbonatblock wurde erfolgreich gebildet, sobald CO_2 angelegt wird (AB Block, Route A). Im Gegensatz dazu kommt es zur ausschließlichen Polycarbonat-Bildung, wenn CO_2 bereits zu Beginn der Reaktion zugeführt wird. Der Polyesterblock wird erst gebildet, nachdem Kohlenstoffdioxid vom Autoklaven abgelassen wurde (Route B). Eine weitere interessante, dritte Route wurde durch eine Verminderung des CO_2-Drucks auf 3 bar gefunden (Route C). Hierbei werden beide Monomertypen (CHO/CO_2 und BBL) aufgrund ähnlicher Reaktionsraten des Katalysators **4** für die Copolymerisation und die Ringöffnungspolymerisation zu einem statistischen Polymer eingebaut. Ein möglicher Mechanismus für diese statistische Polymerisation wurde basierend auf Polarimetriemessungen von PHB und zweidimensionaler NMR-Spektroskopie postuliert. Ein näherer Blick auf die Reaktionsordnungen der Copolymerisationsreaktion offenbarte einen interessanten Wechsel in der Reaktionsordnung von CO_2. Während CO_2 in der

CHO/CO_2 Copolymerisation bei hohen Drücken (40 bar) nicht ratenlimitierend ist (Reaktionsordnung 0), ändert sich die Reaktionsordnung zu einer Abhängigkeit erster Ordnung bei niedrigerer CO_2-Konzentration. Der Wechsel der Polymerarchitektur (Block vs statistisch) hat entscheidenden Einfluss auf die thermischen und mechanischen Eigenschaften. PHB/PCHC Terpolymere in Blockstruktur zeigten zwei getrennte Glasübergangspunkte aufgrund von Phasenseparation (PHB-Block ~5 °C, PCHC Block ~115 °C), wohingegen jene in statistischer Struktur einen Misch-T_g aufweisen, welcher je nach Polymerzusammensetzung einstellbar ist.

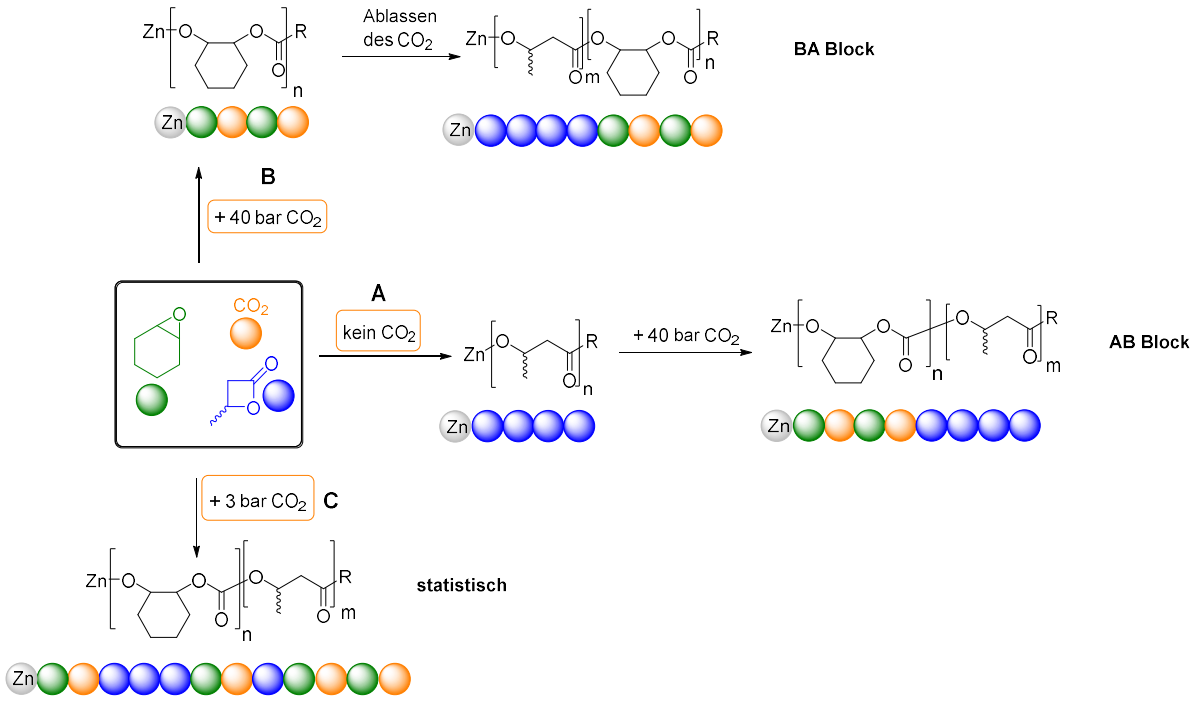

Figure 25. Überblick über die drei möglichen Reaktionsrouten.

Außerdem wurden die Terpolymere hinsichtlich ihres mechanischen Verhaltens getestet, indem sie in hundeknochenförmige Prüfkörper verpresst und mittels einer Zugdehnungsmaschine analysiert wurden. Das Gesamtziel dabei war die Sprödigkeit von PCHC (E-Modul: 3600 MPa, Bruchdehnung: 1.7%[13]) durch den Einbau des weichen PHB-Blocks zu verbessern. Terpolymere in statistischer Struktur zeigten ein verringertes E-Modul, jedoch weiterhin eine sehr geringe Bruchdehnung. PCHC/PHB Polymere in Blockstruktur und hohen Molekulargewichten ($M_{n,\,rel.}$>100 kg/mol) hingegen zeigten ein verbessertes mechanisches Verhalten (1170 MPa, 5.0%) verglichen mit reinem PCHC. Daraufhin wurden die etablierten Reaktionsrouten auf weitere Epoxide, Cyclopentenoxid (CPO) und Limonenoxid, getestet. Im Falle von CPO wurde ein sehr ähnliches Reaktionsverhalten zu CHO beobachtet und alle drei Reaktionswege führten zu den gewünschten Terpolymeren. Reines Poly(cyclopentencarbonat) zeigt einen verringerter T_g von 91 °C im Vergleich zu PCHC aufgrund des Ringgröße des jeweiligen Epoxids. Die resultierenden Terpolymere zeigten wieder ein phasensepariertes Verhalten im Falle der Blockstruktur und einen einstellbaren T_g als bei 3 bar CO_2 polymerisiert wurde. Ein interessanter Reaktivitätswechsel wurde bei der Verwendung von Limonenoxid enthüllt. Das Anlegen von CO_2 zu

Beginn der Reaktion führte zur Bildung von PLC. Nach Ablassen des CO_2, um die Polyesterbildung zu ermöglichen, wurde die Depolymerisation von PLC beobachtet. Eine detaillierte Studie der Copolymerisation von LO und CO_2 mit BDI Zinkkatalysatoren erfolgte 2017.[50] Dabei wurde die Depolymerisation des Polycarbonats bei erhöhten Temperaturen und moderat hohen Umsätzen als vorherrschend bestimmt. Nun zeigt sich, dass der CO_2 Druck ebenfalls entscheidend für das Polymerisations-Depolymerisationsgleichgewicht ist. Als Ergebnis dieser Depolymerisation wurde die zweite Reaktionsroute A gewählt, um beginnend mit der Polyesterbildung gefolgt von der PLC-Bildung PHB/PLC Terpolymere in Blockstruktur herzustellen. Letztere zeigten vielversprechende mechanische Eigenschaften. Eine verändernde PHB/PLC Zusammensetzung ergibt ein Material mit unterschiedlichen Bruchdehnungen. Reines PLC zeigt ein E-Modul von 2350 MPa und versagt meist bei einer Bruchdehung von 4-6%. Der Einbau von weichem PHB in einem Verhältnis von 20% bzw. 50% bewirkt eine Verringerung des E-Moduls auf 1800 MPa bzw. 1450 MPa und die Probenkörper widerstehen einer Dehnung von 13% bzw. 18%.

In der zweiten Methode der Kombination verschiedener Mechanismen war das Ziel die Copolymerisation von CO_2 und Epoxiden mit der seltenerdmetallkatalysierten Gruppentransfer-polymerisation zu koppeln. Da der BDI Zinkkatalysator **4** keine Aktivität in der Polymerisation von Michael-Monomeren wie zum Beispiel 2-Vinylpyridin und 2-Isopropenyl-2-oxazoline zeigte, wurde ein anderer Ansatz verfolgt.

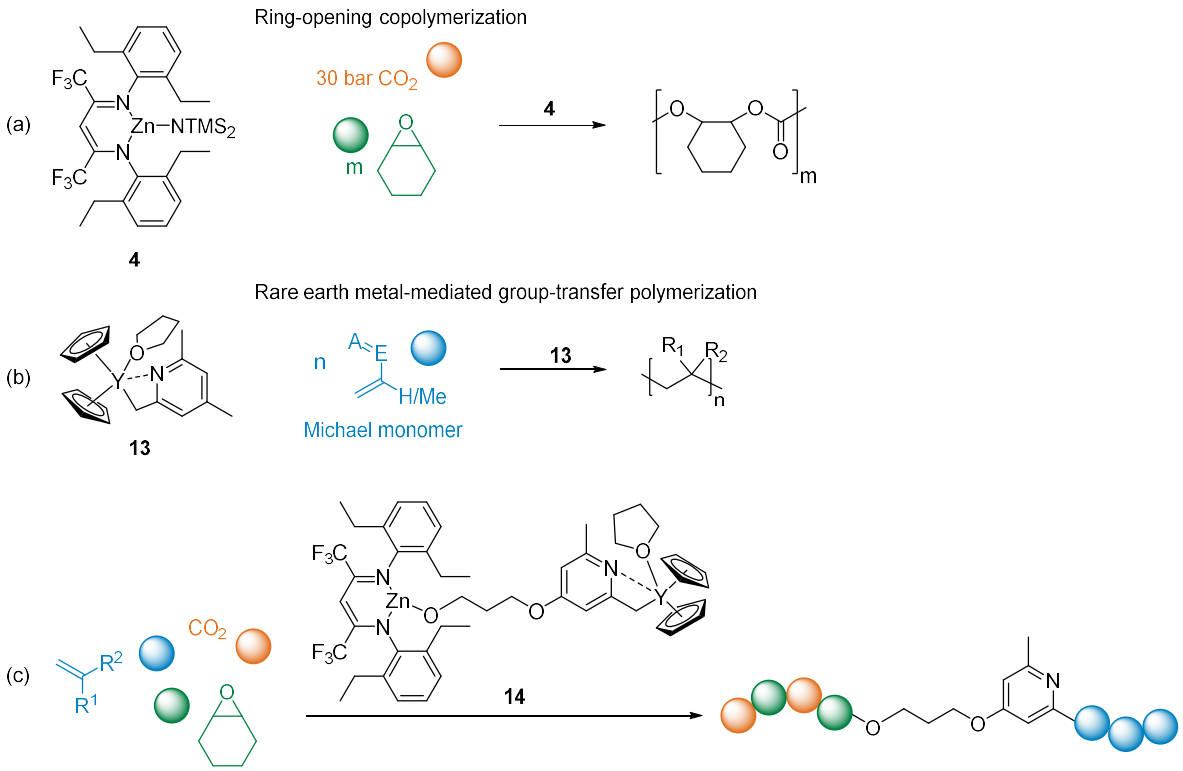

Figure 26. Copolymerisation von Epoxiden und CO_2 (a), seltenerdmetall-katalysierte Gruppentransferpoly-merisation von vinylischen Monomeren (b) und die Idee der Überbrückung zweier aktiven Zentren zur Herstellung eines bifunktionellen Katalysators frü die Terpolymerisation von Epoxiden, CO_2 und vinylischem Monomer (c).

Anstelle einer Polymerisation an einem Metallzentrum, ist geplant zwei Metallzentren mit einer flexiblen Verbindungseinheit zu überbrücken (Figure 26). Ein Pyridylalkohol ersetzt die Initiatorgruppe am bekannten Zinkkomplex **4** und der entstehende Zinkalkoxid Komplex wird mittels CH-Bindungsaktivierung an ein Yttrium Metallocen gekoppelt. Der heteronukleare Komplex **14** wurde hinsichtlich seiner Aktivität in der Terpolymerisation von CHO, CO_2 und 2VP getestet. Vorherige MALDI-TOF-MS Messungen bestätigten, dass die Verbindungseinheit als Endgruppe erfolgreich auf die jeweiligen Homopolymere PCHC und P2VP übertragen wurde. Diese Endgruppe wiederrum ist die Voraussetzung für eine erfolgreiche Verbindung der beiden verschiedenen Polymerblöcke in der folgenden Terpolymerisation. Wird Komplex **14** mit CHO und CO_2 versetzt, bildete sich PCHC, nach Ablassen von CO_2 und Zugabe von 2VP jedoch kein P2VP. Der Grund für dieses Verhalten konnte mittels NMR-Spektroskopie adressiert werden, indem Komplex **14** mit CO_2 bedrückt wurde. Dabei zeigte sich, dass die Yttrium Einheit ihr Funktionalität verlor, weil CO_2 eine Dissoziation des koordinierten THF Moleküls und eine Änderung der CH_2-Y Bindung bewirkt, die zeigt, dass das Pyridyl nicht mehr am Yttrium gebunden ist. Der zweite Reaktionsweg startete mit der REM-GTP von 2VP und der Zugabe von CHO und CO_2 nach vierstündiger Reaktionszeit. Tatsächlich konnte Umsatz sowohl zu P2VP als auch PCHC beobachtet werden. Um die erfolgreiche Blockbildung zu beweisen, wurden Aliquot GPC Messungen und Löslichkeitstests durchgeführt. Eine Verschiebung der Retentionszeit des P2VP/PCHC Terpolymers relativ zum P2VP Aliquot liefert einen ersten Hinweis für eine Verbindung beider Blöcke. Außerdem zeigt das Terpolymer bestehend aus 34% P2VP und 66% PCHC vollständige Löslichkeit in Methanol während reines PCHC in Methanol unlöslich ist. Des Weiteren waren Eintopfreaktionen erfolgreich, wenn 2VP und CHO zu Beginn der Reaktion mit Komplex **4** versetzt wurden und CO_2 nach einem bestimmten 2VP Umsatz zugegeben wird. Die Vielseitigkeit dieser Methode zeigte sich durch das Einführen von IPOx als alternatives Michael Monomer. Insgesamt ermöglicht diese Methode Zugang zu einer Gruppe von Terpolymeren, die vorher synthetisch nicht zugänglich waren. In zukünftigen Arbeiten werden thermische und mechanische Eigenschaften im Detail untersucht. Außerdem werden P2VP Copolymere oft in der Herstellung von temperatur- und pH-abhängigen Mizellen verwendet, dabei bisher aber keine Polycarbonatblöcke getestet.

Im zweiten Teil dieser Arbeit erfolgte eine intensive Untersuchung der beiden Polymere Poly(cyclohexencarbonat) und Poly(limonencarbonat). In situ IR Spektroskopie stellte dabei eine wichtige Möglichkeit dar, die Reaktionsbedingungen zu optimieren und Einsicht in die Kinetik der Reaktion zu gewinnen (Figure 27). Für die Polymerisation von LO und CO_2 konnten zwei wichtige Bedingungen gefunden werden. Vorherige Studien zeigten bereits eine Reaktionsordnung für LO von zwei (im Gegensatz zu eins im Falle von CHO).[14] Dies bedeutet, dass es eine bestimmte Konzentration katalytisch aktiver Zentren und Monomer Molekülen erfordert, um den Koordination-Insertions-Mechanismus ablaufen zu lassen. Erstens kann das Katalysator-zu-Monomer Verhältnis nicht über 1:500 gesteigert werden, wohingegen CHO in Verhältnissen von 1:2500 polymerisiert werden kann. Demzufolge ist für Hochskalierungsreaktionen eine große Menge Katalysator im Falle von

Limonenoxid notwendig. Zweitens kann die Menge an Lösemittel nicht beliebig erhöht werden, da auch dies eine Verringerung der Konzentration aktiver Zentren zur Folge hat. Gewöhnlich wurden die Polymerisationen in 50 mL Autoklaven durchgeführt. Die Reaktion konnte erfolgreich in einem 1 L Büchi Reaktor hochskaliert werden, um eine große Menge an Polymer einer Charge für spätere Charakterisierungen des Materials herzustellen.

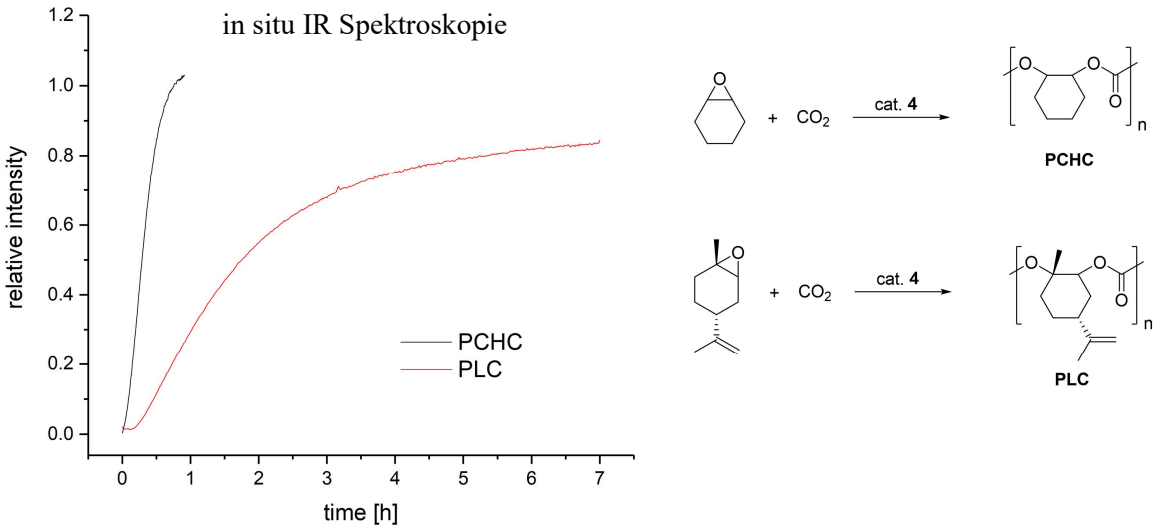

Figure 27. Spektroskopische Verfolgung der Copolymerisation von CO_2 und CHO bzw. LO ($\nu_{C=O}$ = 1745 cm^{-1}).

Die thermische Stabilität der beiden Polymere wurde durch Tempern bei bestimmten Temperaturen für 20 Minuten und folgender Analyse mittel GPC untersucht. Sowohl PCHC als auch PLC sind stabil bis 150 °C. PCHC weist lediglich einen geringen Abbau bei 180 °C auf, wohingegen PLC thermisch-induziertes Quervernetzen bei erhöhten Temperaturen zeigt. Dies konnte aber durch Zusatz von 500 ppm Irganox® verhindert werden. Multiaxiale Drucktests offenbaren ein mechanisches Verhalten zwischen den beiden kommerziellen Polymeren PMMA und Durabio®. PCHC und PLC sind relativ spröde Materialien, brechen aber ohne ein Splittern des Polymers. Die Bestimmung der Glasübergangstemperaturen und der sub-T_g Übergänge war mittels dynamisch-mechanischer Analyse möglich. Aufgrund der Aktivität von Komplex **4** hinsichtlich CHO und LO wurden Terpolymerisation bestehend aus CHO, LO und CO_2 durchgeführt. Die erfolgreiche Bildung des Terpolymers konnte mit Aliquot GPC Analyse und DOSY NMR Spektroskopie überprüft werden. Eine erstaunliche kinetische Eigenschaft konnte mittels Hochdruck-NMR Techniken entdeckt werden. In der Eintopf Polymerisation wird zu Beginn ausschließlich CHO eingebaut, und es erfordert vollen CHO Umsatz, bevor Limonenoxid eingebaut ist. Insgesamt erlauben diesen umfassenden Charakterisierungen ein besseres Verständnis der neuen CO_2-basierten Polymere und erleichtern einen Vergleich mit kommerziellen Kunststoffen.

15. Publications Beyond the Scope of the Thesis

15.1 Synthesis of Lewis Acidic, Aromatic Aminotroponiminate Zinc Complexes for the Ring-Opening Polymerization of Cyclic Esters

Title: "Synthesis of Lewis Acidic, Aromatic Aminotroponiminate Zinc Complexes for the Ring-Opening Polymerization of Cyclic Esters"

Status: Full Paper, published online August 03, 2018

Journal: Inorganic Chemistry, 2018, 57, 9931-9940

Publisher: American Chemical Society

DOI: 10.1021/acs.inorgchem.8b01060

Authors: Sebastian Kernbichl, Marina Reiter, Daniel H. Bucalon, Philipp J. Altmann, A. Kronast, Bernhard Rieger

Content:

β-diiminate ligands are an important structural motif in designing catalysts for the ring-opening polymerization (ROP) of cyclic esters. After complexation of the β-diiminate ligand with a transition metal such as zinc, a six-membered metallacycle is built. Within this study, we examined if the size of the metallacycle has an important influence on the catalytic activity by synthesizing a complex bearing a five-membered cycle with zinc. The structure of aminotroponiminates (ATI) was chosen as an ideal candidate to realize the five-ringed structure. Three differently substituted ATIs were synthesized, structurally characterized with SC-XRD, converted to ATI-Zn-N($SiMe_3$)$_2$ and tested in the ROP of *rac*-β-butyrolactone and *rac*-lactide. In situ IR spectroscopy allowed the monitoring of the polymerization rate and revealed higher activities for the novel ATI based complexes in the ROP of BBL compared to the six-ringed BDI complex. Different reaction conditions were screened by changing reaction temperature, catalyst-to-monomer ratio, solvent type or by adding 2-propanol as in situ generated alkoxy initiating group. Tunable molecular weights were achieved for both polymers, PHB and PLA. Especially in the case of LA, the addition of 2-propanol enhanced the initiator efficiency for the synthesis of a more controlled molecular weight.

S. Kernbichl executed most of the experiments and wrote the manuscript. M. Reiter had the initial idea and performed some initial experiments. D. H. Bucalon performed some ligand and complex synthesis experiments. P. J. Altmann conducted all SC-XRD-measurements and managed the processing of the respective data. A. Kronast performed initial experiments on this topic. All work was carried out under the supervision of B. Rieger.

Inorganic Chemistry
Cite This: Inorg. Chem. 2018, 57, 9931−9940
Article
pubs.acs.org/IC

Synthesis of Lewis Acidic, Aromatic Aminotroponiminate Zinc Complexes for the Ring-Opening Polymerization of Cyclic Esters

Sebastian Kernbichl,[†] Marina Reiter,[†] Daniel H. Bucalon,[†,‡] Philipp J. Altmann,[§] Alexander Kronast,[†] and Bernhard Rieger*[,†]

[†]Wacker-Lehrstuhl für Makromolekulare Chemie, Catalysis Research Center, Technische Universität München, Lichtenbergstraße 4, 85748 Garching bei München, Germany

[‡]Departamento de Química, Universitade Federal de São Carlos, Via Washington Luiz, km 235, 13565-905 São Carlos, SP, Brazil

[§]Catalysis Research Center, Technische Universität München, Ernst-Otto-Fischer Straße 1, 85748 Garching bei München, Germany

Supporting Information

ABSTRACT: Three novel aminotroponiminate (ATI) zinc complexes **I**−**III** (**I** = [(Ph$_2$)ATI]Zn−N(SiMe$_3$)$_2$, **II** = [(C$_6$H$_3$-2,6-C$_2$H$_5$/Ph)ATI]Zn−N(SiMe$_3$)$_2$, and **III** = [(C$_6$H$_3$-2,6-CH(CH$_3$)$_2$/Ph)ATI]Zn−N(SiMe$_3$)$_2$) were synthesized and tested in the ring-opening polymerization of the lactones *β*-*rac*-butyrolactone (BBL) and *rac*-lactide (LA). The ligands, with two of them literature unknown, were readily obtained via a three-step synthesis from tropolone. Forming a five-membered metallacycle with zinc, the complexes were further structurally examined via single-crystal X-ray analysis and compared with that of the established, 6-ringed *β*-diiminate (BDI) complex **IV** ([CH(CMeNPh)$_2$]Zn−N(SiMe$_3$)$_2$). The influence of the varying metallacycle ring size on the polymerization was evaluated. *In situ* IR measurements indicate a higher catalytic activity of the novel ATI complexes **I**−**III** for BBL compared with the BDI system **IV**. The activity and degree of control were further improved by an *in situ* generated alkoxy initiating group generated after the addition of 2-propanol. An enhanced initiator efficiency allowed the synthesis of polymers with controlled molecular weights and narrow polydispersities. Furthermore, **II** and **III** exhibited a high activity in the ring-opening polymerization of *rac*-LA. Hereby, reaction time and initiator efficiency could also be optimized at a higher temperature or by the addition of 2-propanol.

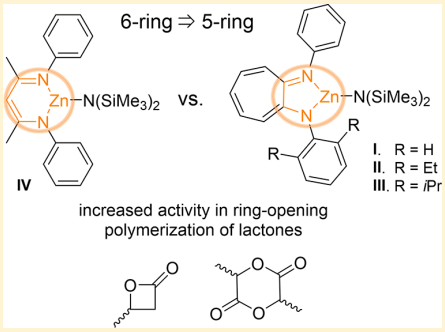

INTRODUCTION

Polyesters, particularly poly(hydroxybutyrate) (PHB) and poly(lactide) (PLA), can be produced by the ring-opening polymerization (ROP) of lactones. These aliphatic polyesters represent a valuable group of polymers with a great range of thermo-mechanical properties along with a renewable origin of quite a number of cyclic esters.[1] PHB, initially identified in *Bacillus megaterium* by M. Lemoigne, serves as a bacterial storage material.[2] In nature, the polymer is produced in its strictly isotactic form; however, controlling the microstructure via synthetic approaches has been attempted for decades. Ring-opening polymerization of *β*-*rac*-butyrolactone (BBL) offers the most promising way of controlling the microstructure with different metals such as aluminum,[3] zinc,[4] chromium,[5] and yttrium.[6] Thereby, *β*-diiminate (BDI) zinc complexes[4d] by Coates et al., yielding atactic PHB, and amino-alkoxy-bis(phenolate) yttrium complexes[6a] by Carpentier et al., giving a syndiotactic microstructure, were introduced as highly active catalysts. In contrast to PHB, the synthesis of PLA is industrially already more applied, making it the leading bioderived polymer. It is usually obtained from lactic acid through condensation reaction or, more promising, from lactide via ring-opening polymerization. The access via ROP enables the production of polymers with high molecular weights, narrow dispersities, and stereoselectivity.[7] Pioneering works using chiral salen aluminum complexes in the polymerization of *rac*-LA showed high isoselectivity.[8] Since then, a variety of ligands were coordinated to different central metals to realize either hetero- or isotactic-enriched PLA.[9] Figure 1 gives an overview of catalysts used in ROP of *rac*-LA starting with a *β*-diiminate zinc complex[4c] producing heterotactic-enriched PLA and ending with the most active and isoselective systems using zinc, yttrium, or indium.

Because the development of new and efficient initiators for this type of polymerization is still an ongoing challenge, the catalytic behavior of a novel type of ligands, the aminotroponimines (ATIHs), was investigated.

Aminotroponimines are a well-known class of ligands initially discovered in 1960. After the insertion of tetrafluoroethylene into cyclopentadiene, the fluorinated cycloheptadiene is subsequently converted into the corresponding ATIHs via

Received: April 17, 2018
Published: August 3, 2018

DOI: 10.1021/acs.inorgchem.8b01060
Inorg. Chem. 2018, 57, 9931−9940

Inorganic Chemistry Article

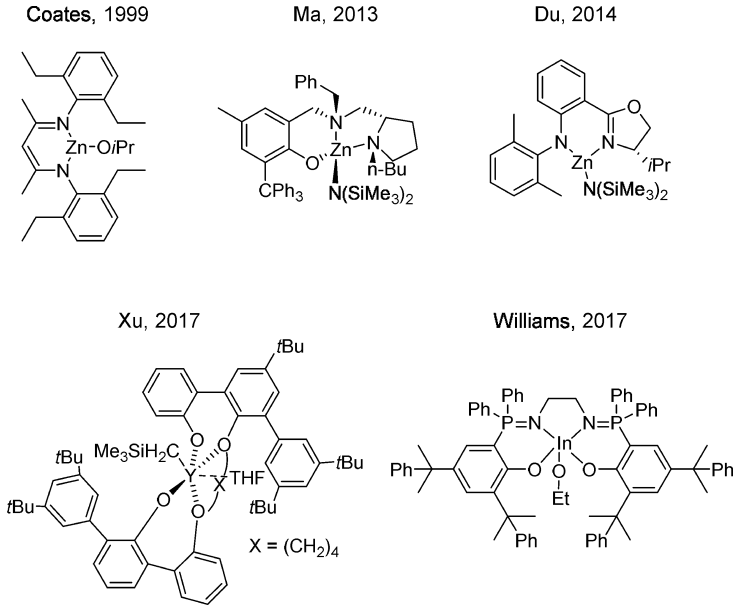

Figure 1. Active complexes for ROP of *rac*-LA with a focus on zinc as central metal.[4c,9b,c,d,g]

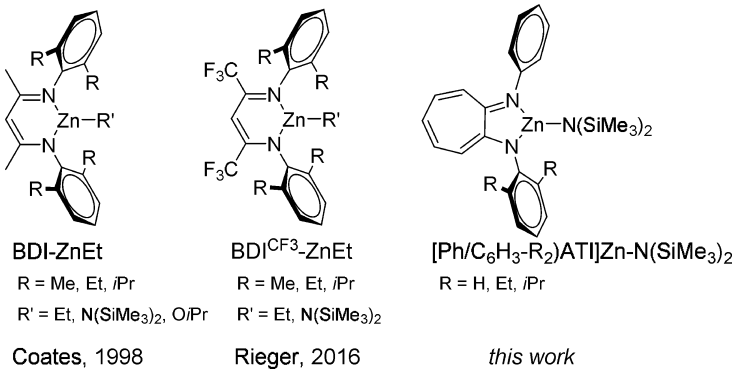

Figure 2. BDI zinc complexes established in polymerization catalysis by Coates (left); introduction of electron-withdrawing groups at the pentane backbone (center); realization of a five-membered metallacycle by synthesis of aminotroponiminate complexes (right).[14,15a]

condensation reaction with primary amines.[10] Deprotonated ATIHs act as anionic, bidentate ligands with a delocalization of the negative charge over the 7-membered ring, giving a 10π-electron backbone. A wide range of main group, transition, and f-block elements[11] have been introduced as central metal, but Roesky et al. were the first to bring aminotroponiminate (ATI) ligands into the coordination sphere of zinc.[12] A vast variety of ATI ligands with different amines were converted to zinc complexes and tested in intramolecular hydroamination reactions.[13] However, to the best of our knowledge, they have not been used in ROP.

Recently, we showed that BDI complexes bearing two electron-withdrawing trifluoromethyl groups in the pentane backbone show enhanced activity in the ring-opening polymerization of lactones when compared with BDI-ZnEt.[14] This can be attributed to an increased Lewis acidity at the metal center. Thus far, the influence of substituted anilines, the pentane backbone, and the initiating group on the catalytic activity was systematically investigated.[4c,d,15] Nevertheless, the 6-membered ring structure around the zinc center was not modified yet. It is expected that changing the ring size will have a decisive influence in terms of catalytic activity of the corresponding complexes (Figure 2).

In this work, we report on the synthesis of three novel, aromatic aminotroponiminate complexes **I**–**III**. Two of the ligands have not been previously reported. The complexes were structurally compared with the BDI model complex **IV** via single-crystal X-ray diffraction (SC-XRD), and the catalytic activity in ring-opening polymerization of BBL and *rac*-LA was examined.

RESULTS AND DISCUSSION

Synthesis. Aromatic aminotroponimine ligands were obtained via a 3-step synthesis starting from tropolone. First, trifluoromethanesulfonyl was introduced as a good leaving group for the following cross-coupling. The palladium-catalyzed Buchwald–Hartwig-like coupling converts the triflatotropone to the aminotropones **1a**–**3a**. This readily works for sterically hindered anilines substituted in the 2,6-position.[16] After activation with Meerwein's salt, the resulting

DOI: 10.1021/acs.inorgchem.8b01060
Inorg. Chem. 2018, 57, 9931–9940

Inorganic Chemistry Article

Scheme 1. Synthesis Route toward Aminotroponimine Ligands 1b−3b

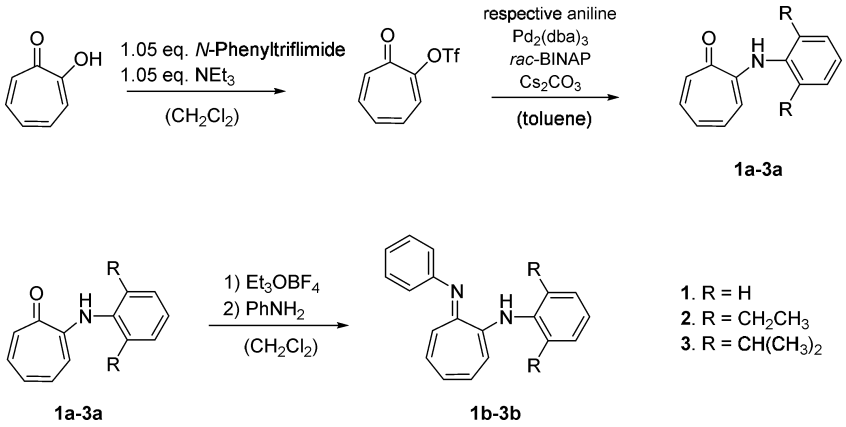

Scheme 2. Complex Synthesis with Ligands 1b−3b and $Zn(NTMS_2)_2$

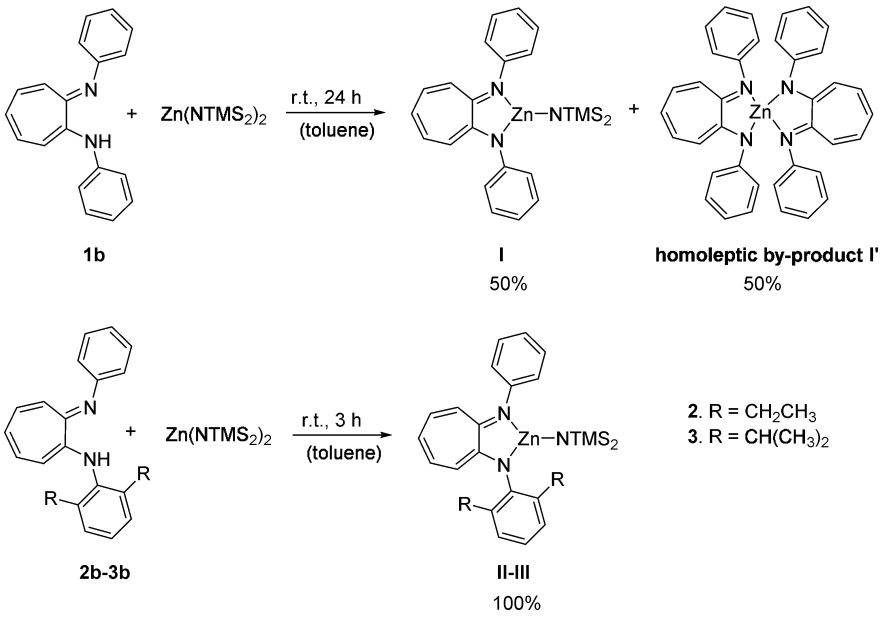

vinylogous ether was converted by aminolysis to the respective aminotroponimines (**1b−3b**).[13] Thus, bidentate, N-donor ligands bearing two different rests (**2**: R = CH_2CH_3; **3**: R = $CH(CH_3)_2$) at the 2,6-positions of one of the anilines were obtained (Scheme 1). In order to realize symmetrical, 2,6 disubstituted ATIHs, the aim was to introduce another triflate leaving group at the aminotropone **2a** and subsequently couple this with a 2,6 disubstituted aniline. The reduction of the carbonyl unit with lithium diisopropylamide was unsuccessful, most likely, because of the conjugated system at the amide. Therefore, only unsymmetrical ATIHs were accessible via this synthesis route.

BDI complexes bearing bis(trimethylsilyl)-amido ($NTMS_2$) initiators coordinated to the zinc center show high activities in the ring-opening polymerization of lactones.[17] Therefore, **1b−3b** were treated with $Zn(NTMS_2)_2$ to obtain ATI zinc amido complexes. Recently, Roesky et al. reported the complexation of aminotroponimines with $ZnMe_2$ and $ZnEt_2$. Depending on the substituents of the amines, either the desired complex with the general formula [(R_2)ATI]Zn-Alkyl (R = cyclohexyl, 1-ethylpropyl) or the corresponding homoleptic complex [(R_2)ATI]$_2$Zn (R = Ph, Me, *i*Pr) was obtained.[20] Complexation of the symmetric, unsubstituted ligand **1b** with $Zn(NTMS_2)_2$ at room temperature resulted in the formation of two different products (Scheme 2): The target structure **I** was only formed to an amount of 50%, whereas the homoleptic byproduct constituted the remaining 50%. Metal−organic complexes used in polymerization catalysis usually bear a nucleophilic group that serves as an initiator for the ring-opening step. Although there are some systems of homoleptic complexes which are active in polymerization, it is assumed for ATI-based complexes that an initiating group is necessary.[1d,18] Hence, **I′**, in contrast to **I**, might be inactive in ROP of lactones (tested for BBL polymerization, result shown in Table 1, entry 13). In order to overcome this high amount of homoleptic byproduct **I′**, different temperatures were applied and the influence on the complexation behavior was investigated (Table S1): Performing the complexation reaction

DOI: 10.1021/acs.inorgchem.8b01060
Inorg. Chem. 2018, 57, 9931−9940

Inorganic Chemistry Article

Scheme 3. Synthesis of β-Diiminate Zinc Complex IV. Reaction of BDI Ligand 4a with the Zinc Precursor

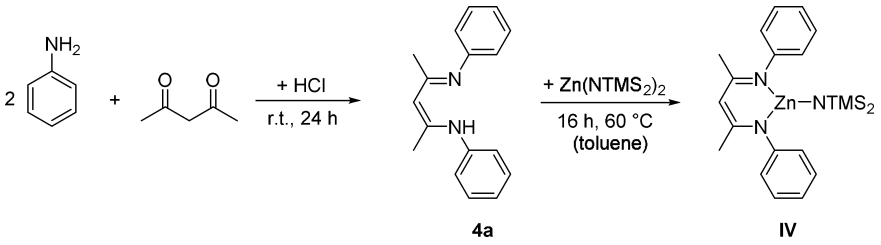

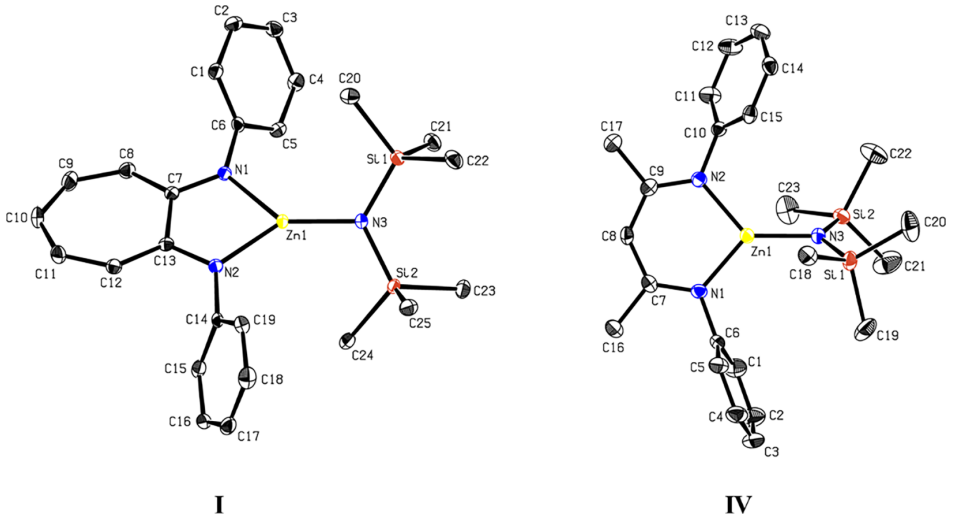

Figure 3. ORTEP style representation of **I** (left, CCDC 1837008) and **IV** (right, CCDC 1837010) with ellipsoids drawn at a 50% probability level. Hydrogen atoms are omitted for clarity. Selected bond lengths (Å) and angles (deg): **I**. Zn1−N1 1.9659(16), Zn1−N2 1.9707(17), Zn1−N3 1.8653(16), N1−Zn1−N2 82.41(7), Zn1−N1−C6 123.67, and Zn1−N2−C14 124.19; **IV**. Zn1−N1 1.9460(16), Zn1−N2 1.9530(16), Zn1−N3 1.8832(16), N1−Zn1−N2 98.59(7), Zn1−N1−C6 117.73, and Zn1−N2−C10 119.46.

at 100 °C resulted in the formation of 59% homoleptic complex **I′**. Lower temperatures, in this case 0 °C, result again in an equal 50/50 mixture of **I** and **I′**. ^{1}H NMR spectroscopy still shows the presence of unreacted ligand **1b**. Thus, a temperature of 25 °C for 24 h was chosen as the best condition for the complexation reaction of **1b**. Treatment of ligands **2b** and **3b**, bearing substituents at the 2,6-positions of the aniline, with the zinc precursor led to the exclusive formation of the desired structures [(C_6H_3-R_2/Ph)ATI]Zn−$NTMS_2$ **II**−**III**. This clearly shows that the steric demand of the ligand plays a decisive role in the complexation reaction.

The mixture of **I** and **I′** was separated based on the different crystallization behavior: Diffusion of pentane into a saturated solution of **I** and **I′** in dichloromethane at −35 °C selectively led to the crystallization of **I′**, whereas **I** remained in solution. Thus, aminotroponiminate complexes derived from aromatic anilines with the general formula [Ph_2ATI]Zn−initiator were isolated for the first time. Crystals suitable for single-crystal X-ray diffraction analysis were obtained via recrystallization of a saturated solution of **I** in pentane at −35 °C.

It is of interest to compare the molecular structure and the activity of the novel ATI complexes with the established BDI complexes. Via acid-catalyzed condensation reaction of aniline and acetylacetone, BDI ligand **4a** was obtained[19] and readily converted to the respective zinc−$NTMS_2$ complex **IV** by stirring the ligand **4a** with $Zn(NTMS_2)_2$ in toluene at 60 °C for 16 h (Scheme 3). Recrystallization from toluene at −35 °C afforded colorless crystals that were suitable for X-ray diffraction.

Figure 3 shows the ORTEP style representations of **I** and **IV**. Both metal cores adopt a trigonal-planar geometry. Because **I** and **IV** are iminate-derived ligands without any substituents at the anilines, the 5- and 6-ringed structures can be directly compared to investigate the influence of the ring size on the molecular structure. The N1−Zn1−N2 angle was 82.41(7)° in the 5-ringed structure and 98.59(7)° in the 6-membered ring. The angle Zn1−N1−C6 also differs (123.67(5) for **I** and 117.73(4) for **IV**), indicating a larger space in **I** for a possible monomer coordination. A shortening of the Zn1−N3 bond was observed for the ATI−Zn−$NTMS_2$ **I** (1.8653(16)) with respect to the BDI−Zn−$NTMS_2$ **IV** (1.8832(16)).

Crystals suitable for SC-XRD were obtained via diffusion of pentane into a saturated solution of **II** and **III** in dichloromethane. Their molecular structures are depicted in Figure 4. The substituents in the 2,6-position of the aniline showed little influence over the molecular structure compared with **I**. Again, a trigonal-planar coordination geometry and very similar Zn1−N3 distances (**I**. 1.8653(16) Å, **II**. 1.865(4) Å, and **III**. 1.8631(17) Å) were observed. The substituted phenyl moieties were almost perpendicular to the coordination plane.

Polymerization Results. The catalytic activity of **I**−**IV** was tested in the polymerization of BBL and *rac*-LA under

DOI: 10.1021/acs.inorgchem.8b01060
Inorg. Chem. 2018, 57, 9931−9940

Inorganic Chemistry Article

Table 1. Ring-Opening Polymerization of BBL Using Catalysts I–IV[a]

entry	cat.	T [°C]	time [h]	conv.[b] [%]	$M_{n,calc}$[c] [kg/mol]	$M_{n,exp}$[d] [kg/mol]	$Đ$[e]	P_m[f]
1	**I**	60	8	>99	52	129	1.22	55
2	**II**	60	15	>99	52	75	1.28	56
3	**III**	60	8	>99	52	122	1.16	55
4[g]	**III**	25	20	4	2	36	1.22	53
5	**III**	80	3.5	>99	52	116	1.15	54
6[h]	**III**	60	7	95	49	53	1.05	54
7[i]	**III**	60	3	98	5	7.5	1.02	53
8[j]	**III**	60	8	97	17	56	1.13	54
9[k]	**III**	60	8	96	33	65	1.51	53
10[g,l]	**III**	25	20	7	3.6	29	1.33	54
11[l]	**III**	60	14	61	31	58	1.78	55
12[h]	**I**	60	4.5	93	48	49	1.07	55
13	**I′**	60	20	2	n.d.	n.d.	n.d.	n.d.
14[m]	**I′**	60	12	1	n.d.	n.d.	n.d.	n.d.
15	**IV**	60	16	76	39	84	1.05	47

[a]All polymerizations were performed with n_{LA} = 17.4 mmol in a BBL/cat. ratio of 600 in 5.0 g of toluene in an autoclave with *in situ* IR monitoring under an argon atmosphere; polymerizations in entries 7–10 were performed in preheated glasses with magnetic stirring under anargon atmosphere, with the equivalents of BBL indicated. [b]Conversion determined by ^{1}H NMR spectroscopy. [c]$M_{n,calc}$ [kg/mol] = 0.01·conv.·86 g/mol·equiv. [d]$M_{n,exp}$ determined by GPC in THF vs polystyrene standards. [e]$Đ = M_w/M_n$. [f]Determined by ^{13}C NMR spectrum of the carbonyl C atom of PHB (Figure S5). [g]Not precipitated. [h]1.0 equiv of *i*PrOH was added. [i]10 equiv of *i*PrOH was added. [j]200 equiv of BBL was used. [k]400 equiv of BBL was used. [l]THF as solvent. [m]2.0 equiv of *i*PrOH was added.

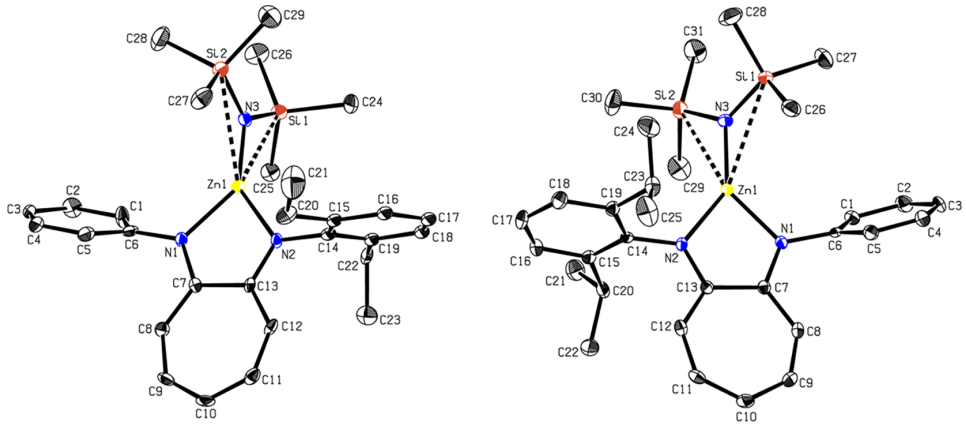

II **III**

Figure 4. ORTEP style representation of **II** (left, CCDC 1837009) and **III** (right, CCDC 1837007) with ellipsoids drawn at a 50% probability level. Hydrogen atoms are omitted for clarity. Selected bond lengths (Å) and angles (deg): **II**. Zn1–N1 1.970(4), Zn1–N2 1.961(4), Zn1–N3 1.865(4), N1–Zn1–N2 82.61(16), Zn1–N1–C6 123.53, and Zn1–N2–C14 125.05; **III**. Zn1–N1 1.9547(17), Zn1–N2 1.9553(17), Zn1–N3 1.8631(17), N1–Zn1–N2 82.80(7), Zn1–N1–C6 122.75, and Zn1–N2–C14 124.48.

different conditions (Tables 1 and 2). The polymerization of BBL was conducted with a catalyst/monomer ratio of 1:600 at 60 °C in an autoclave with *in situ* IR monitoring. The three ATI-based complexes **I**–**III** were active initiators for the ring-opening of BBL, and the ligands had a different influence on the activity of the respective catalysts.

According to *in situ* IR spectroscopy (Figure 5), complex **I** (Table 1, entry 1) showed the highest activity of all the catalysts used with an induction period of about 30 min. The obtained polymer has a molecular weight of 129 kg/mol and a narrow polydispersity index ($Đ$) of 1.22. The more sterically demanding complexes **II** and **III** (Table 1, entries 2 and 3) also exhibited good activity along with a molecular weight of 75 kg/mol using **II** and 122 kg/mol with **III**. Different conditions such as temperature, addition of an external alcohol, concentration, and THF as solvent were tested using complex **III**. At first, polymerizations at 25 °C (Table 1, entry 4) and 80 °C (Table 1, entry 5) were performed. Activity and initiator efficiency at room temperature were low for **III**, leading to 4% conversion and a molecular weight of 36 kg/mol. Higher temperatures resulted in increased activity of **III** and the same initiator efficiency as for 60 °C. A plot of the *in situ* IR spectroscopy versus reaction time for the three temperatures is shown in Figure S1. The influence of adding an external alcohol, in this case, 1.0 equiv of 2-propanol, on complex **III** was studied via ^{1}H NMR spectroscopy. After 10 min reaction time, –O*i*Pr is bonded to the metal center, creating an alkoxy initiating group by a release of $HNTMS_2$ (see Figure S2). This *in situ* formed catalyst was subsequently tested in ROP of BBL at 60 °C (Table 1, entry 6), revealing a higher activity

DOI: 10.1021/acs.inorgchem.8b01060
Inorg. Chem. 2018, 57, 9931–9940

Inorganic Chemistry Article

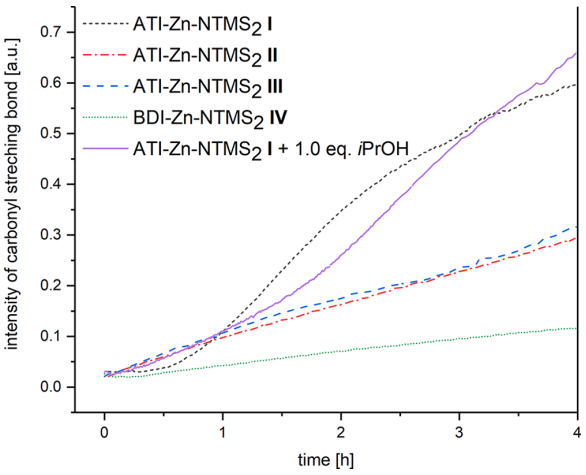

Figure 5. Polymerization of BBL with catalysts **I**–**IV** under the same conditions monitored by *in situ* IR spectroscopy ($\nu_{C=O,\ PHB}$ = 1750 cm^{-1}).

compared to **III** without the addition of *i*PrOH (Figure S3). Most importantly, the initiator efficiency of the *in situ* formed alkoxy group is higher, enabling the synthesis of controlled molecular weights and narrow polydispersities. This worked also for 10 equiv of *i*PrOH, producing PHB with 7.5 kg/mol (Table 1, entry 7). By variation of the monomer-to-catalyst ratio, polymers with different chain lengths were accessible in still good conversions (Table 1, entries 8 and 9). Polymerization experiments using THF as coordinating solvent (Table 1, entries 10 and 11) were successful, although lower conversions were observed compared to toluene as solvent. The use of THF did not influence the stereoselectivity of the reaction. In all polymerizations, atactic PHB was obtained. As mentioned, complex **I** showed an induction time of about 30 min. This can be overcome by adding 1.0 equiv of *i*PrOH prior to monomer addition (Table 1, entry 12). An immediate start of the polymerization as well as controlled molecular weights could be observed. The homoleptic complex **I′** with the general formula $[(Ph_2)ATI]_2Zn$ was also tested (Table 1, entry 13) in the polymerization. **I′** did not show significant activity, demonstrating that the catalyst requires a nucleophilic leaving group to start the ring-opening of the monomer. Complex **I′** was treated with 2.0 equiv of *i*PrOH to check if an active complex can be formed by the addition of an alcohol. No conversion to PHB could be observed after a reaction time of 12 h at 60 °C. This clearly demonstrates that no active complex could be formed by the addition of 2-propanol.

Once the behavior of the ATI complexes in the polymerization of BBL was evaluated, they were compared with the BDI complex model system, in this case, exemplary with complex **IV**: Both **I** and **IV** have the same initiating group and were synthesized from unsubstituted anilines, allowing a direct comparison of the influence of the 5- vs 6-membered ring around zinc. BDI complex **IV** showed lower activity in polymerization compared with **I**, yet the molecular weight (84 kg/mol) and *Đ* (1.05) were still in a good range. There may be various steric and electronic effects involved; thus, the reason for the higher activity is difficult to address. According to the molecular structures of **I** and **IV**, revealing a larger Zn1–N1–C6 angle for **I** compared to **IV** (**I**. 123.67(5)°, **IV**. 117.73(4)°), steric reasons seem to be more decisive rather than electronic effects.

As an example, catalyst **II** was tested in the ring-opening polymerization reaction to assess the possible living-type character (Figure 6). The conversion–time plot is shown on the left. Molecular weights, as well as the polydispersity indices as a function of the conversion, show a linear increase, indicating a living-type character of the polymerization.

Coates et al. investigated the influence of the initiating group of BDI zinc complexes in the ROP of LA. In that work, $-N(SiMe_3)_2$ substituted complexes show slightly lower activity than the –O*i*Pr substituted analogue but maintained a good control of the molecular weight with a moderate *Đ* of 2.95.[4b] Catalysts **I**–**IV** were also tested in the ROP of *rac*-LA under different conditions (Table 2).

Both **II** and **III** (Table 2, entries 2 and 3) were active initiators at room temperature, producing PLA in high conversion and very high molecular weight, whereas catalyst **I** had a very poor activity, resulting in a low conversion of 12% after 16 h. The obtained molecular weights indicate a rather low initiator efficiency of **II** and **III** at room temperature. It can also be concluded that ATI complexes with a higher steric demand of the ligand had better activity in the *rac*-LA polymerization. To get a closer insight why complex **I** showed such a low activity, the stability of **I** and **III** was investigated in different solvents (toluene-d_8 and dichloromethane-d_2, 15 min and 12 h) via ^{1}H NMR spectroscopy and ^{1}H DOSY NMR. In both solvents, **I** and **III** remained stable and showed a single diffusion coefficient for all resonances. Hence, the reason for this activity difference might be caused by the steric demand of the aniline rests. The substituted complexes **II** and **III** likely enable a better coordination of *rac*-LA, thus accelerating the

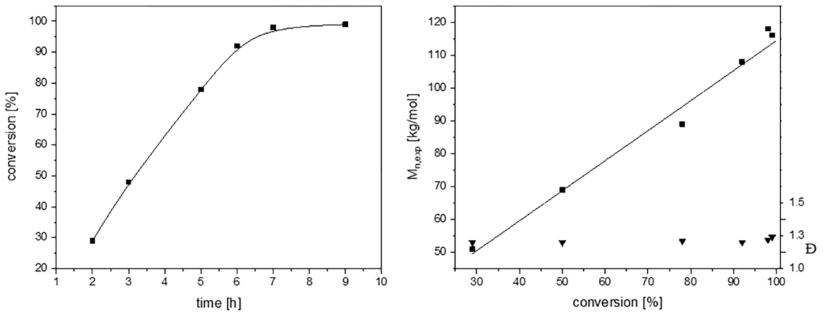

Figure 6. Polymerization of BBL with catalyst **II**. Plot of PHB conversion (%) vs time (h) (left), and PHB molecular weight ■ ($M_{n,\ exp}$ vs polystyrene standard in THF) and polydispersity index ▼ as a function of conversion (right).

DOI: 10.1021/acs.inorgchem.8b01060
Inorg. Chem. 2018, 57, 9931–9940

Inorganic Chemistry Article

Table 2. Ring-Opening Polymerization of *rac*-LA Using Catalysts I–IV[a]

entry	cat.	T [°C]	time [h]	conv.[b] [%]	$M_{n,calc}$[c] [kg/mol]	$M_{n,exp}$[d] [kg/mol]	$Đ$[e]	P_r[f]
1[g]	I	25	16	12	3.5	7.5	1.28	n.d.
2	II	25	16	91	26	168	1.63	50
3	III	25	16	97	28	125	1.89	54
4	II	40	8	97	28	41	1.69	60
5[h]	II	25	1.5	90	26	26	1.23	50
6[h]	II	40	1.5	97	28	30	1.74	60
7[i]	II	40	16	99	56	68	2.05	55
8[j]	II	40	16	94	84	111	1.83	57
9[k]	II	25	16	62	18	109	2.43	47
10[k]	II	40	8	86	25	70	1.81	53
11	IV	25	16	94	27	101	1.43	62

[a]All polymerizations were performed, except otherwise indicated, with n_{LA} = 0.8 mmol in a *rac*-LA/cat. ratio of 200 in 2.65 mL of dichloromethane under an argon atmosphere. [b]Conversion determined by ^{1}H NMR spectroscopy. [c]$M_{n,calc}$ [kg/mol] = 0.01·conv.·144 g/mol·equiv. [d]$M_{n,exp}$ determined by GPC in THF vs polystyrene standards; $M_{n,exp}$ values are corrected with a 0.58 factor for PLA. [e]$Đ = M_w/M_n$. [f]Determined by homo-decoupled ^{1}H NMR spectroscopy considering the methine region of PLA (Figure S6). [g]Not precipitated. [h]1.0 equiv of *i*PrOH was added. [i]400 equiv of *rac*-LA was used. [j]600 equiv of *rac*-LA was used. [k]THF as solvent.

monomer ring-opening step. Due to a low initiator efficiency, polymerizations using **II** both at higher temperature and with the addition of an external alcohol were performed. Molecular weights are determined by GPC in THF and corrected with a factor of 0.58.[1d,18] Increasing the temperature from 25 to 40 °C (Table 2, entry 4) already enhanced the initiator efficiency by a factor of 4 to a molecular weight of 41 kg/mol. The addition of 2-propanol decisively influenced the reaction time and the obtained molecular weights: Polymerizing *rac*-LA at room temperature in the presence of 1.0 equiv of *i*PrOH (Table 2, entry 5) led to full conversion within 1.5 h, compared to 16 h when no external alcohol was used. The obtained molecular weights are in good range with the theoretical values. Performing the polymerization at 40 °C in the presence of 2-propanol (Table 2, entry 6) led to the same reaction time of 1.5 h and a comparable control over the molecular weight. Additionally, polymerization experiments with different monomer-to-initiator ratios (Table 2, entries 7 and 8) and with tetrahydrofuran as coordinating solvent (Table 2, entries 9 and 10) were conducted. Because both the substituents at the ligand and the nature of the solvent influence stereoselectivity, the polymer microstructure was examined via homo-decoupled ^{1}H NMR spectroscopy. It has been reported that increased heterotacticity can be observed for complexes bearing bulkier ligands.[1d,18] This trend was also observed for the ATI complexes **II–III**, although P_r is generally lower when compared to BDI complexes. Complex **II** exhibited higher heterotacticity when a higher temperature (40 °C) was applied. The use of THF had no decisive influence on the tacticity of the PLA. BDI model catalyst **IV** also allowed the polymerization of *rac*-LA in 16 h with a 94% yield (M_n = 101 kg/mol, $Đ$ = 1.43). The living-type character was assessed for *rac*-LA polymerization with **III** (Figure S7).

CONCLUSION

Three novel zinc complexes **I–III** were synthesized from aminotroponimine ligands, two of which were literature unknown. The ligands were obtained via a three-step synthesis starting from tropolone. The molecular structures were compared with the established *β*-diiminate model system **IV** via SC-XRD. Catalysts **I–IV** were tested in the ring-opening polymerization of the cyclic esters, *rac*-BBL and *rac*-LA. *In situ* IR spectroscopy revealed a higher activity for the ATI complexes **I–III** in the production of PHB than the BDI model system **IV**. This clearly demonstrates that the ring size of the metal core decisively influences the catalytic behavior of the complexes. The bulkier complexes **II–III** were also highly active initiators in the ring-opening polymerization of *rac*-LA. For both monomers, an optimization of the reaction conditions regarding reaction time, concentration, influence of the solvent, and the addition of an external alcohol was carried out. The addition of 2-propanol generated a zinc-alkoxy initiator group showing higher activity and initiator efficiency in the ring-opening polymerization. This allowed the synthesis of polymers with controlled molecular weights and narrow polydispersities. Further modifications of the ligands' structure may improve the activity and the stereospecificity of the polymerization.

EXPERIMENTAL SECTION

General. All reactions containing air- and/or moisture-sensitive compounds were performed under an argon atmosphere using standard Schlenk or glovebox techniques. All chemicals, unless otherwise stated, were purchased from Aldrich and used as received. Dry toluene, dichloromethane, and pentane were obtained from an MBraun MB-SPS-800 solvent purification system. 2-Propanol was dried over molecular sieves.

β-Butyrolactone was treated with BaO to remove crotonic acid contaminants. After checking the purity via ^{1}H NMR spectroscopy, BBL was dried over calcium hydride and distilled prior to polymerization. NMR spectra were recorded on Bruker AVIII-300 and AVIII-500 Cryo spectrometers. ^{1}H NMR spectroscopic shifts are reported in ppm relative to tetramethylsilane and calibrated to the residual proton signal of the deuterated solvent. The deuterated solvents were obtained from Aldrich and dried over 3 Å molecular sieves. The following abbreviations are used to describe the peak patterns when appropriate: s (singlet), d (doublet), dd (doublet of doublets), t (triplet), m (multiplet), and br (broad). *In situ* IR measurements were performed under an argon atmosphere using an ATR-IR MettlerToledo system with mechanical stirring. Gel permeation chromatography analysis was performed with a Varian PL-GPC 50 using THF (HPLC grade) with 0.22 g L^{-1} 2.6 di-*tert*-butyl-4-methylphenol and a flow rate of 1 mL/min at 40 °C. Polystyrene standards were used for calibration. Molecular weights of PLA were corrected with a Mark–Houwink factor of 0.58.[20] Elemental analysis was performed at the microanalytic laboratory of the Department of Inorganic Chemistry at the Technical University of Munich. Mass spectra were recorded with an Agilent Technologies Mass Hunter Spectrometer (EI, 70 eV). Single-crystal X-ray

DOI: 10.1021/acs.inorgchem.8b01060
Inorg. Chem. 2018, 57, 9931–9940

crystallography was performed at the SCXRD laboratory of the Catalysis Research Center.

Ligands. *2-Triflatotropone.* This compound was synthesized according to a modified literature procedure.[21] 2-Hydroxycyclohepta-2,4,6-trienone (tropolone) (2.50 g, 20.5 mmol, 1.00 equiv), triethylamine (2.17 g, 21.5 mmol, 1.05 equiv), and *N*-phenyltriflimide (7.68 g, 21.5 mmol, 1.05 equiv) were dissolved in dry dichloromethane and stirred for 48 h at r.t. After extraction with water (20 mL) and dichloromethane (2 × 20 mL), the main product was concentrated *in vacuo* and purified via silica gel column chromatography (hexane/ethyl acetate = 2:1, TLC R_f = 0.3) yielding a brownish oil (86%). ^{1}H NMR (500 MHz, $CDCl_3$, 298 K): δ (ppm) = 9.07 (br s, OH), 7.42−7.22 (m, 4H, H_{Ar}), 7.07 (t, J = 10.2 Hz, 1H, H_{Ar}). ^{13}C NMR (126 MHz, $CDCl_3$, 298 K): δ [ppm] = 178.5 (s), 156.4 (s), 141.2 (s), 137.6 (s), 136.4 (s), 130.7 (s), 128.6 (s), 121.4 ($^1J_{CF}$ = 323 Hz).

Aromatic 2-Aminotropones (1a−3a). In a preheated Schlenk flask, 2-triflatotropone (1.20 g, 4.72 mmol, 1.00 equiv), cesium carbonate (2.15 g, 6.61 g, 1.40 equiv), *rac*-2,2′-bis-(diphenylphosphino)-1,1′-binaphthalene (29.4 mg, 47.2 μmol, 0.01 equiv), tris(dibenzylideneacetone)dipalladium (21.6 mg, 23.6 μmol, 0.005 equiv), and the respective aniline (6.14 mmol, 1.30 equiv) were dissolved in toluene and heated to 90 °C for 24 h.[16] The crude product was filtered, concentrated *in vacuo*, and purified via silica gel chromatography (hexane/ethyl acetate = 20:1, TLC R_f = 0.2).

2-(Phenylamino)tropone ***1a***. ^{1}H NMR (500 MHz, $CDCl_3$, 298 K): δ (ppm) = 8.84 (br s, 1H, NH), 7.53−7.19 (m, 9H, H_{Ar}), 6.88 (dd, J = 7.1 Hz, J = 8.9 Hz, 1H, H_{Ar}).

2-(2,6-Diethylphenylamino)tropone ***2a***. ^{1}H NMR (500 MHz, $CDCl_3$, 298 K): δ (ppm) = 8.47 (br s, 1H, NH), 7.36−7.23 (m, 5H, H_{Ar}), 7.07 (t, J = 10.3 Hz, 1H, H_{Ar}), 6.73 (t, J = 8.9 Hz, 1H, H_{Ar}), 6.26 (d, J = 10.3 Hz, 1H, H_{Ar}), 2.55−2.42 (m, 4H, $-CH_2-$), 1.14 (t, J = 7.6 Hz, 6H, $-CH_3$). ^{13}C NMR (126 MHz, $CDCl_3$, 298 K): δ [ppm] = 176.5, 155.6, 142.1, 137.5, 136.7, 133.9, 129.8, 128.4, 127.0, 123.6, 110.2, 24.7, 14.9. Anal. Calcd for $C_{17}H_{19}NO$: C, 80.60; H, 7.56; N, 5.53. Found C, 80.67; H, 7.64; N, 5.46. MS (EI, 70 eV): 253.2 m/z [M^+].

2-(2,6-Diisopropylphenylamino)tropone ***3a***. ^{1}H NMR (500 MHz, $CDCl_3$, 298 K): δ (ppm) = 8.42 (br s, 1H, NH), 7.41−7.26 (m, 5H, H_{Ar}), 7.07 (t, J = 10.3 Hz, 1H, H_{Ar}) 6.73 (t, J = 9.8 Hz, 1H, H_{Ar}), 6.27 (d, J = 10.3 Hz, 1H, H_{Ar}) 2.94−2.85 (m, 2H, −CH−), 1.13 (dd, J = 20.3 Hz, J = 6.9 Hz, 6H, $-CH_3$). ^{13}C NMR (126 MHz, $CDCl_3$, 298 K): δ [ppm] = 176.4, 156.5, 146.9, 137.7, 136.4, 132.4, 130.0, 128.9, 124.4, 123.8, 110.7, 28.6, 24.6, 23.5. Anal. Calcd for $C_{19}H_{16}N_2$: C, 81.10; H, 8.24; N, 4.98. Found C, 81.10; H, 8.47; N, 4.74. MS (EI, 70 eV): 281.2 m/z [M^+].

***N,N′*-Disubstituted Aminotroponimines (1b−3b).** Triethyloxonium tetrafluoroborate (0.47 g, 2.48 mmol, 1.05 equiv) was dissolved in a preheated flask in dry dichloromethane and added to a solution of the respective 2-aminotropone **2a−c** (2.36 mmol, 1.00 equiv) and dichloromethane. After stirring for 3 h at r.t., aniline (1.10 g, 11.4 mmol, 5.00 equiv) was added and the resulting solution was stirred for 48 h. The crude product was extracted with a NaOH solution (1M, 10 mL) and dichloromethane (2 × 10 mL). A dark brownish oil was obtained after silica gel column chromatography (hexane/ethyl acetate = 30:1, TLC R_f = 0.6).

N-Phenyl-2-(phenylamino)troponimine ***1b***. ^{1}H NMR (500 MHz, $CDCl_3$, 298 K): δ (ppm) = 9.18 (br s, 1H, NH), 7.40 (t, J = 7.9 Hz, 4H), 7.16−7.12 (m, 6H), 6.84 (d, J = 10.4 Hz, 2H, H_{Ar}), 6.73 (t, J = 10.3 Hz, 2H, H_{Ar}), 6.34 (t, J = 9.2 Hz, 1H). ^{13}C NMR (126 MHz, $CDCl_3$, 298 K): δ [ppm] = 152.0, 145.3, 133.6, 129.6, 124.1, 122.7, 122.2, 115.0. Anal. Calcd for $C_{19}H_{16}N_2$: C, 83.79; H, 5.92; N, 10.29. Found C, 83.95; H, 6.00; N, 10.23. MS (EI, 70 eV): 273.2 m/z [M + H].

N-Phenyl-2-(2,6-diethylphenylamino)troponimine ***2b***. ^{1}H NMR (500 MHz, $CDCl_3$, 298 K): δ (ppm) = 9.10 (br s, 1H, NH), 7.41 (t, J = 7.8 Hz, 2H), 7.18−7.13 (m, 6H), 6.88 (d, J = 10.9 Hz, 1H), 6.73 (dd, J = 10.6 Hz, J = 9.5 Hz, 1H), 6.66 (dd, J = 10.6 Hz, J = 9.5 Hz, 1H), 6.28 (t, J = 9.5 Hz, 1H), 6.14 (d, J = 10.6 Hz, 1H), 2.53−2.39 (m, 4H), 7.54 (t, J = 7.5 Hz, 6H). ^{13}C NMR (126 MHz, $CDCl_3$, 298 K): δ [ppm] = 152.8, 151.0, 144.9, 141.9, 137.6, 133.6, 133.5, 129.6, 126.5, 125.1, 124.0, 122.9, 121.3, 115.4, 113.1, 24.8, 14.6. Anal. Calcd for $C_{23}H_{24}N_2$: C, 84.11; H, 7.37; N, 8.53. Found C, 83.83; H, 7.60; N, 8.24. MS (EI, 70 eV): 329.2 m/z [M + H].

N-Phenyl-2-(2,6-diisophenylamino)troponimine ***3b***. ^{1}H NMR (500 MHz, $CDCl_3$, 298 K): δ (ppm) = 9.16 (br s, 1H, NH), 7.46 (t, J = 7.9 Hz, 2H), 7.28−7.17 (m, 6H), 6.93 (d, J = 11.0 Hz, 1H), 6.77 (dd, J = 10.7 Hz, J = 9.6 Hz, 1H), 6.69 (dd, J = 10.7 Hz, J = 9.6 Hz, 1H) 6.31 (t, J = 9.6 Hz, 1H), 6.19 (d, J = 10.7 Hz, 1H), 2.97−2.89 (m, 2H), 1.20 (dd, J = 11.1 Hz, 6.9 Hz, 12H). ^{13}C NMR (126 MHz, $CDCl_3$, 298 K): δ [ppm] = 151.3, 145.4, 142.6, 140.0, 133.5, 133.5, 129.6, 125.7, 123.9, 123.8, 122.8, 121.3, 115.1, 113.9, 28.5, 24.2, 23.5. Anal. Calcd for $C_{25}H_{28}N_2$: C, 84.23; H, 7.92; N, 7.86. Found C, 84.24; H, 8.29; N, 7.57. MS (EI, 70 eV): 357.3 m/z [M + H].

*N-(Phenylimino)pent-2-en-2-yl)aniline (****4a****).* The ligand was synthesized by a modified literature procedure.[19] A solution of 2,4-pentadione (5.00 g, 49.9 mmol, 1.00 equiv) and aniline (9.18 g, 100 mmol, 2.00 equiv) was treated with concentrated hydrochloric acid (4.90 g, 49.9 mmol) at 0 °C. After stirring the mixture for 24 h, the precipitate was filtered, washed with hexane, and dissolved in a solution of CH_2Cl_2 (4 mL), H_2O, and triethylamine (10.0 mL). The crude product was recrystallized from ethanol. ^{1}H NMR (500 MHz, $CDCl_3$, 298 K): δ (ppm) = 12.7 (s, 1H, NH), 7.29 (m, 4H, H_{Ar}), 7.06 (t, J = 7.4 Hz, 2H, H_{Ar}), 6.97 (d, J = 8.5 Hz, 4H, H_{Ar}), 4.89 (s, 1H, CH), 2.01 (s, 6H, CH_3).

Complexes. The ligands **1b−3b** (0.610 mmol, 1.00 equiv) were dissolved in a Schlenk flask in 10 mL of toluene. $Zn(NTMS_2)_2$ (0.670 mmol, 1.10 equiv) was added to the solution and stirred for 3 h (ligand **3a** for 24 h in the case of 0 °C/25 °C and 72 h at 100 °C) at room temperature; then the solvent was removed *in vacuo*. Complexes **II** and **III** were obtained by recrystallization in CH_2Cl_2/pentane at −35 °C. Complexation of **1b** yielded 50% homoleptic and 50% heteroleptic complex. Recrystallization of a saturated solution in CH_2Cl_2/pentane resulted in the exclusive crystallization of the homoleptic complex, whereas the heteroleptic one remains in solution and can be successfully separated.

I. ^{1}H NMR (300 MHz, $CDCl_3$, 298 K): δ [ppm] = 7.46 (t, J = 9.6 Hz, 4H, H_{Ar}), 7.22 (t, J = 7.3 Hz, 2H, H_{Ar}), 7.14 (dd, J = 7.4 Hz, J = 1.1 Hz, 4H, H_{Ar}), 7.07 (m, 3H, H_{Ar}), 6.72 (m, 2H, H_{Ar}), −0.18 (s, 18H, $Si-CH_3$). ^{13}C NMR (126 MHz, $CDCl_3$, 298 K): δ [ppm] = 160.3, 159.7, 149.4, 148.1, 135.2, 134.8, 129.9, 129.8, 124.8, 124.5, 124.1, 122.3, 117.6, 116.2. Anal. Calcd for $C_{25}H_{33}N_3Si_2Zn$: C, 60.40; H, 6.69; N, 8.45. Found C, 60.09; H, 6.79; N, 8.59.

II. ^{1}H NMR (500 MHz, $CDCl_3$, 298 K): δ (ppm) = 7.46 (t, J = 7.9 Hz, 2H, H_{Ar}), 7.25−7.00 (m, 9H, H_{Ar}), 6.57 (t, J = 9.2 Hz, 1H, H_{Ar}), 6.53 (d, J = 11.2 Hz, 1H, H_{Ar}), 2.55−2.37 (m, 4H, $-CH_2-$), 1.15 (t, J = 7.6 Hz, 6H, $-CH_3$), −0.25 (s, 18H, $Si-CH_3$). ^{13}C NMR (126 MHz, $CDCl_3$, 298 K): δ [ppm] = 159.5, 159.0, 147.8, 143.7, 137.2, 135.1, 135.0, 129.7, 126.2, 125.2, 125.0, 124.7, 121.8, 117.2, 116.7, 23.9, 14.0, 4.65. Anal. Calcd for $C_{29}H_{41}N_3Si_2Zn$: C, 62.96; H, 7.47; N, 7.60. Found C, 62.63; H, 7.43; N, 7.30.

III. ^{1}H NMR (500 MHz, $CDCl_3$, 298 K): δ (ppm) = 7.46 (t, J = 7.9 Hz, 2H, H_{Ar}), 7.26−6.97 (m, 7H, H_{Ar}), 7.07 (t, J = 10.7 Hz, 1H, H_{Ar}), 6.99 (t, J = 10.5 Hz, 1H, H_{Ar}), 6.55 (t, J = 9.4 Hz, 2H, H_{Ar}), 2.87 (m, 2H, CH), 1.22 (d, J = 6.8 Hz, 6H, CH_3), 1.04 (d, J = 6.8 Hz, 6H, CH_3), −0.23 (s, 18H, $Si-CH_3$). ^{13}C NMR (126 MHz, $CDCl_3$, 298 K): δ [ppm] = 160.7, 159.0, 147.6, 142.6, 142.3, 135.2, 134.8, 129.8, 125.9, 125.1, 124.8, 124.4, 122.0, 118.5, 116.9, 28.4, 25.4, 24.3, 4.78. Anal. Calcd for $C_{31}H_{45}N_3Si_2Zn$: C, 64.06; H, 7.80; N, 7.23. Found C, 63.96; H, 7.79; N, 6.96.

Ligand **4a** (0.68 mmol, 1.0 equiv) was dissolved in 5.0 mL of toluene. $Zn(NTMS_2)_2$ (0.82 mmol, 1.2 equiv) was added to the solution and stirred for 20 h at 80 °C; then the solvent was removed *in vacuo*. Complex **IV** was obtained via recrystallization in toluene at −35 °C. **IV**. ^{1}H NMR (500 MHz, $CDCl_3$, 298 K): δ (ppm) = 7.33 (m, 4H, H_{Ar}), 7.15 (t, J = 7.4 Hz, 2H, H_{Ar}), 6.98 (d, J = 8.2 Hz, 4H, H_{Ar}), 4.91 (s, 1H, CH), 1.95 (s, 6H, CH_3), −0.33 (s, 18H, $Si-CH_3$). ^{13}C NMR (126 MHz, $CDCl_3$, 298 K): δ [ppm] = 167.8, 148.7, 128.9,

DOI: 10.1021/acs.inorgchem.8b01060
Inorg. Chem. 2018, 57, 9931−9940

125.2, 124.7, 96.2, 23.9, 4.53. Anal. Calcd for $C_{23}H_{35}N_3Si_2Zn$: C, 58.15; H, 7.43; N, 8.84. Found C, 58.18; H, 7.28; N, 8.69.

General Polymerization Procedure for BBL. The polymerizations performed in the *in situ* IR autoclave were performed in the following way: The corresponding catalyst **I**−**IV** (1.00 equiv) was dissolved in dry toluene (5.0 mL) and placed in a syringe. BBL was stored in a second syringe. The two filled syringes were transported to an *in situ* IR autoclave with mechanical stirring. The autoclave was pretempered to a certain temperature under an argon atmosphere, and the solution of the catalyst in toluene and BBL were transferred into the reactor. After full conversion, an aliquot was taken to determine the conversion via ^{1}H NMR spectroscopy. The amount of toluene was reduced under vacuum prior to precipitation of the polymer in 100 mL of pentane/diethyl ether (1:1). The polymerizations without IR monitoring were carried out in glass vials with magnetic stirring under an argon atmosphere under the same conditions as in the autoclave. In the case of using 2-propanol as external alcohol, the catalyst was dissolved in toluene and treated with the respective amount of *i*PrOH. This solution was stirred for 10 min prior to monomer addition. Conversion was determined via ^{1}H NMR spectroscopy, and the polymers were precipitated in 100 mL of pentane/diethyl ether (1:1).

General Polymerization Procedure for *rac*-Lactide. *rac*-LA was dissolved in dry dichloromethane (2.65 mL), and the respective catalyst (4.00 μmol, 1.00 equiv) was added. After stirring for a certain time, an aliquot was taken to determine the conversion via ^{1}H NMR spectroscopy. In the case of using 2-propanol as external alcohol, the catalyst was dissolved in dichloromethane and treated with the respective amount of *i*PrOH. This solution was stirred for 10 min prior to monomer addition. The polymeric solution was precipitated in 60 mL of pentane/diethyl ether (1:1); then the resulting polymer was dried *in vacuo* to constant weight.

■ ASSOCIATED CONTENT

Supporting Information

The Supporting Information is available free of charge on the ACS Publications website at DOI: 10.1021/acs.inorgchem.8b01060.

In situ IR spectroscopy plots, NMR data for microstructure determination of PHB and PLA, ^{1}H DOSY NMRs, GPC data, and SC-XRD data (PDF)

Accession Codes

CCDC 1837007−1837010 contain the supplementary crystallographic data for this paper. These data can be obtained free of charge via www.ccdc.cam.ac.uk/data_request/cif, or by emailing data_request@ccdc.cam.ac.uk, or by contacting The Cambridge Crystallographic Data Centre, 12 Union Road, Cambridge CB2 1EZ, UK; fax: +44 1223 336033.

■ AUTHOR INFORMATION

Corresponding Author

*E-mail: rieger@tum.de. Tel: +49-89-289-13570. Fax: +49-89-289-13562.

ORCID

Bernhard Rieger: 0000-0002-0023-884X

Author Contributions

M.R. substantially contributed to this work during her time as a co-worker of the Wacker-Lehrstuhl für Makromolekulare Chemie. D.H.B. did a 6-month part of his Ph.D. at the Wacker-Lehrstuhl für Makromolekulare Chemie.

Funding

Financial support for D.H.B.'s research at the Wacker-Lehrstuhl for Makromolekulare Chemie was provided by the Coordenação de Aperfeiçoamento de Pessoal de Nível Superior (Process no. 88881.131708/2016-01).

Notes

The authors declare no competing financial interest.

■ ACKNOWLEDGMENTS

The authors thank Rike Adams for valuable discussions and Christian Jandl and Alexander Pöthig for crystallographic advice.

■ REFERENCES

(1) (a) Reichardt, R.; Rieger, B. Poly(3-Hydroxybutyrate) from Carbon Monoxide. *Adv. Polym. Sci.* **2011**, *245*, 49. (b) Carpentier, J.-F. Rare-Earth Complexes Supported by Tripodal Tetradentate Bis(phenolate) Ligands: A Privileged Class of Catalysts for Ring-Opening Polymerization of Cyclic Esters. *Organometallics* **2015**, *34*, 4175. (c) Guillaume, S. M.; Kirillov, E.; Sarazin, Y.; Carpentier, J. F. Beyond Stereoselectivity, Switchable Catalysis: Some of the Last Frontier Challenges in Ring-Opening Polymerization of Cyclic Esters. *Chem. - Eur. J.* **2015**, *21*, 7988. (d) Thomas, C. M. Stereocontrolled ring-opening polymerization of cyclic esters: synthesis of new polyester microstructures. *Chem. Soc. Rev.* **2010**, *39*, 165. (e) Dechy-Cabaret, O.; Martin-Vaca, B.; Bourissou, D. Controlled Ring-Opening Polymerization of Lactide and Glycolide. *Chem. Rev.* **2004**, *104*, 6147. (f) Dagorne, S.; Normand, M.; Kirillov, E.; Carpentier, J.-F. Gallium and indium complexes for ring-opening polymerization of cyclic ethers, esters and carbonates. *Coord. Chem. Rev.* **2013**, *257*, 1869.

(2) Lemoigne, M. Produit de déshydratation et de polymérisation de l'acide β-oxybutyrique. *Bull. Soc. Chim. Biol.* **1926**, 770.

(3) (a) Yasuda, T.; Aida, T.; Inoue, S. Living polymerization of β-butyrolactone catalysed by tetraphenylporphinatoaluminum chloride. *Makromol. Chem., Rapid Commun.* **1982**, *3*, 585. (b) Asano, S.; Aida, T.; Inoue, S. Polymerization of epoxide and.beta.-lactone catalyzed by aluminum porphyrin. Exchange of alkoxide or carboxylate group as growing species on aluminum porphyrin. *Macromolecules* **1985**, *18*, 2057. (c) Bloembergen, S.; Holden, D. A.; Bluhm, T. L.; Hamer, G. K.; Marchessault, R. H. Stereoregularity in synthetic β-hydroxybutyrate and β-hydroxyvalerate homopolyesters. *Macromolecules* **1989**, *22*, 1656.

(4) (a) Le Borgne, A.; Spassky, N. Stereoelective polymerization of β-butyrolactone. *Polymer* **1989**, *30*, 2312. (b) Chamberlain, B. M.; Cheng, M.; Moore, D. R.; Ovitt, T. M.; Lobkovsky, E. B.; Coates, G. W. Polymerization of Lactide with Zinc and Magnesium β-Diiminate Complexes: Stereocontrol and Mechanism. *J. Am. Chem. Soc.* **2001**, *123*, 3229. (c) Cheng, M.; Attygalle, A. B.; Lobkovsky, E. B.; Coates, G. W. Single-Site Catalysts for Ring-Opening Polymerization: Synthesis of Heterotactic Poly(lactic acid) from rac-Lactide. *J. Am. Chem. Soc.* **1999**, *121*, 11583. (d) Rieth, L. R.; Moore, D. R.; Lobkovsky, E. B.; Coates, G. W. Single-Site β-Diiminate Zinc Catalysts for the Ring-Opening Polymerization of β-Butyrolactone and β-Valerolactone to Poly(3-hydroxyalkanoates). *J. Am. Chem. Soc.* **2002**, *124*, 15239.

(5) (a) Vagin, S. I.; Reichardt, R.; Klaus, S.; Rieger, B. Conformationally Flexible Dimeric Salphen Complexes for Bifunctional Catalysis. *J. Am. Chem. Soc.* **2010**, *132*, 14367. (b) Zintl, M.; Molnar, F.; Urban, T.; Bernhart, V.; Preishuber-Pflügl, P.; Rieger, B. Variably Isotactic Poly(hydroxybutyrate) from Racemic β-Butyrolactone: Microstructure Control by Achiral Chromium(III) Salophen Complexes. *Angew. Chem., Int. Ed.* **2008**, *47*, 3458.

(6) (a) Amgoune, A.; Thomas, C. M.; Ilinca, S.; Roisnel, T.; Carpentier, J.-F. Highly Active, Productive, and Syndiospecific Yttrium Initiators for the Polymerization of Racemic β-Butyrolactone. *Angew. Chem., Int. Ed.* **2006**, *45*, 2782. (b) Bouyahyi, M.; Ajellal, N.; Kirillov, E.; Thomas, C. M.; Carpentier, J.-F. Exploring Electronic versus Steric Effects in Stereoselective Ring-Opening Polymerization

DOI: 10.1021/acs.inorgchem.8b01060
Inorg. Chem. 2018, 57, 9931−9940

of Lactide and β-Butyrolactone with Amino-alkoxy-bis(phenolate)−Yttrium Complexes. *Chem. - Eur. J.* **2011**, *17*, 1872.
(7) Stanford, M. J.; Dove, A. P. Stereocontrolled ring-opening polymerisation of lactide. *Chem. Soc. Rev.* **2010**, *39*, 486.
(8) Spassky, N.; Wisniewski, M.; Pluta, C.; Le Borgne, A. Highly stereoelective polymerization of rac-(D,L)-lactide with a chiral schiff's base/aluminium alkoxide initiator. *Macromol. Chem. Phys.* **1996**, *197*, 2627.
(9) (a) Williams, C. K.; Breyfogle, L. E.; Choi, S. K.; Nam, W.; Young, V. G.; Hillmyer, M. A.; Tolman, W. B. A Highly Active Zinc Catalyst for the Controlled Polymerization of Lactide. *J. Am. Chem. Soc.* **2003**, *125*, 11350. (b) Wang, H.; Ma, H. Highly diastereoselective synthesis of chiral aminophenolate zinc complexes and isoselective polymerization of rac-lactide. *Chem. Commun.* **2013**, *49*, 8686. (c) Abbina, S.; Du, G. Zinc-Catalyzed Highly Isoselective Ring Opening Polymerization of rac-Lactide. *ACS Macro Lett.* **2014**, *3*, 689. (d) Myers, D.; White, A.; Forsyth, C. M.; Bown, M.; Williams, C. K. Phosphasalen Indium Complexes Showing High Rates and Isoselectivities in rac-Lactide Polymerizations. *Angew. Chem., Int. Ed.* **2017**, *56*, 5277. (e) Normand, M.; Roisnel, T.; Carpentier, J. F.; Kirillov, E. Dinuclear vs. mononuclear complexes: accelerated, metal-dependent ring-opening polymerization of lactide. *Chem. Commun.* **2013**, *49*, 11692. (f) Piedra-Arroni, E.; Ladavière, C.; Amgoune, A.; Bourissou, D. Ring-Opening Polymerization with Zn(C6F5)2-Based Lewis Pairs: Original and Efficient Approach to Cyclic Polyesters. *J. Am. Chem. Soc.* **2013**, *135*, 13306. (g) Xu, T.-Q.; Yang, G.-W.; Liu, C.; Lu, X.-B. Highly Robust Yttrium Bis(phenolate) Ether Catalysts for Excellent Isoselective Ring-Opening Polymerization of Racemic Lactide. *Macromolecules* **2017**, *50*, 515.
(10) (a) Brasen, W. R.; Holmquist, H. E.; Benson, R. E. NOVEL ANALOGS OF TROPOLONE. *J. Am. Chem. Soc.* **1960**, *82*, 995. (b) Brasen, W. R.; Holmquist, H. E.; Benson, R. E. *N,N'*-Disubstituted-1-amino-7-imino-1,3,5-cycloheptatrienes, a Non-classical Aromatic System. *J. Am. Chem. Soc.* **1961**, *83*, 3125.
(11) Roesky, P. W. The co-ordination chemistry of aminotroponiminates. *Chem. Soc. Rev.* **2000**, *29*, 335.
(12) (a) Gamer, M. T.; Roesky, P. W. Bridged Aminotroponiminate Complexes of Zinc. *Eur. J. Inorg. Chem.* **2003**, *2003*, 2145. (b) Herrmann, J.-S.; Luinstra, G. A.; Roesky, P. W. Aminotroponiminate alkyl and alkoxide complexes of zinc. *J. Organomet. Chem.* **2004**, *689*, 2720.
(13) Dochnahl, M.; Löhnwitz, K.; Pissarek, J.-W.; Biyikal, M.; Schulz, S. R.; Schön, S.; Meyer, N.; Roesky, P. W.; Blechert, S. Intramolecular Hydroamination with Homogeneous Zinc Catalysts: Evaluation of Substituent Effects in *N,N'*-Disubstituent Aminotroponiminate Zinc Complexes. *Chem. - Eur. J.* **2007**, *13*, 6654.
(14) Kronast, A.; Reiter, M.; Altenbuchner, P. T.; Jandl, C.; Pöthig, A.; Rieger, B. Electron-Deficient β-Diiminato-Zinc-Ethyl Complexes: Synthesis, Structure, and Reactivity in Ring-Opening Polymerization of Lactones. *Organometallics* **2016**, *35*, 681.
(15) (a) Cheng, M.; Lobkovsky, E. B.; Coates, G. W. Catalytic Reactions Involving C1 Feedstocks: New High-Activity Zn(II)-Based Catalysts for the Alternating Copolymerization of Carbon Dioxide and Epoxides. *J. Am. Chem. Soc.* **1998**, *120*, 11018. (b) Cheng, M.; Moore, D. R.; Reczek, J. J.; Chamberlain, B. M.; Lobkovsky, E. B.; Coates, G. W. Single-Site β-Diiminate Zinc Catalysts for the Alternating Copolymerization of CO2 and Epoxides: Catalyst Synthesis and Unprecedented Polymerization Activity. *J. Am. Chem. Soc.* **2001**, *123*, 8738. (c) Kissling, S.; Lehenmeier, M. W.; Altenbuchner, P. T.; Kronast, A.; Reiter, M.; Deglmann, P.; Seemann, U. B.; Rieger, B. Dinuclear zinc catalysts with unprecedented activities for the copolymerization of cyclohexene oxide and CO_2. *Chem. Commun.* **2015**, *51*, 4579. (d) Lehenmeier, M. W.; Kissling, S.; Altenbuchner, P. T.; Bruckmeier, C.; Deglmann, P.; Brym, A.-K.; Rieger, B. Flexibly Tethered Dinuclear Zinc Complexes: A Solution to the Entropy Problem in CO_2/Epoxide Copolymerization Catalysis? *Angew. Chem., Int. Ed.* **2013**, *52*, 9821. (e) Chen, H.-Y.; Huang, B.-H.; Lin, C.-C. A Highly Efficient Initiator for the Ring-Opening Polymerization of Lactides and ε-Caprolactone: A Kinetic Study. *Macromolecules* **2005**, *38*, 5400. (f) Ajellal, N.; Carpentier, J.-F.; Guillaume, C.; Guillaume, S. M.; Helou, M.; Poirier, V.; Sarazin, Y.; Trifonov, A. Metal-catalyzed immortal ring-opening polymerization of lactones, lactides and cyclic carbonates. *Dalton Transactions* **2010**, *39*, 8363.
(16) Hicks, F. A.; Brookhart, M. Synthesis of 2-Anilinotropones via Palladium-Catalyzed Amination of 2-Triflatotropone. *Org. Lett.* **2000**, *2*, 219.
(17) Kernbichl, S.; Reiter, M.; Adams, F.; Vagin, S.; Rieger, B. CO_2-Controlled One-Pot Synthesis of AB, ABA Block, and Statistical Terpolymers from β-Butyrolactone, Epoxides, and CO_2. *J. Am. Chem. Soc.* **2017**, *139*, 6787.
(18) (a) Gibson, V. C.; Redshaw, C.; Solan, G. A. Bis(imino)-pyridines: Surprisingly Reactive Ligands and a Gateway to New Families of Catalysts. *Chem. Rev.* **2007**, *107*, 1745. (b) Roesky, P. W.; Gamer, M. T.; Puchner, M.; Greiner, A. Homoleptic Lanthanide Complexes of Chelating Bis(phosphanyl)amides: Synthesis, Structure, and Ring-Opening Polymerization of Lactones. *Chem. - Eur. J.* **2002**, *8*, 5265.
(19) Tang, L.-M.; Duan, Y.-Q.; Li, X.-F.; Li, Y.-S. Syntheses, structure and ethylene polymerization behavior of β-diiminato titanium complexes. *J. Organomet. Chem.* **2006**, *691*, 2023.
(20) Baran, J.; Duda, A.; Kowalski, A.; Szymanski, R.; Penczek, S. Intermolecular chain transfer to polymer with chain scission: general treatment and determination of kp/ktr in L,L-lactide polymerization. *Macromol. Rapid Commun.* **1997**, *18*, 325.
(21) Mc Murry, J. E.; Scott, W. J. A method for the regiospecific synthesis of enol triflates by enolate trapping. *Tetrahedron Lett.* **1983**, *24*, 979.

DOI: 10.1021/acs.inorgchem.8b01060
Inorg. Chem. 2018, 57, 9931−9940

15.2 (Co)polymerization of *(-)*-Menthide and β-Butyrolactone with Yttrium *bis*(phenolates): Tuning Material Properties of Sustainable Polyesters

Title: **"**(Co)polymerization of (-)-Menthide and β-Butyrolactone with Yttrium-*bis*(phenolates): Tuning Material Properties of Sustainable Polyester"

Status: Full Paper, manuscript in preparation

Journal:

Authors: Friederike Adams, Thomas M. Pehl, Moritz Kränzlein, Sebastian A. Kernbichl, Jia-Jhen Kang, Christine M. Papadakis, Bernhard Rieger

Abstract

A series of pyrazine-containing heteroaromatic yttrium-bis(phenolate) complexes were synthesized and tested in the ring-opening polymerization of racemic β-butyrolactone and *(-)*-menthide. Besides the two homopolymers, AB and BAB copolymers were produced consisting of poly(*(-)*-menthide) (PM, block A) and poly(3-hydroxybutyrate) (block B) in a sequential addition pathway. The synthesis of BAB copolymers was enabled by the introduction of a bifunctional pyrazine initiator which allowed polymerization in two directions. The influence of the block formation was investigated via thermal analysis, X-ray diffraction, small-angle X-ray scattering, and stress-strain experiments. A microphase separation of the semicrystalline BAB materials was revealed. Stress-strain measurements render the syndiotactic PHB less brittle than natural PHB. The incorporation of PM in the polymer architecture led to a reduced Young modulus and an increased elongation at break was observed.

F. Adams planned and executed all experiments and wrote the manuscript. T. M. Pehl, M. Kränzlein and S. A. Kernbichl helped with measurements and proofreading of the manuscript. J.-J. Jhen and C. K. Papadakis performed and evaluated SAXS measurements. All work was supervised by B. Rieger.

16. Appendix

16.1 Supporting Information: CO_2-Controlled One-Pot Synthesis of AB, ABA Block, and Statistical Terpolymers from β-Butyrolactone, Epoxides, and CO_2

CO_2-Controlled One-Pot Synthesis of AB, ABA Block, and Statistical Terpolymers from β-Butyrolactone, Epoxides, and CO_2

Sebastian Kernbichl[‡], Marina Reiter[‡], Friederike Adams, Sergei Vagin, and Bernhard Rieger*

Table of contents

1. Experimental Section

General

All reactions containing air- and/or moisture sensitive compounds were performed under dry argon using standard Schlenk or glovebox techniques. All chemicals were purchased from Aldrich or ABCR. Monomers were dried over calcium hydride and distilled prior to polymerization. CO_2 was purchased from Westfalen (purity 4.6). Toluene was obtained from an MBraun MB-SPS-800 solvent purification system. NMR spectra were recorded on a Bruker AVIII500 Cryo and an AVHD500 spectrometer. ^{1}H NMR spectroscopic chemical shifts δ are reported in ppm relative to tetramethylsilane and calibrated to the residual proton signal of the deuterated solvent. Deuterated solvents were obtained from Aldrich and dried over 3 Å molecular sieves. Gel permeation chromatography (GPC) analysis was performed on a Varian PL-GPC 50 using THF (HPLC grade) with 0.22 g L^{-1} 2.6 di-*tert*-butyl-4-methylphenol and a flow rate of 1 ml/min at 40 °C. Polystyrene standards were used for calibration. DSC measurements were carried out at a DSC G2000 of TA Instruments with a heating rate of 5 °C/min. ESI-MS analytical measurements were performed in acetonitrile solutions on a Varian 500 MS spectrometer. UV-Vis spectra were recorded on a Varian Cary-50. *In situ* IR measurements were performed under argon atmosphere using an ATR IR MettlerToledo system. Elemental analysis was performed at the microanalytic laboratory of the Department of Inorganic Chemistry at the Technical University of Munich. Stress-strain measurements were performed on a ZwickRoell with a strain rate of 5 mm/min and analyzed with testXpert II software. Specimen (dog bone shape, 50 mm long, 4 mm wide (smallest point)) were produced by dissolving the polymer in dichloromethane and subsequent evaporation of the solvent. Complete removal of DCM was checked *via* ^{1}H NMR. Optical Rotation measurements were performed on a Perkin-Elmer 241 MC Polarimeter in $CHCl_3$ using a Hg-lamp at a wavelength of 365 nm. The catalyst was removed prior to measure optical rotation by stirring a polymer/dichloromethane solution in an aqueous EDTA solution.

Ligand Synthesis

Ligand $CH(CCF_3NC_6H_4\text{-}2,6C_2H_5)_2$ was synthesized according to literature procedures.[1]

Complex Synthesis

$[CH(CCF_3NC_6H_4\text{-}2,6C_2H_5)_2]ZnN(SiMe_3)_2$, Complex 1 was synthesized according to literature procedures. [2]

Polymerization Procedure

All Polymerizations were performed with *in situ* monitoring using a React-IR/MultiMax four-autoclave system (Mettler-Toledo). The 50 mL steel autoclaves are equipped with a diamond window, a mechanic stirring and a heating device. The autoclaves were heated to 130 °C under vacuum overnight prior to polymerization.

ROP-Polymerization of BBL

For the homopolymerizations of BBL (Table S1, entries S1-S5) 28.9 µmol of complex 1 were dissolved in 5.0 g toluene and taken to a syringe. 17.4 mmol BBL were stored in a second syringe. The two syringes were rapidly transported to the reactor using a vial equipped with an injection septum. The autoclave was pretempered to 60 °C under argon atmosphere und the two syringes were transferred into the reactor. After full conversion an aliquot was taken to determine the conversion *via* ^{1}H-NMR spectroscopy. Toluene was removed under vacuum prior to precipitation of the polymer in pentane/diethylether (1:1).

[1] A. Kronast, M. Reiter, P. T. Altenbuchner, C. Jandl, A. Pöthig and B. Rieger, *Organometallics* **2016**, *35*, 681-685.

[2] M. Reiter, S. Vagin, A. Kronast, C. Jandl and B. Rieger, *Chem. Sci.* **2017**, 10.1039/C6SC04477H.

Terpolymerization of BBL/Epoxide/CO_2 *via* Procedure A1

For terpolymerizations (Table 1, entries 1+6) 40 µmol complex 1 were dissolved in 2.0 g toluene and 20 mmol epoxide (CHO or CPO) and transferred to a syringe. 20 mmol BBL were stored in a second syringe. The two syringes were rapidly transported to the reactor using a vial equipped with an injection septum. The autoclave was pretempered to 60 °C in case of CHO, to 50 °C for CPO under argon atmosphere and the two syringes were transferred into the reactor. After full conversion of BBL, 40 bar CO_2 were applied. At the end of the reaction, CO_2 was released and the product was dissolved in dichloromethane and transferred to a flask. Consequent removal of the solvent under vacuum allowed the determination of yield and selectivity via NMR/weight of the polymer. The dissolved polymer (dichloromethane) was precipitated in methanol and dried under vacuum.

Terpolymerization of BBL/Epoxide/CO_2 *via* Procedure A1+A2

For terpolymerizations (Table 1, entries 2+7) 40 µmol complex 1 were dissolved in 2.0 g toluene and 20 mmol epoxide (CHO or CPO) and transferred to a syringe. 20 mmol BBL were stored in a second syringe. The two syringes were rapidly transported to the reactor using a vial equipped with an injection septum. The autoclave was pretempered to 60 °C in case of CHO, to 50 °C for CPO under argon atmosphere and the two syringes were transferred into the reactor. After half conversion of BBL, 40 bar CO_2 were applied. After full conversion of CHO, CO_2 was slowly released to allow the residual BBL to polymerize. It is important to release all CO_2 by an Argon counterflow and repeat the purging process until CO_2 can not be measured anymore. The product was dissolved in dichloromethane and transferred to a flask. Consequent removal of the solvent under vacuum allowed the determination of yield and selectivity *via* NMR/weight of the polymer. The dissolved polymer (dichloromethane) was precipitated in methanol and dried under vacuum.

Terpolymerization of BBL/Epoxide/CO_2 *via* Procedure B

For terpolymerizations (Table 1, entries 3, 8) 40 µmol complex 1 were dissolved in 2.0 g toluene and the amount of epoxide (CHO or CPO) and transferred to a syringe. A total amount of 40 mmol monomer (BBL + epoxide) was applied with a definite composition as indicated in Table 1 or Table S2. The amount of BBL was stored in a second syringe. The two syringes were rapidly transported to the reactor using a vial equipped with an injection septum. The autoclave was pretempered to 60 °C in case of CHO, to 50 °C for CPO under argon atmosphere and the two syringes were transferred into the reactor. 40 bar CO_2 were applied. After full conversion of CHO, CO_2 is released slowly allowing BBL to polymerize. It is important to release all CO_2 by an Argon counterflow and repeat the purging process until CO_2 can not be measured anymore. After full conversion the product was dissolved in dichloromethane and transferred to a flask. Consequent removal of the solvent under vacuum allowed the determination of yield and selectivity via NMR/weight of the polymer. The dissolved polymer (dichloromethane) was precipitated in methanol and dried under vacuum.

Terpolymerization of BBL/Epoxide/CO_2 *via* Procedure C

For the terpolymerization (Table 1, entries 4, 5, 9) 40 µmol complex 1 were dissolved in 2.0 g toluene and 20 mmol epoxide (CHO or CPO) and transferred to a syringe. 20 mmol BBL were stored in a second syringe. The two syringes were rapidly transported to the reactor using a vial equipped with an injection septum. The autoclave was pretempered to 60 °C in case of CHO, to 50 °C for CPO under argon atmosphere und the two syringes were transferred into the reactor. 3 bar CO_2 were applied. After the desired conversion of the epoxide and BBL, CO_2 is released. The product was dissolved in dichloromethane and transferred to a flask. Consequent removal of the solvent under vacuum allowed the determination of yield and selectivity *via* NMR/weight of the polymer. The dissolved polymer (dichloromethane) was precipitated in methanol and dried under vacuum.

Copolymerization of CPO and CO_2

For copolymerizations of cyclopentane oxide 57.3 µmol complex 1 were dissolved in 57.3 mmol cyclopentane oxide and rapidly transferred to the autoclave using a syringe in a vial with an injection septum. The reactor was pretempered to 50 °C under argon

atmosphere and the syringe is given into the reactor. 40 bar CO_2 were applied and the reaction was terminated as no linear increase in polymer formation could be detected. The product was dissolved in dichloromethane and transferred to a flask. Consequent removal of the solvent under vacuum allowed the determination of yield and selectivity *via* NMR/weight of the polymer. The dissolved polymer (dichloromethane) was precipitated in methanol and dried under vacuum.

2. Formation of PHB and the carbonyl region of ^{13}C-NMR Spectra (Table S1)

Table S1. ROP of BBL in the absence, presence, and subsequent release of CO_2.

entry	BBL/cat	CO_2 [bar]	Conversion [%][a]	M_n (calc.) [kg/mol][b]	M_n (exp.) [kg/mol] (PDI)[c]	Tacticity P_m[d]
S1	600	-	91	47	145 (1.6)	0.53
S2	600 (*R*-BBL)	-	98	51	n.d.[f]	0.95
S3	600	40	17	9	14 (1.2)	0.47
S4	600	40 + release	87	45	48 (1.1)	0.43
S5[e]	600	-	99	51	76 (1.5)	0.52

5.0 g toluene, 28 µmol 1, 17.4 mmol BBL, 60 °C; [a]Determined with an aliquot ^{1}H-NMR spectrum; [b]Calculated using the following equation: M_n = 600·86.09 g/mol·conversion; [c]PHB precipitated in pentane/Et_2O (1:1), measured via GPC in THF (polystyrene standard). [d]Determined by ^{13}C spectrum of the carbonyl C atom of PHB (Figure S1). [e]17.4 mmol CHO, 17.4 mmol BBL, and 3.48 g toluene were used. [f]n.d. = not determined.

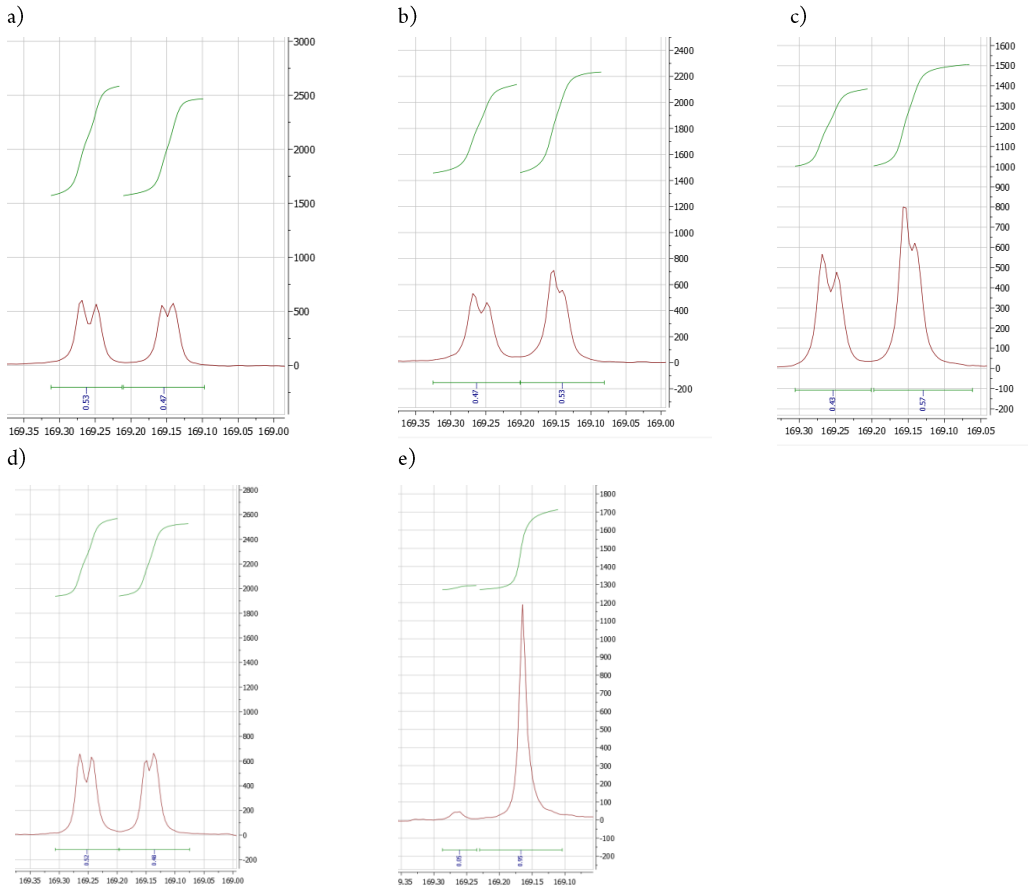

Figure S1. Carbonyl region of PHB in ^{13}C spectra: a) Table S1, entry 1; b) Table S1, entry 2; c) Table S1, entry 3; d) Table S1, entry 4; e) Table S1, entry 5.

3. *In situ* IR data for ROP of BBL with catalyst 1

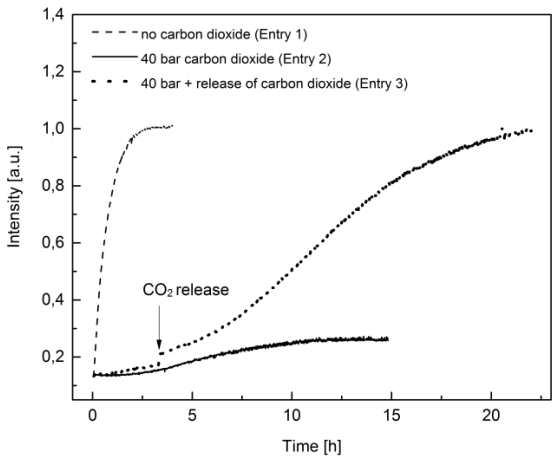

Figure S2. ROP of BBL with catalyst 1 in an autoclave with *in situ* IR monitoring (Intensity $\nu_{(C=O,\,PHB)}$ = 1744 cm^{-1} against time). Dashed line: without CO_2, black line: 40 bar CO_2, dotted line: 3.5 h and 40 bar CO_2, subsequent CO_2 release.

4. ^{13}C-NMR spectrum of PHB-Homopolymer (Table S1, entry S3)

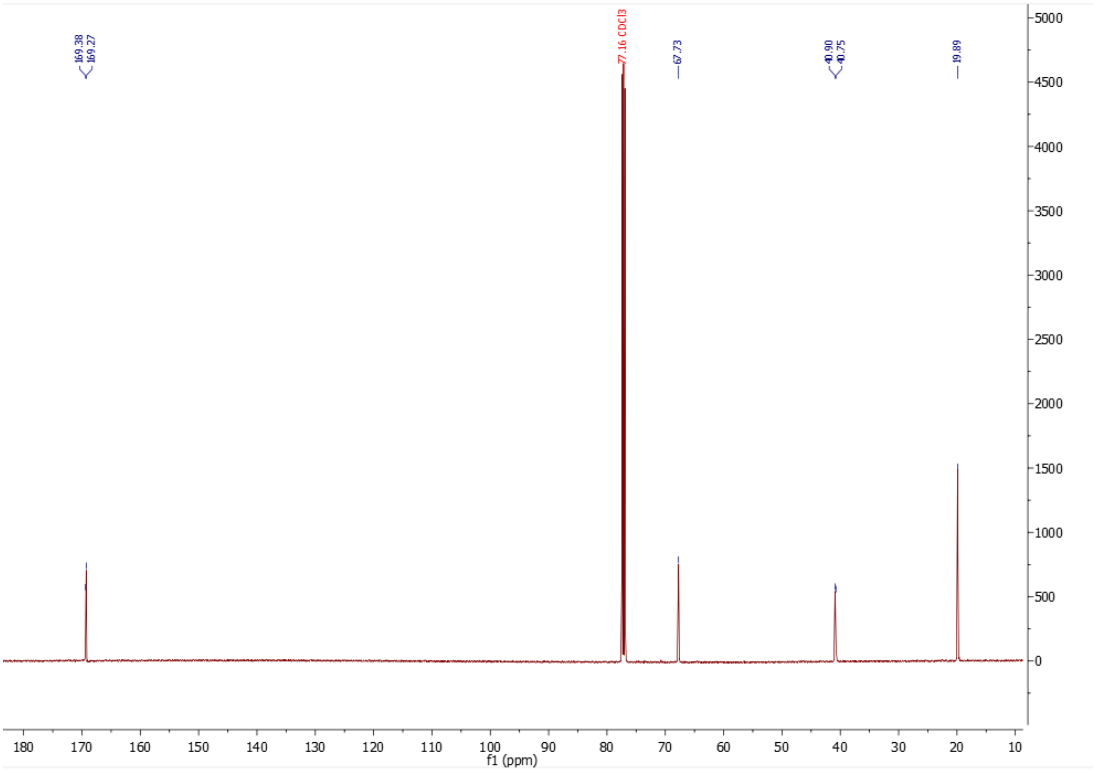

Figure S3. ^{13}C NMR spectrum of PHB homopolymer in presence of CO_2 (Table S1, entry S3).

5. Polymerization Experiments using *R*-BBL for mechanistic investigations, further Terpolymerization Experiments with *rac*-BBL, CPO or CHO and CO_2

Table S2: Terpolymerizations of CHO/CPO, CO_2 and *rac*-BBL/*R*-BBL and Copolymerisation of CPO and CO_2.

Entry	[epoxide]:[BBL]:[cat]	reaction pathway[a]	CO_2 [bar]	conv. BBL [%][c]	conv. epoxide [%][c]	[PC]:[PHB] prior to prec. [%][d]	[PC]:[PHB] after prec. [%][e]	Tg [°C][f]	M_n (PDI) [kg/mol][g]	$[\alpha]^{25}_{365}$[h]
S1	500 (CHO):500 (*rac*-BBL):1	C	3	39	32	45:55	45:55	57	64 (1.2)	-
S2	500 (CHO):500 (*rac*-BBL):1	C	1	60	21	27:73	28:72	26	53 (1.2)	-
S3	500 (CHO):500 (*R*-BBL):1	C	3	76	79	51:49	51:49	49	n.d.	+8.1
S4	850(CHO):150:1	B	40	78	95	89:11[h]	92:8	108	174 (1.4)	-
S5	400(CHO):600:1	B	40	89	73	45:55	55:45	2/114	108 (1.2)	-
S6	150(CHO):850:1	B	40	58	72	17:83	22:78	5	73 (1.5)	-
S7	1000 (CPO):1[i]	-	40	-	61	-	-	91	122 (1.3)	-
S8	500 (CPO):500 (*rac*-BBL):1	B	50	47	73	61:39	65:35	7/67	64 (1.5)	-
S9	500 (CPO):500 (*rac*-BBL):1	C	6	6	53	90:10	90:10	n.d.	46 (1.3)	-

Reaction conditions: CHO/BBL/CO_2: 60 °C, CPO/CO_2: 50 °C, 2.0 g toluene, 40 µmol catalyst 1. [a]According to Figure 1. [b]Whole polymerization time, followed by the *in situ* ATR-IR. [c]Determined by ^{1}H-NMR spectroscopy of a crude polymer sample. [d]Determined by ^{1}H-NMR spectroscopy of a crude polymer sample. [e]Composition of terpolymer after precipitation (homopolymeric PHB stays in solution after precipitation). [f]Determined by DSC, heating rate 5 K/min. [g]Measured via GPC in thf. [h]Optical activity measured with a polarimeter at 365 nm. [i]4.82 g CPO, 57 µmol catalyst 1, no toluene was added.

6. Modes of ROP of BBL

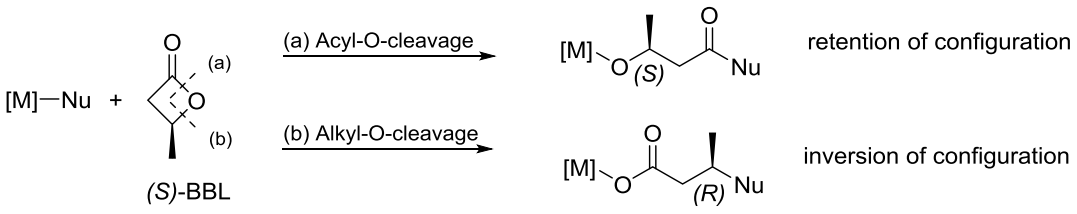

Figure S4. Possible modes of ROP for BBL: (a) *via* Acyl-O-cleavage or (b) *via* Alkyl-O-cleavage.

7. GPC results of Table S1 and Table 1

Table S1

Entry S1

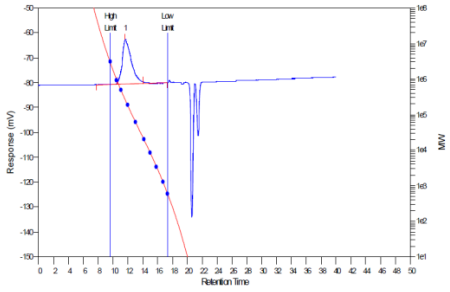

MW Averages

Peak No	Mp	Mn	Mw	Mz	Mz+1	Mv	PD
1	261366	145590	227435	313838	397863	215107	1.56216

Entry S3

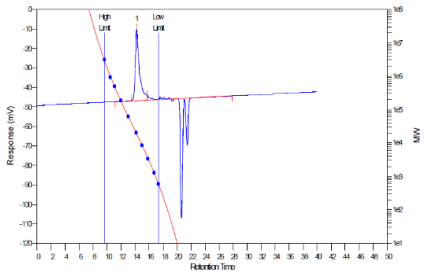

MW Averages

Peak No	Mp	Mn	Mw	Mz	Mz+1	Mv	PD
1	19416	13917	16426	18399	19868	16089	1.18028

Entry S4

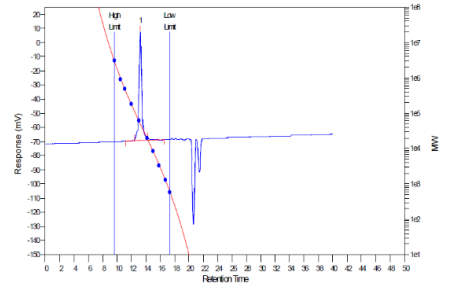

MW Averages

Peak No	Mp	Mn	Mw	Mz	Mz+1	Mv	PD
1	51649	48337	51436	54774	58252	50919	1.06411

Entry S5

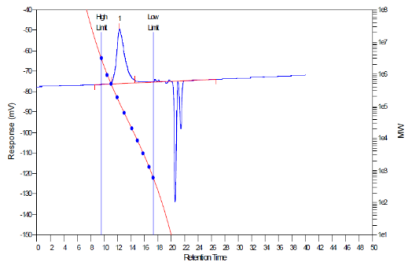

MW Averages

Peak No	Mp	Mn	Mw	Mz	Mz+1	Mv	PD
1	131061	76443	117141	159861	201705	111027	1.5324

Table 1

Entry 1

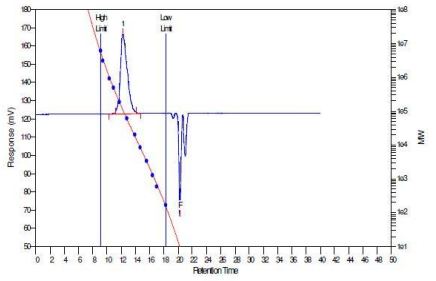

MW Averages

Peak No	Mp	Mn	Mw	Mz	Mz+1	Mv	PD
1	113485	75809	100599	127336	156291	96854	1.32701
2	0	0	0	0	0	0	0

Entry 2

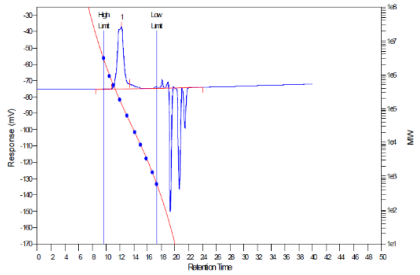

MW Averages

Peak No	Mp	Mn	Mw	Mz	Mz+1	Mv	PD
1	145450	145598	178690	217479	260901	173268	1.22728

Entry 3

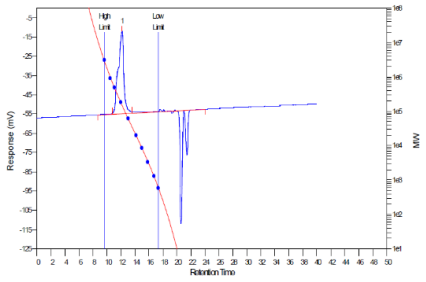

MW Averages

Peak No	Mp	Mn	Mw	Mz	Mz+1	Mv	PD
1	155968	165976	202931	246123	293319	196976	1.22265

Entry 4

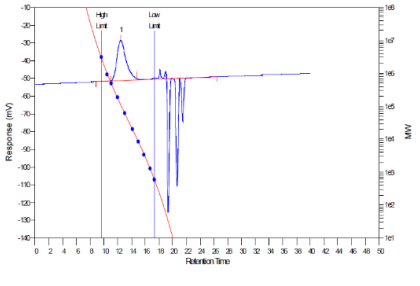

MW Averages

Peak No	Mp	Mn	Mw	Mz	Mz+1	Mv	PD
1	112232	69280	111646	156855	202474	105293	1.61152

Entry 5

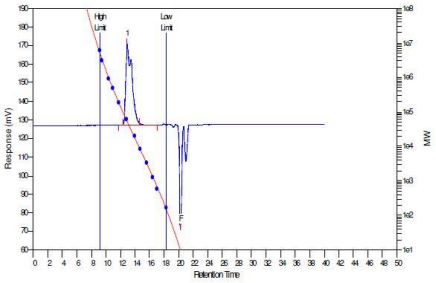

MW Averages

Peak No	Mp	Mn	Mw	Mz	Mz+1	Mv	PD
1	52319	33799	40786	47143	52460	39799	1.20672
2	0	0	0	0	0	0	0

Entry 6

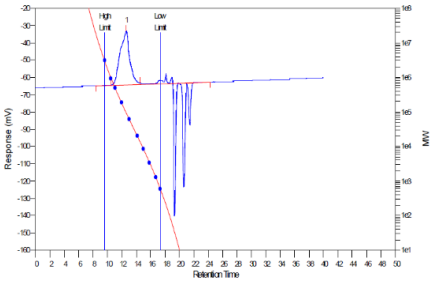

MW Averages

Peak No	Mp	Mn	Mw	Mz	Mz+1	Mv	PD
1	94605	91798	146056	220544	307954	136705	1.59106

Entry 7

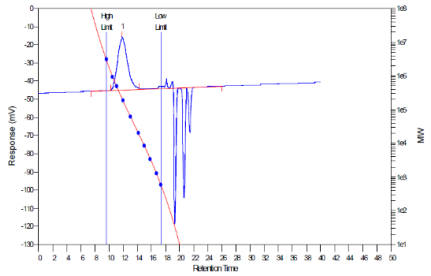

MW Averages

Peak No	Mp	Mn	Mw	Mz	Mz+1	Mv	PD
1	210608	142583	240154	363162	498937	224175	1.68431

Entry 8

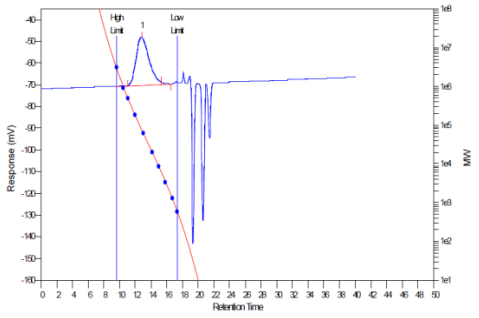

MW Averages

Peak No	Mp	Mn	Mw	Mz	Mz+1	Mv	PD
1	79855	45305	82011	127810	177016	75994	1.8102

Entry 9

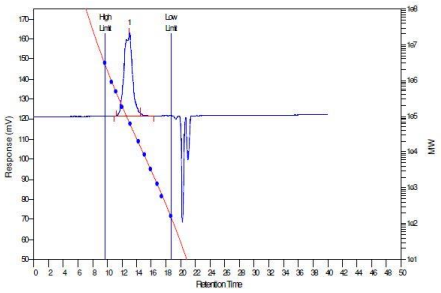

MW Averages

Peak No	Mp	Mn	Mw	Mz	Mz+1	Mv	PD
1	66036	67510	92172	122427	157009	88132	1.36531

Table S2, entry S7

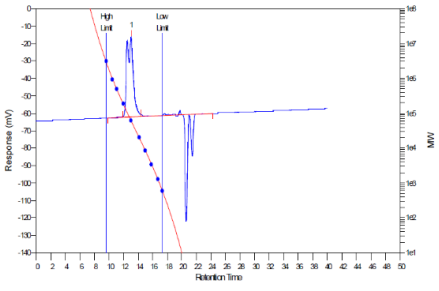

MW Averages

Peak No	Mp	Mn	Mw	Mz	Mz+1	Mv	PD
1	61030	63680	76227	88080	98340	74398	1.19703

8. DSC Analysis of Terpolymers (Table 1)

a)

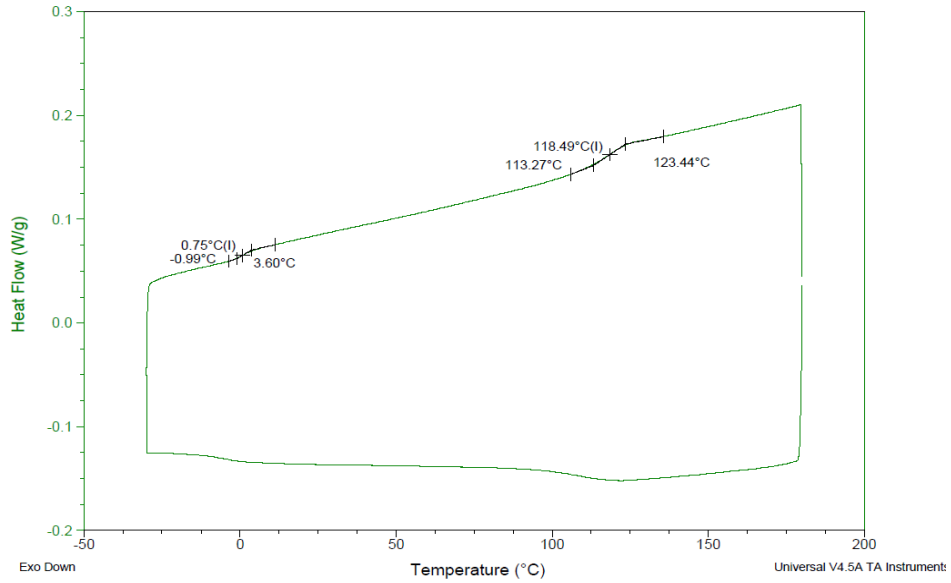

b)

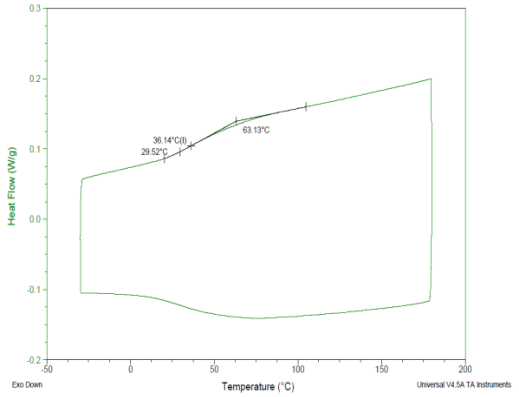

c)

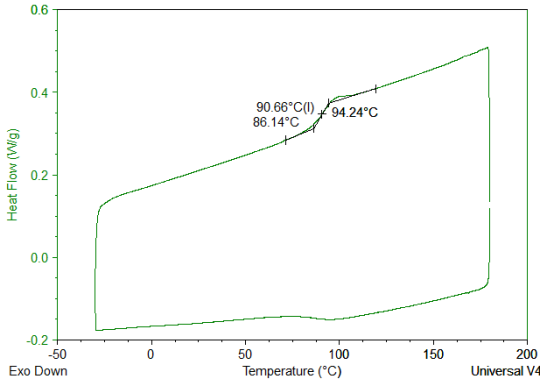

Figure S5. DSC curve (heating rate 5 K/min) a) for terpolymer Table 1, entry 3 (polymerization according to procedure B). b) for terpolymer Table 1, entry 4 (polymerization according to procedure C). c) for terpolymer Table 1, entry 5 (76:24, PCHC:PHB, Procedure C).

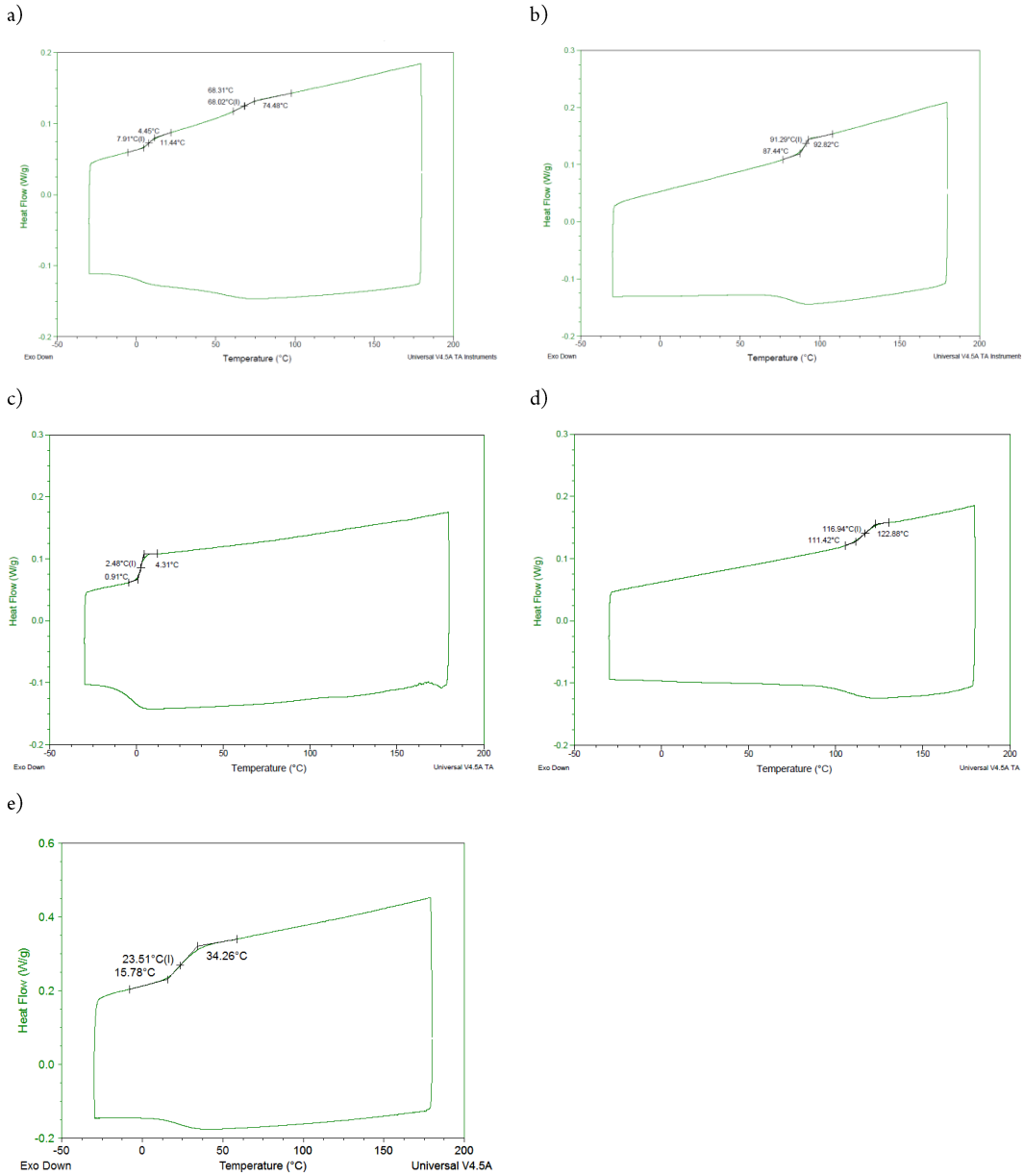

Figure S6. DSC curve (heating rate 5 K/min) a) for terpolymer out of CPO, BBL and CO_2, Table 1, entry 8 (polymerization according to procedure B) b) for PCPC copolymer (Table S2, entry S7) c) PHB homopolymer (Table S1, entry S1) d) PCHC copolymer, and e) statistical terpolymer out of CPO, BBL and CO_2 (Table 1, entry 9).

9. UV-Vis Analysis of Terpolymer (Table S2, entry S6)

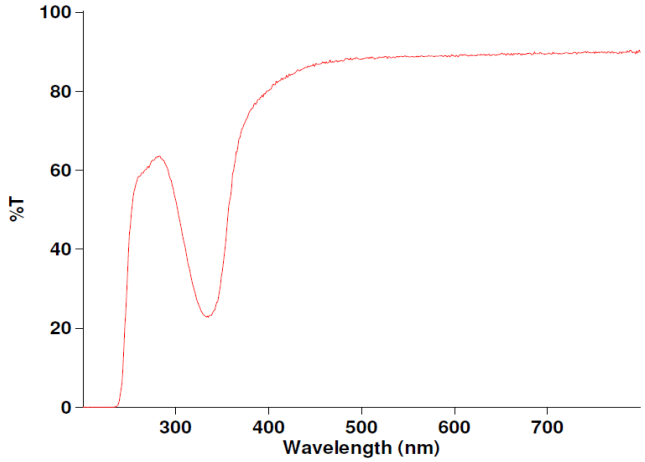

Figure S7. UV-Vis spectrum of terpolymer consisting of 22% PCHC/78% PHB from 200-800 nm (Table S2, entry S6).

10. Tensile Test of PHB/PCHC Terpolymers

Table S3. Comparison of mechanical properties of three different terpolymers.

	[PC]:[PHB] [%]	Young's modulus [MPa]	Tensile strength [MPa]	elongation at break [%]
Table 1, entry 4	47:53	1340	13.1	1.2
Table S2, entry S5	55:45	1250	13.1	1.3
Table S2, entry S6	22:78	261	5.8	225

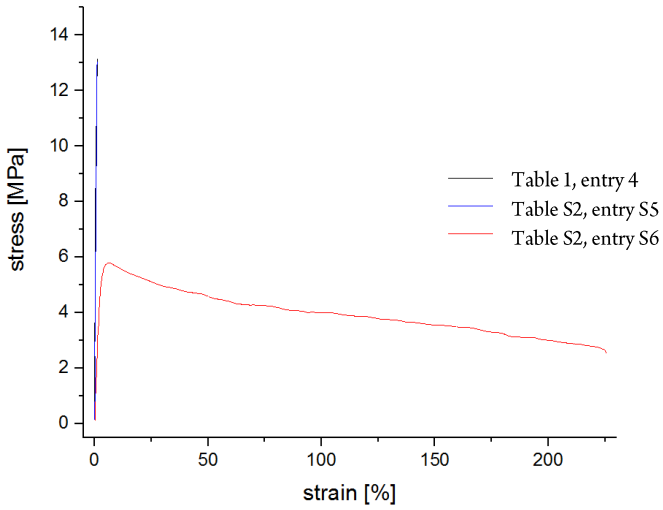

Figure S8. Stress-Strain curve of three different terpolymers (measured with 5 mm/min, thickness of all three specimen about 30 µm).

11. ^{1}H, ^{13}C, COSY and HMBC spectra of Terpolymer (Table 1, Entry 4) produced *via* Procedure C

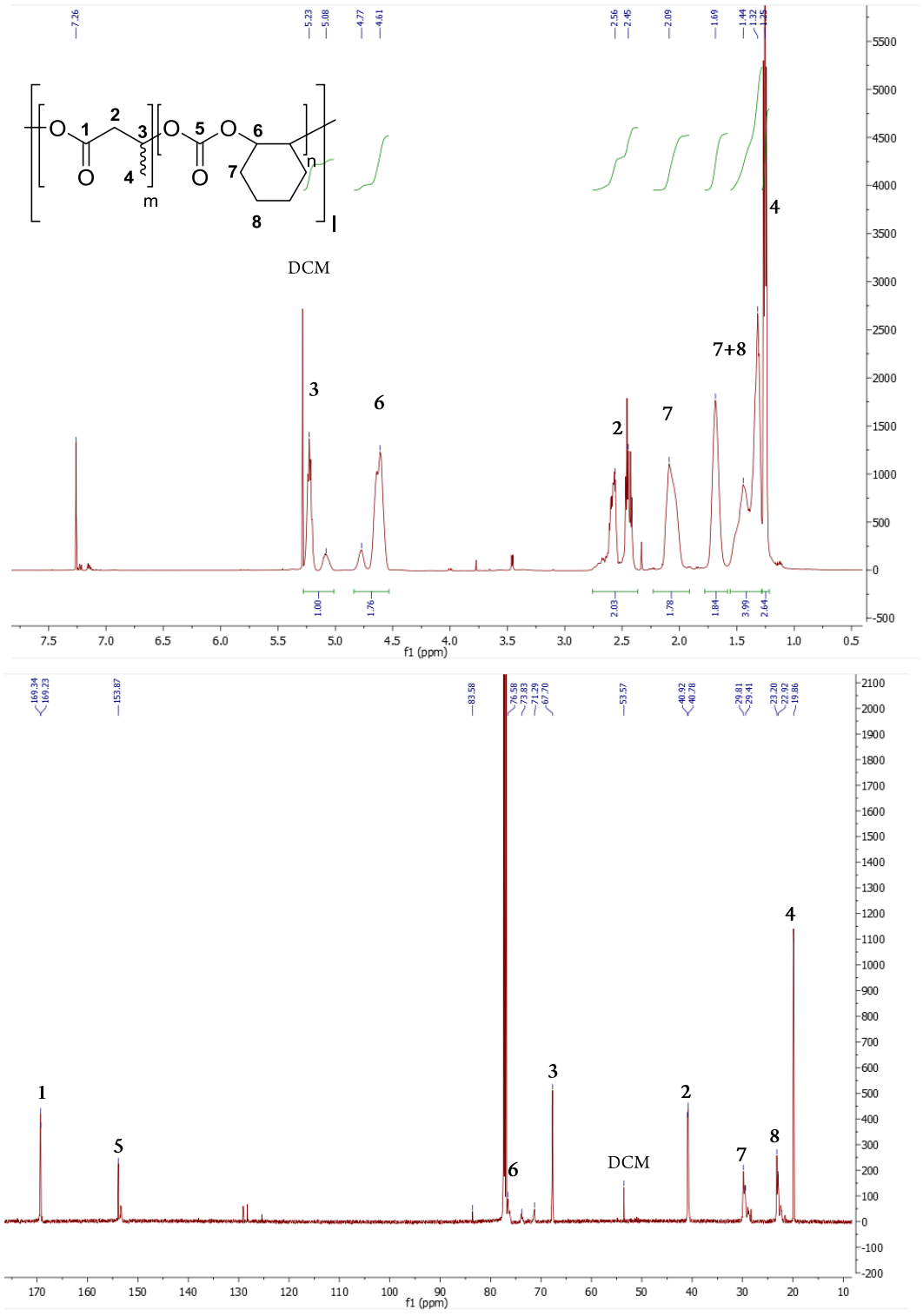

Figure S9. ^{1}H and ^{13}C NMR spectra of terpolymer produced *via* procedure C prior to precipitation (Table 1, entry 4).

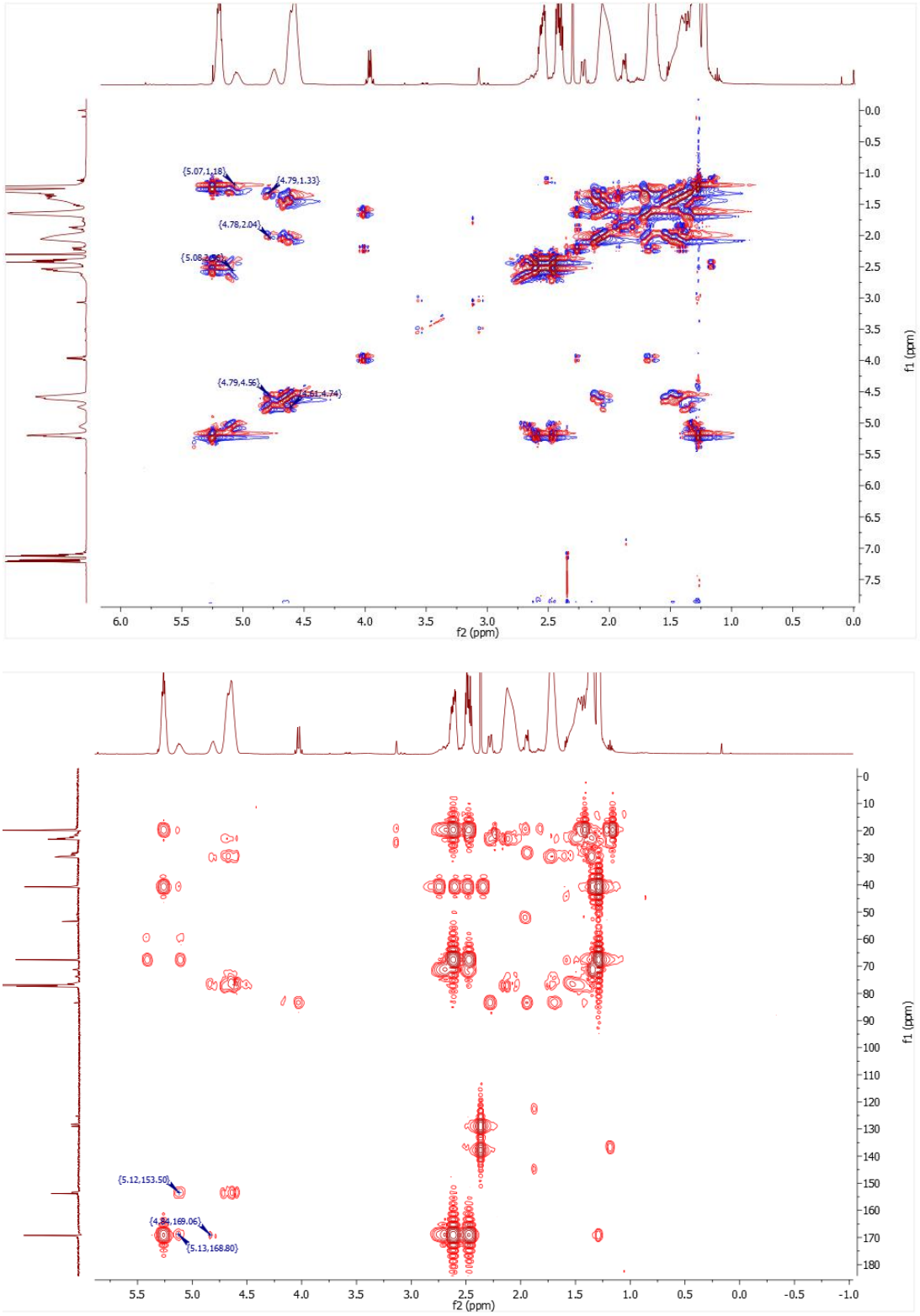

Figure S10. COSY (4 scans) and HMBC (32 scans) of terpolymer produced via procedure C prior to precipitation (Table 1, entry 4).

12. *In situ* IR Spectroscopy for Terpolymerizations according to different Reaction Pathways

a)

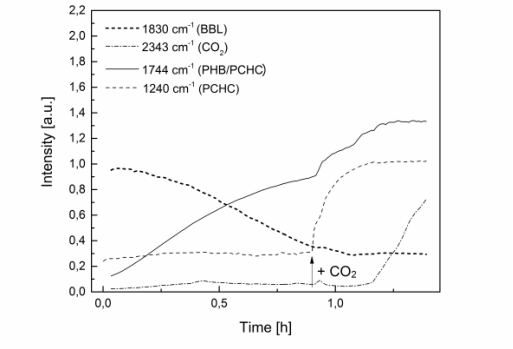

b)

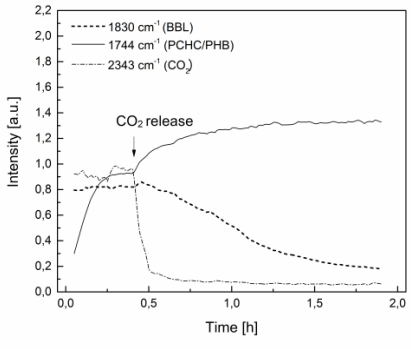

c)

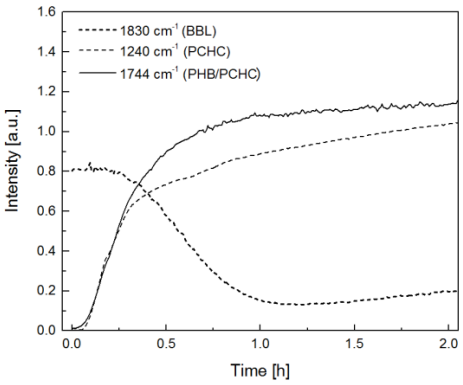

Figure S11. Formation of terpolymers monitored by *in situ* IR spectroscopy: a) procedure A1 (Table 1, entry 1) procedure B (Table 1, entry 3) and c) procedure C with 3 bar CO_2 within the whole reaction (Table 1, entry 4) (assignment of procedures according to Figure 1).

13. ^{1}H NMR Spectra of precipitated Terpolymers (Table 1)

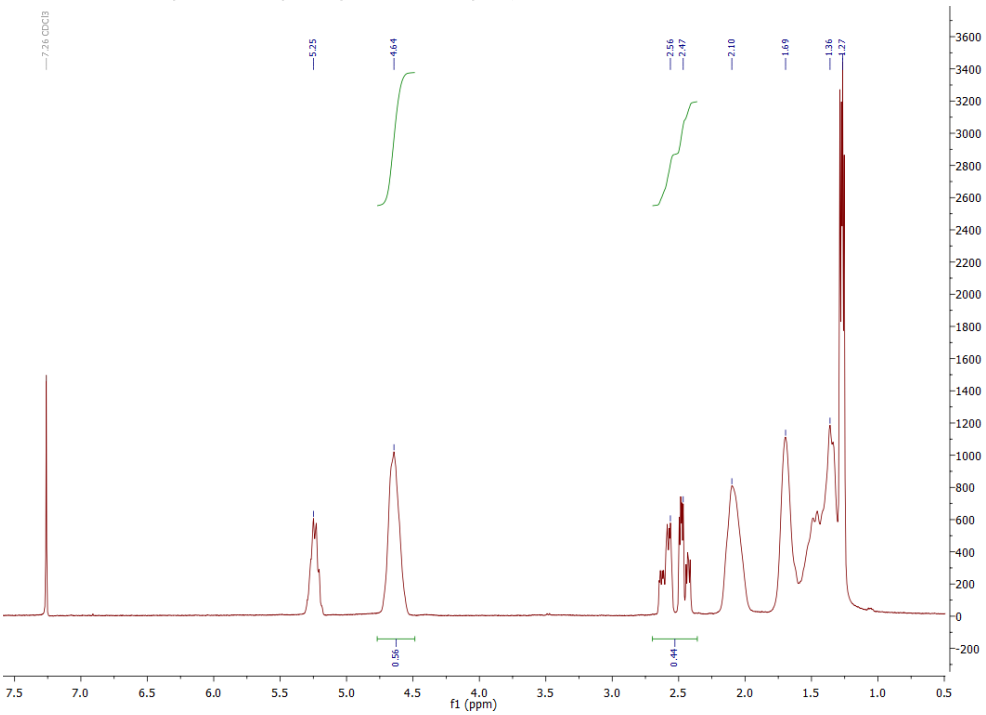

Figure S12. ^{1}H NMR spectrum of terpolymer (Table 1, entry 1).

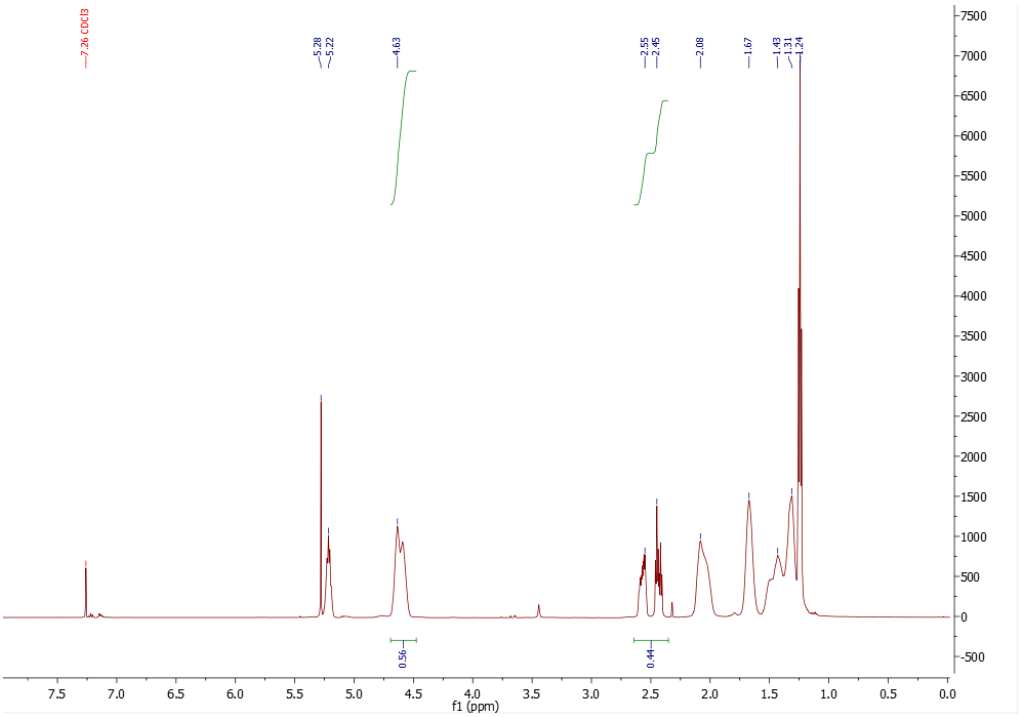

Figure S13. ^{1}H NMR spectrum of terpolymer (Table 1, entry 2).

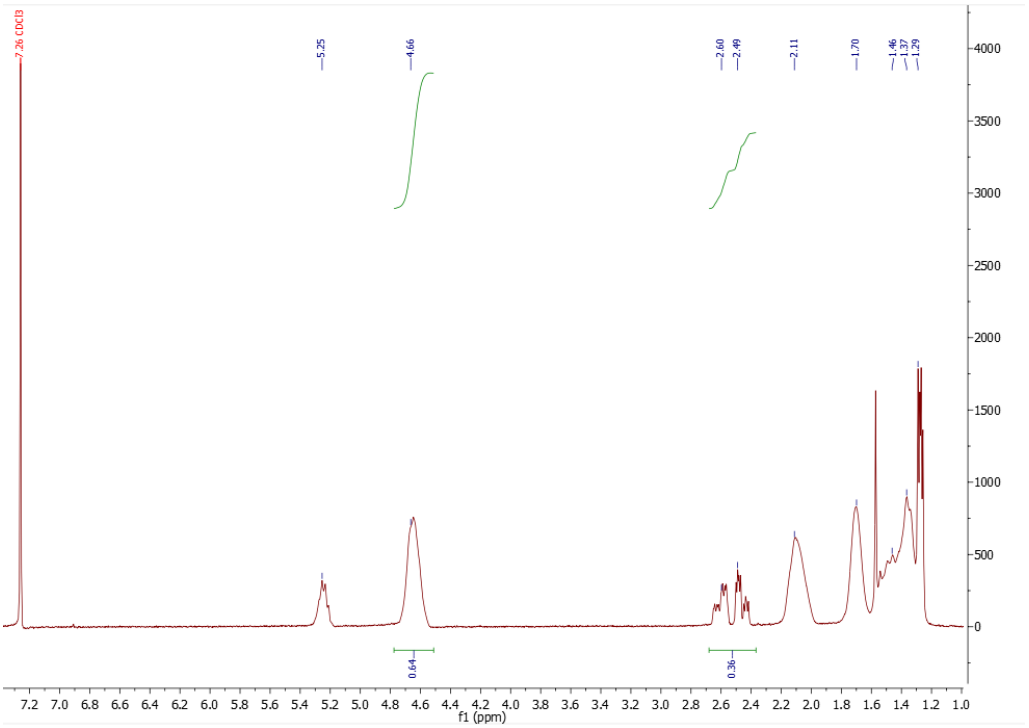

Figure S14. ^{1}H NMR spectrum of terpolymer (Table 1, entry 3).

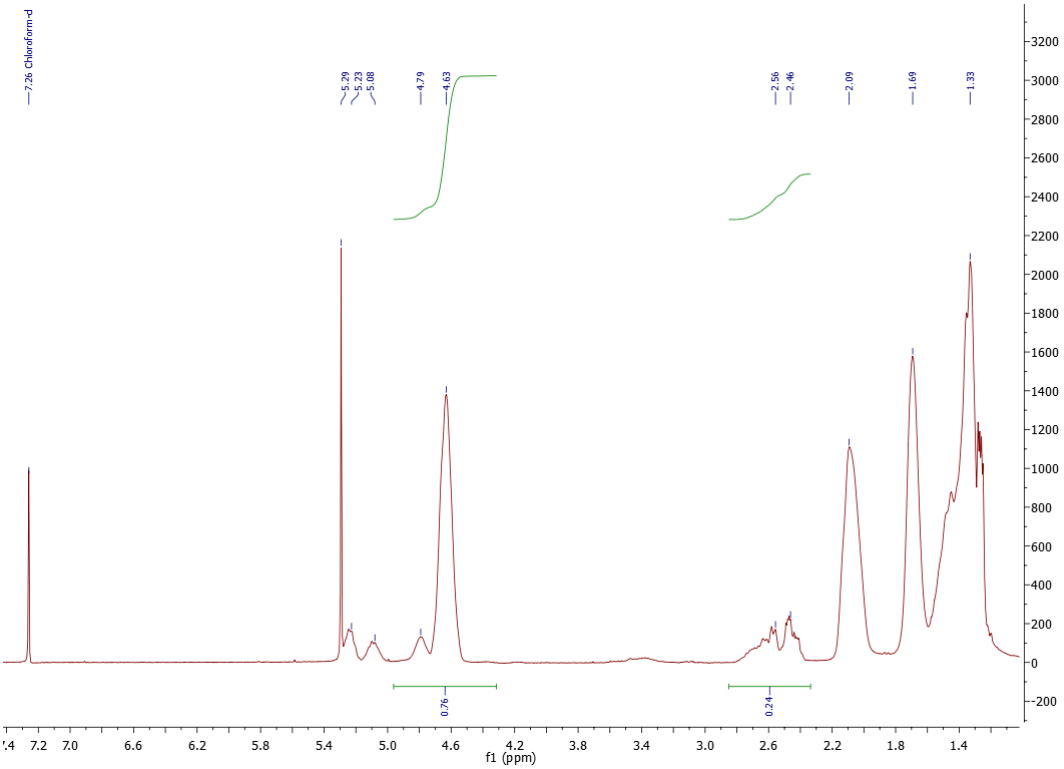

Figure S15. ^{1}H NMR spectrum of terpolymer (Table 1, entry 5).

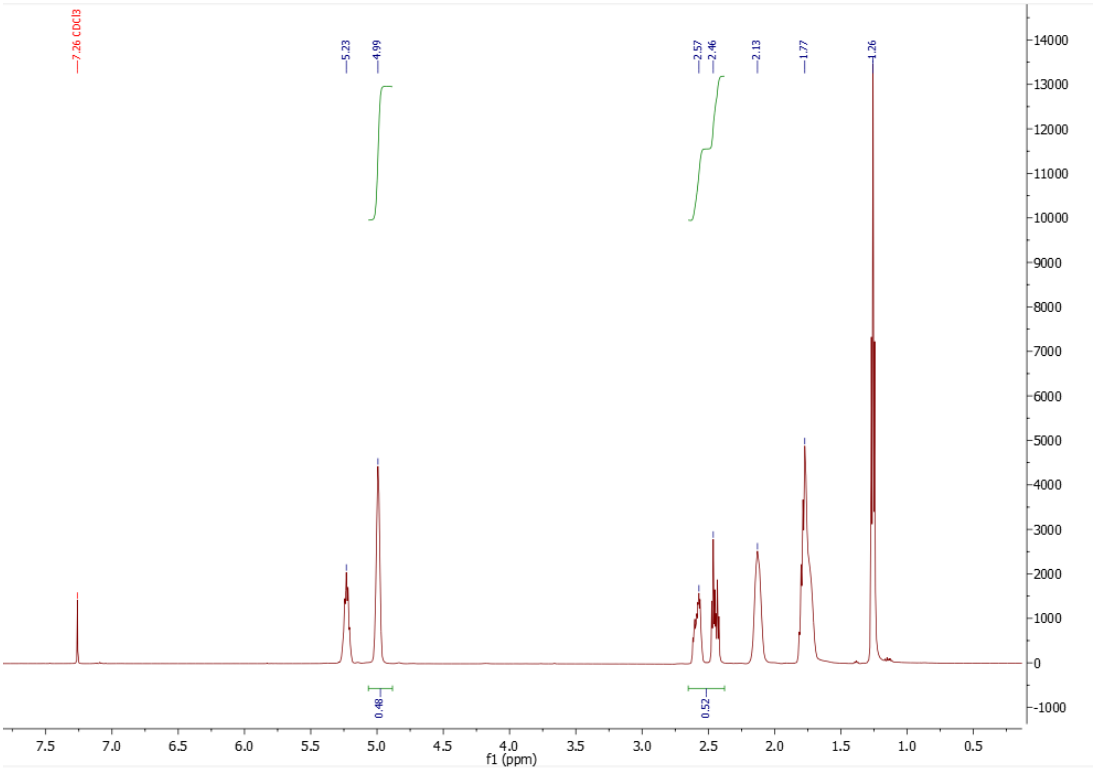

Figure S16. ^{1}H NMR spectrum of terpolymer (Table12, entry 6).

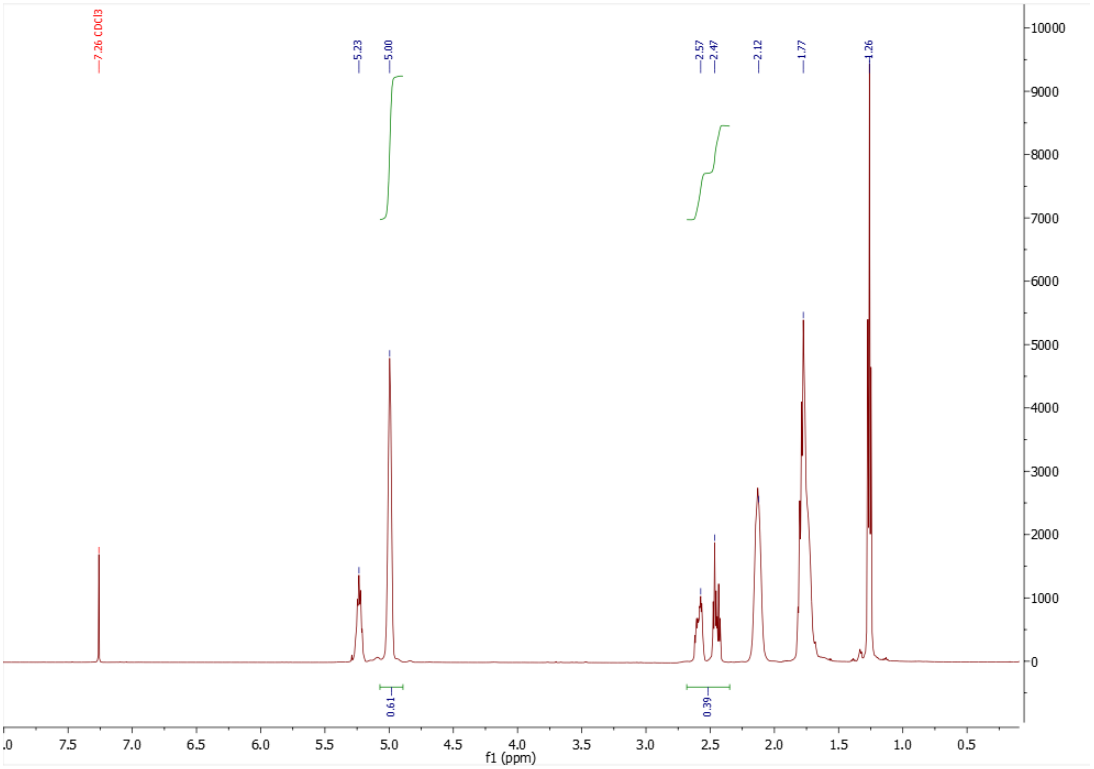

Figure S2. ^{1}H spectrum of terpolymer (Table 1, entry 7).

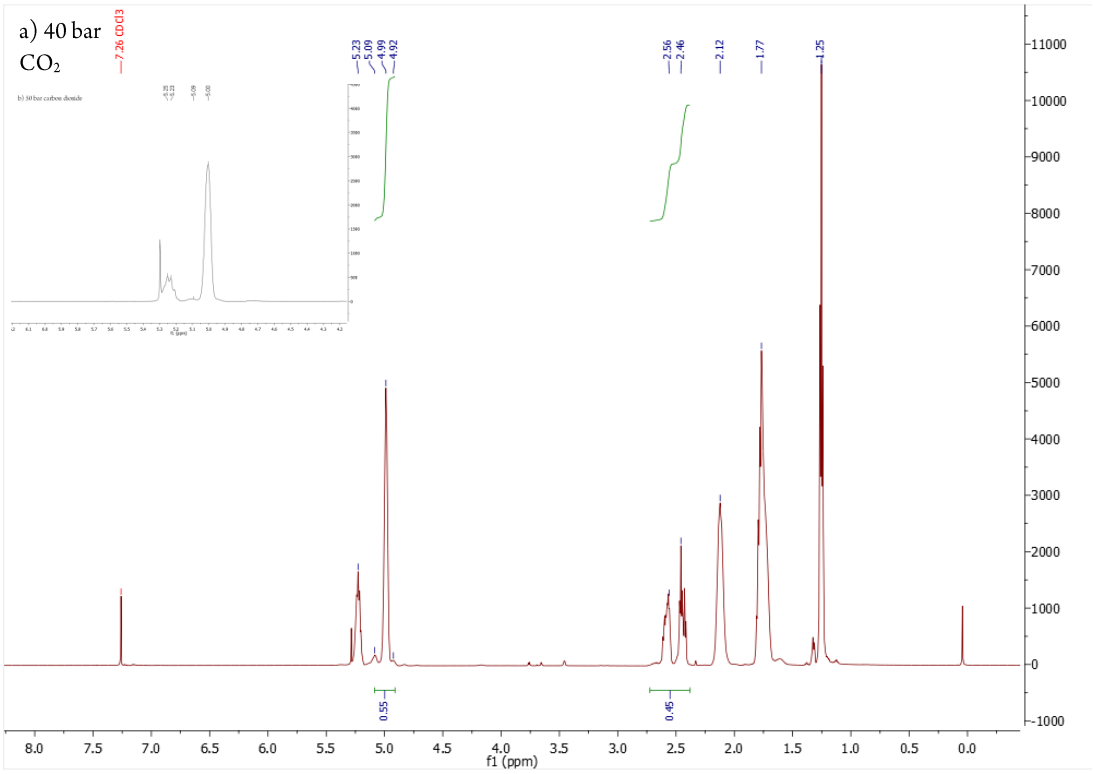

Figure S18a. ^{1}H spectrum of terpolymer (Table 1, entry 8); b. Extract of ^{1}H spectrum of terpolymer (Table S2, entry S8).

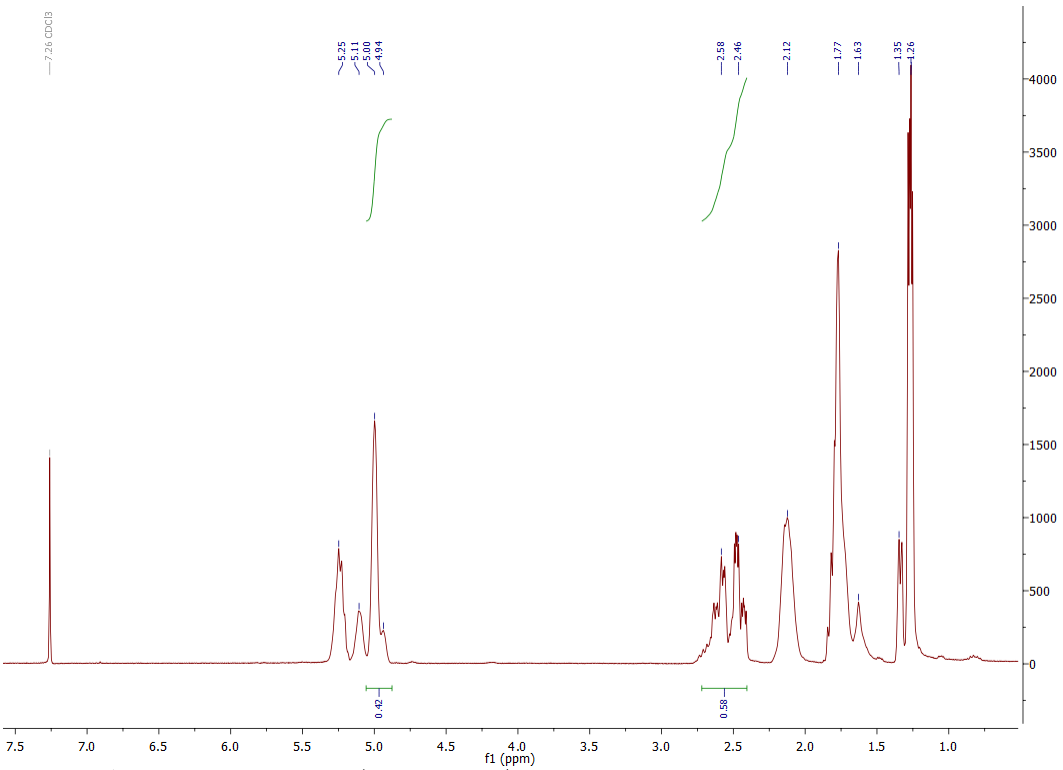

Figure S19. ^{1}H spectrum of terpolymer (Table 1, entry 9)

14. Investigations towards the Block Structures (GPC and ^{1}H NMR data)

Table S4: Terpolymerization of CHO, BBL and CO_2 according pathways A and B.[a]

entry	[epoxide]:[BBL]:[cat]	reaction pathway[a]	CO_2 [bar]	conv. BBL [%][b]	conv. epoxide [%][b]	[PC]:[PHB][c] prior to prec.	[PC]:[PHB][c] after prec.	M_n (PDI) first block (not prec.) [kg/mol][d]	M_n (PDI) terpolymer (not prec.) [kg/mol][d]
S1	500 (CHO):500:1	A1	40	98	81	46:54	75:25	73 (PHB) (1.5)	94 (1.3)
S2	500 (CHO):500:1	B	40	83	74	45:55	63:37	128 (PCHC) (1.1)	169 (1.2)

Reaction conditions: CHO/BBL/CO_2: 60 °C, 2.0 g toluene, 40 µmol catalyst 1. [a]According to Figure 1. [b]Determined by ^{1}H-NMR spectroscopy of a crude polymer sample. [c]Determined by ^{1}H-NMR spectroscopy of a crude polymer sample. [d]Measured *via* GPC in THF against a polystyrene standard.

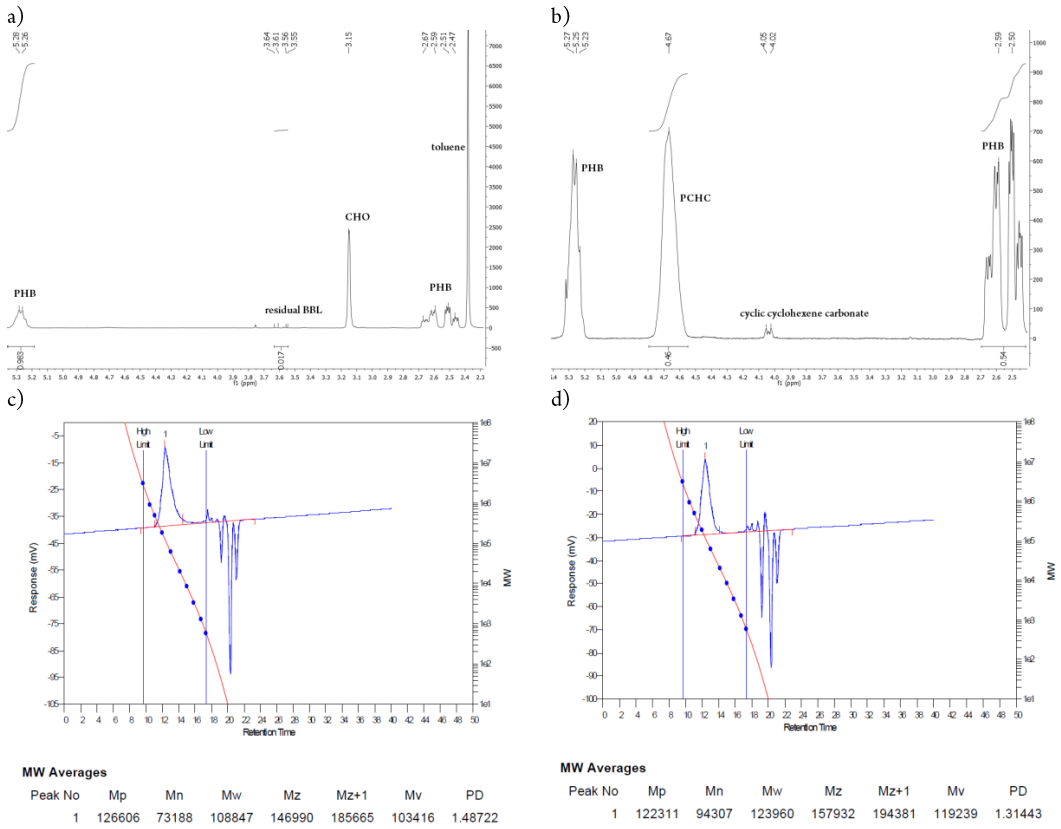

Figure S20: Procedure A1: Table S4, entry S1: a)^{1}H NMR spectrum of the first block (PHB) directly before adding CO_2; b) a) ^{1}H NMR spectrum of the non-precipitated terpolymer; c) GPC of the first block (PHB) d) GPC of the non-precipitated terpolymer.

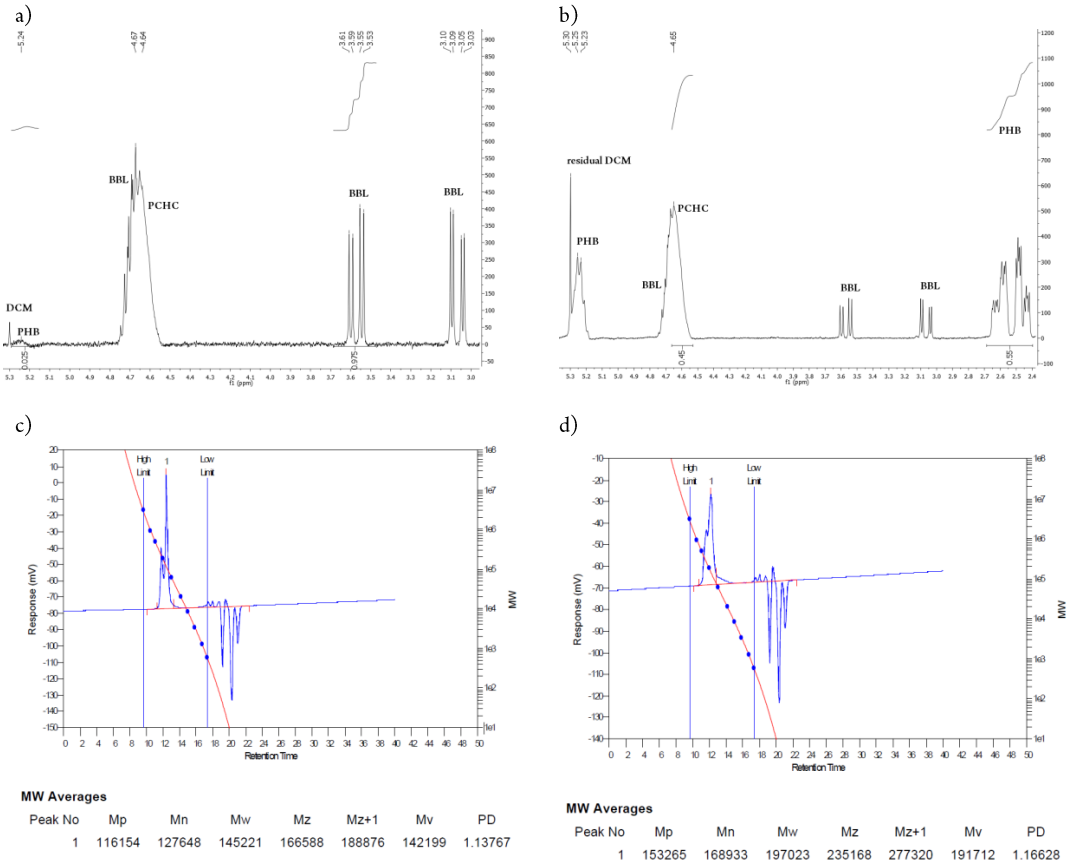

Figure S21: Procedure B: Table S4, entry S2: a)^{1}H NMR spectrum of the first block (PCHC) directly after CO_2 release; b) a) ^{1}H NMR spectrum of the non-precipitated terpolymer; c) GPC of the first block (PCHC) d) GPC of the non-precipitated terpolymer.

Remark to Figure S21a. The CO_2 release takes few minutes, as it has to be done carefully at 60 °C. Therefore, there is enough time for realizing 2% conversion of BBL.

15. Side reactions of the Catalyst with PHB

Table S5. Terpolymerization of BBL, CHO and CO_2 with complex 1.

entry	[epoxide]:[BBL]:[cat]	reaction path-way[a]	CO_2 [bar]	time [h][b]	conv. BBL [%][c]	conv. epoxide [%][c]	[PC]:[PHB][d] prior to prec.	[PC]:[PHB][e] after prec.	T_g [°C][f]	M_n (PDI) [kg/mol][g]
S1	500 (CHO):500 :1	A1	40	2	99	89	47:53	85:15	102	79 (1.6)

Reaction conditions: CHO/BBL/CO_2: 60 °C, 2.0 g toluene, 40 µmol catalyst 1. [a]According to Figure 1. [b]Complete polymerization time followed by *in situ* ATR-IR. [c]Determined by ^{1}H-NMR spectroscopy of a crude polymer sample. [d]Determined by ^{1}H-NMR spectroscopy of a crude polymer sample. [e]Composition of terpolymer after precipitation in MeOH (homopolymeric PHB stays in solution). [f]Determined by DSC, heating rate: 5 K/min. [g]Measured *via* GPC in THF.

Table S6: Reaction of complex 1 and PHB at 60 °C and 1 hour.

[PHB]:[cat]	CO_2 [bar]	M_n (prior treatment with cat) [kg/mol] (PDI)[c]	M_n (after treatment with cat) [kg/mol] (PDI)[c]
40:1[a]	-	160 (1.8)	69 (1.7)
40:1[b]	40	160 (1.8)	91 (1.8)
40:0[a]	-	160 (1.8)	160 (1.8)

Reaction conditions: 100 mg PHB, 60 °C, 1.0 mL toluene. [a]Performed in a pressure flask. [b]Performed in a hand autoclave. [c]Measured via GPC in thf against a polystyrene standard.

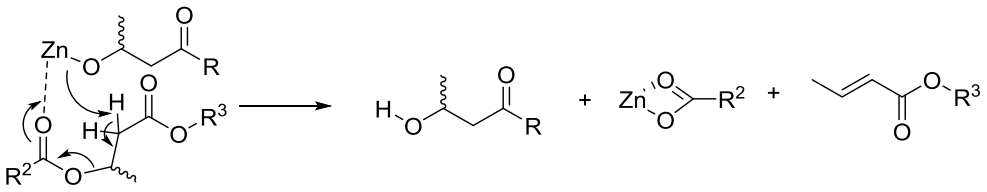

Scheme S1: Possible side reaction, which leads to decreased molecular weights.[3, 4]

[3] Rieth, L. R.; Moore, D. R.; Lobkovsky, E. B.; Coates, G. W. *J. Am. Chem. Soc.* **2002**, *124*, 15239-15248.

[4] Kurcok, P.; Dubois, P.; Jèrôme, R. *Polym. Int.* **1996**, *41*, 479.

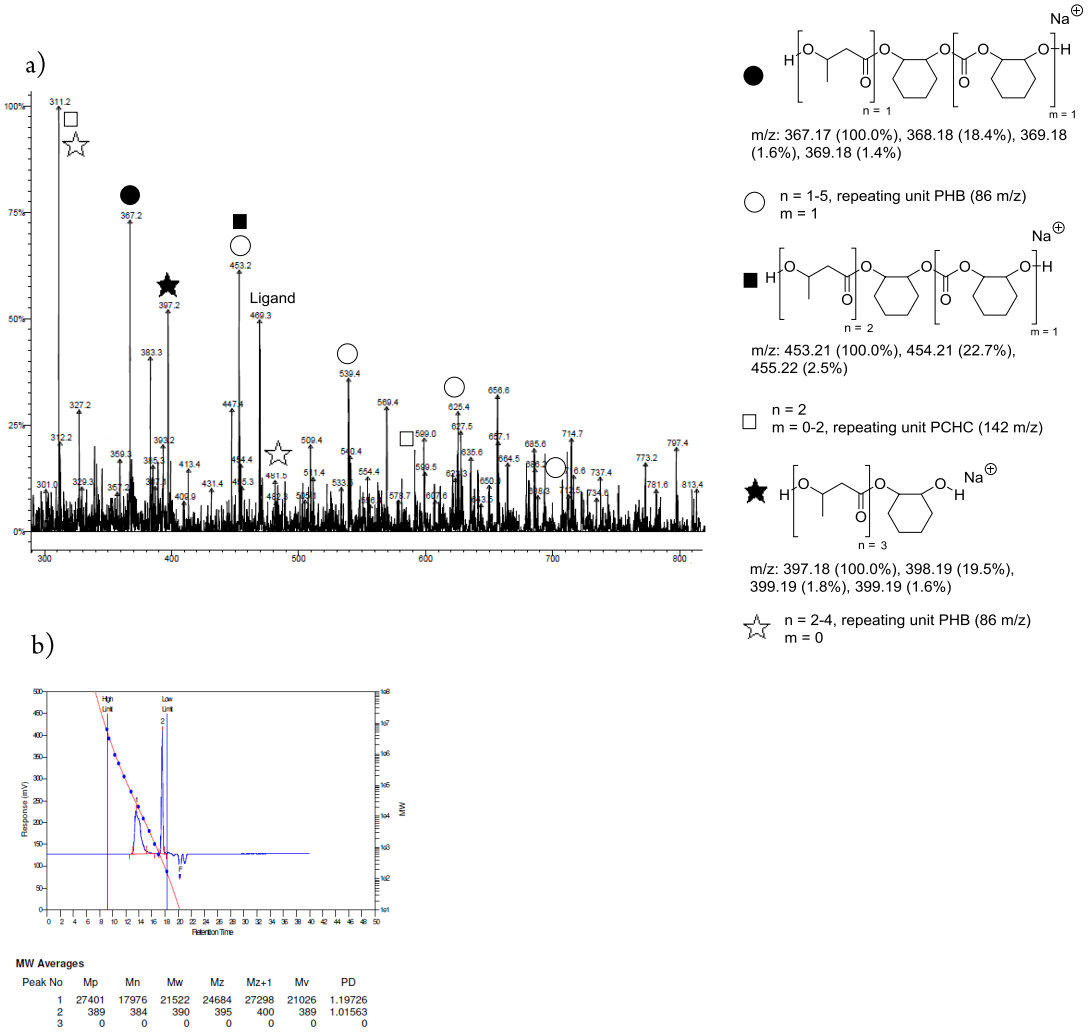

Figure S22. a) ESI-MS in MeCN of an oligomeric PCHC-PHB block terpolymer (reaction conditions: standard autoclave with magnetic stirrer/agitators, catalyst 71.9 µmol, 1.0 eq., CHO 0.36 mmol, 5.0 eq., BBL 0.36 mmol, 5.0 eq., 36 µL toluene, route B: 25 minutes with 40 bar CO_2 at 60 °C, after CO_2 release 60 minutes reaction time, 36:64 / PCHC: PHB, 99% yield, M_n = 18 kg/mol (1.2), M_n = 0.4 kg/mol (1.0)), indicating the presence of low molecular weight diols. b) GPC result for the oligomerization with two peaks at 18 kg/mol and 0.4 kg/mol.

16.2 Supporting Information: Terpolymerization of β-Butyrolactone, Epoxides, and CO_2: Chemoselective CO_2-Switch and its Impact on Kinetics and Material Properties

Terpolymerization of β-Butyrolactone, Epoxides, and CO_2: Chemoselective CO_2-Switch and its Impact on Kinetics and Material Properties

Sebastian Kernbichl[‡], *Marina Reiter*[‡], *Josef Mock*[§], *Bernhard Rieger*[*, ‡]

[‡]WACKER-Chair of Macromolecular Chemistry, Catalysis Research Center, Technical University Munich, Lichtenbergstr. 4, 85748 Garching, Germany

[§]Chair of Nanoelectronics, Technical University Munich, Theresienstraße 90, 80333 Munich, Germany

1. Polymerization Procedure

Copolymerization of epoxide and CO_2. In case no BBL was added, 40 bar CO_2 were added in the beginning and the reaction was quenched after full conversion to the polycarbonate.

Block pathway. Epoxide, BBL, complex **1** and toluene were added to the autoclave at the respective temperature. After a conversion of BBL of ca. 80%, 40 bar CO_2 were applied enabling the copolymerization to start. The polymerization was quenched after almost full conversion to the polycarbonate.

In case of limonene oxide, the reverse block order was also tested. Epoxide, BBL, complex **1** and toluene were added to the autoclave at the respective temperature. 40 bar CO_2 are applied in the beginning. After a certain conversion to PLC, CO_2 was released slowly to let the ROP of BBL start. The polymerization was quenched after the indicated time.

Statistical pathway. Epoxide, BBL, complex **1** and toluene were added to the autoclave at the respective temperature. 3 bar CO_2 (in case of LO 9 bar) were applied immediately. The polymerization was quenched after the desired conversion.

CHO/CO_2/BBL. Polymerizations ran at 60 °C.

CPO/CO_2/BBL. Polymerizations ran at 50 °C.

LO/CO_2/BBL. ROP of BBL ran at 60 °C. Due to the ceiling temperature of PLC, copolymerization of LO and CO_2 was performed at 40 °C. The statistical terpolymerization at 9 bar CO_2 was done at 40 °C.

2. Kinetic investigation of the copolymerization of CHO and CO_2

2.1 Order in CO_2

Table S1. Summary of the in-situ IR experiment with varying CO_2 pressure

m (CHO) [g]	n (CHO) [mmol]	Total volume [mL]	CO_2 pressure	ln (CO_2 pressure)	k_{obs} [a.u.s-1][a]	ln k_{obs}
1.96	20.0	6.31	2	0.6931	0.00028	-8.18
1.96	20.0	6.31	3	1.0986	0.00040	-7.82
1.96	20.0	6.31	5	1.6094	0.00072	-7.23
1.96	20.0	6.31	10	2.3025	0.00082	-7.11
1.96	20.0	6.31	14	2.6390	0.00082	-7.11
1.96	20.0	6.31	20	2.9957	0.00083	-7.10
1.96	20.0	6.31	30	3.4011	0.00088	-7.03
1.96	20.0	6.31	40	3.6887	0.00086	-7.06

[a] k_{obs} is defined as the biggest slope of the respective curve

2.2 Order in CHO

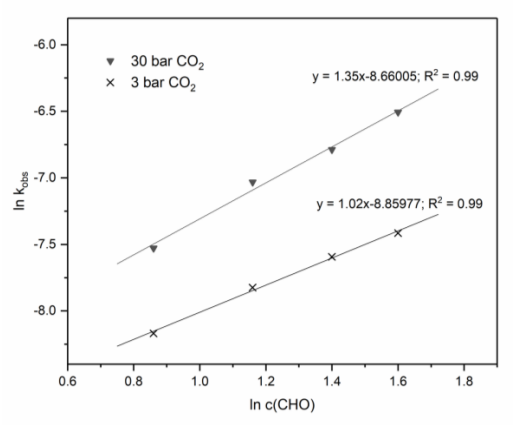

Figure S1. Determination of CHO order in CHO/CO_2 copolymerization. Plot of ln k_{obs} vs ln c(CHO) for 3 bar and 30 bar CO_2 under the conditions shown in Table S2.

Table S2. Summary of the in-situ IR experiment with varying CHO concentration at 3 bar and 30 bar CO_2

m (CHO) [g]	n (CHO) [mmol]	Total volume [mL]	[CHO]/[M]	CO_2 pressure	ln c(CHO)	k_{obs} [a.u.s-1][a]	ln k_{obs}
1.46	14.9	6.31	2.36	3	0.8587	0.00028	-8.17
1.96	20.0	6.31	3.20	3	1.1631	0.00040	-7.82
2.46	25.1	6.31	4.06	3	1.4011	0.00050	-7.59
2.96	30.2	6.31	4.95	3	1.5994	0.00060	-7.41
1.46	14.9	6.31	2.36	30	0.8587	0.00053	-7.53
1.96	20.0	6.31	3.20	30	1.1631	0.00088	-7.03
2.46	25.1	6.31	4.06	30	1.4011	0.00113	-6.79
2.96	30.2	6.31	4.95	30	1.5994	0.00149	-6.51

[a] k_{obs} is defined as the biggest slope of the respective curve

2.3 Order in catalyst

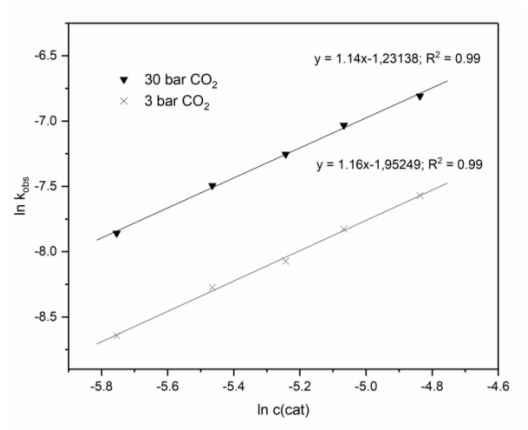

Figure S2. Determination of catalyst order in CHO/CO_2 copolymerization. Plot of ln k_{obs} vs ln c(cat) for 3 bar and 30 bar CO_2 under the conditions shown in Table S3.

Table S3. Summary of the in-situ IR experiment with varying catalyst concentration at 3 bar and 30 bar CO_2

m (CHO) [g]	Total volume [mL]	n (Zn) / [mmol]	[Zn] / [M]	CO_2 pressure	ln c(Zn)	k_{obs} [a.u.s-1][a]	ln k_{obs}
1.96	6.31	0.0500	0.0079	3	-4.84	0.00051	-7.58
1.96	6.31	0.0399	0.0063	3	-5.07	0.00040	-7.82
1.96	6.31	0.0333	0.0052	3	-5.26	0.00031	-8.08
1.96	6.31	0.0267	0.0042	3	-5.47	0.00026	-8.25
1.96	6.31	0.0200	0.0032	3	-5.74	0.00018	-7.58
1.96	6.31	0.0500	0.0079	30	-4.84	0.00110	-6.81
1.96	6.31	0.0399	0.0063	30	-5.07	0.00088	-7.04
1.96	6.31	0.0333	0.0052	30	-5.26	0.00071	-7.25
1.96	6.31	0.0267	0.0042	30	-5.47	0.00056	-7.49
1.96	6.31	0.0200	0.0032	30	-5.74	0.00039	-7.85

[a]k_{obs} is defined as the biggest slope of the respective curve

3. DSC analysis of PCHC/PCPC-containing terpolymers

Table 1, entry 1

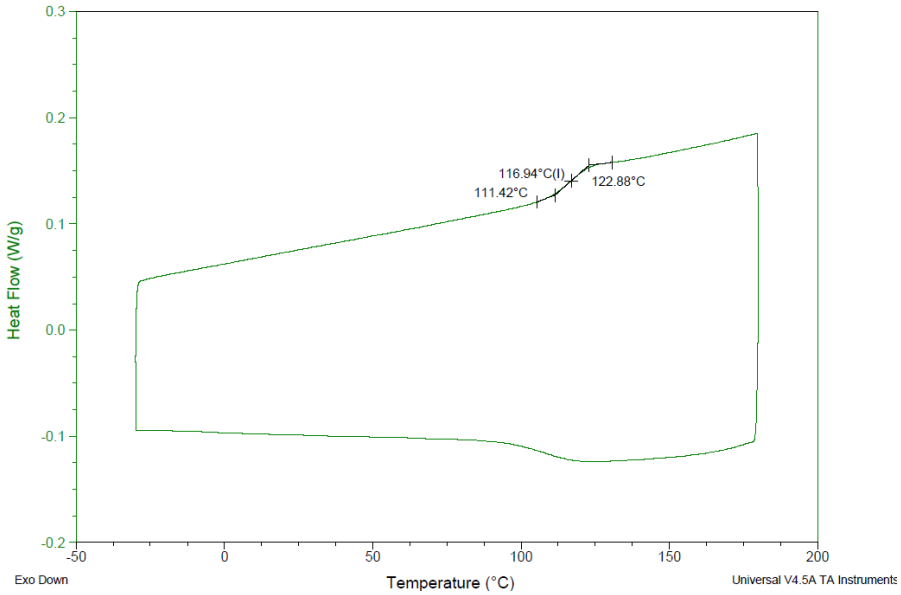

Table 1, entry 2

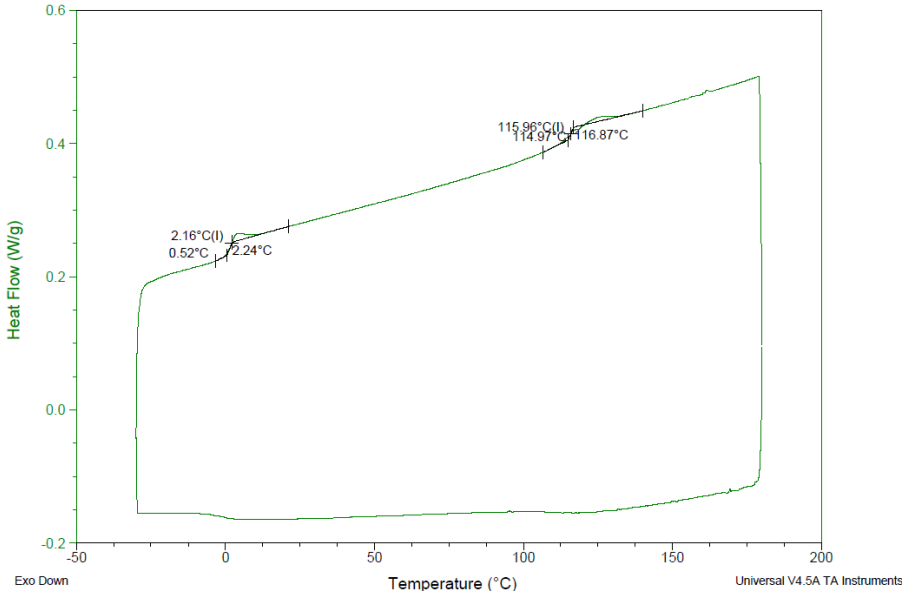

6

Table 1, entry 3

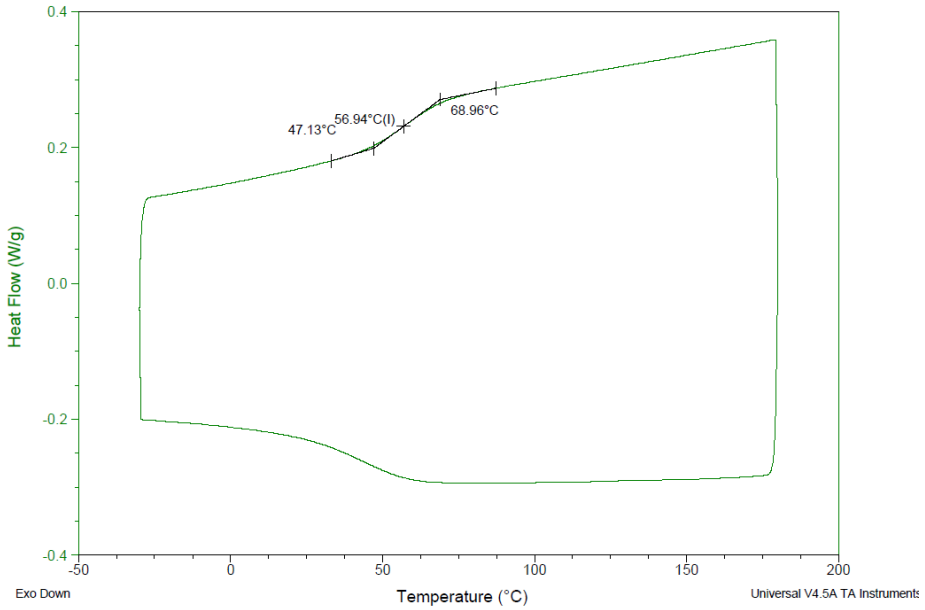

Table 1, entry 8

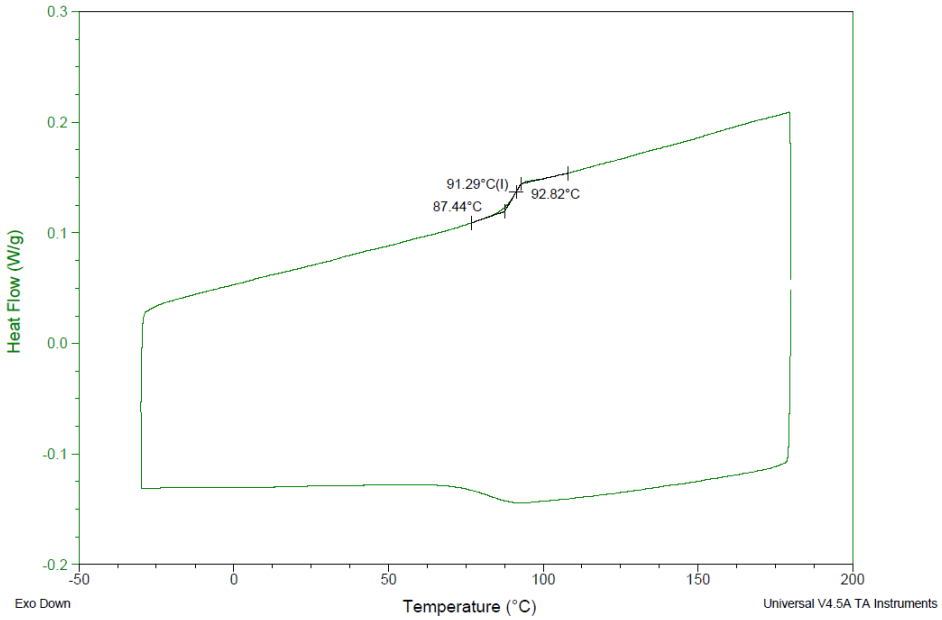

7

Table 1, entry 11

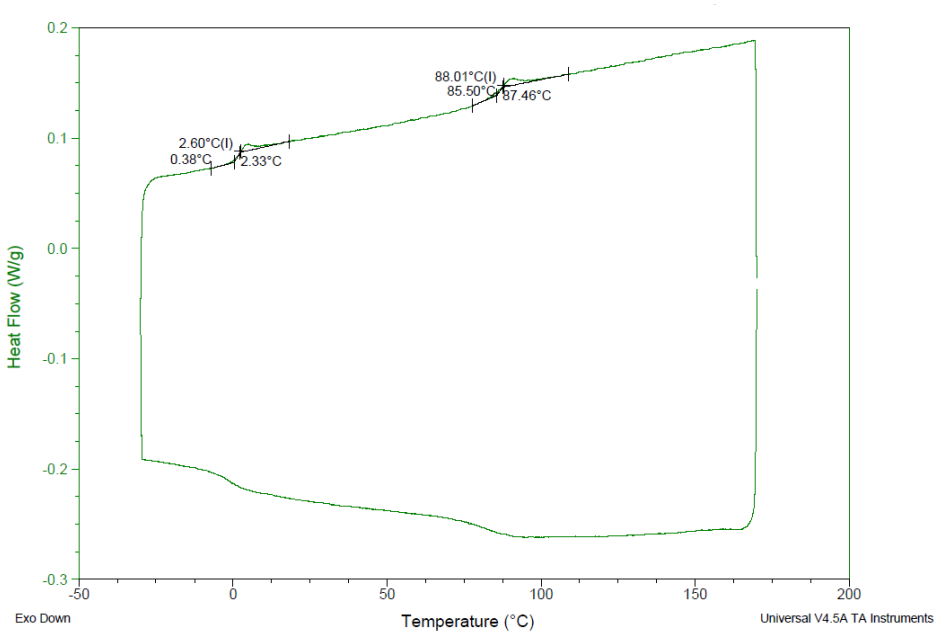

Table 1, entry 12

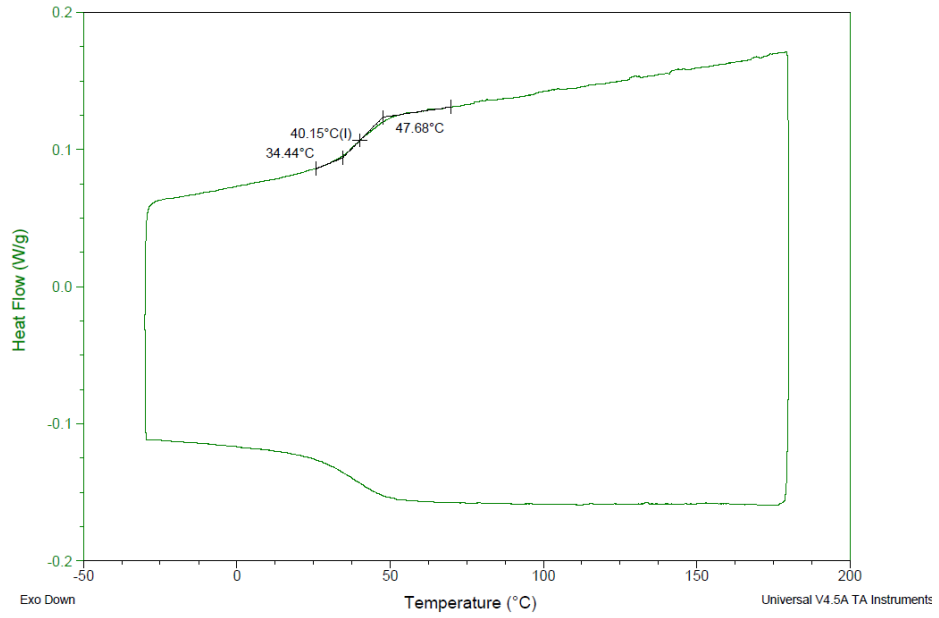

Figure S3. DSC curves (heating rate 5 K/min) for different terpolymers.

8

4. GPC traces of PCHC/PCPC-containing terpolymers

Table 1, entry 1

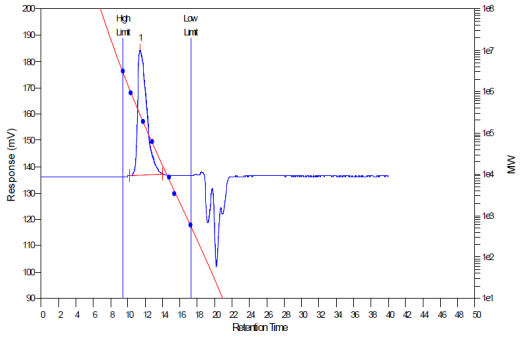

MW Averages

Peak No	Mp	Mn	Mw	Mz	Mz+1	Mv	PD
1	284523	149142	219643	280139	331517	210270	1.47271

Table 1, entry 2

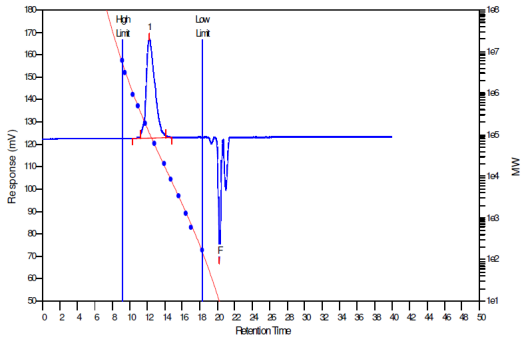

MW Averages

Peak No	Mp	Mn	Mw	Mz	Mz+1	Mv	PD
1	113485	75809	100599	127336	156291	96854	1.32701

Table 1, entry 3

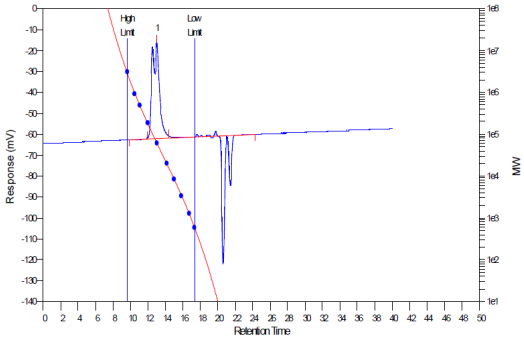

MW Averages

Peak No	Mp	Mn	Mw	Mz	Mz+1	Mv	PD
1	61030	63680	76227	88080	98340	74398	1.19703

Table 1, entry 4

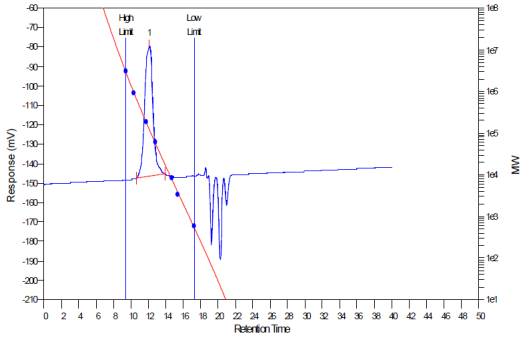

MW Averages

Peak No	Mp	Mn	Mw	Mz	Mz+1	Mv	PD
1	124701	115338	149648	188712	234287	144348	1.29747

Table 1, entry 5

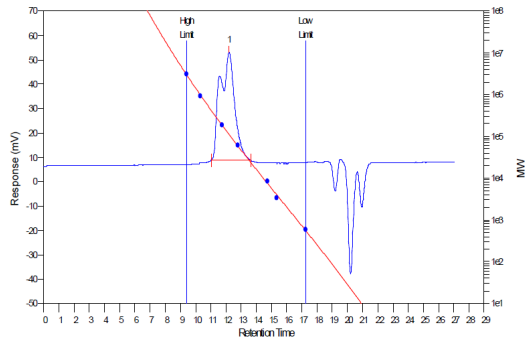

MW Averages

Peak No	Mp	Mn	Mw	Mz	Mz+1	Mv	PD
1	111638	111494	143154	175893	204970	138335	1.28396

Table 1, entry 6

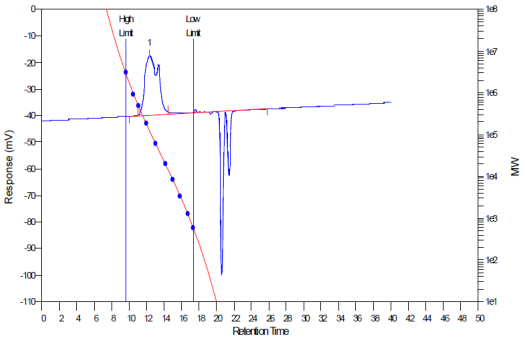

MW Averages

Peak No	Mp	Mn	Mw	Mz	Mz+1	Mv	PD
1	128813	72976	113031	161572	208539	106348	1.54888

Table 1, entry 7

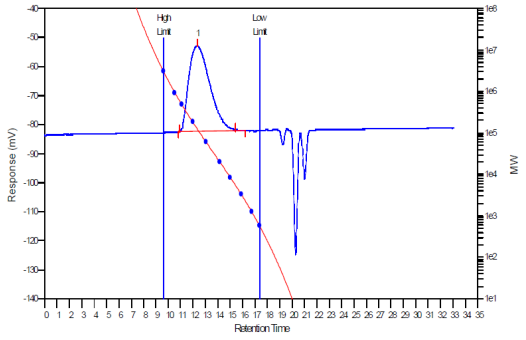

MW Averages

Peak No	Mp	Mn	Mw	Mz	Mz+1	Mv	PD
1	124439	63145	119997	180829	234153	111350	1.90034

Table 1, entry 8

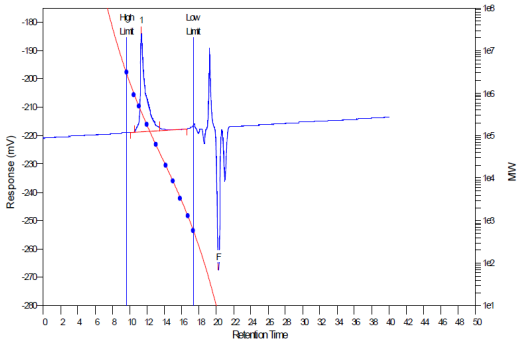

MW Averages

Peak No	Mp	Mn	Mw	Mz	Mz+1	Mv	PD
1	363846	202302	276202	334938	382285	266618	1.3653

Table 1, entry 9

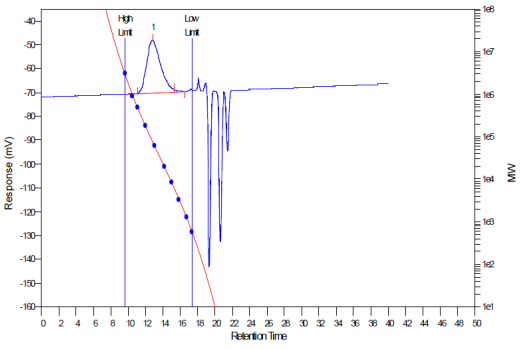

MW Averages

Peak No	Mp	Mn	Mw	Mz	Mz+1	Mv	PD
1	79855	45305	82011	127810	177016	75994	1.8102

Table 1, entry 10

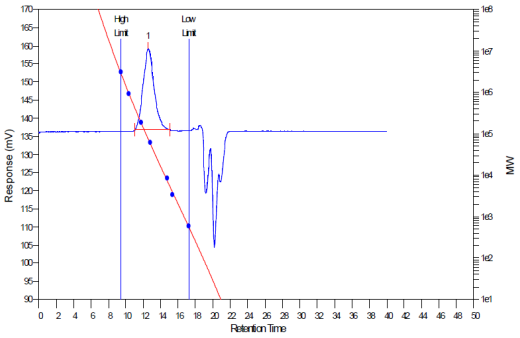

MW Averages

Peak No	Mp	Mn	Mw	Mz	Mz+1	Mv	PD
1	76026	53466	85265	123315	164025	80201	1.59475

Table 1, entry 11

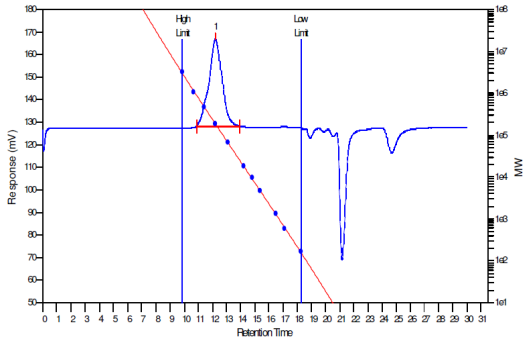

MW Averages

Peak No	Mp	Mn	Mw	Mz	Mz+1	Mv	PD
1	188127	157714	213054	282629	362531	203924	1.35089

Table, entry 12

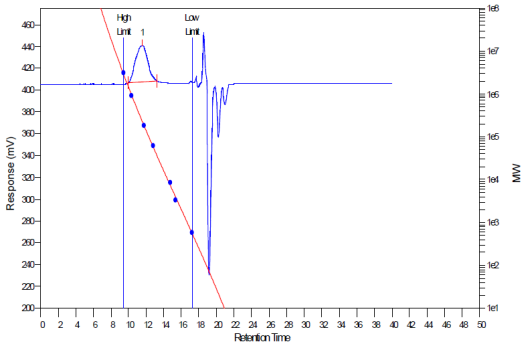

MW Averages

Peak No	Mp	Mn	Mw	Mz	Mz+1	Mv	PD
1	239860	203323	319410	473091	632563	299377	1.57095

Figure S4. GPC traces of terpolymers with different compositions measured in THF relative to polystyrene.

5. Terpolymerizations with different [epoxide]:[BBL] ratios

Table S4. Terpolymerizations with CHO/CPO, CO_2 and BBL according to the statistical pathway[a]

entry	[epoxide]:[BBL]:[cat]	time [h]	conv. epoxide[b] [%]	conv. BBL[b] [%]	[PC]:[PHB][c]	T_g [°C][d]	M_n ($Đ$) [kg/mol][e]
1	350 (CHO):650:1	1.0	59	52	38:62	44	70 (1.16)
2	500 (CHO):500:1	0.2	32	39	45:55	57	64 (1.20)
3	650 (CHO):350:1	0.2	31	36	66:34	73	80 (1.21)
4	350 (CPO):650:1	1.2	27	25	37:63	24	89 (1.42)
5	500 (CPO):500:1	1.2	45	52	65:35	55	53 (1.59)
6	650 (CPO):350:1	0.8	35	28	79:21	62	91 (1.40)

[a]Polymerizations were quenched at low conversions to show that the two catalytic cycles run with comparable rates. [b]Conversions were determined by ^{1}H NMR spectroscopy of a crude polymer sample. [c]Determined via ^{1}H NMR of the precipitated polymer. [d]Determined by DSC, heating rate of 5 K/min. [e]Measured via GPC in THF relative to polystyrene.

6. Investigation towards the block structure via GPC

Table S5. Terpolymerization of BBL, LO and CO_2[a]

entry	[epoxide]:[BBL]:[cat]	time [h]	conv. epoxide[b] [%]	conv. BBL[b] [%]	[PC]:[PHB][c]	T_g [°C][d]	M_n ($Đ$) [kg/mol][e]
S1	250 (LO):250:1	7	60	59	50:50	n.d.	201 (1.29)

[a]Polymerizations were conducted according to block pathway A with BBL in the beginning. [b]Conversions were determined by ^{1}H NMR spectroscopy of a crude polymer sample. [c]Determined via ^{1}H NMR of the precipitated polymer. [d]Determined by DSC with a heating rate of 5 K/min. [e]Measured via GPC in $CHCl_3$ relative to polystyrene.

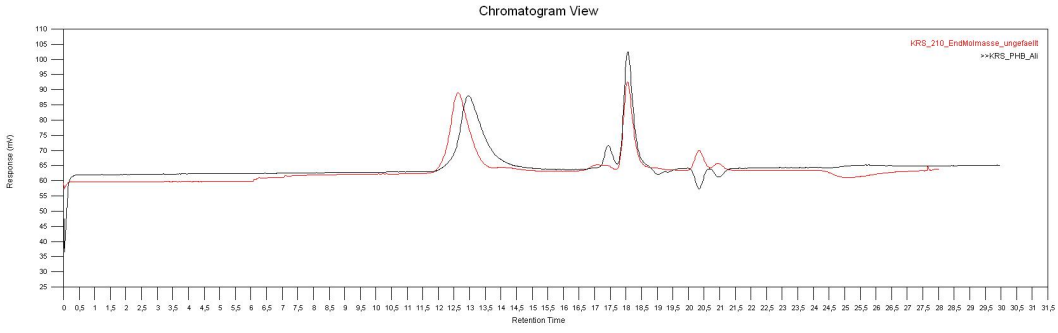

Figure S5. GPC analysis of the first block, PHB, (black line) and of the terpolymer with PLC (red line). GPC measured in $CHCl_3$ relative to polystyrene.

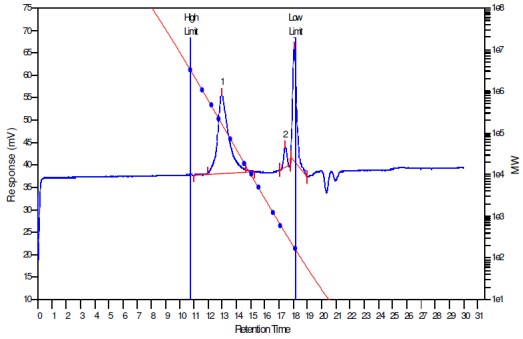

MW Averages

Peak No	Mp	Mn	Mw	Mz	Mz+1	Mv	PD
1	163548	104159	153602	204295	259694	146499	1.47469

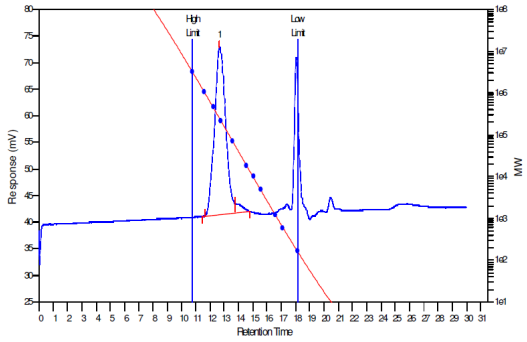

MW Averages

Peak No	Mp	Mn	Mw	Mz	Mz+1	Mv	PD
1	246415	201255	259932	328287	401840	250546	1.29156

Figure S6. GPC traces of the PHB/PLC terpolymer. PHB aliquot GPC (left) and final molecular weight after PLC incorporation (right).

7. DSC analysis of PLC-containing terpolymers

Table 3, entry 2

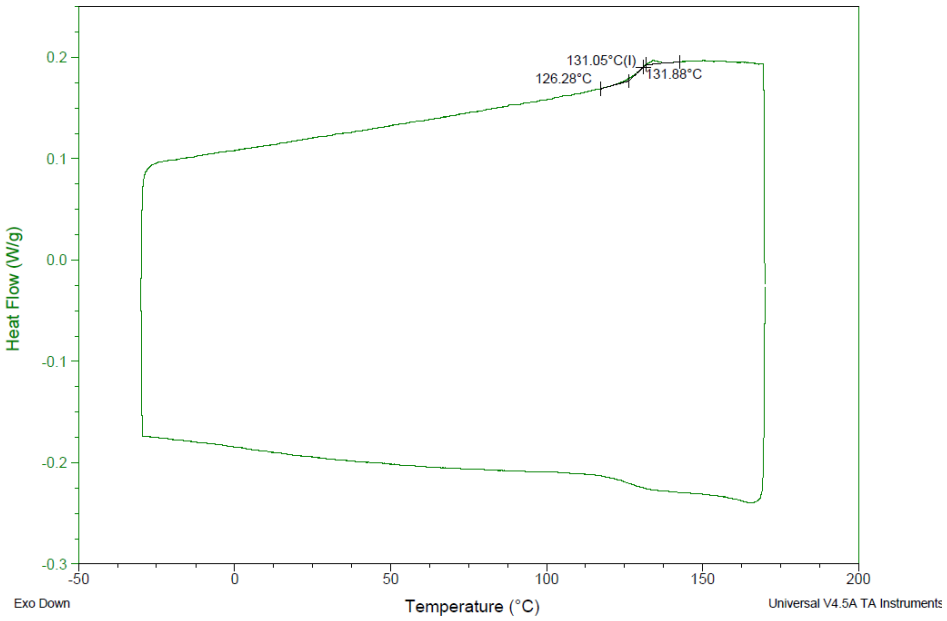

Table 3, entry 4

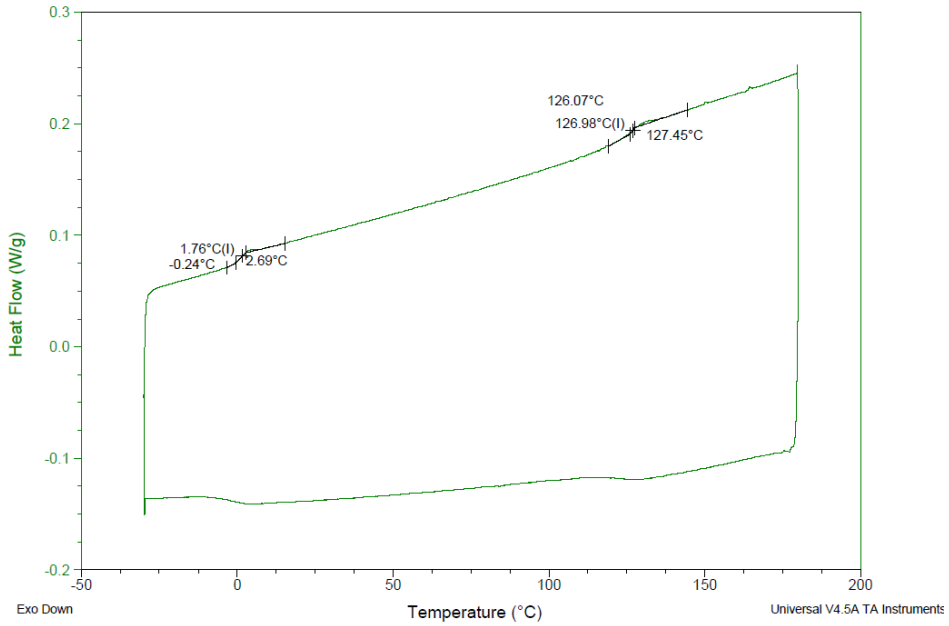

15

Table 3, entry 6

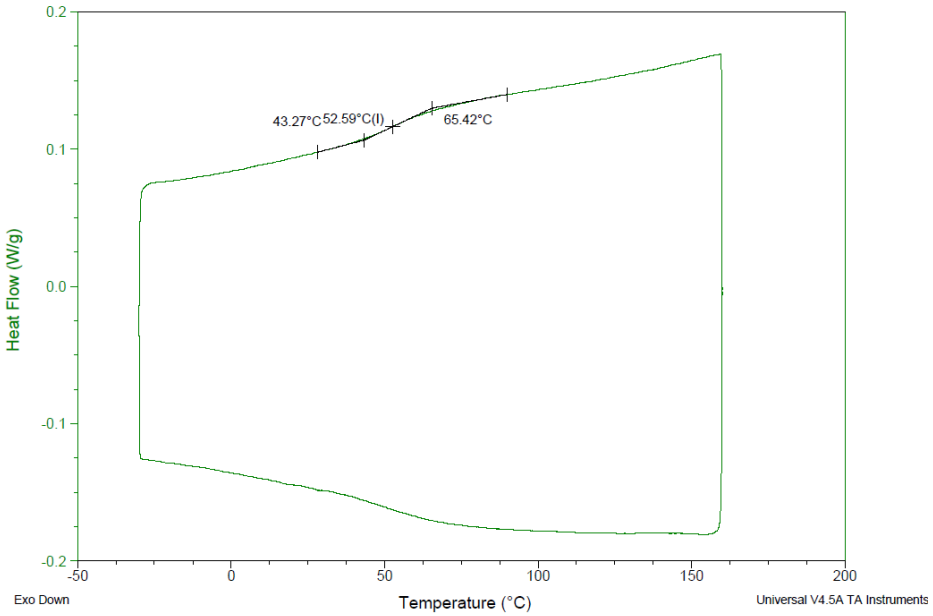

Figure S7. DSC curves of different PLC-containing co-and terpolymers (heating rate 5 K/min).

8. GPC traces of PLC-containing terpolymers

Table 3, entry 1

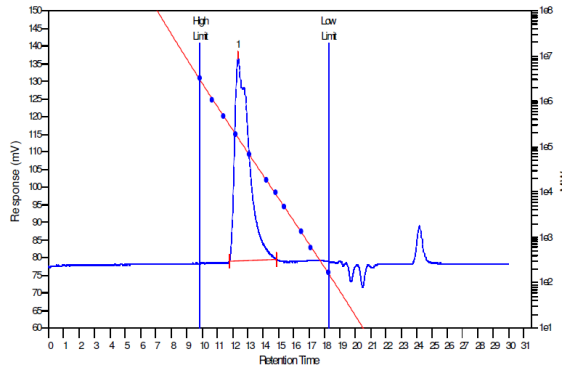

MW Averages

Peak No	Mp	Mn	Mw	Mz	Mz+1	Mv	PD
1	157836	80425	114490	141357	161763	110157	1.42356

Table 3, entry 2

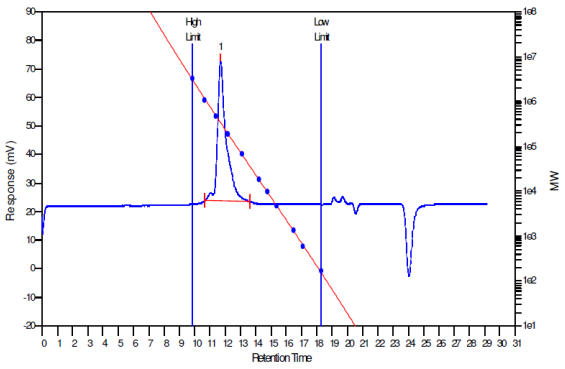

MW Averages

Peak No	Mp	Mn	Mw	Mz	Mz+1	Mv	PD
1	338484	244261	303833	360963	427793	295633	1.24389

Table 3, entry 4

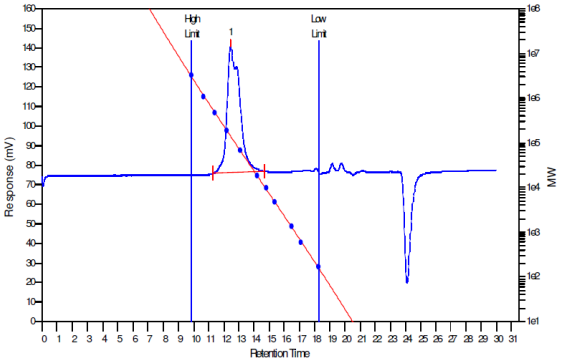

MW Averages

Peak No	Mp	Mn	Mw	Mz	Mz+1	Mv	PD
1	140424	90498	117341	145332	177674	113430	1.29661

Table 3, entry 5

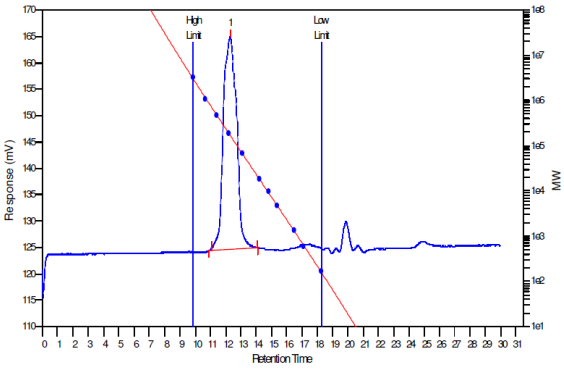

MW Averages

Peak No	Mp	Mn	Mw	Mz	Mz+1	Mv	PD
1	174000	149984	184701	223530	268233	179345	1.23147

Table 3, entry 6

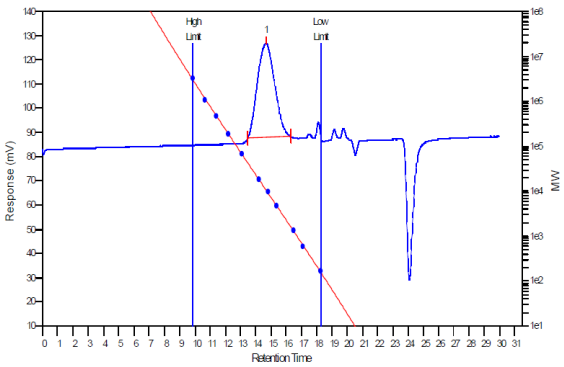

MW Averages

Peak No	Mp	Mn	Mw	Mz	Mz+1	Mv	PD
1	10720	8615	11955	15691	19323	11429	1.3877

Table 3, entry 7

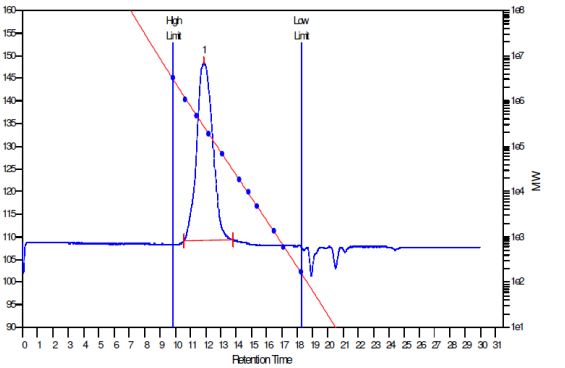

MW Averages

Peak No	Mp	Mn	Mw	Mz	Mz+1	Mv	PD
1	267496	210901	289059	384301	492283	276392	1.37059

Table 3, entry 8

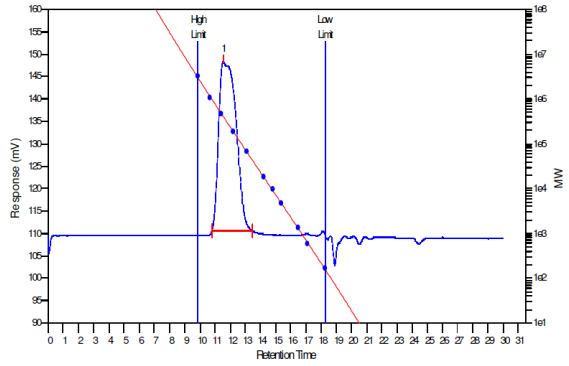

MW Averages

Peak No	Mp	Mn	Mw	Mz	Mz+1	Mv	PD
1	403999	233355	313108	396373	470643	300905	1.34177

Figure S8. GPC traces of PLC containing terpolymers measured in $CHCl_3$ relative to polystyrene.

9. Mechanical properties of different CPO containing co- and terpolymers

Table S6. Mechanical properties of PCPC containing co-and terpolymers measured with hot-pressed specimens with dog-bone shape at a stress-strain machine

entry	structure	[PCHC]: [PHB]	M_n ($Đ$) [kg/mol][d]	Young modulus [MPa]	tensile strength [MPa]	elongation at break [%]
1	-	100:0	202 (1.37)	3000 (±100)	42 (±5)	2 (±0.3)
2	block, low MW	55:45	45 (1.81)	1250 (±200)	14 (±3)	1.1 (±0.3)
3	block, high MW	60:40	158 (1.35)	1500 (±100)	34 (±2)	5 (±0.2)
4	stat., high MW	46:54	203 (1.28)	2040 (±40)	22 (±3)	1.2 (±0.2)

10. NMR spectra of PLC containing terpolymer in block structure (Table 3, entry 7)

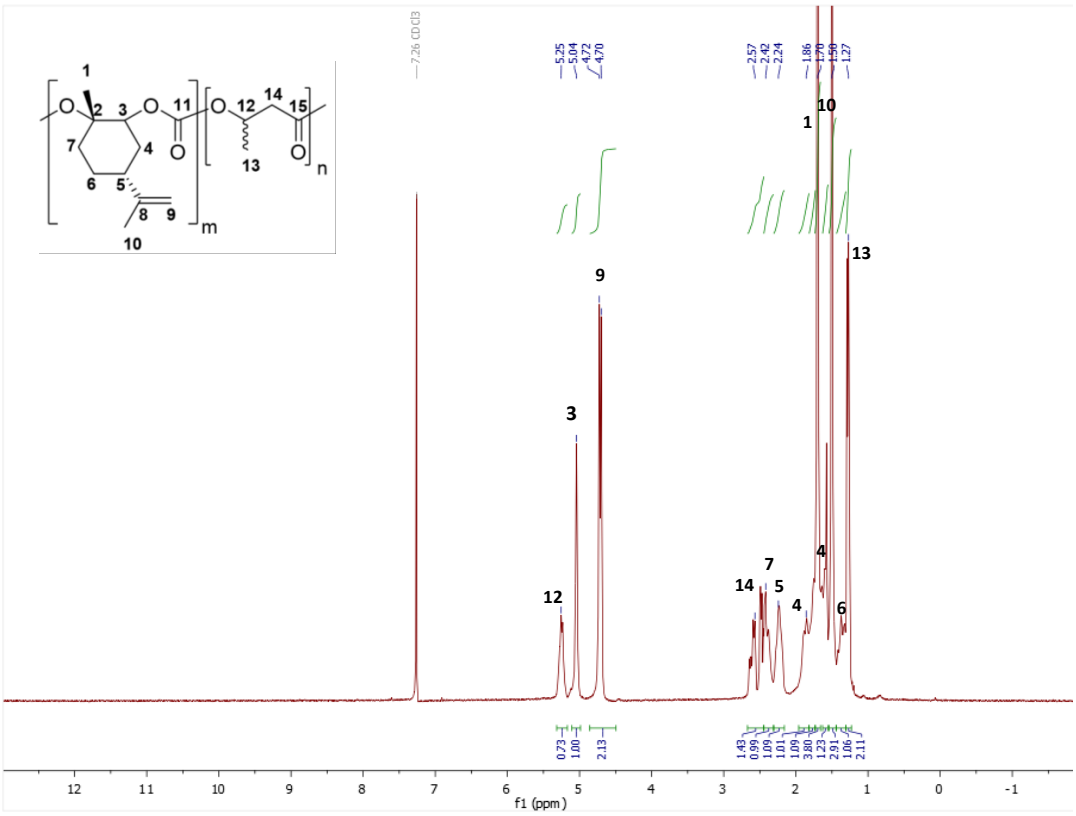

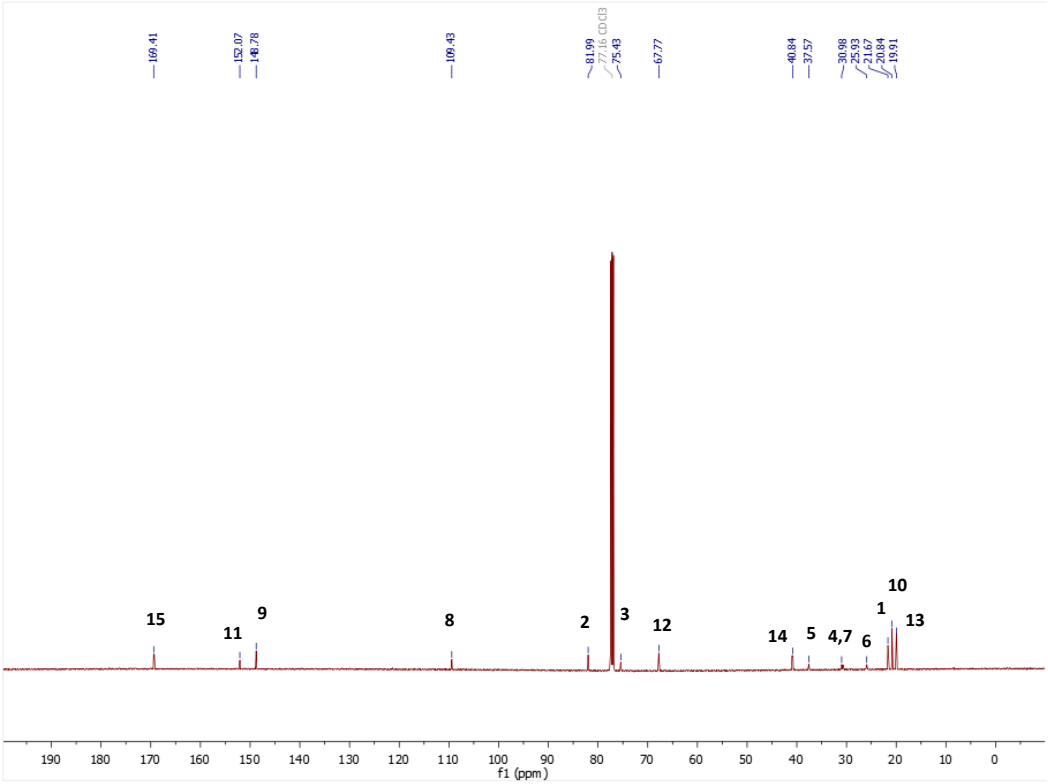

20

11. NMR spectra of PLC containing terpolymer in statistical structure (Table 3, entry 6)

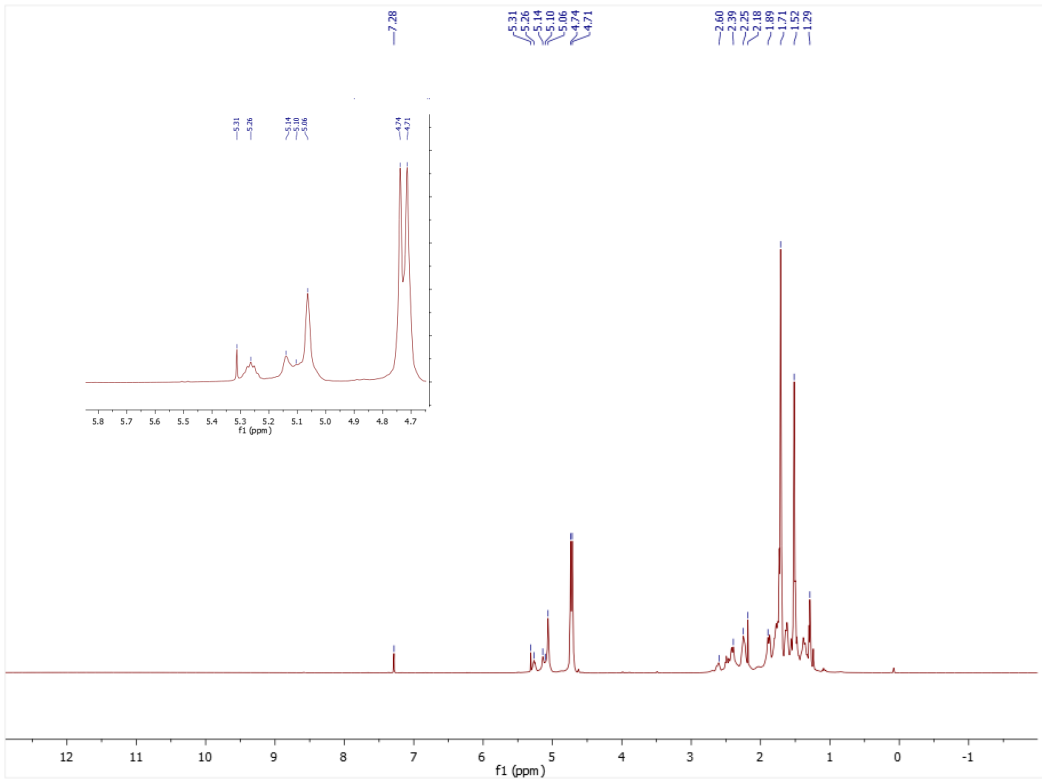

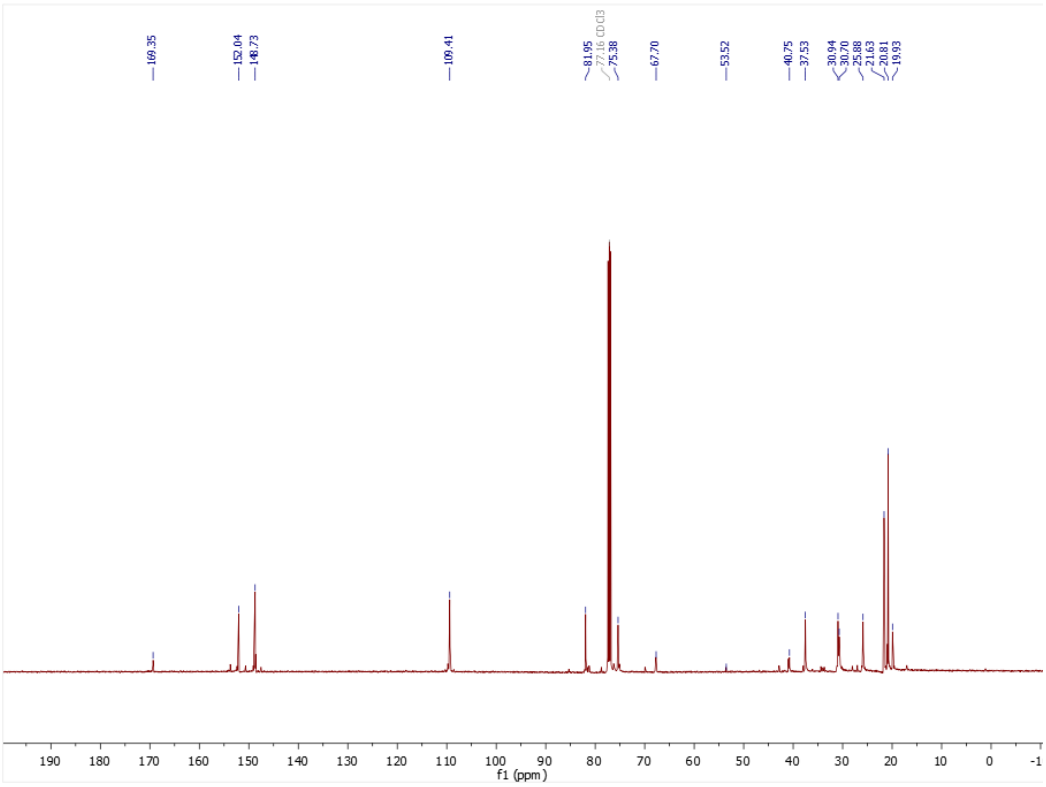

16.3 Supporting Information: A Heteronuclear, Monomer-Selective Zn/Y Catalyst Combines Copolymerization of Epoxides and CO_2 with Group Transfer Polymerization of Michael-type Monomers

A Heteronuclear, Monomer-Selective Zn/Y Catalyst Combines Copolymerization of Epoxides and CO_2 with Group-Transfer Polymerization of Michael-type Monomers

*Alina Denk,[‡] Sebastian Kernbichl,[‡] Andreas Schaffer, Moritz Kränzlein, Thomas Pehl, and Bernhard Rieger**

WACKER-Chair of Macromolecular Chemistry, Catalysis Research Center, Technical University Munich, Lichtenbergstr. 4, 85748 Garching, Germany

Content

1. Synthesis procedures

General

All reactions containing air- and/or moisture sensitive compounds were carried out under dry argon 4.6 (99.996%, *Westfalen AG*) using standard Schlenk or glovebox techniques. Toluene was dried with a solvent purification system (SPS) MB SPS-800 of the company *M. Braun* and stored over molecular sieve under argon atmosphere. Commercially available chemicals were purchased from *Sigma-Aldrich, ABCR, TCI Chemicals* or the central administration of materials of the Technical University of Munich and, unless otherwise specified, used without further purification. The compounds **1**,[1] 3-((2,6-dimethylpyridin-4-yl)oxy)propan-1-ol[2] and $Cp_2Y(CH_2TMS)(thf)$[3] were synthesized according to procedures from literature. Monomers were dried and purified prior to polymerization. Cyclohexene oxide was dried over NaH and purified by distillation. The monomers 2-vinylpyridine and 2-isopropenyl-2-oxazoline were dried over CaH_2 and purified by distillation. NMR-measurements (^1H, ^{13}C) were carried out on the spectrometers AV-400 and AV-500 Cryo of the company *Bruker*. Deuterated solvents were purchased from *Sigma-Aldrich* and for substances susceptible to hydrolysis stored over molecular sieves and under argon. The chemical shifts (δ) are given in parts per million (ppm) and are calibrated to the signals of the deuterated solvents. Mass spectra were carried out either on a *Varian* 500-MS with electron spray ionization (ESI) in acetonitrile using positive ionization mode at 70 eV or on a *Bruker Daltonics ultraflex TOF/TOF* with matrix assisted laser desorption ionization (MALDI). For MALDI-MS measurements the polymer sample is dissolved in dichloromethane and mixed with a saturated solution of α-cyano-4-hydroxycinnamic acid in a 0.1 vol% solution of trifluoroacetic acid in water/acetonitrile. The instrument has been calibrated with a protein standard in the same matrix as the sample prior to use. Gel permeation chromatography experiments were carried out at a PL-GPC 50 of the company *Agilent* with DMF (HPLC grade, 2.17 g/L LiBr) as solvent and PMMA calibration standards. Absolute molar masses of P2VP aliquots were determined via concentration measurement with a two-angle light scattering, viscosimetry and refractive index detection (dn/dc = 0.149 mL/g). Elemental analysis measurements were performed by the microanalytical laboratory of the Inorganic-chemical Institute of the Technical University Munich. *In situ* ATR-IR measurements were performed under argon atmosphere using a *Mettler Toledo MultiMax Pressure* system.

(1) Reiter, M.; Vagin, S.; Kronast, A.; Jandl, C.; Rieger, B., A Lewis acid β-diiminato-zinc-complex as all-rounder for co- and terpolymerisation of various epoxides with carbon dioxide. *Chemical Science* 2017, *8* (3), 1876-1882.

(2) Wang, Q.; Chen, S.; Liang, Y.; Dong, D.; Zhang, N., Bottle-Brush Brushes: Surface-Initiated Rare Earth Metal Mediated Group Transfer Polymerization from a Poly(3-((2,6-dimethylpyridin-4-yl)oxy)propyl methacrylate) Backbone. *Macromolecules* 2017, *50* (21), 8456-8463.

(3a) Hultzsch, K. C.; Voth, P.; Beckerle, K.; Spaniol, T. P.; Okuda, J., Single-Component Polymerization Catalysts for Ethylene and Styrene: Synthesis, Characterization, and Reactivity of Alkyl and Hydrido Yttrium Complexes Containing a Linked Amido−Cyclopentadienyl Ligand.

Organometallics 2000, *19* (3), 228-243; (b) Salzinger, S.; Soller, B. S.; Plikhta, A.; Seemann, U. B.; Herdtweck, E.; Rieger, B., Mechanistic Studies on Initiation and Propagation of Rare Earth Metal-Mediated Group Transfer Polymerization of Vinylphosphonates. *J Am Chem Soc* 2013, *135* (35), 13030-13040.

Synthesis of catalyst 3'

In a glovebox 52.1 mg (288 µmol, 1.0 eq.) 3-((2,6-dimethylpyridin-4-yl)oxy)propan-1-ol are dissolved in 1.0 mL toluene and a solution of 200 mg (288 µmol, 1.0 eq.) **1** in 1.0 mL toluene is added. Immediate precipitation of a light-yellow solid can be observed, which is separated from the supernatant solution by decantation. Complex **3'** in form of a light-yellow solid is dried under vacuum (yield: 61%).

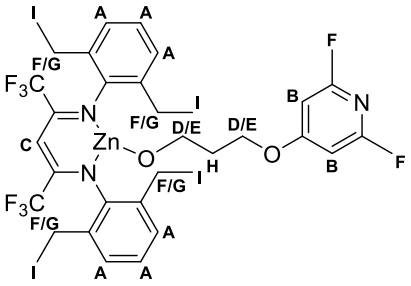

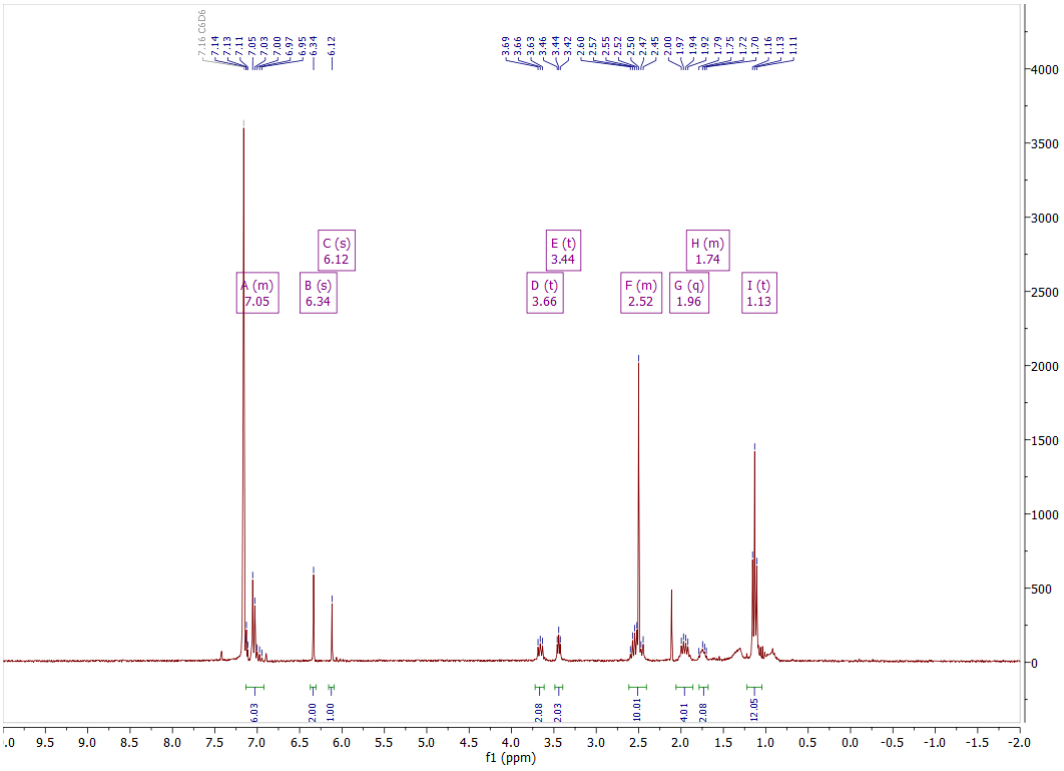

Figure S1. ^{1}H NMR spectrum of complex **3'** in benzene-d_6.

3

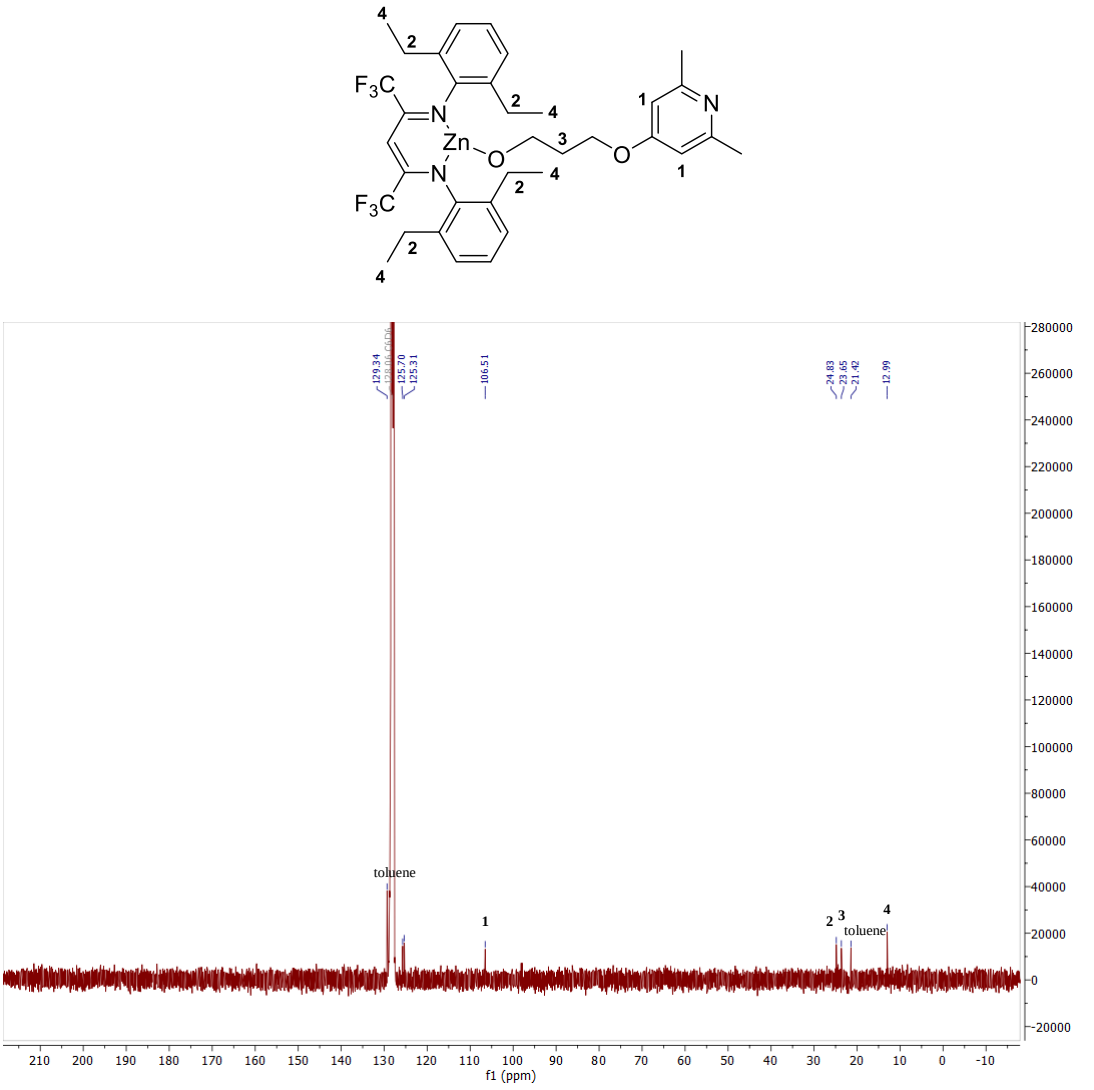

Figure S2. ^{13}C NMR spectrum of a saturated solution of complex **3'** in benzene-d_6 (due to the low solubility of the complex the signals of Pyr-C^{Ar}-Me, Pyr-C^{Ar}-O, CF_3, BDI-C^{Ar}, *C*-CF_3, *C*H-C-CF_3 and CH_2-O are not visible in the spectrum).

EA: [%] calculated: C 58.79, H 5.78, N 5.88

found: C 60.06, H 6.13, N 5.67

4

Synthesis of catalyst 3

In a vial 6.00 mg (8.39 µmol, 1.0 eq.) **3'** and 3.18 mg (8.39 µmol, 1.0 eq.) $Cp_2Y(CH_2TMS)(thf)$ are suspended in 1.2 mL toluene and stirred at room temperature for four hours. The resulting solution of the dinuclear complex **3** is used directly for a polymerization reaction.

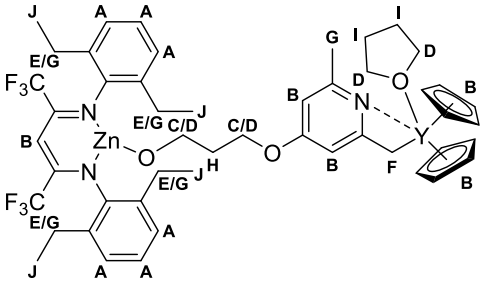

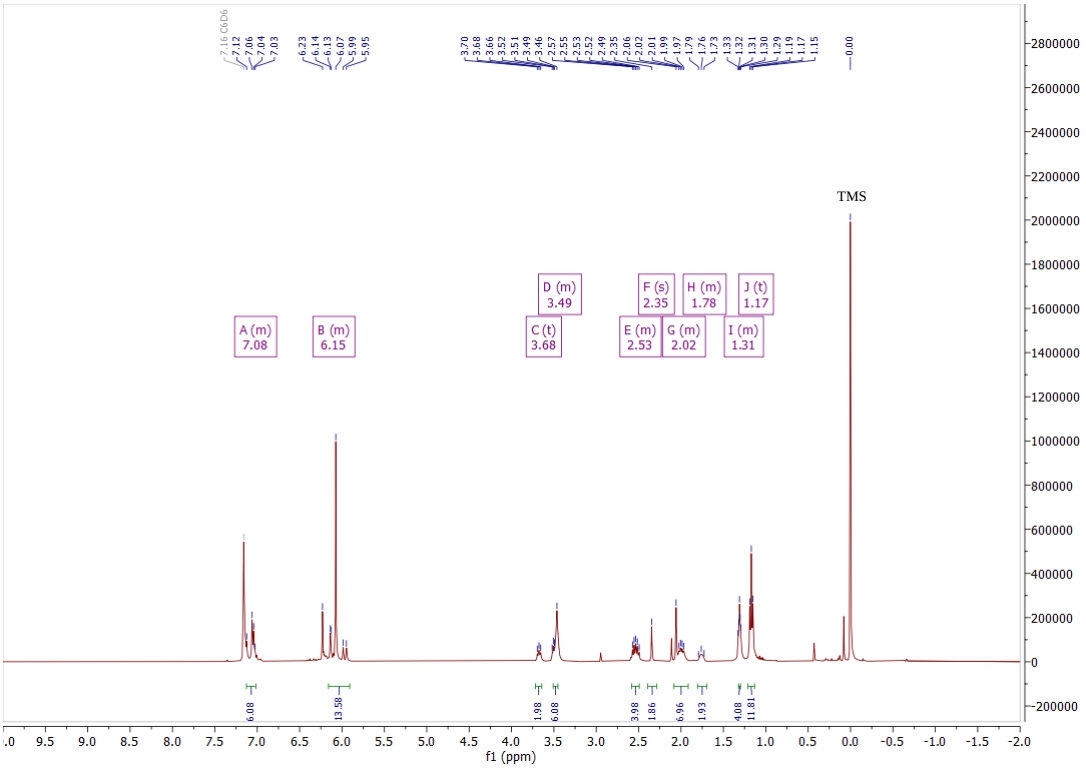

Figure S3. ^{1}H NMR spectrum of complex **3** in benzene-d_6.

5

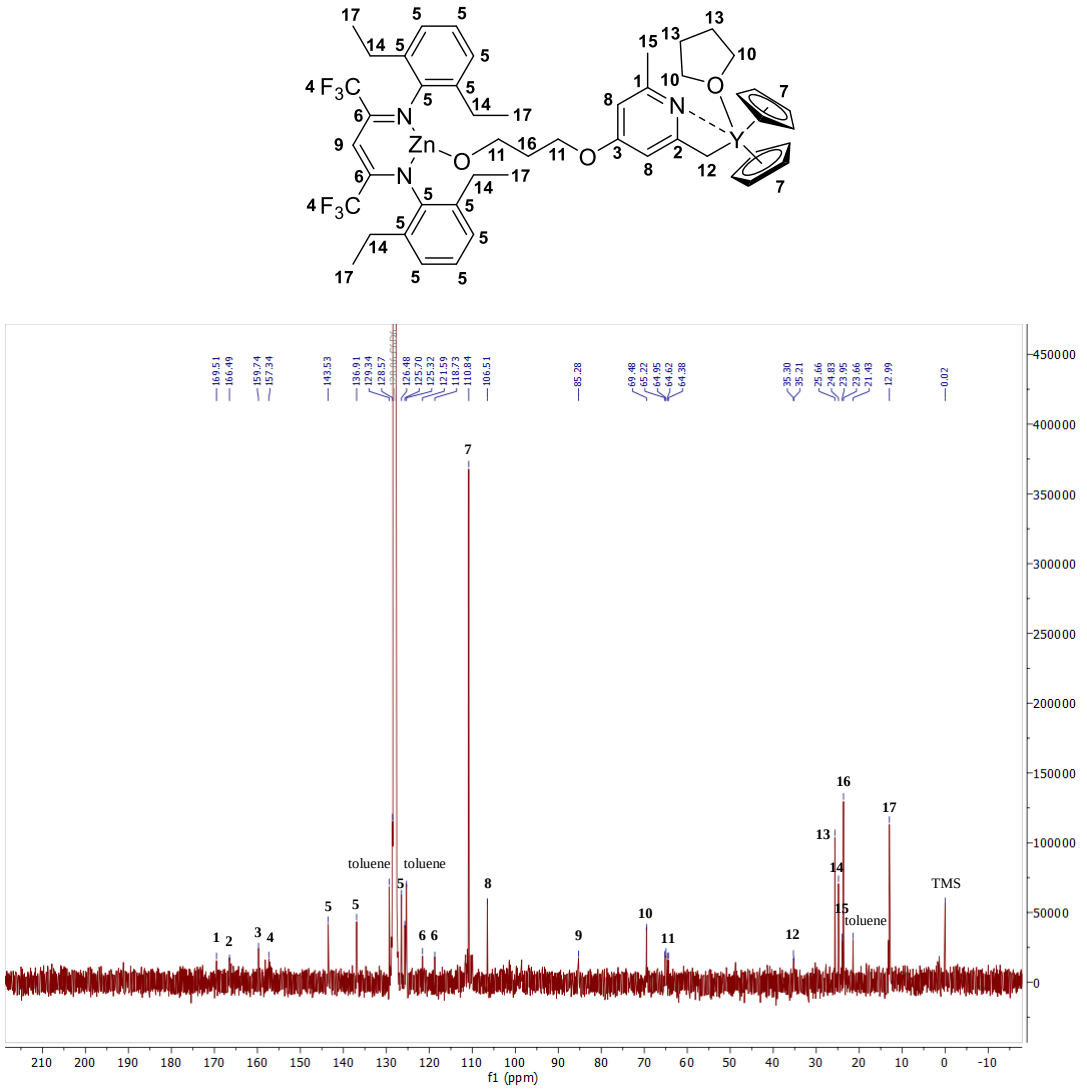

Figure S4. ^{13}C NMR spectrum of complex **3** in benzene-d_6.

EA: [%] calculated: C 58.54, H 5.82, N 4.18

found: C 57.45, H 5.48, N 4.17

6

2. NMR spectra of CH-bond activation

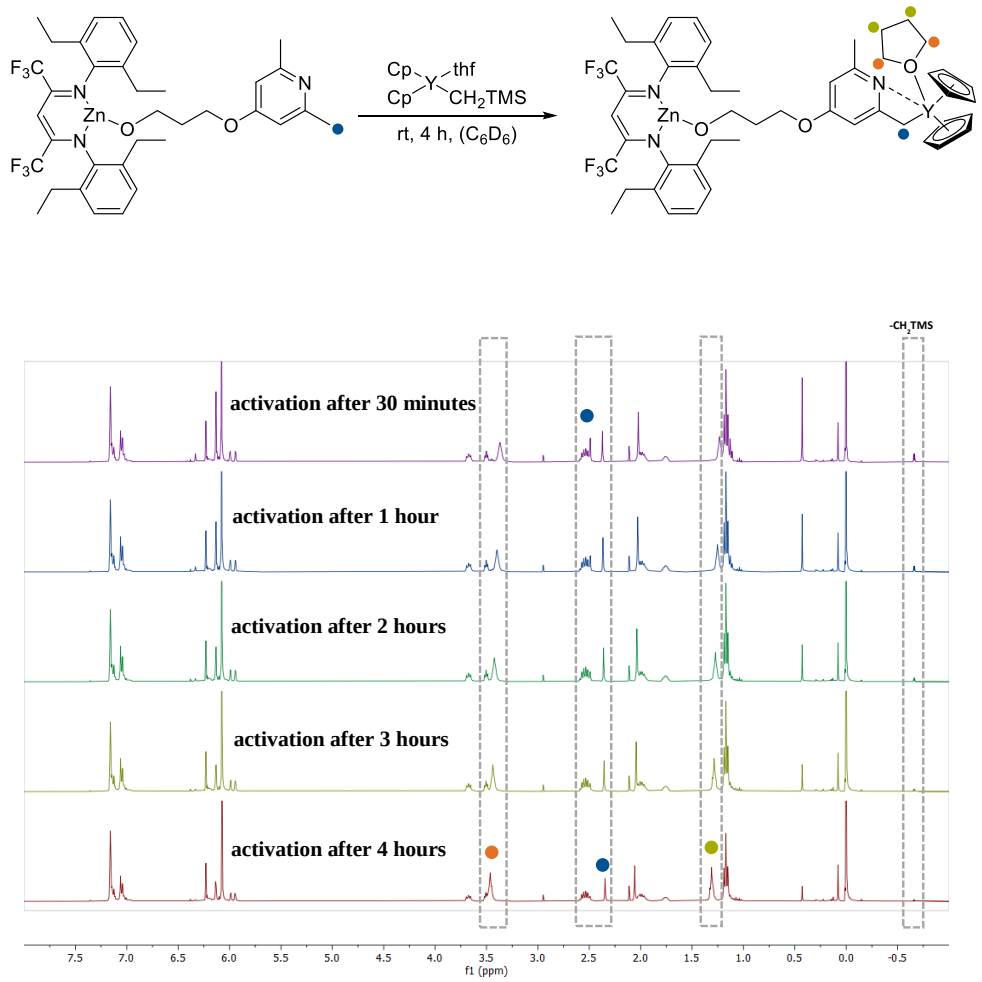

Figure S5. ^{1}H NMR spectra of the CH-bond activation of complex **3'** over four hours in benzene-d_6.

3. Mononuclear catalysts in P2VP and PCHC polymerization

$Cp_2Y(thf)(CH_2TMS)$ in the copolymerization of cyclohexene oxide/CO_2

In the glovebox 40.8 µmol (1.0 eq.) $Cp_2Y(thf)(CH_2TMS)$ are dissolved in 4.0 g toluene and transferred into a handheld autoclave together with 20.4 mmol (500 eq.) cyclohexene oxide. The reaction mixture is pressurized with 30 bar CO_2 and stirred at 40 °C. After 17 hours no generation of PCHC product could be observed.

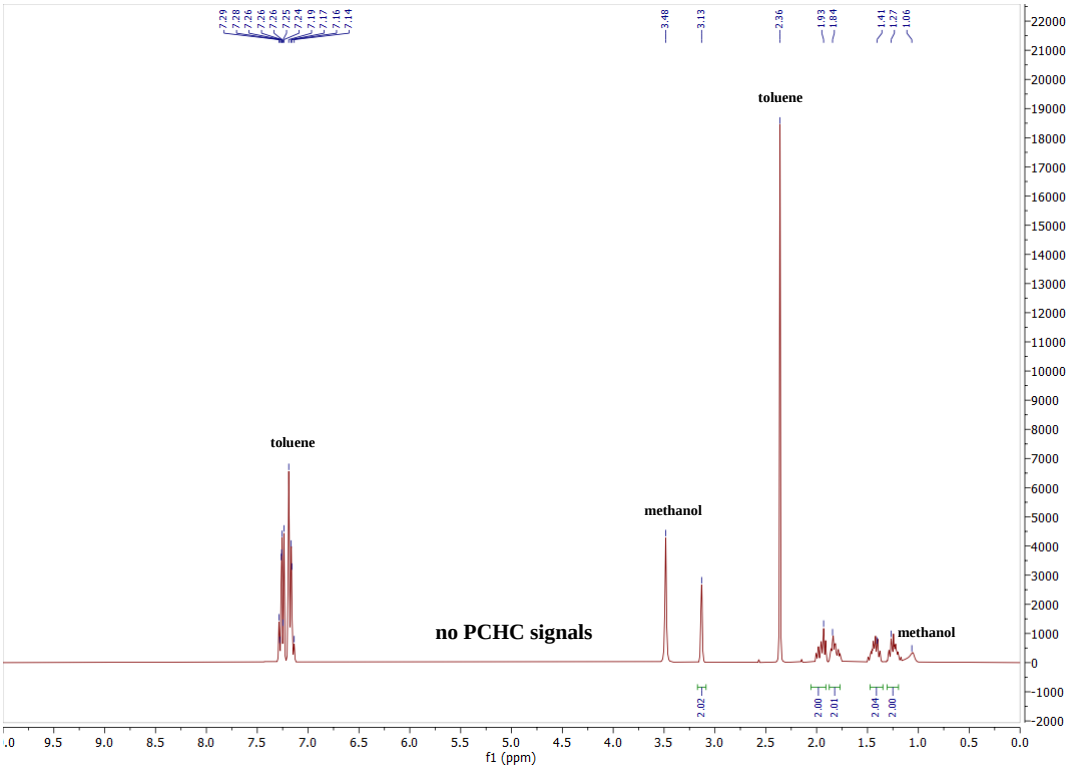

Figure S6. ^1H NMR spectrum of the reaction of CHO and CO_2 with catalyst **2** after 17 hours with no visible polymerization in benzene-d_6.

8

Catalyst 3' in the polymerization of 2-vinylpyridine

In a glovebox 2.80 µmol (1.0 eq.) **3'** are dissolved in 1.2 mL C_6D_6 and mixed with 280 µmol (100 eq.) 2-vinylpyridine. The reaction mixture is stirred at room temperature for five hours without observable generation of P2VP product.

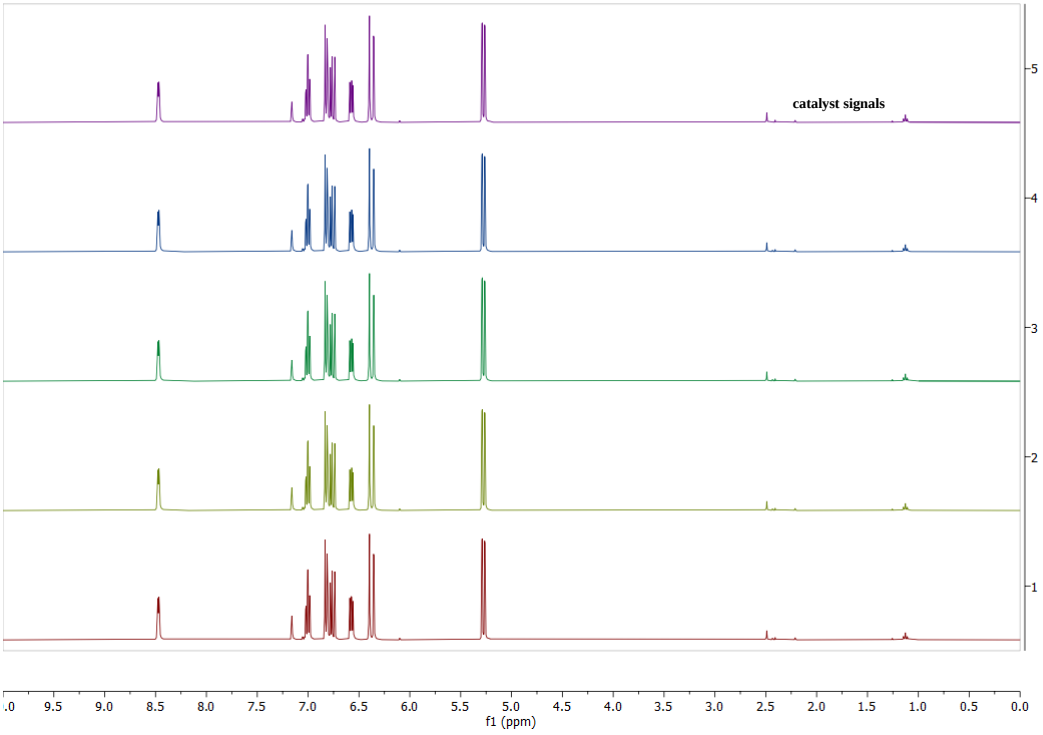

Figure S7. ^{1}H NMR spectra of the reaction of 2VP with **3'** after over five hours without polymerization in benzene-d_6.

9

4. MALDI-MS of oligomeric P2VP synthesized with catalyst 3

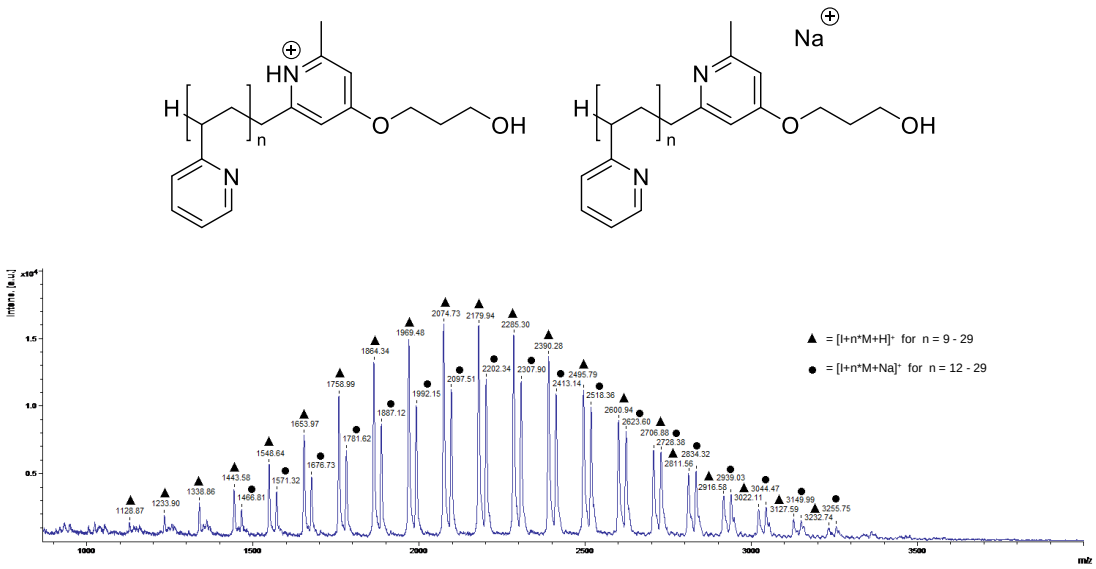

Figure S8. MALDI-MS of oligomeric P2VP synthesized with catalyst **3**.

10

5. Polymerization procedures

Sequential terpolymerization of cyclohexene oxide, and CO_2 with 2-vinylpyridine or 2-isopropenyl-2-oxazoline

In a glovebox 8.39 µmol (1.0 eq.) **3'** is used for the CH-bond activation with 8.39 µmol (1.0 eq.) $Cp_2Y(thf)(CH_2TMS)$ in 1.2 mL toluene. After four hours the reaction mixture is transferred into a handheld autoclave together with 2-vinylpyridine or 2-isopropenyl-2-oxazoline and stirred again for the respective time at room temperature. Cyclohexene oxide is added, the reaction mixture is pressurized with 30 bar CO_2 and stirred at 40 °C. The CO_2 pressure is released and the resulting product is precipitated from *n*-pentane and dried under vacuum.

One-pot terpolymerization of 2-vinylpyridine or 2-isopropenyl-2-oxazoline, cyclohexene oxide, and CO2

In a glovebox 8.39 µmol (1.0 eq.) **3'** is used for the CH-bond activation with 8.39 µmol (1.0 eq.) $Cp_2Y(thf)(CH_2TMS)$ in 1.2 mL toluene. After four hours the reaction mixture is transferred into a handheld autoclave together with 2-vinylpyridine or 2-isopropenyl-2-oxazoline and cyclohexene oxide and stirred at room temperature. After conversion of the Michael-type monomer, the reaction mixture is pressurized with 30 bar CO_2 and stirred at 40 °C. The CO_2 pressure is released and the resulting product is precipitated from *n*-pentane and dried under vacuum.

6. *In situ* ATR-IR spectrum of the CHO/CO_2 copolymerization with catalyst 3

In a glovebox 20.4 µmol (1.0 eq.) **1** is dissolved in 4.0 g toluene and transferred into a steel autoclave together with cyclohexene oxide. The reaction mixture is pressurized with 30 bar CO_2 and stirred at 40 °C with *in situ* IR monitoring.

In a glovebox 9.38 µmol (1.0 eq.) **3'** is used for the CH-bond activation with 9.38 µmol (1.0 eq.) $Cp_2Y(thf)(CH_2TMS)$ in 2.0 mL toluene. After four hours the reaction mixture is transferred into a steel autoclave together with cyclohexene oxide. The reaction mixture is pressurized with 30 bar CO_2 and stirred at 40 °C with *in situ* IR monitoring.

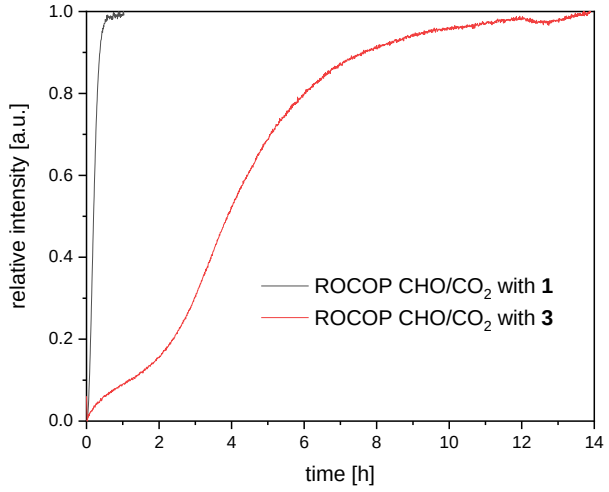

Figure S9. Relative intensity of the absorption of the C=O stretching bond in PCHC at 1750 cm^{-1} measured via *in situ* ATR-IR spectroscopy during the CHO/CO_2 copolymerization with catalysts **1** (black) and **3** (red).

12

7. ESI- and MALDI-MS of oligomeric PCHC synthesized with catalyst 3

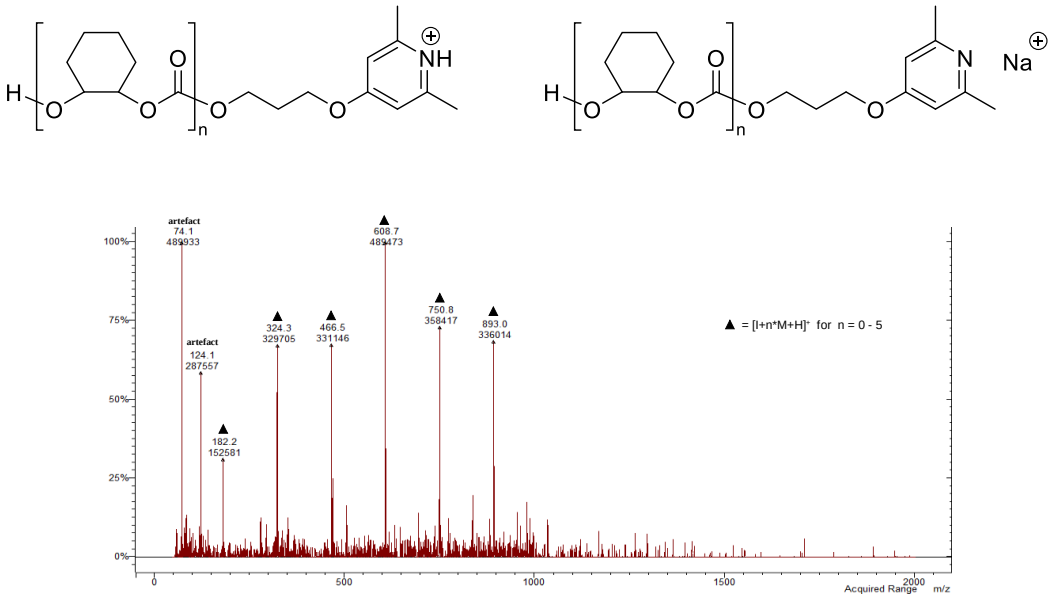

Figure S10. ESI-MS of oligomeric PCHC synthesized with catalyst **3** (signals at 74.1 and 124.1 m/z are artefacts from the spectrometer).

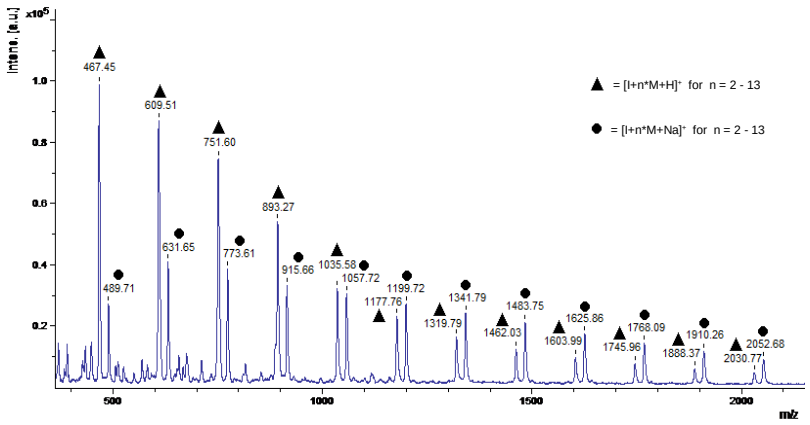

Figure S11. MALDI-MS of oligomeric PCHC synthesized with catalyst **3**.

8. NMR spectrum of catalyst 3 pressurized with CO_2

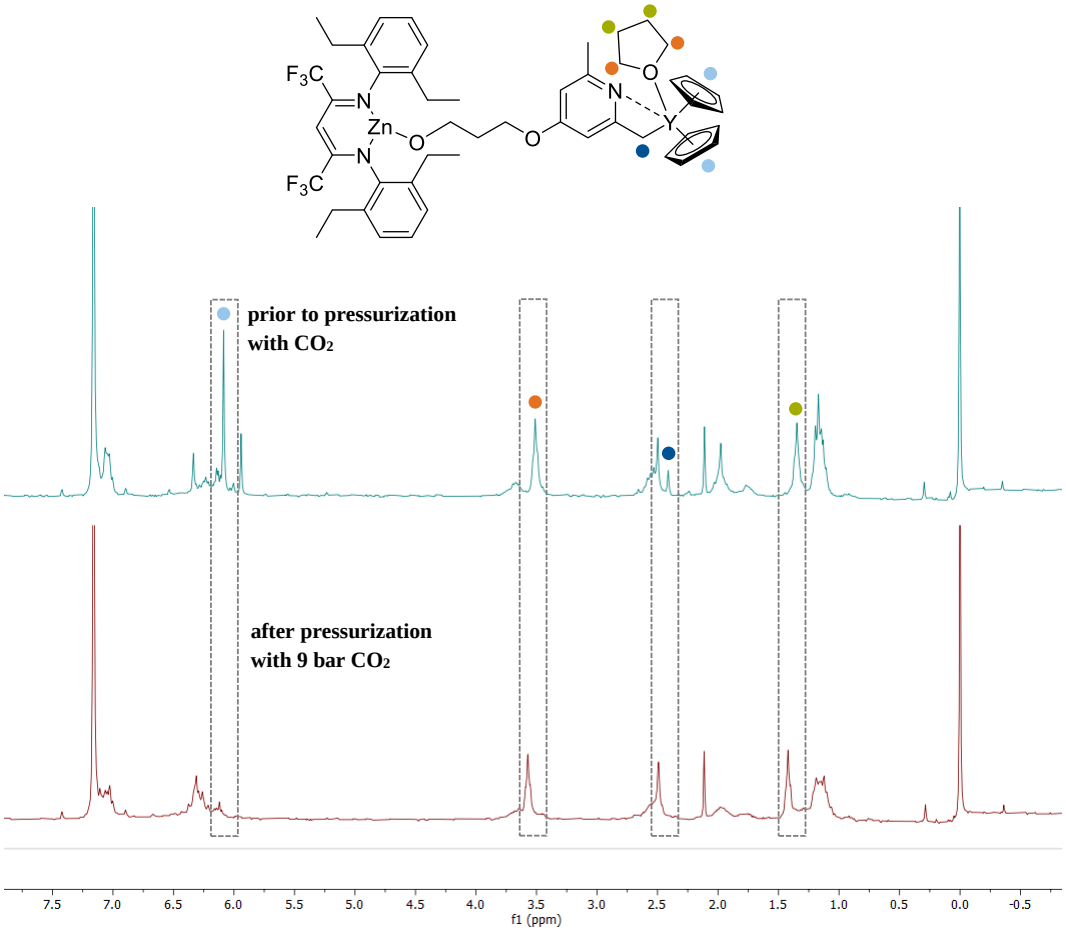

Figure S12. ^{1}H-NMR spectra of complex **3** prior and after pressurization with 9 bar CO_2 in benzene-d_6.

9. GPC traces of P2VP/PCHC and PIPOx/PCHC terpolymers

Table 1, entry 1

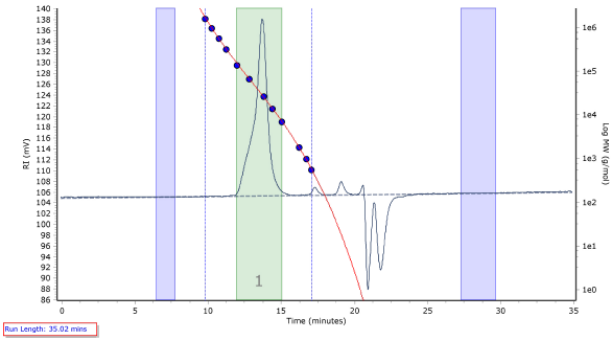

Molecular Weight Averages

Peak	Mp (g/mol)	Mn (g/mol)	Mw (g/mol)	Mz (g/mol)	Mz+1 (g/mol)	Mv (g/mol)	PD
Peak 1	27698	28225	37358	50659	67101	48409	1.324

Figure S13. GPC trace of a PCHC copolymer (table 1, entry 1).

Table 1, entry 2

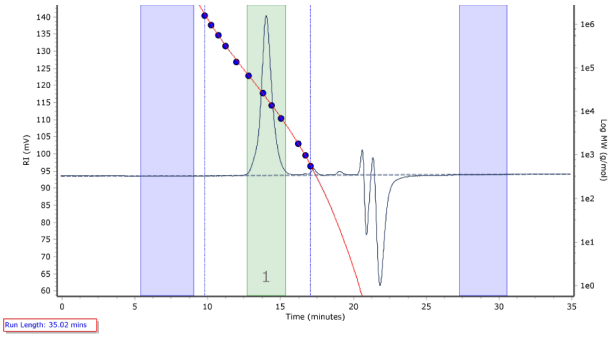

Molecular Weight Averages

Peak	Mp (g/mol)	Mn (g/mol)	Mw (g/mol)	Mz (g/mol)	Mz+1 (g/mol)	Mv (g/mol)	PD
Peak 1	20254	17495	21050	25181	30140	24511	1.203

Figure S14. GPC trace of a PCHC copolymer (table 1, entry 2).

15

Table 1, entry 3

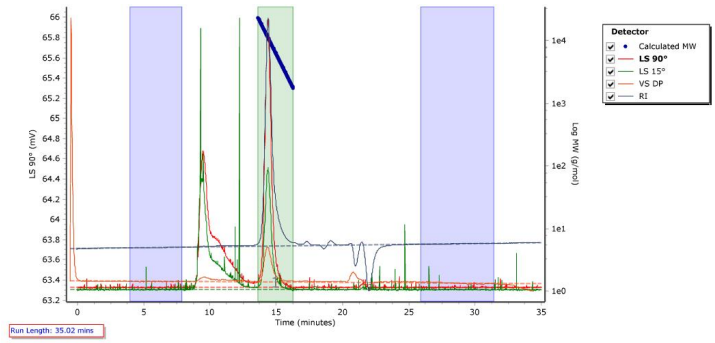

Molecular Weight Averages

Peak	Mp (g/mol)	Mn (g/mol)	Mw (g/mol)	Mz (g/mol)	Mz+1 (g/mol)	Mv (g/mol)	PD
Peak 1	11076	8743	10219	11277	12130	0	1.169

Figure S15. GPC traces of a P2VP aliquot (table 1, entry 3).

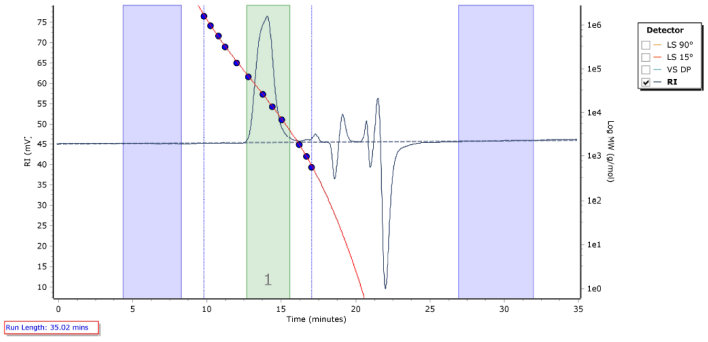

Molecular Weight Averages

Peak	Mp (g/mol)	Mn (g/mol)	Mw (g/mol)	Mz (g/mol)	Mz+1 (g/mol)	Mv (g/mol)	PD
Peak 1	19268	19975	24870	30357	35819	29543	1.245

Figure S16. GPC traces of a P2VP/PCHC terpolymer (table 1, entry 3).

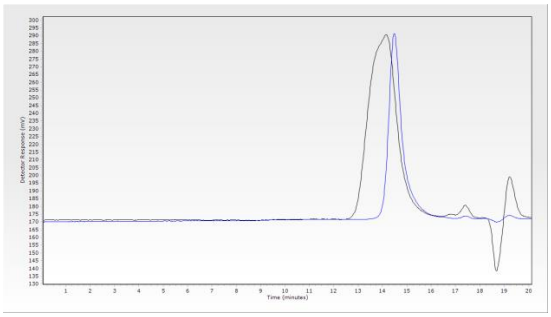

Figure S17. GPC traces (RI) of a P2VP aliquot (blue) and the corresponding P2VP/PCHC terpolymer (black, table 1, entry 3).

Table 1, entry 4

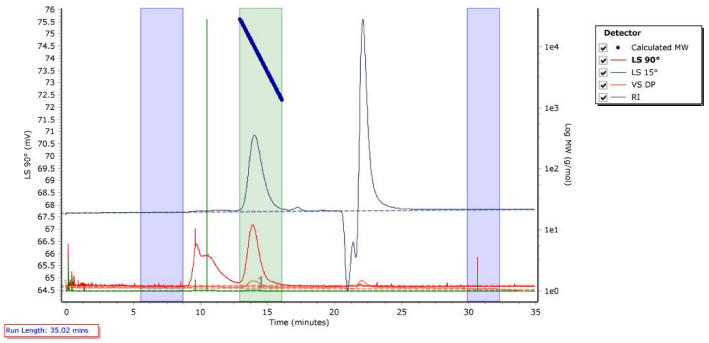

Molecular Weight Averages

Peak	Mp (g/mol)	Mn (g/mol)	Mw (g/mol)	Mz (g/mol)	Mz+1 (g/mol)	Mv (g/mol)	PD
Peak 1	10004	6976	9271	11394	13344	10460	1.329

Figure S18. GPC traces of a P2VP aliquot (table 1, entry 4).

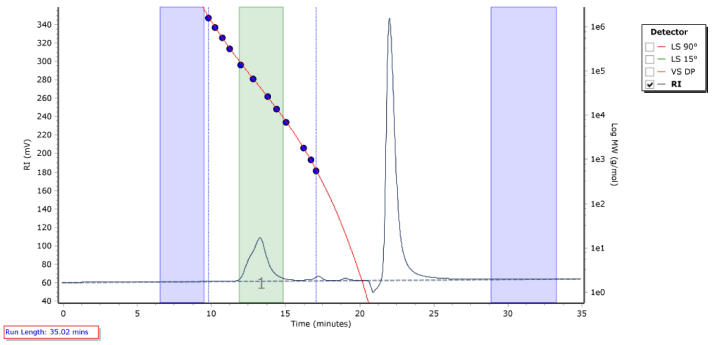

Molecular Weight Averages

Peak	Mp (g/mol)	Mn (g/mol)	Mw (g/mol)	Mz (g/mol)	Mz+1 (g/mol)	Mv (g/mol)	PD
Peak 1	42253	37153	50950	66150	81144	63919	1.371

Figure S19. GPC traces of a P2VP/PCHC terpolymer (table 1, entry 4).

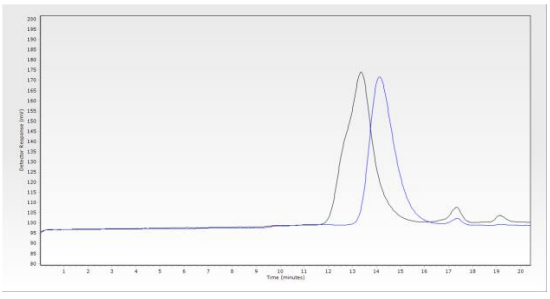

Figure S20. GPC traces (RI) of a P2VP aliquot (blue) and the corresponding P2VP/PCHC terpolymer (black, table 1, entry 4).

Table 1, entry 5

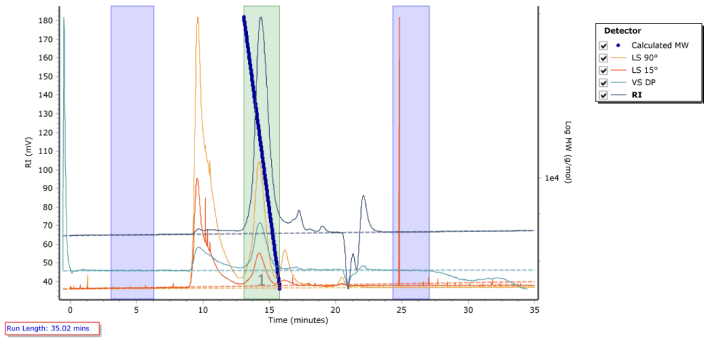

Figure S21. GPC traces of a P2VP aliquot (table 1, entry 5), the absolute molar mass was calculated via ^{1}H NMR spectroscopy.

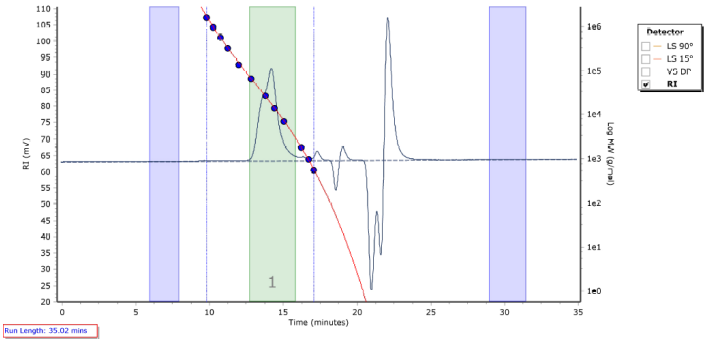

Molecular Weight Averages

Peak	Mp (g/mol)	Mn (g/mol)	Mw (g/mol)	Mz (g/mol)	Mz+1 (g/mol)	Mv (g/mol)	PD
Peak 1	17140	16991	22045	27690	33222	26860	1.297

Figure S22. GPC traces of a P2VP/PCHC terpolymer (table 1, entry 5).

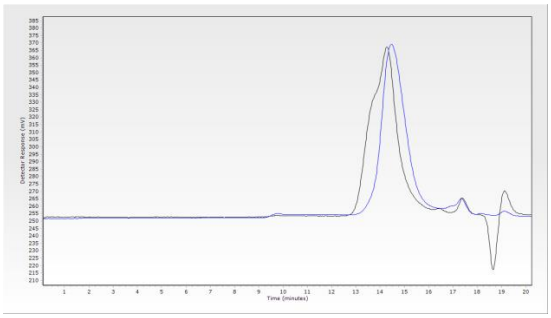

Figure S23. GPC traces (RI) of a P2VP aliquot (blue) and the corresponding P2VP/PCHC terpolymer (black, table 1, entry 5).

Table 1, entry 6

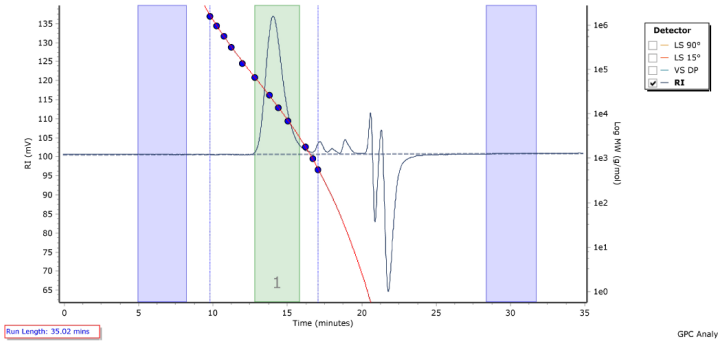

Figure S24. GPC traces of a PIPOx aliquot (table 1, entry 6), the absolute molar mass was calculated via ^{1}H NMR spectroscopy.

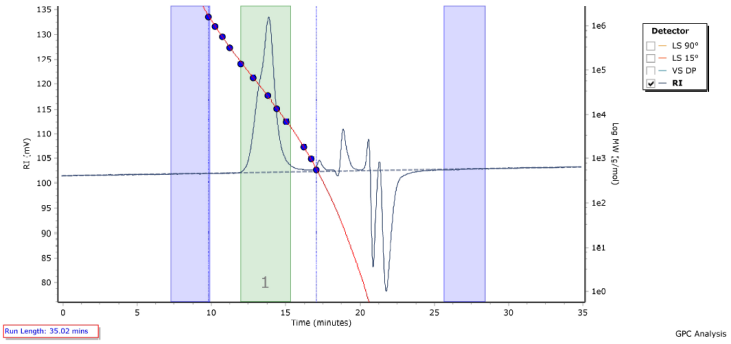

Molecular Weight Averages

Peak	Mp (g/mol)	Mn (g/mol)	Mw (g/mol)	Mz (g/mol)	Mz+1 (g/mol)	Mv (g/mol)	PD
Peak 1	23895	22995	31405	42061	54600	40346	1.366

Figure S25. GPC traces of a PIPOx/PCHC terpolymer (table 1, entry 6).

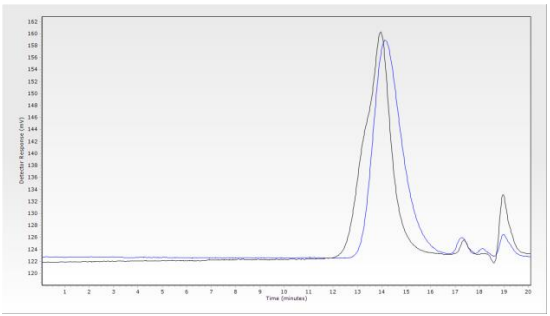

Figure S26. GPC traces (RI) of a PIPOx aliquot (blue) and the corresponding PIPOx/PCHC terpolymer (black, table 1, entry 6).

Table 1, entry 7

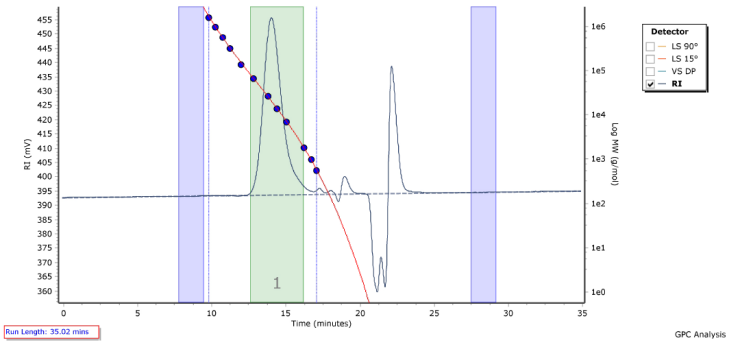

Figure S27. GPC traces of a PIPOx aliquot (table 1, entry 7), the absolute molar mass was calculated via ^{1}H NMR spectroscopy

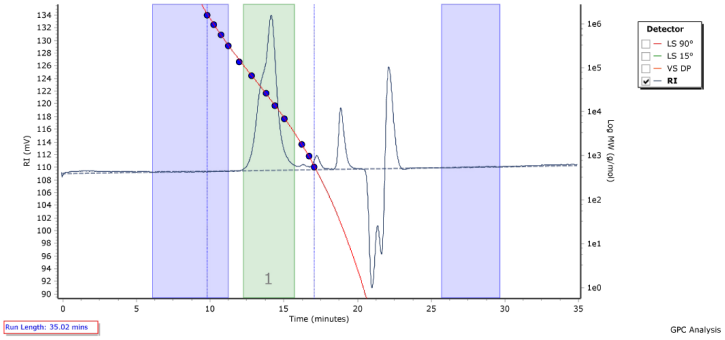

Molecular Weight Averages

Peak	Mp (g/mol)	Mn (g/mol)	Mw (g/mol)	Mz (g/mol)	Mz+1 (g/mol)	Mv (g/mol)	PD
Peak 1	18023	17657	24630	33474	43921	32047	1.395

Figure S28. GPC traces of a PIPOx/PCHC terpolymer (table 1, entry 7).

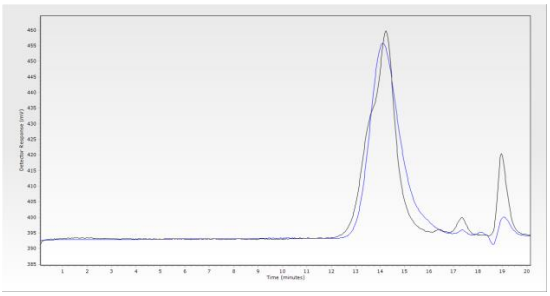

Figure S29. GPC traces (RI) of a PIPOx aliquot (blue) and the corresponding PIPOx/PCHC terpolymer (black, table 1, entry 7).

10. NMR after extraction/washing of an artificial P2VP/PCHC blend with methanol

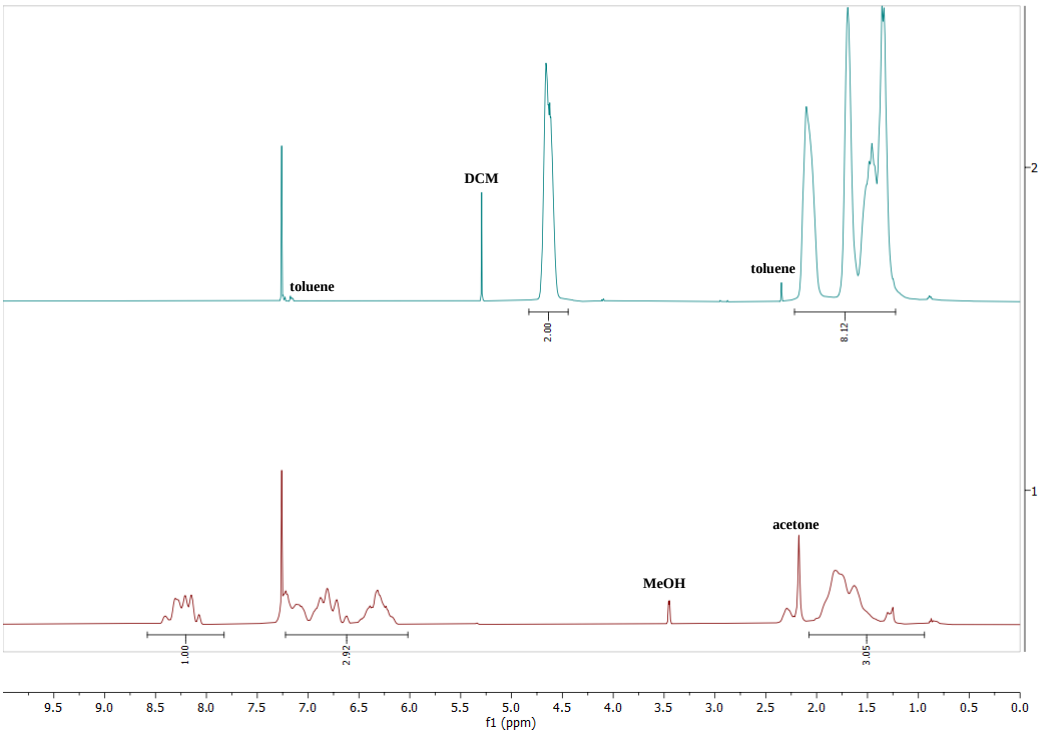

Figure S30. ^{1}H NMR spectra in chloroform-d of the methanol phase (1) and the remaining solid (2) of an artificial P2VP/PCHC blend (M_n(P2VP) = 22 kg/mol, M_n(PCHC) = 33 kg/mol) after extraction/washing with methanol.

21

11. NMR after extraction/washing of a P2VP/PCHC terpolymer with methanol

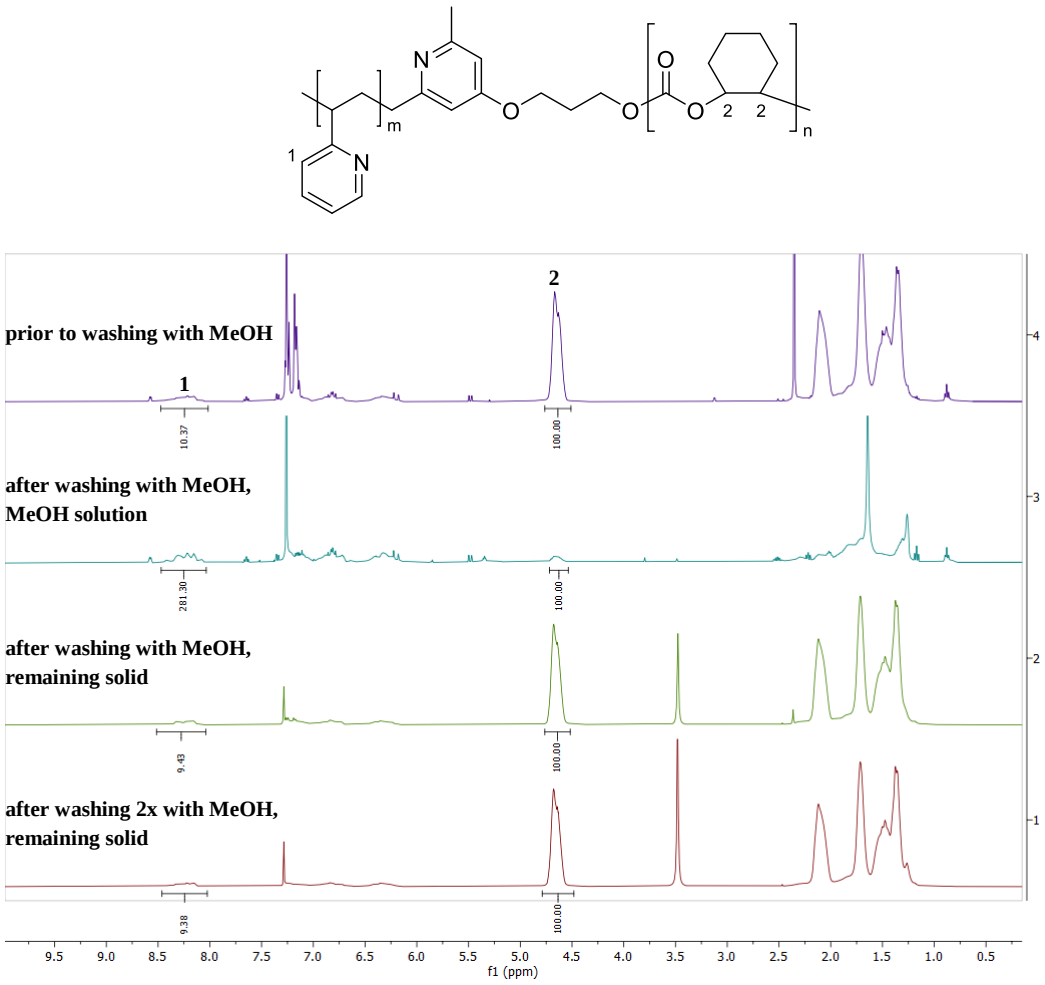

Figure S31. NMR spectra of a P2VP/PCHC terpolymer (table 1, entry 4) prior (4) and after washing with methanol (3–1) in chloroform-d.

22

12. GPC after extraction/washing of a P2VP/PCHC terpolymer with methanol

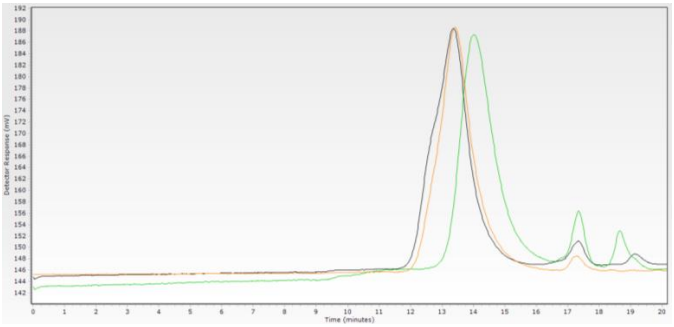

black:

Molecular Weight Averages

Peak	Mp (g/mol)	Mn (g/mol)	Mw (g/mol)	Mz (g/mol)	Mz+1 (g/mol)	Mv (g/mol)	PD
Peak 1	42253	37153	50950	66150	81144	63919	1.371

orange:

Molecular Weight Averages

Peak	Mp (g/mol)	Mn (g/mol)	Mw (g/mol)	Mz (g/mol)	Mz+1 (g/mol)	Mv (g/mol)	PD
Peak 1	40252	37096	44712	53524	62453	52193	1.205

green:

Molecular Weight Averages

Peak	Mp (g/mol)	Mn (g/mol)	Mw (g/mol)	Mz (g/mol)	Mz+1 (g/mol)	Mv (g/mol)	PD
Peak 1	22370	16163	21339	26722	31930	25948	1.32

Figure S32. GPC traces (RI) of a P2VP/PCHC terpolymer (table 1, entry 4) prior (black) and after washing with methanol (orange, remaining solid and green, methanol phase).

13. DSC Analysis of P2VP/PCHC terpolymer

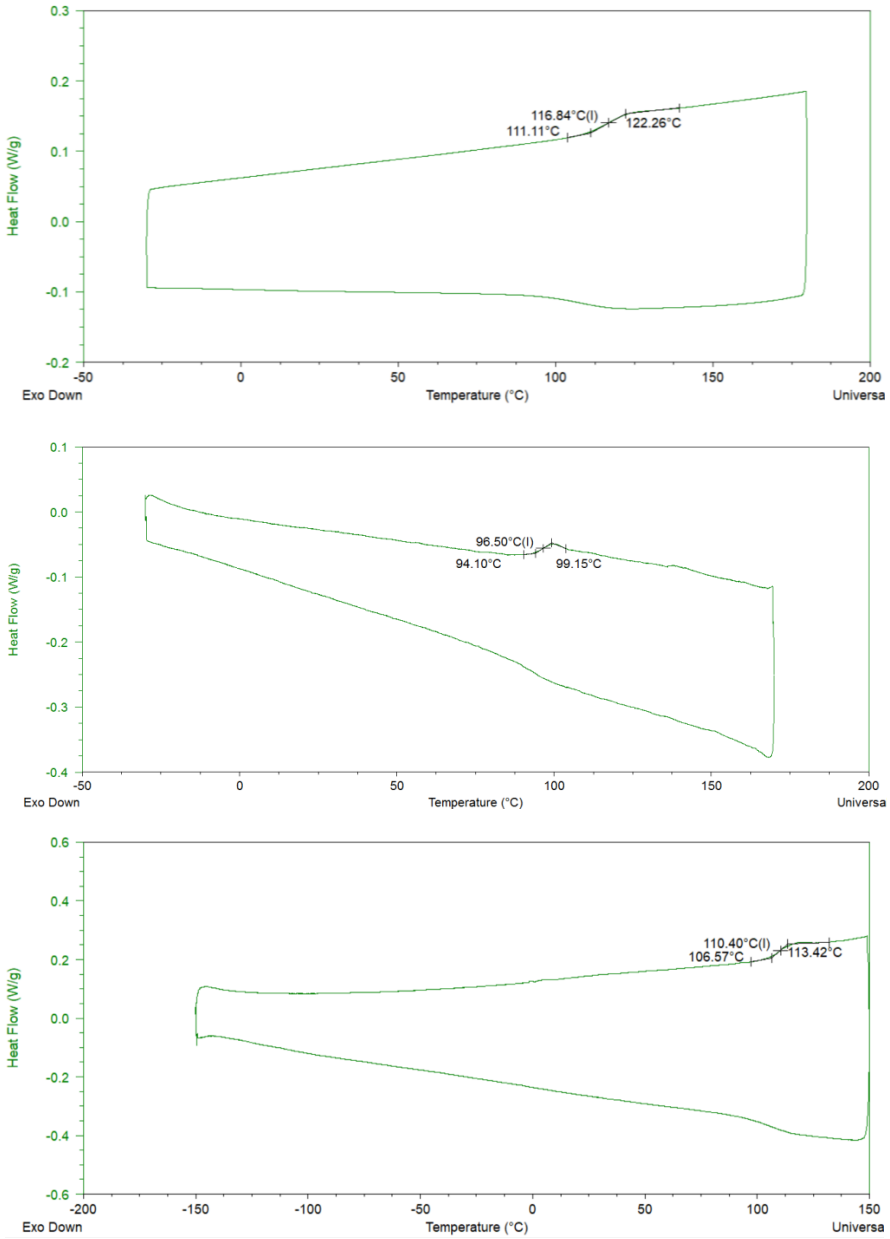

(1)

(2)

(3)

Figure S33. DSC measurement of PCHC (1), P2VP (2) and a P2VP/PCHC terpolymer (table 1, entry 3) (3).

24

14. TGA of P2VP/PCHC and PIPOx/PCHC terpolymers

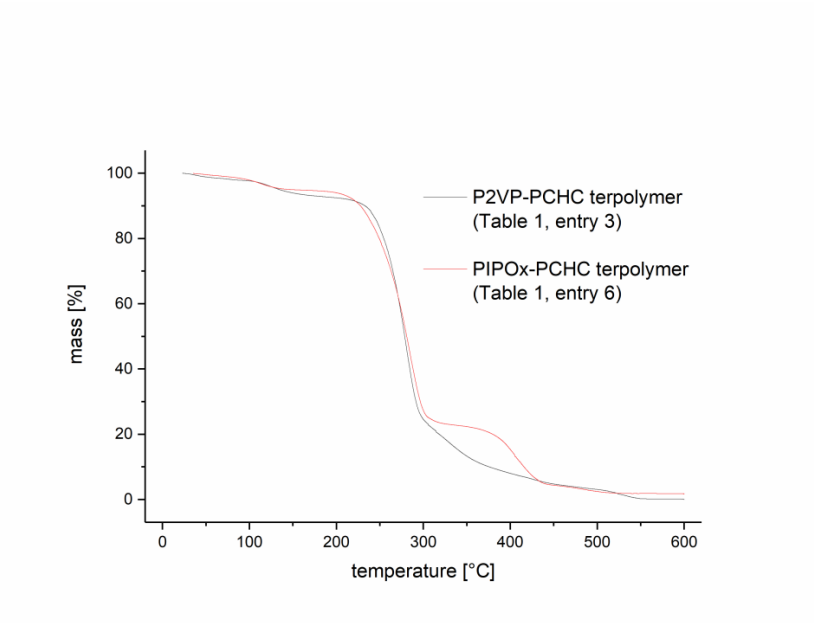

Figure S34. TGA of a P2VP/PCHC (table 1, entry 3) and a PIPOx/PCHC terpolymer (table 1, entry 6).

15. ESI-MS of oligomeric PIPOx synthesized with catalyst 3

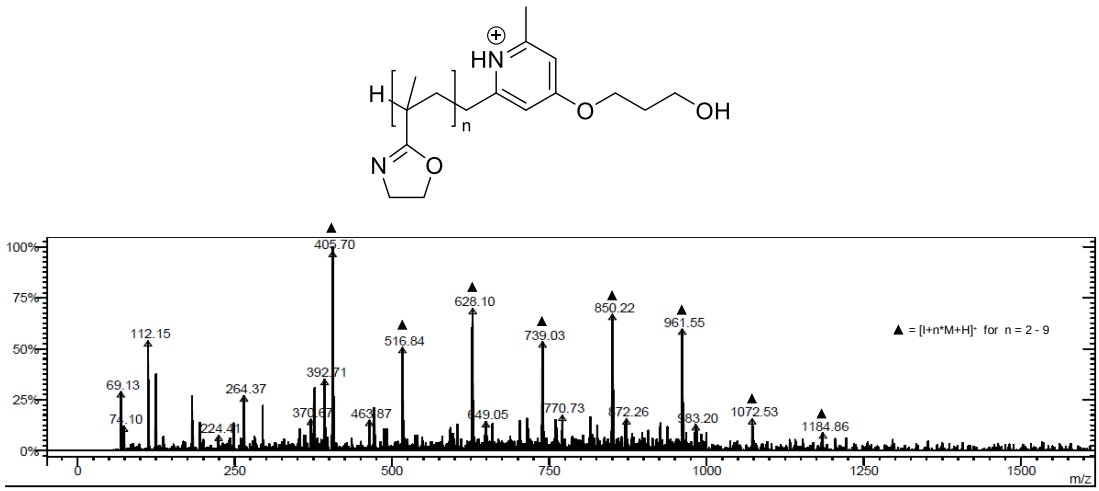

Figure S35. ESI-MS of oligomeric PIPOx synthesized with catalyst **3** (the signal at 112.15 m/z is the mass of the protonated monomer).

16. DSC Analysis of PIPOx/PCHC terpolymer

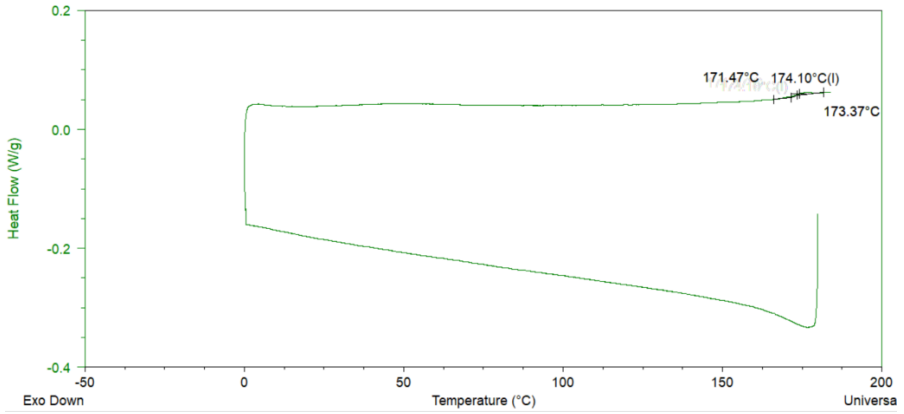

(1)

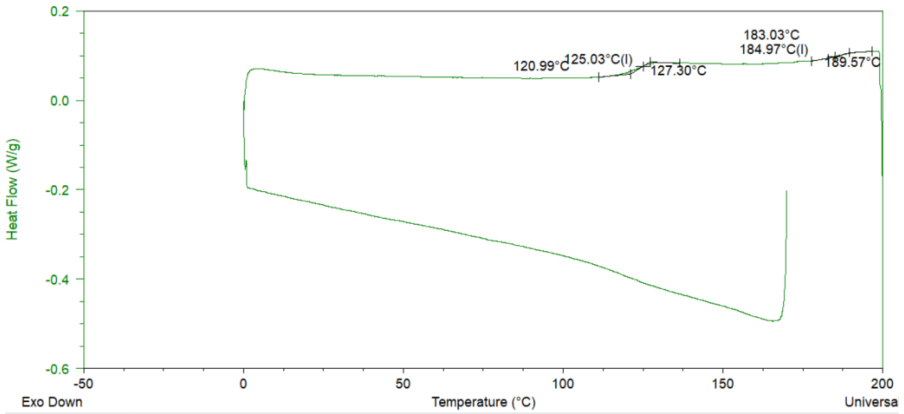

(2)

Figure S36. DSC measurement of PIPOx homopolymer (1) and of a PIPOx/PCHC terpolymer (table 1, entry 6) (2).

26

17. NMR spectra of P2VP/PCHC and PIPOx/PCHC terpolymers

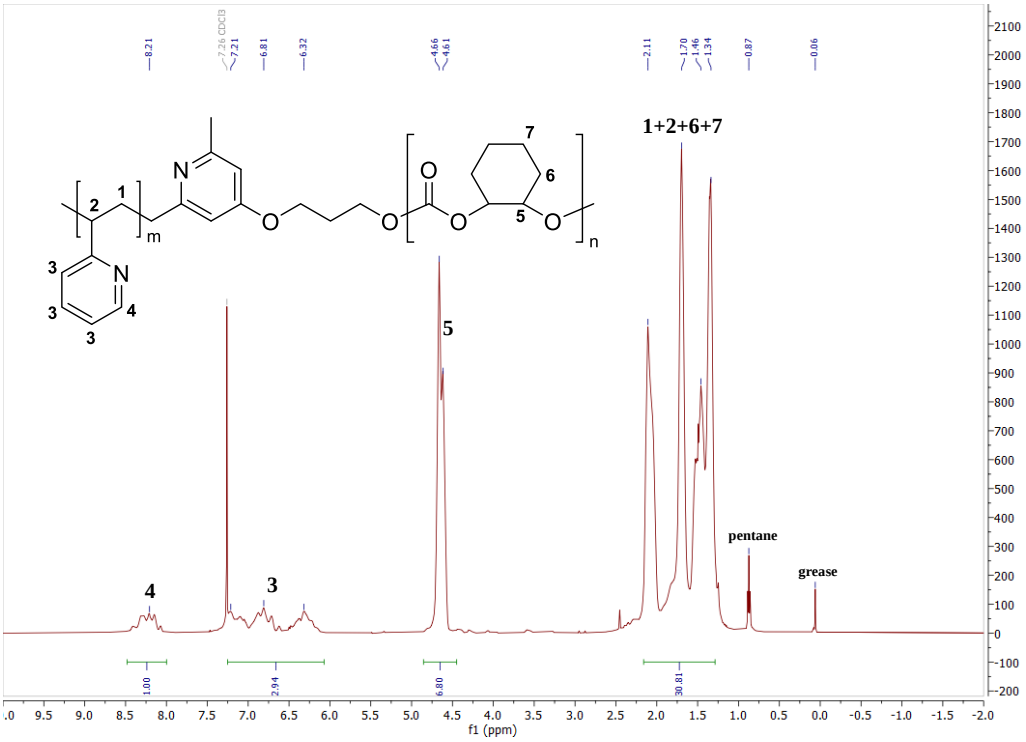

Figure S37. ^{1}H NMR spectrum of a P2VP/PCHC terpolymer (table 1, entry 5) in chloroform-d.

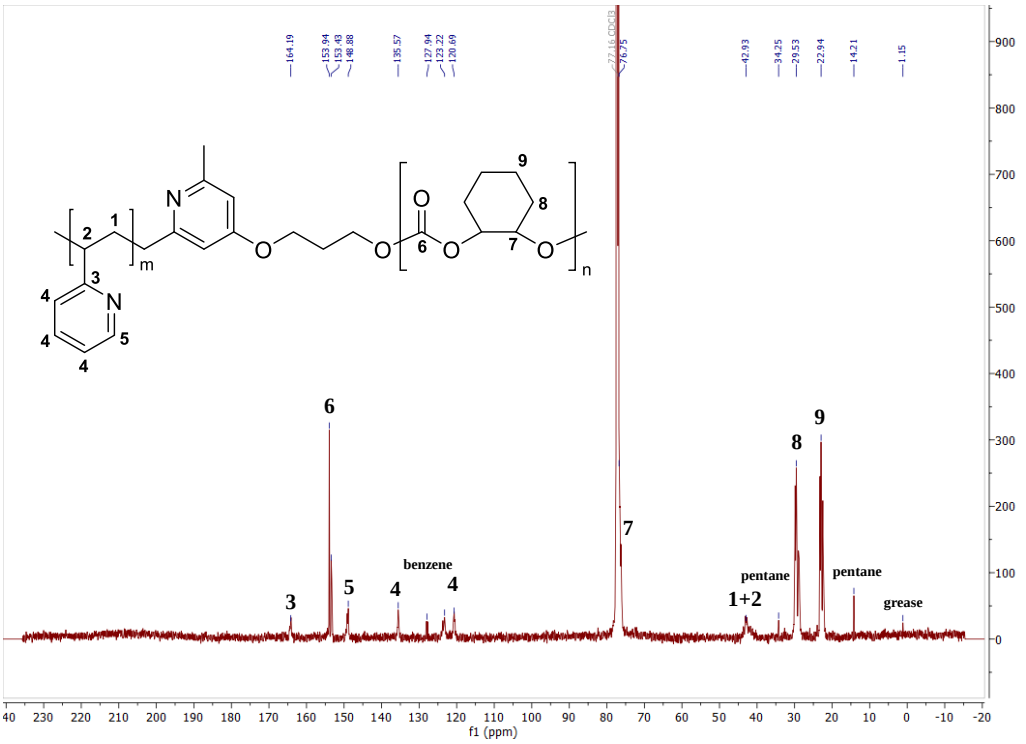

Figure S38. ^{13}C NMR spectrum of a P2VP/PCHC terpolymer (table 1, entry 5) in chloroform-d.

27

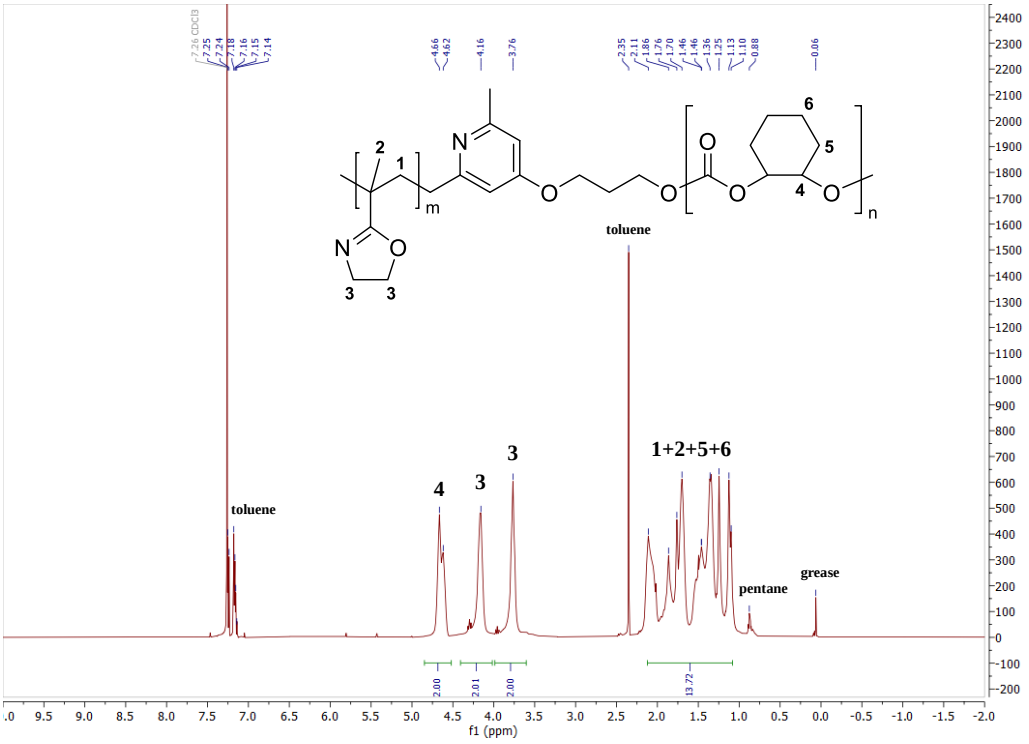

Figure S39. ^{1}H NMR spectrum of a PIPOx/PCHC terpolymer (table 1, entry 6) in chloroform-d.

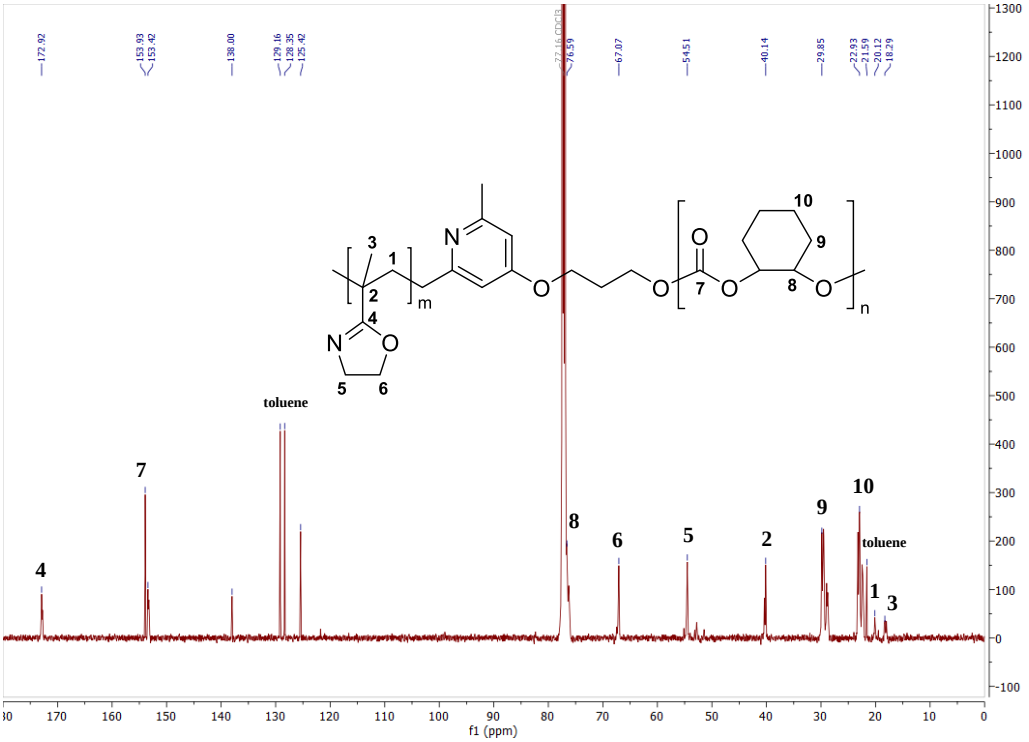

Figure S40. ^{13}C NMR spectrum of a PIPOx/PCHC terpolymer (table 1, entry 6) in chloroform-d.

28

16.4 Supporting Information: Aliphatic Polycarbonates Derived From Epoxides and CO_2: A Comparative Study of Poly(cyclohexene carbonate) and Poly(limonene carbonate)

Aliphatic Polycarbonates Derived From Epoxides and CO_2: A Comparative Study of Poly(cyclohexene carbonate) and Poly(limonene carbonate)

Sebastian Kernbichl, and Bernhard Rieger

WACKER-Chair of Macromolecular Chemistry, Catalysis Research Center, Technical University Munich, Lichtenbergstr. 4, 85748 Garching, Germany

Content

1. Polymerization Procedure

Copolymerization of CO_2 with CHO and LO, respectively:

50 mL autoclave: The polymerizations were performed with in situ monitoring using a React-IR/MultiMax four-autoclave system (Mettler-Toledo). The 50 mL steel autoclaves are equipped with a diamond window, a mechanic stirring and a heating device. The autoclaves were heated to 130 °C under vacuum overnight prior to polymerization. Complex **1** was dissolved in the amount of toluene. In a second syringe, the amount of epoxide was stored. Both syringes were rapidly transferred to the autoclave by attaching the syringes to a vial with an injection septum. The reactor was pretempered to the desired temperature under argon atmosphere and the syringe is given into the reactor. 40 bar CO_2 were applied. The product was dissolved in dichloromethane and transferred to a flask. Consequent removal of the solvent under vacuum allowed the determination of yield and selectivity via NMR/weight of the polymer. The dissolved polymer was precipitated in methanol and dried under vacuum.

1 L Buchi reactor: The amount of complex **1** was dissolved in toluene in a glovebox. The amount of epoxide was filled in a second preheated flask. Both flasks were rapidly transported to the reactor and cannulated into the preheated reactor under argon atmosphere. 40 bar CO_2 were applied for the desired time. The polymeric mixture could be released via a valve at the bottom of the reactor. The product was dissolved in dichloromethane and transferred to a flask. Consequent removal of the solvent under vacuum allowed the determination of yield and selectivity via NMR/weight of the polymer. The dissolved polymer (dichloromethane) was precipitated in methanol and dried under vacuum.

Terpolymerization of CHO, LO, and CO_2:

The terpolymerizations were performed with in situ monitoring using a React-IR/MultiMax four-autoclave system (Mettler-Toledo). Complex **1** was dissolved in the amount of toluene. In a second syringe, the amount of both epoxides was stored. Both syringes were rapidly transferred to the autoclave by attaching the syringes to a vial with an injection septum. The reactor was pretempered to the desired temperature under argon atmosphere and the syringe is given into the reactor. 40 bar CO_2 were applied. The product was dissolved in dichloromethane and transferred to a flask. Consequent removal of the solvent under vacuum allowed the determination of yield and selectivity via NMR/weight of the polymer. The dissolved polymer (dichloromethane) was precipitated in methanol and dried under vacuum.

Catalyst removal:

In a first attempt, the dissolved polymer was precipitated in methanol and dried to constant weight. The polymer was again dissolved in dichloromethane extracted with a saturated aqueous EDTA-solution. This procedure was repeated until the UV-Vis spectrum of solution of the polymer in chloroform did show high transmission in the range from 200 to 800 nm.

2. Cross-linking of PLC

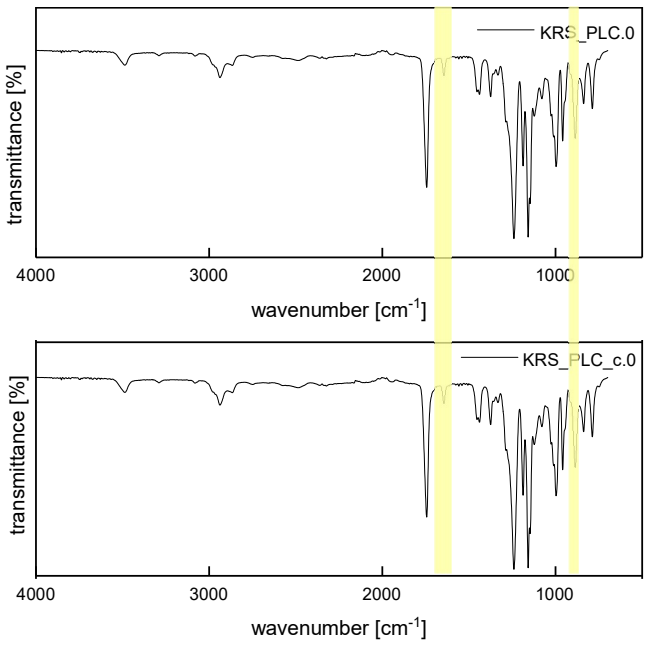

Figure S1. IR spectrum of PLC (top) and thermally treated, insoluble PLC (bottom).

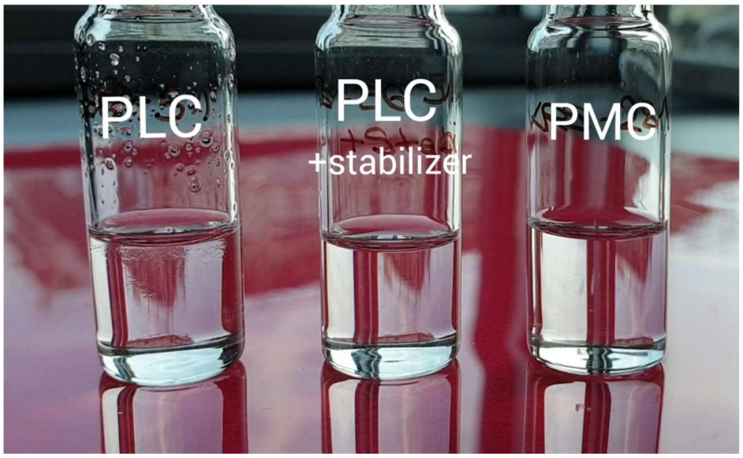

Figure S2. Mixing the polymer with chloroform. PLC(left) is no longer soluble while PLC with Irganox® (middle) and PMC are well soluble (right).

3. In situ IR monitoring of the terpolymerization of CHO, LO, and CO_2

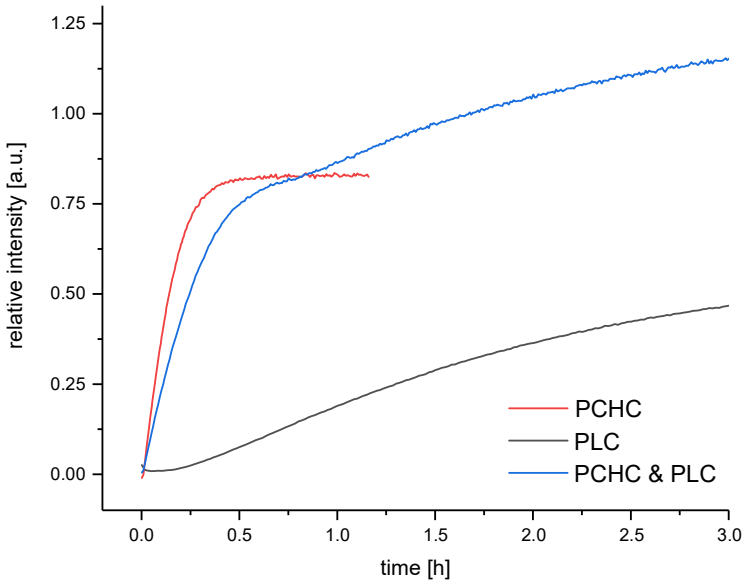

4. GPC traces of co- and terpolymers

Table 1, entry 1

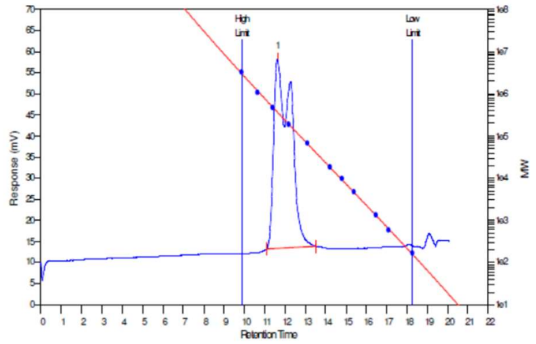

MW Averages

Peak No	Mp	Mn	Mw	Mz	Mz+1	Mv	PD
1	366160	219423	269095	317238	358396	261792	1.22638

Table 1, entry 2

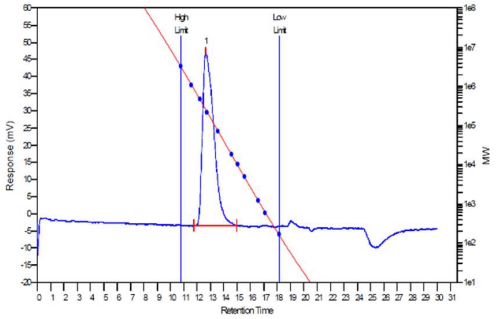

MW Averages

Peak No	Mp	Mn	Mw	Mz	Mz+1	Mv	PD
1	252084	142074	201190	250763	291706	193448	1.41609

Table 1, entry 3

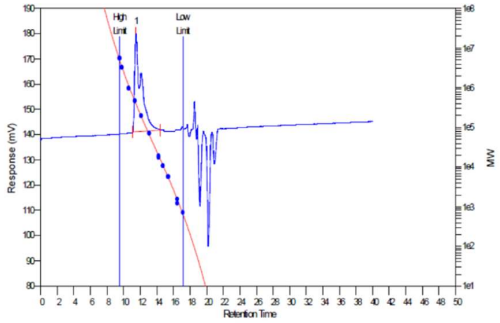

MW Averages

Peak No	Mp	Mn	Mw	Mz	Mz+1	Mv	PD
1	409676	176005	267199	334557	378827	255897	1.51813

Table 1, entry 4

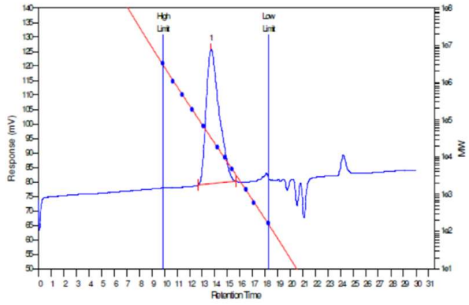

MW Averages

Peak No	Mp	Mn	Mw	Mz	Mz+1	Mv	PD
1	32825	21064	29355	37486	44764	28146	1.39361

Table 1, entry 5

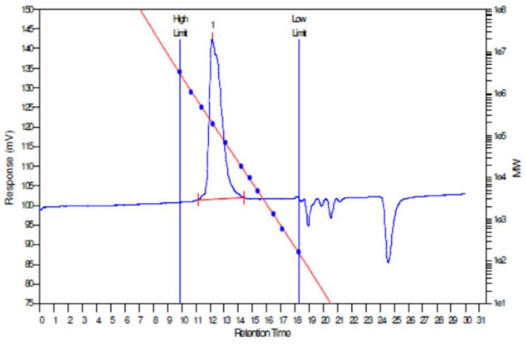

MW Averages

Peak No	Mp	Mn	Mw	Mz	Mz+1	Mv	PD
1	195619	116750	153033	186053	218779	148087	1.31078

Table 1, entry 6

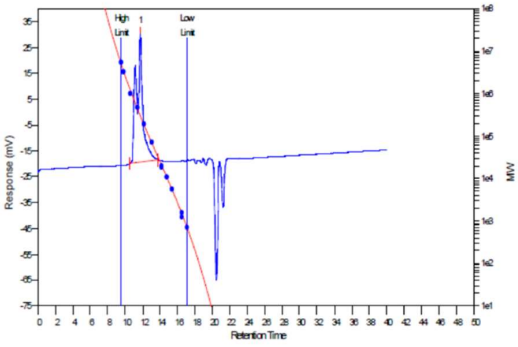

MW Averages

Peak No	Mp	Mn	Mw	Mz	Mz+1	Mv	PD
1	305780	275113	389482	490206	571850	373935	1.41572

Table 3, entry 1

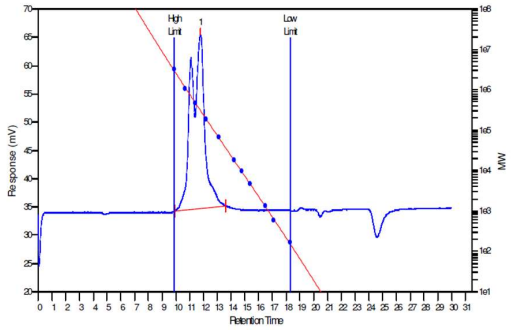

MW Averages

Peak No	Mp	Mn	Mw	Mz	Mz+1	Mv	PD
1	300882	316745	470289	649533	855221	446334	1.48476

Table 3, entry 2

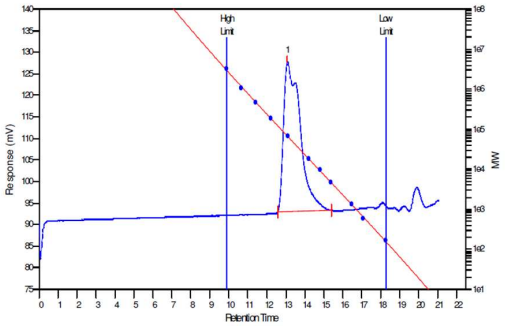

MW Averages

Peak No	Mp	Mn	Mw	Mz	Mz+1	Mv	PD
1	67138	37931	50023	59651	67152	48474	1.31879

Table 3, entry 3

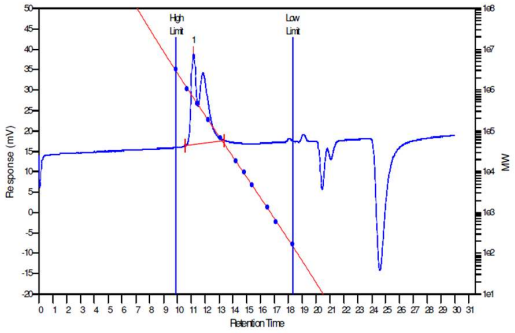

MW Averages

Peak No	Mp	Mn	Mw	Mz	Mz+1	Mv	PD
1	648781	299951	419795	534714	622493	402132	1.39955

5. Aliquot GPC analysis for the proof of block formation

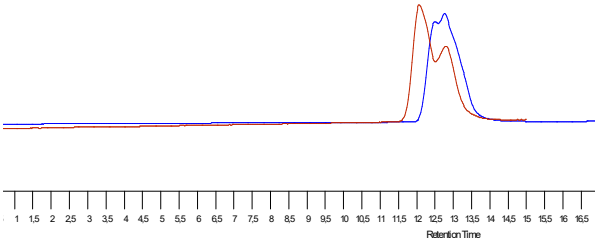

Figure S3. GPC traces of the PCHC aliquot (blue) and the resulting PCHC/PLC terpolymer (red).

16.5 Licenses for Copyrighted Content

Rightslink® by Copyright Clearance Center https://s100.copyright.com/AppDispatchServlet

Copyright Clearance Center RightsLink®

Home | Help | Live Chat | Sign in | Create Account

ACS Publications
Most Trusted. Most Cited. Most Read.

CO2-Controlled One-Pot Synthesis of AB, ABA Block, and Statistical Terpolymers from β-Butyrolactone, Epoxides, and CO2

Author: Sebastian Kernbichl, Marina Reiter, Friederike Adams, et al
Publication: Journal of the American Chemical Society
Publisher: American Chemical Society
Date: May 1, 2017

Copyright © 2017, American Chemical Society

PERMISSION/LICENSE IS GRANTED FOR YOUR ORDER AT NO CHARGE

This type of permission/license, instead of the standard Terms & Conditions, is sent to you because no fee is being charged for your order. Please note the following:

- Permission is granted for your request in both print and electronic formats, and translations.
- If figures and/or tables were requested, they may be adapted or used in part.
- Please print this page for your records and send a copy of it to your publisher/graduate school.
- Appropriate credit for the requested material should be given as follows: "Reprinted (adapted) with permission from (COMPLETE REFERENCE CITATION). Copyright (YEAR) American Chemical Society." Insert appropriate information in place of the capitalized words.
- One-time permission is granted only for the use specified in your request. No additional uses are granted (such as derivative works or other editions). For any other uses, please submit a new request.

BACK CLOSE WINDOW

Heteronuclear, Monomer-Selective Zn/Y Catalyst Combines Copolymerization of Epoxides and CO2 with Group-Transfer Polymerization of Michael-Type Monomers

Author: Alina Denk, Sebastian Kernbichl, Andreas Schaffer, et al

Publication: ACS Macro Letters

Publisher: American Chemical Society

Date: Apr 1, 2020

Permission to reproduce book chapter for 'Engineering Solutions for CO_2 Conversion' (Licenses for included schemes and figures attached)

Sehr geehrter Herr Kernbichl,

gerne erteilen wir Ihnen hiermit die Genehmigung für die unten beschriebene Nutzung unter der Voraussetzung, dass der Text nur im Rahmen der Doktorarbeit genutzt wird und daß ein entsprechendes Quellenzitat erfolgt.

Wenn in unserem Werk Material mit einer Quellenangabe abgedruckt ist, müssen Sie eine Genehmigung von der angegebenen Quelle einholen.

Das Quellenzitat muß folgende Bestandteile haben:

- Bücher: Autor(en)/ Herausgeber Name(n): Titel des Buches. Seite(n). Publikationsjahr. Copyright Wiley-VCH Verlag GmbH & Co. KGaA. Reproduced with permission.

Mit freundlichen Grüßen

Bettina Loycke
Senior Rights Manager
Rights & Licenses

Wiley-VCH Verlag GmbH & Co. KGaA
Boschstraße 12
69469 Weinheim
Germany
www.wiley-vch.de

T +(49) 6201 606-280
F +(49) 6201 606-332
rightsDE@wiley.com

WILEY

Herausgeber: Tomas R. Reina et al.
Titel: Engineering Solutions for CO2 Conversion
ISBN: **9783527346394**
Erscheint: voraussichtlich Ende 2020 / Copyrightjahr 2021
Kapitelautoren: Sebastian Kernbichl, Bernhard Rieger
Kapitel: Aliphatic Polycarbonates Derived from Epoxides and CO2

A Lewis acid β-diiminato-zinc-complex as all-rounder for co- and terpolymerisation of various epoxides with carbon dioxide

M. Reiter, S. Vagin, A. Kronast, C. Jandl and B. Rieger, *Chem. Sci.*, 2017, **8**, 1876
DOI: 10.1039/C6SC04477H

Bio-based polycarbonate from limonene oxide and CO_2 with high molecular weight, excellent thermal resistance, hardness and transparency

O. Hauenstein, M. Reiter, S. Agarwal, B. Rieger and A. Greiner, *Green Chem.*, 2016, **18**, 760
DOI: 10.1039/C5GC01694K

16.6 Experimental Section for Chapter 12

General Information. Moisture sensitive reactions were performed under standard Schlenk techniques in argon atmosphere (purity 4.6) in preheated glassware or in a glovebox LABmaster 130 of *M. Braun Inertgas-Systeme GmbH* (Garching, Germany). The synthesized monomers were stirred over CaH_2 or NaH and freshly distilled prior to use. All commercially available reagents were supplied by *Sigma-Aldrich* (St. Louis, USA) *and TCI* (Tokyo, Japan) and used without further purification. Dry solvents were obtained via purification with an MBraun MB-SPS-800 solvent purification system.

NMR. ^{1}H and ^{13}C NMR measurements were performed on a Bruker AV-500C spectrometer. Chemical shifts were reported in ppm relative to tetramethylsilane and calibrated to the residual ^{1}H or ^{13}C signal of the deuterated signal. Deuterated solvents were purchased from *Sigma-Aldrich*. The following abbreviations were applied: s (singlet), d (doublet), dd (double doublet), dt (double triplet), t (triplet), m (multiplet).

$CDCl_3$: ^{1}H-NMR: δ [ppm] = 7.26 (s)

^{13}C-NMR: δ [ppm] = 77.16 (t)

GC-MS. Mass spectra were recorded with an *Agilent Technologies* Mass Hunter Spectrometer (EI, 70 eV).

2-Trimethylsilyloxirane. 4.00 g (39.9 mmol, 1.00 eq.) vinyltrimethylsilane is dissolved in 100 mL dichloromethane and stirred at 0 °C. 12.2 g *meta*-chloroperoxybenzoic acid (77wt-%, 59.8 mmol, 1.50 eq.) is also dissolved in 100 mL DCM and slowly added to the reaction mixture under vigorous stirring. After one hour, the ice bath is removed, and the solution stirred overnight. A white solid precipitates after a few minutes which corresponds to the side product *meta*-chlorobenzoic acid. The precipitate is filtrated off and the solution is washed five times with 5% Na_2CO_3 solution. The product is distilled at reduced pressure to yield the product as a colorless liquid.

^{1}H NMR (500 MHz, $CDCl_3$, 298 K): δ (ppm) = 2.93 (t, ^{3}J = 5.7 Hz, 1H, CH), 2.58 (dd, ^{3}J = 5.7 Hz, ^{2}J = 4.1 Hz, 1H, CH), 2.22 (dd, ^{3}J = 5.7 Hz, ^{2}J = 4.1 Hz, 1H, CH), 0.09 (s, 9H, $SiMe_3$).

3-Carene oxide. 3-Carene oxide was prepared according to a modified literature procedure.[14] 10.0 g 3-carene (73.4 mmol, 1.00 eq.) is dissolved in 38.0 ml acetone and 8.00 mL H_2O. 13.6 g *N*-bromosuccinimide (76.6 mmol, 1.05 eq.) is added slowly under stirring at 0 °C. The solution is stirred for another hour. Acetone and water are removed under vacuum and the organic phase diluted with diethyl ether. The organic phase is washed with water before the ether gets removed again. The crude bromohydrin is directly converted to the epoxide via addition of 17.0 mL 6 M NaOH solution. The reaction mixture is stirred at room temperature for 2 h. The alkaline solution is removed, the crude product is diluted with ether and extracted with a $NaHCO_3$ solution and water. After evaporating the

solvent, the product is obtained as a yellowish liquid. Fractional distillation (15 mbar, 80 °C) allowed the isolation of 3-carene oxide in high purity (determined via GC-MS analysis).

^{1}H NMR (500 MHz, $CDCl_3$, 298 K): δ (ppm) = 2.84 (s, 1H, epoxy-H), 2.31 (ddd, *J* = 16.4 Hz, 8.9 Hz, 2.0 Hz, 1H, CH), 2.15 (dd, *J* = 16.4 Hz, 8.9 Hz, 1H, CH), 1.65 (dt, *J* = 16.4 Hz, 2.2 Hz, 1H, CH), 1.50 (dd, *J* = 16.2 Hz, 2.2 Hz, 1H, CH), 1.27 (s, 3H, Me), 1.02 (s, 3H, Me), 0.74 (s, 3H, Me), 0.50 (m, 2H, CH).

^{13}C NMR (500 MHz, $CDCl_3$, 298 K): δ (ppm) = 58.2 (s), 55.8 (s), 29.1 (s), 24.8 (s), 23.9 (s), 19.8 (s), 18.3 (s), 17.5 (s), 17.3 (s), 14.7 (s).

MS (EI, 70 eV): 153.1 m/z [M+H]

Polymerization procedure. In the glovebox, 8.76 mmol (100 eq.) of the respective epoxide (trimethylsilyloxirane, 3-carene oxide) is stored in one syringe. In a second one, 87.6 µmol of complex **4** (1.00 eq.) is dissolved in 1.00 mL toluene. The syringes are rapidly transported to a high-pressure autoclave and pressurized with 30 bar CO_2 for 16 h at rt. The polymerization is quenched with the addition of DCM and analyzed via ^{1}H NMR spectroscopy.

17. Bibliography

(1) Jambeck, J. R.; Geyer, R.; Wilcox, C.; Siegler, T. R.; Perryman, M.; Andrady, A.; Narayan, R.; Law, K. L. Plastic waste inputs from land into the ocean. *Science* **2015**, *347*, 768-771.

(2) https://www.plasticseurope.org/download_file/view/3355/310 status: january, **2020.**

(3) Ziegler, K.; Holzkamp, E.; Breil, H.; Martin, H. Das Mülheimer Normaldruck-Polyäthylen-Verfahren. *Angew. Chem.* **1955**, *67*, 541-547.

(4) Chen, E. Y. X. Coordination Polymerization of Polar Vinyl Monomers by Single-Site Metal Catalysts. *Chem. Rev.* **2009**, *109*, 5157-5214.

(5) Walsh, D. J.; Hyatt, M. G.; Miller, S. A.; Guironnet, D. Recent Trends in Catalytic Polymerizations. *ACS Catal.* **2019**, *9*, 11153-11188.

(6) Haider, T. P.; Völker, C.; Kramm, J.; Landfester, K.; Wurm, F. R. Plastics of the Future? The Impact of Biodegradable Polymers on the Environment and on Society. *Angew. Chem. Int. Ed.* **2019**, *58*, 50-62.

(7) https://www.european-bioplastics.org/market/ status: january, **2020**.

(8) Kember, M. R.; Buchard, A.; Williams, C. K. Catalysts for CO2/epoxide copolymerisation. *Chem. Comm.* **2011**, *47*, 141-163.

(9) Quadrelli, E. A.; Centi, G.; Duplan, J.-L.; Perathoner, S. Carbon Dioxide Recycling: Emerging Large-Scale Technologies with Industrial Potential. *ChemSusChem* **2011**, *4*, 1194-1215.

(10) https://www.novomer.com/novomer-completes-ppc-polyol-manufacturing-run status: january, **2020**.

(11) Langanke, J.; Wolf, A.; Hofmann, J.; Böhm, K.; Subhani, M. A.; Müller, T. E.; Leitner, W.; Gürtler, C. Carbon dioxide (CO2) as sustainable feedstock for polyurethane production. *Green Chem.* **2014**, *16*, 1865-1870.

(12) https://press.covestro.com/news.nsf/id/first-thermoplastic-polyurethane-based-on-co2-technology# status: january, **2020**.

(13) Koning, C.; Wildeson, J.; Parton, R.; Plum, B.; Steeman, P.; Darensbourg, D. J. Synthesis and physical characterization of poly(cyclohexane carbonate), synthesized from CO2 and cyclohexene oxide. *Polymer* **2001**, *42*, 3995-4004.

(14) Hauenstein, O.; Reiter, M.; Agarwal, S.; Rieger, B.; Greiner, A. Bio-based polycarbonate from limonene oxide and CO2 with high molecular weight, excellent thermal resistance, hardness and transparency. *Green Chem.* **2016**, *18*, 760-770.

(15) Rieger, B.; Künkel, A.; Coates, G. W. *Synthetic Biodegradable Polymers* Springer, Berlin/Heidelberg, Germany, 2012.

(16) Phillips, O.; Schwartz, J. M.; Kohl, P. A. Thermal decomposition of poly(propylene carbonate): End-capping, additives, and solvent effects. *Polym. Degrad. Stab.* **2016**, *125*, 129-139.

(17) Li, X.-G.; Huang, M.-R. Thermal degradation of bisphenol A polycarbonate by high-resolution thermogravimetry. *Polym. Int.* **1999**, *48*, 387-391.

(18) Li, G.; Qin, Y.; Wang, X.; Zhao, X.; Wang, F. Study on the influence of metal residue on thermal degradation of poly(cyclohexene carbonate). *Journal of Polymer Research* **2011**, *18*, 1177-1183.

(19) Cyriac, A.; Lee, S. H.; Varghese, J. K.; Park, E. S.; Park, J. H.; Lee, B. Y. Immortal CO2/Propylene Oxide Copolymerization: Precise Control of Molecular Weight and Architecture of Various Block Copolymers. *Macromolecules* **2010**, *43*, 7398-7401.

(20) Qin, Y.; Chen, L.; Wang, X.; Zhao, X.; Wang, F. Enhanced mechanical performance of poly(propylene carbonate) via hydrogen bonding interaction with o-lauroyl chitosan. *Carbohyd. Polym.* **2011**, *84*, 329-334.

(21) Seong, J. E.; Na, S. J.; Cyriac, A.; Kim, B.-W.; Lee, B. Y. Terpolymerizations of CO2, Propylene Oxide, and Various Epoxides Using a Cobalt(III) Complex of Salen-Type Ligand Tethered by Four Quaternary Ammonium Salts. *Macromolecules* **2010**, *43*, 903-908.

(22) Thorat, S. D.; Phillips, P. J.; Semenov, V.; Gakh, A. Physical properties of aliphatic polycarbonates made from CO2 and epoxides. *J. Appl. Polym. Sci.* **2003**, *89*, 1163-1176.

(23) Kindermann, N.; Cristòfol, À.; Kleij, A. W. Access to Biorenewable Polycarbonates with Unusual Glass-Transition Temperature (Tg) Modulation. *ACS Catal.* **2017**, *7*, 3860-3863.

(24) Li, C.; Sablong, R. J.; Koning, C. E. Chemoselective Alternating Copolymerization of Limonene Dioxide and Carbon Dioxide: A New Highly Functional Aliphatic Epoxy Polycarbonate. *Angew. Chem.* **2016**, *128*, 11744-11748.

(25) Kreimeyer, A.; Eckes, P.; Fischer, C.; Lauke, H.; Schuhmacher, P. "We Create Chemistry for a Sustainable Future": Chemistry Creates Sustainable Solutions for a Growing World Population. *Angew. Chem. Int. Ed.* **2015**, *54*, 3178-3195.

(26) Yilmaz, B.; Müller, U. Catalytic Applications of Zeolites in Chemical Industry. *Top. Catal.* **2009**, *52*, 888-895.

(27) Gall, R. J.; Greenspan, F. P.; Google Patents US2745848 A: 1956.

(28) Zhou, X.-T.; Ji, H.-B.; Xu, J.-C.; Pei, L.-X.; Wang, L.-F.; Yao, X.-D. Enzymatic-like mediated olefins epoxidation by molecular oxygen under mild conditions. *Tetrahedron Lett.* **2007**, *48*, 2691-2695.

(29) Inoue, S.; Koinuma, H.; Tsuruta, T. Copolymerization of carbon dioxide and epoxide with organometallic compounds. *Die Makromolekulare Chemie* **1969**, *130*, 210-220.

(30) Inoue, S.; Koinuma, H.; Tsuruta, T. Copolymerization of carbon dioxide and epoxide. *J. Polym. Sci.* **1969**, *7*, 287-292.

(31) Soga, K.; Imai, E.; Hattori, I. Alternating Copolymerization of CO2 and Propylene Oxide with the Catalysts Prepared from Zn(OH)2 and Various Dicarboxylic Acids. *Polym. J.* **1981**, *13*, 407-410.

(32) Klaus, S.; Lehenmeier, M. W.; Herdtweck, E.; Deglmann, P.; Ott, A. K.; Rieger, B. Mechanistic Insights into Heterogeneous Zinc Dicarboxylates and Theoretical Considerations for CO2–Epoxide Copolymerization. *J. Am. Chem. Soc.* **2011**, *133*, 13151-13161.

(33) Meng, Y. Z.; Du, L. C.; Tiong, S. C.; Zhu, Q.; Hay, A. S. Effects of the structure and morphology of zinc glutarate on the fixation of carbon dioxide into polymer. *J. Polym. Sci. Pol. Chem.* **2002**, *40*, 3579-3591.

(34) Takeda, N.; Inoue, S. Polymerization of 1,2-epoxypropane and copolymerization with carbon dioxide catalyzed by metalloporphyrins. *Die Makromolekulare Chemie* **1978**, *179*, 1377-1381.

(35) Qin, Y.; Wang, X.; Zhang, S.; Zhao, X.; Wang, F. Fixation of carbon dioxide into aliphatic polycarbonate, cobalt porphyrin catalyzed regio-specific poly(propylene carbonate) with high molecular weight. *J. Polym. Sci. Pol. Chem.* **2008**, *46*, 5959-5967.

(36) Kruper, W. J.; Dellar, D. D. Catalytic Formation of Cyclic Carbonates from Epoxides and CO2 with Chromium Metalloporphyrinates. *J. Org. Chem.* **1995**, *60*, 725-727.

(37) Darensbourg, D. J.; Holtcamp, M. W.; Struck, G. E.; Zimmer, M. S.; Niezgoda, S. A.; Rainey, P.; Robertson, J. B.; Draper, J. D.; Reibenspies, J. H. Catalytic Activity of a Series of Zn(II) Phenoxides for the Copolymerization of Epoxides and Carbon Dioxide. *J. Am. Chem. Soc.* **1999**, *121*, 107-116.

(38) Darensbourg, D. J.; Wildeson, J. R.; Yarbrough, J. C.; Reibenspies, J. H. Bis 2,6-difluorophenoxide Dimeric Complexes of Zinc and Cadmium and Their Phosphine Adducts: Lessons Learned Relative to Carbon Dioxide/Cyclohexene Oxide Alternating Copolymerization Processes Catalyzed by Zinc Phenoxides. *J. Am. Chem. Soc.* **2000**, *122*, 12487-12496.

(39) Cheng, M.; Lobkovsky, E. B.; Coates, G. W. Catalytic Reactions Involving C1 Feedstocks: New High-Activity Zn(II)-Based Catalysts for the Alternating Copolymerization of Carbon Dioxide and Epoxides. *J. Am. Chem. Soc.* **1998**, *120*, 11018-11019.

(40) Moore, D. R.; Cheng, M.; Lobkovsky, E. B.; Coates, G. W. Mechanism of the Alternating Copolymerization of Epoxides and CO2 Using β-Diiminate Zinc Catalysts: Evidence for a Bimetallic Epoxide Enchainment. *J. Am. Chem. Soc.* **2003**, *125*, 11911-11924.

(41) Darensbourg, D. J. Making Plastics from Carbon Dioxide: Salen Metal Complexes as Catalysts for the Production of Polycarbonates from Epoxides and CO2. *Chem. Rev.* **2007**, *107*, 2388-2410.

(42) Allen, S. D.; Moore, D. R.; Lobkovsky, E. B.; Coates, G. W. High-Activity, Single-Site Catalysts for the Alternating Copolymerization of CO2 and Propylene Oxide. *J. Am. Chem. Soc.* **2002**, *124*, 14284-14285.

(43) Qin, Z.; Thomas, C. M.; Lee, S.; Coates, G. W. Cobalt-Based Complexes for the Copolymerization of Propylene Oxide and CO2: Active and Selective Catalysts for Polycarbonate Synthesis. *Angew. Chem. Int. Ed.* **2003**, *42*, 5484-5487.

(44) S, S.; Min, J. K.; Seong, J. E.; Na, S. J.; Lee, B. Y. A Highly Active and Recyclable Catalytic System for CO2/Propylene Oxide Copolymerization. *Angew. Chem. Int. Ed.* **2008**, *47*, 7306-7309.

(45) Kember, M. R.; Knight, P. D.; Reung, P. T. R.; Williams, C. K. Highly Active Dizinc Catalyst for the Copolymerization of Carbon Dioxide and Cyclohexene Oxide at One Atmosphere Pressure. *Angew. Chem. Int. Ed.* **2009**, *48*, 931-933.

(46) Kember, M. R.; Williams, C. K. Efficient Magnesium Catalysts for the Copolymerization of Epoxides and CO2; Using Water to Synthesize Polycarbonate Polyols. *J. Am. Chem. Soc.* **2012**, *134*, 15676-15679.

(47) Byrne, C. M.; Allen, S. D.; Lobkovsky, E. B.; Coates, G. W. Alternating Copolymerization of Limonene Oxide and Carbon Dioxide. *J. Am. Chem. Soc.* **2004**, *126*, 11404-11405.

(48) Auriemma, F.; De Rosa, C.; Di Caprio, M. R.; Di Girolamo, R.; Ellis, W. C.; Coates, G. W. Stereocomplexed Poly(Limonene Carbonate): A Unique Example of the Cocrystallization of Amorphous Enantiomeric Polymers. *Angew. Chem. Int. Ed.* **2015**, *54*, 1215-1218.

(49) Peña Carrodeguas, L.; González-Fabra, J.; Castro-Gómez, F.; Bo, C.; Kleij, A. W. AlIII-Catalysed Formation of Poly(limonene)carbonate: DFT Analysis of the Origin of Stereoregularity. *Chem. Eur. J.* **2015**, *21*, 6115-6122.

(50) Reiter, M.; Vagin, S.; Kronast, A.; Jandl, C.; Rieger, B. A Lewis acid [small beta]-diiminato-zinc-complex as all-rounder for co- and terpolymerisation of various epoxides with carbon dioxide. *Chem. Sci.* **2017**, *8*, 1876-1882.

(51) Luinstra, G. A.; Haas, G. R.; Molnar, F.; Bernhart, V.; Eberhardt, R.; Rieger, B. On the Formation of Aliphatic Polycarbonates from Epoxides with Chromium(III) and Aluminum(III) Metal–Salen Complexes. *Chem. Eur. J.* **2005**, *11*, 6298-6314.

(52) Lu, X. B. *Carbon Dioxide and Organometallics*; Springer International Publishing, 2015.

(53) Darensbourg, D. J.; Yarbrough, J. C.; Ortiz, C.; Fang, C. C. Comparative Kinetic Studies of the Copolymerization of Cyclohexene Oxide and Propylene Oxide with Carbon Dioxide in the Presence of Chromium Salen Derivatives. In Situ FTIR Measurements of Copolymer vs Cyclic Carbonate Production. *J. Am. Chem. Soc.* **2003**, *125*, 7586-7591.

(54) https://www.plasticsinsight.com/resin-intelligence/resin-prices/polyester/ status: january, **2020**.

(55) Lemoigne, M. Produit de déshydratation et de polymérisation de l'acide β-oxybutyrique. *Bull. Soc. Chim. Biol.* **1926**, 770-782.

(56) Grothe, E.; Moo-Young, M.; Chisti, Y. Fermentation optimization for the production of poly(β-hydroxybutyric acid) microbial thermoplastic. *Enzyme Microb. Technol.* **1999**, *25*, 132-141.

(57) Thomas, C. M. Stereocontrolled ring-opening polymerization of cyclic esters: synthesis of new polyester microstructures. *Chem. Soc. Rev.* **2010**, *39*, 165-173.

(58) Ajellal, N.; Carpentier, J.-F.; Guillaume, C.; Guillaume, S. M.; Helou, M.; Poirier, V.; Sarazin, Y.; Trifonov, A. Metal-catalyzed immortal ring-opening polymerization of lactones, lactides and cyclic carbonates. *Dalton Trans.* **2010**, *39*, 8363-8376.

(59) Carpentier, J.-F. Discrete Metal Catalysts for Stereoselective Ring-Opening Polymerization of Chiral Racemic β-Lactones. *Macromol. Rapid Commun.* **2010**, *31*, 1696-1705.

(60) Olah, G. A.; Goeppert, A.; Prakash, G. K. S. Chemical Recycling of Carbon Dioxide to Methanol and Dimethyl Ether: From Greenhouse Gas to Renewable,

Environmentally Carbon Neutral Fuels and Synthetic Hydrocarbons. *J. Org. Chem.* **2009**, *74*, 487-498.

(61) Koempel, H.; Liebner, W. In *Studies in Surface Science and Catalysis*; Bellot Noronha, F., Schmal, M., Falabella Sousa-Aguiar, E., Eds.; Elsevier: 2007; Vol. 167, p 261-267.

(62) Khanmohammadi, M.; Amani, S.; Garmarudi, A. B.; Niaei, A. Methanol-to-propylene process: Perspective of the most important catalysts and their behavior. *Chin. J. Chem* **2016**, *37*, 325-339.

(63) Buchler, J.; Schmidt, M.; Prescher, G. 1990.

(64) Clerici, M. G.; Bellussi, G.; Romano, U. Synthesis of propylene oxide from propylene and hydrogen peroxide catalyzed by titanium silicalite. *J. Catal.* **1991**, *129*, 159-167.

(65) Mahadevan, V.; Getzler, Y. D. Y. L.; Coates, G. W. [Lewis Acid]+[Co(CO)4]− Complexes: A Versatile Class of Catalysts for Carbonylative Ring Expansion of Epoxides and Aziridines. *Angew. Chem.* **2002**, *114*, 2905-2908.

(66) Getzler, Y. D. Y. L.; Mahadevan, V.; Lobkovsky, E. B.; Coates, G. W. Synthesis of β-Lactones: A Highly Active and Selective Catalyst for Epoxide Carbonylation. *J. Am. Chem. Soc.* **2002**, *124*, 1174-1175.

(67) Tschan, M. J. L.; Brulé, E.; Haquette, P.; Thomas, C. M. Synthesis of biodegradable polymers from renewable resources. *Polymer Chem.* **2012**, *3*, 836-851.

(68) Castillo Martinez, F. A.; Balciunas, E. M.; Salgado, J. M.; Domínguez González, J. M.; Converti, A.; Oliveira, R. P. d. S. Lactic acid properties, applications and production: A review. *Trends Food Sci. Tech.* **2013**, *30*, 70-83.

(69) Ghaffar, T.; Irshad, M.; Anwar, Z.; Aqil, T.; Zulifqar, Z.; Tariq, A.; Kamran, M.; Ehsan, N.; Mehmood, S. Recent trends in lactic acid biotechnology: A brief review on production to purification. *J. Radiat. Res.* **2014**, *7*, 222-229.

(70) Ouhadi, T.; Hamitou, A.; Jerome, R.; Teyssie, P. Soluble Bimetallic μ-Oxo-alkoxides. 8. Structure and Kinetic Behavior of the Catalytic Species in Unsubstituted Lactone Ring-Opening Polymerization. *Macromolecules* **1976**, *9*, 927-931.

(71) Aida, T.; Sanuki, K.; Inoue, S. Well-controlled polymerization by metalloporphyrin. Synthesis of copolymer with alternating sequence and regulated molecular weight from cyclic acid anhydride and epoxide catalyzed by the system of aluminum porphyrin coupled with quaternary organic salt. *Macromolecules* **1985**, *18*, 1049-1055.

(72) Billingham, N. C.; Proctor, M. G.; Smith, J. D. Polymerization and copolymerization of β-butyrolactone by aluminium compounds. *J. Organomet. Chem.* **1988**, *341*, 83-93.

(73) Yasuda, T.; Aida, T.; Inoue, S. Living polymerization of β-butyrolactone catalysed by tetraphenylporphinatoaluminum chloride. *Makromol. Chem. Rapid Commun.* **1982**, *3*, 585-588.

(74) Le Borgne, A.; Spassky, N. Stereoelective polymerization of β-butyrolactone. *Polymer* **1989**, *30*, 2312-2319.

(75) Rieth, L. R.; Moore, D. R.; Lobkovsky, E. B.; Coates, G. W. Single-Site β-Diiminate Zinc Catalysts for the Ring-Opening Polymerization of β-Butyrolactone and

β-Valerolactone to Poly(3-hydroxyalkanoates). *J. Am. Chem. Soc.* **2002**, *124*, 15239-15248.

(76) Zintl, M.; Molnar, F.; Urban, T.; Bernhart, V.; Preishuber-Pflügl, P.; Rieger, B. Variably Isotactic Poly(hydroxybutyrate) from Racemic β-Butyrolactone: Microstructure Control by Achiral Chromium(III) Salophen Complexes. *Angew. Chem. Int. Ed.* **2008**, *47*, 3458-3460.

(77) Cai, C.-X.; Toupet, L.; Lehmann, C. W.; Carpentier, J.-F. Synthesis, structure and reactivity of new yttrium bis(dimethylsilyl)amido and bis(trimethylsilyl)methyl complexes of a tetradentate bis(phenoxide) ligand. *J. Organomet. Chem.* **2003**, *683*, 131-136.

(78) Amgoune, A.; Thomas, C. M.; Ilinca, S.; Roisnel, T.; Carpentier, J.-F. Highly Active, Productive, and Syndiospecific Yttrium Initiators for the Polymerization of Racemic β-Butyrolactone. *Angew. Chem. Int. Ed.* **2006**, *45*, 2782-2784.

(79) Ajellal, N.; Bouyahyi, M.; Amgoune, A.; Thomas, C. M.; Bondon, A.; Pillin, I.; Grohens, Y.; Carpentier, J.-F. Syndiotactic-Enriched Poly(3-hydroxybutyrate)s via Stereoselective Ring-Opening Polymerization of Racemic β-Butyrolactone with Discrete Yttrium Catalysts. *Macromolecules* **2009**, *42*, 987-993.

(80) Bouyahyi, M.; Ajellal, N.; Kirillov, E.; Thomas, C. M.; Carpentier, J.-F. Exploring Electronic versus Steric Effects in Stereoselective Ring-Opening Polymerization of Lactide and β-Butyrolactone with Amino-alkoxy-bis(phenolate)–Yttrium Complexes. *Chem. Eur. J.* **2011**, *17*, 1872-1883.

(81) Guillaume, S. M.; Kirillov, E.; Sarazin, Y.; Carpentier, J. F. Beyond Stereoselectivity, Switchable Catalysis: Some of the Last Frontier Challenges in Ring-Opening Polymerization of Cyclic Esters. *Chem. Eur. J.* **2015**, *21*, 7988-8003.

(82) Altenbuchner, P. T.; Soller, B. S.; Kissling, S.; Bachmann, T.; Kronast, A.; Vagin, S. I.; Rieger, B. Versatile 2-Methoxyethylaminobis(phenolate)yttrium Catalysts: Catalytic Precision Polymerization of Polar Monomers via Rare Earth Metal-Mediated Group Transfer Polymerization. *Macromolecules* **2014**, *47*, 7742-7749.

(83) Altenbuchner, P. T.; Kronast, A.; Kissling, S.; Vagin, S. I.; Herdtweck, E.; Pöthig, A.; Deglmann, P.; Loos, R.; Rieger, B. Mechanistic Investigations of the Stereoselective Rare Earth Metal-Mediated Ring-Opening Polymerization of β-Butyrolactone. *Chem. Eur. J.* **2015**, *21*, 13609-13617.

(84) Nie, K.; Fang, L.; Yao, Y.; Zhang, Y.; Shen, Q.; Wang, Y. Synthesis and Characterization of Amine-Bridged Bis(phenolate)lanthanide Alkoxides and Their Application in the Controlled Polymerization of rac-Lactide and rac-β-Butyrolactone. *Inorg. Chem.* **2012**, *51*, 11133-11143.

(85) Inoue, S. Immortal polymerization: The outset, development, and application. *J. Polym. Sci. Pol. Chem.* **2000**, *38*, 2861-2871.

(86) Zhuo, Z.; Zhang, C.; Luo, Y.; Wang, Y.; Yao, Y.; Yuan, D.; Cui, D. Stereoselectivity switchable ROP of rac-β-butyrolactone initiated by salan-ligated rare-earth metal amide complexes: the key role of the substituents on ligand frameworks. *Chem. Comm.* **2018**, *54*, 11998-12001.

(87) Tang, X.; Westlie, A. H.; Watson, E. M.; Chen, E. Y.-X. Stereosequenced crystalline polyhydroxyalkanoates from diastereomeric monomer mixtures. *Science* **2019**, *366*, 754-758.

(88) Webster, O. W.; Hertler, W. R.; Sogah, D. Y.; Farnham, W. B.; RajanBabu, T. V. Group-transfer polymerization. 1. A new concept for addition polymerization with organosilicon initiators. *J. Am. Chem. Soc.* **1983**, *105*, 5706-5708.

(89) Sogah, D. Y.; Hertler, W. R.; Webster, O. W.; Cohen, G. M. Group transfer polymerization - polymerization of acrylic monomers. *Macromolecules* **1987**, *20*, 1473-1488.

(90) Quirk, R. P.; Ren, J. Mechanistic studies of group transfer polymerization. Silyl group exchange studies. *Macromolecules* **1992**, *25*, 6612-6620.

(91) Mueller, A. H. E. Kinetic Discrimination between Various Mechanisms in Group-Transfer Polymerization. *Macromolecules* **1994**, *27*, 1685-1690.

(92) Müller, A. H. E.; Litvinenko, G.; Yan, D. Kinetic Analysis of "Living" Polymerization Systems Exhibiting Slow Equilibria. 4. "Dissociative" Mechanism of Group Transfer Polymerization and Generation of Free Ions in Cationic Polymerization. *Macromolecules* **1996**, *29*, 2346-2353.

(93) Webster, O. W. Group Transfer Polymerization: A Critical Review of Its Mechanism and Comparison with Other Methods for Controlled Polymerization of Acrylic Monomers. *Adv. Polym. Sci.* **2004**, *167*, 1-34.

(94) Soller, B. S.; Salzinger, S.; Rieger, B. Rare Earth Metal-Mediated Precision Polymerization of Vinylphosphonates and Conjugated Nitrogen-Containing Vinyl Monomers. *Chem. Rev.* **2016**, *116*, 1993-2022.

(95) Collins, S.; Ward, D. G. Group-transfer polymerization using cationic zirconocene compounds. *J. Am. Chem. Soc.* **1992**, *114*, 5460-5462.

(96) Yasuda, H. Organo-rare-earth-metal initiated living polymerizations of polar and nonpolar monomers. *J. Organomet. Chem.* **2002**, *647*, 128-138.

(97) Mariott, W. R.; Chen, E. Y. X. Mechanism and Scope of Stereospecific, Coordinative-Anionic Polymerization of Acrylamides by Chiral Zirconocenium Ester and Amide Enolates. *Macromolecules* **2005**, *38*, 6822-6832.

(98) Zhang, N.; Salzinger, S.; Soller, B. S.; Rieger, B. Rare Earth Metal-Mediated Group-Transfer Polymerization: From Defined Polymer Microstructures to High-Precision Nano-Scaled Objects. *J. Am. Chem. Soc.* **2013**, *135*, 8810-8813.

(99) Zhang, N.; Salzinger, S.; Rieger, B. Poly(vinylphosphonate)s with Widely Tunable LCST: A Promising Alternative to Conventional Thermoresponsive Polymers. *Macromolecules* **2012**, *45*, 9751-9758.

(100) Seemann, U. B.; Dengler, J. E.; Rieger, B. High-Molecular-Weight Poly(vinylphosphonate)s by Single-Component Living Polymerization Initiated by Rare-Earth-Metal Complexes. *Angew. Chem. Int. Ed.* **2010**, *49*, 3489-3491.

(101) Adams, F.; Pahl, P.; Rieger, B. Metal-Catalyzed Group-Transfer Polymerization: A Versatile Tool for Tailor-Made Functional (Co)Polymers. *Chem. Eur. J.* **2018**, *24*, 509-518.

(102) Altenbuchner, P. T.; Adams, F.; Kronast, A.; Herdtweck, E.; Pöthig, A.; Rieger, B. Stereospecific catalytic precision polymerization of 2-vinylpyridine via rare earth metal-mediated group transfer polymerization with 2-methoxyethylamino-bis(phenolate)-yttrium complexes. *Polymer Chem.* **2015**, *6*, 6796-6801.

(103) Kronast, A.; Reiter, D.; Altenbuchner, P. T.; Vagin, S. I.; Rieger, B. 2-Methoxyethylamino-bis(phenolate)yttrium Catalysts for the Synthesis of Highly

Isotactic Poly(2-vinylpyridine) by Rare-Earth Metal-Mediated Group Transfer Polymerization. *Macromolecules* **2016**, *49*, 6260-6267.

(104) Xu, T.-Q.; Yang, G.-W.; Lu, X.-B. Highly Isotactic and High-Molecular-Weight Poly(2-vinylpyridine) by Coordination Polymerization with Yttrium Bis(phenolate) Ether Catalysts. *ACS Catal.* **2016**, *6*, 4907-4913.

(105) Soller, B. S.; Salzinger, S.; Jandl, C.; Pöthig, A.; Rieger, B. C–H Bond Activation by σ-Bond Metathesis as a Versatile Route toward Highly Efficient Initiators for the Catalytic Precision Polymerization of Polar Monomers. *Organometallics* **2015**, *34*, 2703-2706.

(106) Watson, P. L. Methane exchange reactions of lanthanide and early-transition-metal methyl complexes. *J. Am. Chem. Soc.* **1983**, *105*, 6491-6493.

(107) Deelman, B.-J.; Booij, M.; Meetsma, A.; Teuben, J. H.; Kooijman, H.; Spek, A. L. Activation of Ethers and Sulfides by Organolanthanide Hydrides. Molecular Structures of (Cp*2Y)2(.mu.-OCH2CH2O)(THF)2 and (Cp*2Ce)2(.mu.-O)(THF)2. *Organometallics* **1995**, *14*, 2306-2317.

(108) Ringelberg, S. N.; Meetsma, A.; Troyanov, S. I.; Hessen, B.; Teuben, J. H. Permethyl Yttrocene 2-Furyl Complexes: Synthesis and Ring-Opening Reactions of the Furyl Moiety. *Organometallics* **2002**, *21*, 1759-1765.

(109) Kaneko, H.; Nagae, H.; Tsurugi, H.; Mashima, K. End-Functionalized Polymerization of 2-Vinylpyridine through Initial C–H Bond Activation of N-Heteroaromatics and Internal Alkynes by Yttrium Ene–Diamido Complexes. *J. Am. Chem. Soc.* **2011**, *133*, 19626-19629.

(110) Salzinger, S.; Soller, B. S.; Plikhta, A.; Seemann, U. B.; Herdtweck, E.; Rieger, B. Mechanistic Studies on Initiation and Propagation of Rare Earth Metal-Mediated Group Transfer Polymerization of Vinylphosphonates. *J. Am. Chem. Soc.* **2013**, *135*, 13030-13040.

(111) Natta, G.; Mazzanti, G.; Longi, P.; Dall'Asta, G.; Bernardini, F. Stereospecific polymerization of 2-vinylpyridine. *Journal of Polymer Science* **1961**, *51*, 487-504.

(112) Bräutigam, M.; Weyell, P.; Rudolph, T.; Dellith, J.; Krieck, S.; Schmalz, H.; Schacher, F. H.; Dietzek, B. Porous NiOx nanostructures templated by polystyrene-block-poly(2-vinylpyridine) diblock copolymer micelles. *Journal of Materials Chemistry A* **2014**, *2*, 6158-6166.

(113) Altenbuchner, P. T.; Werz, P. D. L.; Schöppner, P.; Adams, F.; Kronast, A.; Schwarzenböck, C.; Pöthig, A.; Jandl, C.; Haslbeck, M.; Rieger, B. Next Generation Multiresponsive Nanocarriers for Targeted Drug Delivery to Cancer Cells. *Chem. Eur. J.* **2016**, *22*, 14576-14584.

(114) Hückstädt, H.; Göpfert, A.; Abetz, V. Synthesis and morphology of ABC heteroarm star terpolymers of polystyrene, polybutadiene and poly(2-vinylpyridine). *Macromol. Chem. Phys.* **2000**, *201*, 296-307.

(115) Changez, M.; Koh, H.-D.; Kang, N.-G.; Kim, J.-G.; Kim, Y.-J.; Samal, S.; Lee, J.-S. Molecular Level Ordering in Poly(2-vinylpyridine). *Adv. Mater.* **2012**, *24*, 3253-3257.

(116) Schwarzenböck, C.; Nelson, P. J.; Huss, R.; Rieger, B. Synthesis of next generation dual-responsive cross-linked nanoparticles and their application to anti-cancer drug delivery. *Nanoscale* **2018**, *10*, 16062-16068.

(117) Bronstein, L. M.; Sidorov, S. N.; Valetsky, P. M.; Hartmann, J.; Cölfen, H.; Antonietti, M. Induced Micellization by Interaction of Poly(2-vinylpyridine)-block-poly(ethylene oxide) with Metal Compounds. Micelle Characteristics and Metal Nanoparticle Formation. *Langmuir* **1999**, *15*, 6256-6262.

(118) Adams, F.; Altenbuchner, P. T.; Werz, P. D. L.; Rieger, B. Multiresponsive micellar block copolymers from 2-vinylpyridine and dialkylvinylphosphonates with a tunable lower critical solution temperature. *RSC Adv.* **2016**, *6*, 78750-78754.

(119) Magenau, A. J. D.; Strandwitz, N. C.; Gennaro, A.; Matyjaszewski, K. Electrochemically Mediated Atom Transfer Radical Polymerization. *Science* **2011**, *332*, 81-84.

(120) Fors, B. P.; Hawker, C. J. Control of a Living Radical Polymerization of Methacrylates by Light. *Angew. Chem. Int. Ed.* **2012**, *51*, 8850-8853.

(121) Wang, X.; Thevenon, A.; Brosmer, J. L.; Yu, I.; Khan, S. I.; Mehrkhodavandi, P.; Diaconescu, P. L. Redox Control of Group 4 Metal Ring-Opening Polymerization Activity toward l-Lactide and ε-Caprolactone. *J. Am. Chem. Soc.* **2014**, *136*, 11264-11267.

(122) Coulembier, O.; Moins, S.; Todd, R.; Dubois, P. External and Reversible CO2 Regulation of Ring-Opening Polymerizations Based on a Primary Alcohol Propagating Species. *Macromolecules* **2014**, *47*, 486-491.

(123) Jeske, R. C.; Rowley, J. M.; Coates, G. W. Pre-Rate-Determining Selectivity in the Terpolymerization of Epoxides, Cyclic Anhydrides, and CO2: A One-Step Route to Diblock Copolymers. *Angew. Chem. Int. Ed.* **2008**, *47*, 6041-6044.

(124) Darensbourg, D. J.; Holtcamp, M. W. Catalytic Activity of Zinc(II) Phenoxides Which Possess Readily Accessible Coordination Sites. Copolymerization and Terpolymerization of Epoxides and Carbon Dioxide. *Macromolecules* **1995**, *28*, 7577-7579.

(125) Shi, L.; Lu, X.-B.; Zhang, R.; Peng, X.-J.; Zhang, C.-Q.; Li, J.-F.; Peng, X.-M. Asymmetric Alternating Copolymerization and Terpolymerization of Epoxides with Carbon Dioxide at Mild Conditions. *Macromolecules* **2006**, *39*, 5679-5685.

(126) Martín, C.; Kleij, A. W. Terpolymers Derived from Limonene Oxide and Carbon Dioxide: Access to Cross-Linked Polycarbonates with Improved Thermal Properties. *Macromolecules* **2016**, *49*, 6285-6295.

(127) Aida, T.; Inoue, S. Catalytic reaction on both sides of a metalloporphyrin plane. Alternating copolymerization of phthalic anhydride and epoxypropane with an aluminum porphyrin-quaternary salt system. *J. Am. Chem. Soc.* **1985**, *107*, 1358-1364.

(128) Paul, S.; Zhu, Y.; Romain, C.; Brooks, R.; Saini, P. K.; Williams, C. K. Ring-opening copolymerization (ROCOP): synthesis and properties of polyesters and polycarbonates. *Chem. Comm.* **2015**, *51*, 6459-6479.

(129) Longo, J. M.; Sanford, M. J.; Coates, G. W. Ring-Opening Copolymerization of Epoxides and Cyclic Anhydrides with Discrete Metal Complexes: Structure–Property Relationships. *Chem. Rev.* **2016**, *116*, 15167-15197.

(130) Vagin, S. I.; Reichardt, R.; Klaus, S.; Rieger, B. Conformationally Flexible Dimeric Salphen Complexes for Bifunctional Catalysis. *J. Am. Chem. Soc.* **2010**, *132*, 14367-14369.

(131) Wu, G.-P.; Darensbourg, D. J.; Lu, X.-B. Tandem Metal-Coordination Copolymerization and Organocatalytic Ring-Opening Polymerization via Water To Synthesize Diblock Copolymers of Styrene Oxide/CO2 and Lactide. *J. Am. Chem. Soc.* **2012**, *134*, 17739-17745.

(132) Darensbourg, D. J.; Wu, G.-P. A One-Pot Synthesis of a Triblock Copolymer from Propylene Oxide/Carbon Dioxide and Lactide: Intermediacy of Polyol Initiators. *Angew. Chem. Int. Ed.* **2013**, *52*, 10602-10606.

(133) Hwang, Y.; Jung, J.; Ree, M.; Kim, H. Terpolymerization of CO2 with Propylene Oxide and ε-Caprolactone Using Zinc Glutarate Catalyst. *Macromolecules* **2003**, *36*, 8210-8212.

(134) Song, P.; Xu, H.; Mao, X.; Liu, X.; Wang, L. A one-step strategy for aliphatic poly(carbonate-ester)s with high performance derived from CO2, propylene oxide and l-lactide. *Polym. Adv. Technol.* **2016**, n/a-n/a.

(135) Romain, C.; Williams, C. K. Chemoselective Polymerization Control: From Mixed-Monomer Feedstock to Copolymers. *Angew. Chem. Int. Ed.* **2014**, *53*, 1607-1610.

(136) Paul, S.; Romain, C.; Shaw, J.; Williams, C. K. Sequence Selective Polymerization Catalysis: A New Route to ABA Block Copoly(ester-b-carbonate-b-ester). *Macromolecules* **2015**, *48*, 6047-6056.

(137) Romain, C.; Zhu, Y.; Dingwall, P.; Paul, S.; Rzepa, H. S.; Buchard, A.; Williams, C. K. Chemoselective Polymerizations from Mixtures of Epoxide, Lactone, Anhydride, and Carbon Dioxide. *J. Am. Chem. Soc.* **2016**, *138*, 4120-4131.

(138) Chen, T. T. D.; Zhu, Y.; Williams, C. K. Pentablock Copolymer from Tetracomponent Monomer Mixture Using a Switchable Dizinc Catalyst. *Macromolecules* **2018**, *51*, 5346-5351.

(139) Zhu, Y.; Radlauer, M. R.; Schneiderman, D. K.; Shaffer, M. S. P.; Hillmyer, M. A.; Williams, C. K. Multiblock Polyesters Demonstrating High Elasticity and Shape Memory Effects. *Macromolecules* **2018**, *51*, 2466-2475.

(140) Solaro, R.; Cantoni, G.; Chiellini, E. Polymerisability of different lactones and methyl methacrylate in the presence of various organoaluminium catalysts. *Eur. Polym. J.* **1997**, *33*, 205-211.

(141) Yasuda, H.; Ihara, E. Rare earth metal initiated polymerizations of polar and nonpolar monomers to give high molecular weight polymers with extremely narrow molecular weight distribution. *Macromol. Chem. Phys.* **1995**, *196*, 2417-2441.

(142) Kostakis, K.; Mourmouris, S.; Karanikolopoulos, G.; Pitsikalis, M.; Hadjichristidis, N. Ring-opening polymerization of lactones using zirconocene catalytic systems: Block copolymerization with methyl methacrylate. *J. Polym. Sci. Pol. Chem.* **2007**, *45*, 3524-3537.

(143) Wang, Y.; Zhao, Y.; Ye, Y.; Peng, H.; Zhou, X.; Xie, X.; Wang, X.; Wang, F. A One-Step Route to CO2-Based Block Copolymers by Simultaneous ROCOP of CO2/Epoxides and RAFT Polymerization of Vinyl Monomers. *Angew. Chem. Int. Ed.* **2018**, *57*, 3593-3597.

(144) Zhang, Y.-Y.; Yang, G.-W.; Wu, G.-P. A Bifunctional β-Diiminate Zinc Catalyst with CO2/Epoxides Copolymerization and RAFT Polymerization Capacities for Versatile Block Copolymers Construction. *Macromolecules* **2018**, *51*, 3640-3646.

(145) Bhanage, B. M.; Arai, M. *Transformation and Utilization of Carbon Dioxide* Springer, Berlin/Heidelberg, Germany, 2014.

(146) Kernbichl, S.; Reiter, M.; Adams, F.; Vagin, S.; Rieger, B. CO_2-Controlled One-Pot Synthesis of AB, ABA Block, and Statistical Terpolymers from β-Butyrolactone, Epoxides, and CO_2. *J. Am. Chem. Soc.* **2017**, *139*, 6787-6790.

(147) Higashihara, T.; Ueda, M. Recent Progress in High Refractive Index Polymers. *Macromolecules* **2015**, *48*, 1915-1929.

(148) Czepukojc, B., Organische Schwefelverbindungen und ihre vielseitigen, innovativen Anwendungsgebiete, Ph.D. Dissertation, Universität des Saarlandes, Saarbrücken, 2014.

(149) Kanemura, Y.; Imai, M.; K.;, S.; Kajimoto, N.; Nagata, T. 1987; Vol. EP0235743A1.

(150) Nakano, K.; Tatsumi, G.; Nozaki, K. Synthesis of Sulfur-Rich Polymers: Copolymerization of Episulfide with Carbon Disulfide by Using [PPN]Cl/(salph)Cr(III)Cl System. *J. Am. Chem. Soc.* **2007**, *129*, 15116-15117.

(151) Darensbourg, D. J.; Andreatta, J. R.; Jungman, M. J.; Reibenspies, J. H. Investigations into the coupling of cyclohexene oxide and carbon disulfide catalyzed by (salen)CrCl. Selectivity for the production of copolymers vs. cyclic thiocarbonates. *Dalton Trans.* **2009**, 8891-8899.

(152) Marianucci, E.; Berti, C.; Pilati, F.; Manaresi, P.; Guaita, M.; Chiantore, O. Refractive index of poly(thiocarbonate)s and poly(dithiocarbonate)s. *Polymer* **1994**, *35*, 1564-1566.

(153) Winnacker, M. Pinenes: Abundant and Renewable Building Blocks for a Variety of Sustainable Polymers. *Angew. Chem. Int. Ed.* **2018**, *57*, 14362-14371.